A study of swarming in *Proteus mirabilis* and its role in the pathogenesis of catheter-associated urinary tract infections

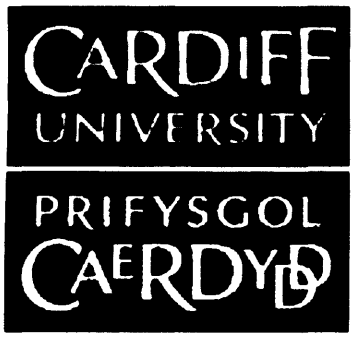

A thesis submitted to the University of Wales

by

Brian Vaughan Jones, BSc (Hons.) Genetics

In candidature for the degree of Philosophiae Doctor

Cardiff School of Biosciences

University of Wales, Cardiff

July 2004

ProQuest LLC
789 East Eisenhower Parkway
P.O. Box 1346
Ann Arbor, MI 48106-1346

Acknowledgements

Firstly, I would like to thank my supervisors Dave and Esh for all their help and support throughout my PhD. You have made the last 3 years stimulating, rewarding, and fun.

Thanks also go to everyone I have worked with: Mike, Hann, and especially Rob for all their help with electron microscopy; Joan, Adam, Sara, Marc and George for being helpful, friendly, and providing moments of comedy genius; and everyone in the lab for all their help.

Lastly (but not least), I would like to thank my parents, my brother, and Caroline for all their support and encouragement. I couldn't have done it without you.

Publications and presentations

Jones, B. V., R. Young, E. Mahenthiralingam, D. J. Stickler. (2004) The ultra-structure of *Proteus mirabilis* swarmer cell rafts, and the role of swarming in catheter-associated urinary tract infection. *Infection and Immunity*. **72**: 3941 - 3950.

Codling, C. E., B. V. Jones, E. Mahenthiralingam, A. D. Russell, J-Y. Maillard. (2004) Identification of genes involved in the resistance of *Serratia marcescens* to polyquaternium-1. *Journal of Antimicrobial Chemotherapy*. **54**: 370 – 375.

Jones, B. V., R. Young, E. Mahenthiralingam, D. J. Stickler. (2003) Characterisation of *Proteus mirabilis* swarming-deficient mutants by electron microscopy. Poster presented at the American Society for Microbiology 103rd Annual General Meeting, Washington D. C. Abstract D-262.

Jones, B. V., E. Mahenthiralingam, D. J. Stickler. (2002) The development of *Proteus mirabilis* crystalline biofilms that encrust indwelling urethral catheters. Poster presented at the American Society for Microbiology 102nd Annual General Meeting, Salt Lake City. Abstract B-196.

Abstract

Proteus mirabilis is a common cause of catheter-associated urinary tract infection (C-UTI). It blocks indwelling urethral catheters through the formation of extensive crystalline biofilms. The obstruction of urine flow from the bladder can induce episodes of pyelonephritis, septicaemia and endotoxic shock. *P. mirabilis* exhibits a type of motility referred to as swarming where multi-cellular rafts of elongated, hyper-flagellated, swarmer cells form and move rapidly in concert over solid surfaces. It has been suggested that swarming is important in the pathogenesis of C-UTI.

In this study a set of stable transposon mutants deficient in swarming were generated, and used to assess the contribution of swarming to the blockage and encrustation of urinary catheters by *P. mirabilis*. The genes disrupted in these mutants were identified, and their function in catheter blockage and swarming examined. The swarming ability, swimming ability, urease production, and growth rates of individual mutants were assessed. In general, all mutants showed severe reductions in swarming, and the majority were also attenuated in swimming. Growth and urease production were not affected in any of the mutants. Complementation studies in several mutants confirmed the genes disrupted as the source of the swarming-deficient phenotype.

The phenotypes of swimmer cells of swarming-deficient mutants were compared to those of wild type strains by transmission electron microscopy (TEM). This revealed that a reduction in flagella production was common to all swarming-deficient mutants. Several mutants also possessed defects in flagella structure or morphology. A novel vapour fixation technique for the preparation of specimens, and scanning electron microscopy was used to resolve the ultra-structure of *P. mirabilis* multi-cellular rafts during active migration over agar. The flagella filaments of *P. mirabilis* were found to be highly organised during migration. Filaments were interwoven in phase, to form helical connections between adjacent swarmer cells. TEM observations of thin sectioned swarm fronts showed that flagella filaments were interwoven in a criss-cross pattern. Helical connections appear to be important for migration and formation of multi-cellular rafts, and mutants lacking these novel organised structures failed to swarm successfully. Studies of complemented mutants revealed that formation of helical connections was also restored in these mutants, and identified genes associated with formation of these structures.

The role of swarming in adherence to and biofilm formation on silicone was examined using a parallel plate flow chamber. These experiments indicated that swarming-deficient mutants attached to silicone at higher rates that the wild type. A negative relationship was observed between both swimming and swarming ability, and adherence to silicone. However, only two mutants showed statistically significant differences in adherence when compared to the wild type. The strength of adherence to silicone was not affected by deficiencies in swarming, or swarm cell differentiation. Swarming-deficient mutants also exhibited alterations in biofilm architecture.

In vitro models of infection were used to investigate the contribution of swarming to the blockage of urinary catheters. The ability of mutants to form crystalline biofilms and block all-silicone catheters was investigated using an *in vitro* model of the catheterised urinary tract. Swarming ability did not significantly affect the time taken for *P. mirabilis* to block all-silicone catheters. A strong positive correlation was observed between the ability of mutants to adhere to silicon in parallel plate flow chambers and the time taken to block catheters.

The role of swarming in the migration of *P. mirabilis* over the surfaces of all-silicone, and hydrogel-coated latex catheters, was assessed using catheter bridge models. Swarming was found to be essential for migration over all-silicone catheters. Swarming-deficient mutants were attenuated in migration over hydrogel-coated latex catheters, but those capable of swimming motility were able to move over and infect these surfaces. Complemented mutants were also restored in their ability to migrate over both types of catheter. These results suggest that while swarming is not directly involved in the formation of crystalline biofilms on catheter surfaces, this form of motility enables *P. mirabilis* to initiate C-UTI by migration over catheter surfaces from the urethral meatus into the bladder.

Table of contents

List of figures

List of tables

Bacteria have these flagella,
They spin like little propellers,
So they can swim for a while,
Up a river of bile,
To your liver,
Which makes you turn yella.

Matthew Pitman

Chapter 1: Introduction

1.1 The indwelling urethral catheter

Indwelling urethral catheters (IUC) are common medical devices used to drain urine from the bladder, and in general constitute a convenient form of bladder management in a wide range of circumstances and conditions. Relief from anatomical and neurophysical bladder obstruction, accurate measure of urinary output from unconscious patients in intensive care units, management of long term incontinence in elderly patients and those suffering neurological pathologies are just a few applications (Stickler & McLean 1995; Stickler 1996a,b).

IUC are tubular structures, usually constructed from latex or silicone, which are inserted into the bladder via the urethra, or supra-pubically by surgery. A small opening at the tip called the eye-hole allows urine to drain into the catheter lumen and out of the bladder (Kunin 1987). The most widely used design is the Foley catheter, which incorporates a balloon near the tip of the catheter that holds the device in place when inflated (Figure 1.1).

The catheter is then connected to an external drainage system, which collects the patient's urine and stores it in a drainage bag. Cuthbert Dukes became the first to describe a closed drainage system for IUCs in 1928. He had become concerned with the inevitable development of urinary tract infections in patients fitted with IUCs following surgery on the rectum for cancer (Kunin 1987). He developed a system in which the urine drained into a sterile bottle, but also went a step further and incorporated a device which allowed intermittent irrigation, that was used to periodically wash the system with oxycyanide of mercury. This method virtually eliminated catheter associated UTI in the post operative period, yet the closed drainage system was not adopted for another 30-40 years and the majority of

Figure 1.1: Foley catheters.
An all silicone Foley catheter with inflated balloon (**A**), and a hydrogel-coated latex catheter with inflated balloon (**B**).

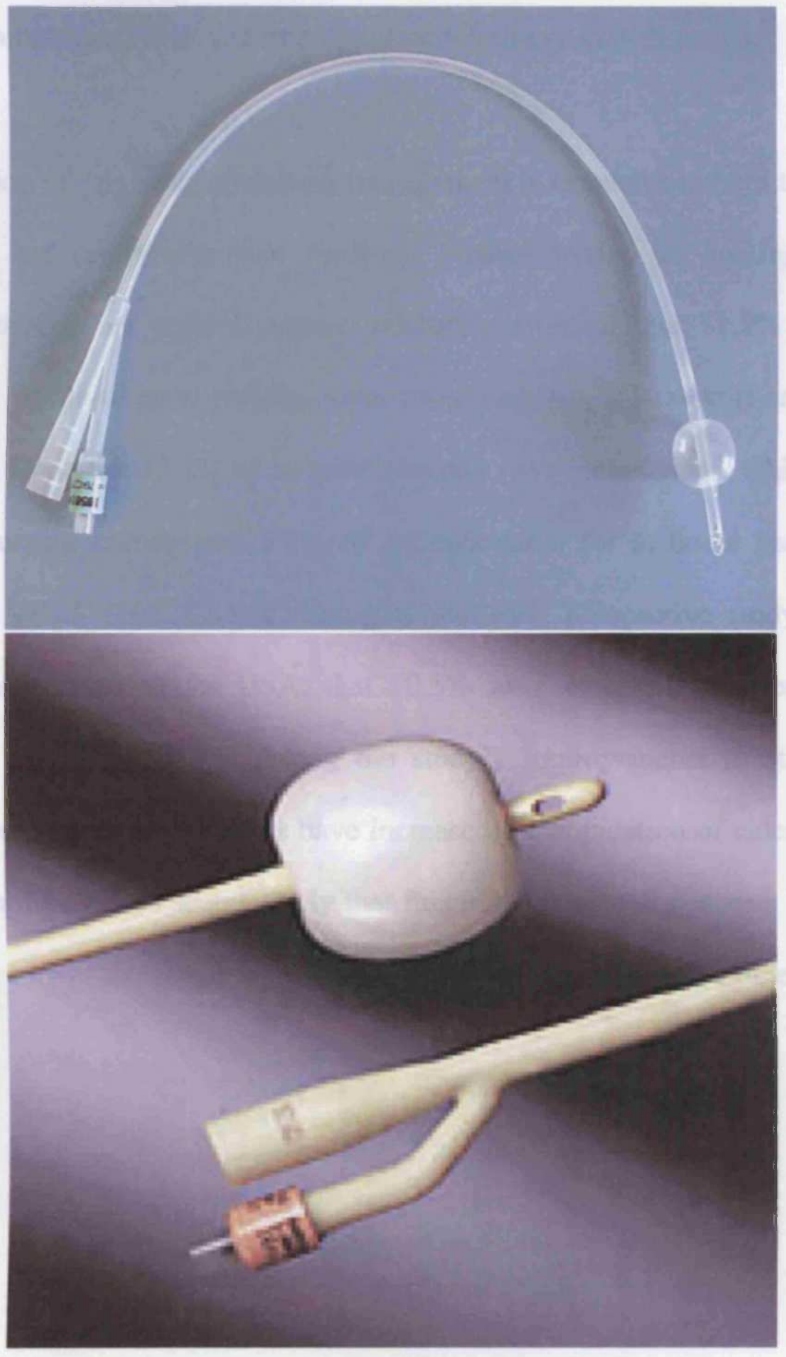

drainage systems remained open (Kunin 1987). Modern medical practice is to use IUCs in conjunction with a sterile, closed drainage system in order to reduce the chances of infection (Gillespie *et al.* 1983; Kunin 1987; Stickler & Zimakoff 1994). Figure 1.2 illustrates a Foley catheter and closed drainage system *in situ*.

The application of this form of bladder management is extensive in both the hospital environment and community care facilities. Studies carried out by Jepsen *et al.* (1982) in hospitals of eight European countries revealed that 11.8% of female patients, and 10.1% of male patients were fitted with IUCs. Zimakoff *et al.* (1993) found that in Denmark 13.2% of hospital patients were catheterised, while 4.9% of patients in nursing homes, and 3.9% of patients cared for at home had catheters fitted. Kunin *et al.* (1992) noted during a year-long prospective study of 1,540 nursing home patients in the USA, that 10.5% were catheterised at entry and a further 10% were catheterised during the study. Improvements to standards of living, healthcare, and other factors have increased the population of elderly citizens in many countries. It also seems likely that this population will continue to increase and therefore so will the use of IUC and other bladder management regimes.

Figure 1.2: Illustration of a Foley catheter and closed drainage system *in situ*.

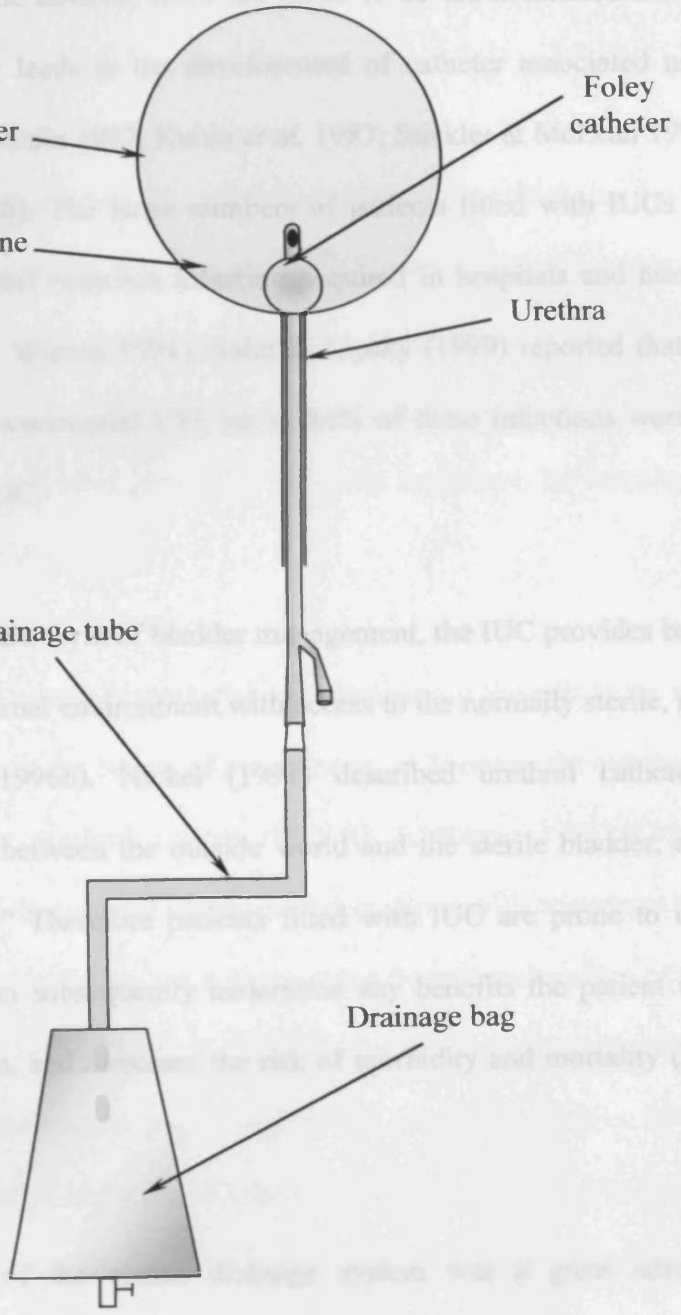

1.2 Catheter associated urinary tract infections

As with all prosthetic devices, IUCs are prone to device associated infections, and their use frequently leads to the development of catheter associated urinary tract infections (C-UTI; Kunin 1987, Kunin *et al.* 1987; Stickler & McLean 1995; Stickler 1996b; Warren 1996). The large numbers of patients fitted with IUCs has helped make C-UTI the most common infection acquired in hospitals and nursing homes (Meers *et al.* 1980; Warren 1991). Saint & Lipsky (1999) reported that in patients who had acquired nosocomial UTI, up to 86% of these infections were associated with the use of an IUC.

Although a convenient form of bladder management, the IUC provides bacteria from a contaminated external environment with access to the normally sterile, nutrient rich bladder (Stickler 1996b). Nickel (1991) described urethral catheterisation as "building a bridge between the outside world and the sterile bladder, along which bacteria can travel." Therefore patients fitted with IUC are prone to urinary tract infection, which can subsequently undermine any benefits the patient may receive from catheterisation, and increases the risk of morbidity and mortality (Kunin *et al.* 1992).

The introduction of the closed drainage system was a great advance in the management of the catheterised urinary tract, and can completely prevent C-UTI in the short term (Kunin 1987; Warren 1991). However, there are still many routes by which bacteria may colonise the catheterised urinary tract, and patients who undergo long-term catheterisation, defined as a period greater than 28 days, will inevitably

develop bacteriuria (Kunin 1987). Figure 1.3 summarised the routes by which bacteria may gain access to the catheterised urinary tract when a closed drainage system is in place.

Initially, insertion of the catheter may push organisms colonising the urethra, or contaminating the catheter into the bladder (Warren 1991). However, with good hygiene and proper aseptic insertion the number of infections initiated by this route is very low (Nickel 1991). Reported epidemics of UTIs associated with indwelling urethral catheters have been greatly reduced, or overcome, by introducing simple hygiene protocols (Kunin 1987).

The most important routes of bacterial colonisation are thought to be migration of bacteria either through the lumen of the catheter, or between the external surface of the catheter and the urethral mucosa (Daifuku & Stamm 1984). Organisms that compose the normal flora of the periurethral skin, along with organisms that colonise this area soon after admission, can migrate along the external surface of the catheter, to gain access to the bladder (Schaffer & Chmiel 1983; Fawcett *et al.* 1986). The first evidence that infection could be initiated by this route came form a study in which the periurethral skin of catheterised comatose patients was inoculated with *Serratia marcescens*. The same organism could often be isolated form catheter urine samples several days later (Kass & Schneiderman 1957).

Drainage taps become contaminated through continual use, and disconnection of the drainage tube to change drainage bags etc, can both lead to contamination of the system (Warren *et al.* 1978; Platt *et al.* 1983; Bradley *et al.* 1986). Once established

Figure 1.3: The routes of infection in a closed drainage system (Modified from Stickler 1996b).

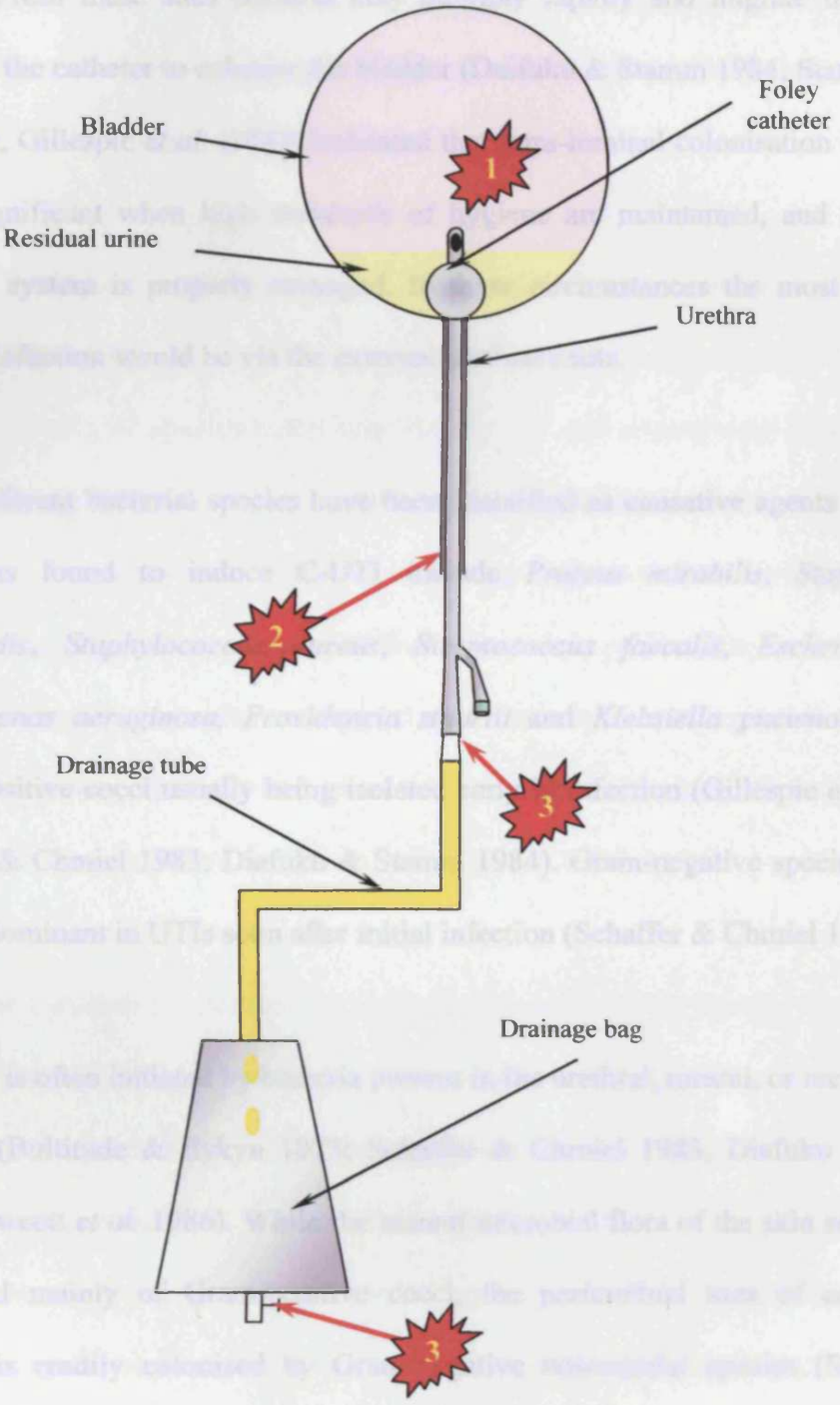

Routes of infection:

1. Bacteria may gain access to the bladder during catheter insertion.
2. Bacteria may migrate form the periurethral skin, along the interface between the catheter and urethral mucosa, to gain access to the bladder.
3. Bacteria may gain access to the closed drainage system during frequent use of taps or disconnection of drainage tube, then migrate through the catheter lumen to the bladder.

in the drainage bags, the contaminating organisms are provided with an excellent growth medium in the form of urine, and can often form dense populations (Stickler 1996b). From these sites bacteria may multiply rapidly and migrate through the lumen of the catheter to colonise the bladder (Daifuku & Stamm 1984; Stamm 1991). However, Gillespie *et al.* (1983) indicated that intra-luminal colonisation is unlikely to be significant when high standards of hygiene are maintained, and the closed drainage system is properly managed. In these circumstances the most important route of infection would be via the external urethral route.

Many different bacterial species have been identified as causative agents of C-UTI. Organisms found to induce C-UTI include *Proteus mirabilis*, *Staphylcoccus epidermidis*, *Staphylococcus aureus*, *Streptococcus faecalis*, *Eschericia coli*, *Pseudomonas aeruginosa*, *Providencia stuartii* and *Klebsiella pneumoniae*, with Gram- positive cocci usually being isolated early in infection (Gillespie *et al.* 1983; Schaffer & Chmiel 1983; Diafuku & Stamm 1984). Gram-negative species seem to become dominant in UTIs soon after initial infection (Schaffer & Chmiel 1983).

Infection is often initiated by bacteria present in the urethral, meatal, or rectal flora of patients (Bultitude & Eykyn 1973; Schaffer & Chmiel 1983; Diafuku & Stamm 1984; Fawcett *et al.* 1986). While the natural microbial flora of the skin seems to be composed mainly of Gram-positive cocci, the periurethral area of catheterised patients is readily colonised by Gram-negative nosocomial species (Schaffer & Chmiel 1983; Fawcett *et al.* 1986). Fawcett *et al.* (1986), compared the skin flora of 11 spine injured patients undergoing intermittent urethral catheterisation, with that of 11 healthy individuals. In all but three cases, Gram-negative bacilli were not isolated

from the urethras of the healthy individuals, but many Gram-negative species could be found colonising the skin of the spine injured patients. The groins, perinea, penile shaft, and urethras of these patients were heavily contaminated with multi-drug resistant Gram-negative organisms which included *P. mirabilis*, *S. marcescens*, *P. stuartii*, *P. aeruginosa*, and *K. pneumoniae*.

In early infections, single species are often isolated in pure culture (Bultitude & Eykyn 1973; Gillespie *et al.* 1983), but as the duration of catheterisation increases so does the number of species colonising the bladder and urinary tract (Clayton *et al.* 1982; Stickler 1996b). Studies of spine injured patients have revealed that in patients undergoing long-term catheterisation, infecting organisms can develop complex mixed communities of up to seven different bacterial species (Clayton *et al.* 1982). These communities are often composed of Gram-negative nosocomial species, of which the most common and persistent organisms include *P. mirabilis*, *K. pneumoniae*, *P. aeruginosa*, and *P. stuartii* (Stickler 1996a,b).

Due to the variation in resistance to antibacterial agents of the species that comprise these communities, their compositions can change in response to treatment with antibiotics (Clayton *et al.* 1982). Such treatment regimes may effectively eliminate one or more predominant species, but in doing so allow other, potentially more problematic species to gain a foot hold (Clayton *et al.* 1982; Fawcett *et al.* 1986). Transient organisms that persist in the urine in small numbers may flourish when competition from faster growing predominant species is removed (Clayton *et al.* 1982). In addition to this, cessation of therapy usually leads to the reappearance of the target organism (Clayton *et al.* 1982).

C-UTIs are a major problem which greatly undermine the effectiveness of the IUC, and in economic terms the cost of C-UTIs is huge. In 1992 it was estimated that approximately 225,000 patients in nursing homes in the USA, are catheterised at any one time (Kunin *et al.* 1992). Assuming that all of these patients may require long term catheterisation, and are therefore more likely to be hospitalised, the cost of excess hospitalisations alone would range from $343,588,500 to $666,112,500 (Kunin *et al.* 1992).

1.3 Complications associated with the indwelling urethral catheter

A wide variety of complications have been associated with the use of indwelling urethral catheters (Stickler & Zimakoff 1994). Complications linked to the use of IUC range from minor infections of the urinary tract to more serious, potentially lethal, conditions such as pyelonephritis, septicaemia, and cancer of the bladder (Kunin 1987; Stickler & Zimakoff 1994). Patients fitted with catheters, especially long-term indwelling catheters, are at greater risk of developing these conditions than non-catheterised patients due to the higher risk of urinary tract infection and bacteriuria associated with catheterisation (Kunin 1987; Stickler & Zimakoff 1994; Stickler 1996a,b). This makes catheterised patients, particularly those undergoing long-term catheterisation, more vulnerable to serious complications than non-catheterised patients (Stickler 1996a,b; Warren 1996).

Due to these factors, it is perhaps unsurprising that the use of IUC have been linked with increased morbidity and mortality in both hospital and nursing home patients (Platt *et al.* 1982; Kunin *et al.* 1992). The association between catheterisation and increased morbidity and mortality was illustrated in a study by Kunin *et al.* (1992), who undertook a year-long prospective study of 1540 residents in 14 nursing homes in Ohio. Regardless of status in relation to age, mobility, independence, sex, diabetes, cancer, heart disease, and skin condition, it was found that catheterised patients were three times more likely to be hospitalised than non-catheterised patients. Those catheterised for 76% or more of their time in the nursing home, were three times more likely to die within the year compared to non-catheterised patients. A similar increase in mortality has also been associated with catheterisation in hospital patients (Platt *et al.* 1982).

In patients undergoing short-term catheterisation complications include fever, acute pyelonephritis, and bacteraemia (Stickler & Zimakoff 1994; Warren 1996). Patients who are catheterised for long periods are not only prone to these complications, but are also susceptible to catheter blockage, bladder or infection stones, local periurinary infection, chronic pyelonephritis, renal failure, and when catheterisation has been undertaken for extensive periods of time (> 10 years) carcinoma of the bladder (Locke *et al.* 1985; Warren 1991; Stickler & Zimakoff 1994; Warren 1996).

Cystitis is an inflammation of the bladder wall and is usually caused by urinary tract infection, and can be characterised by dysuria, frequency and urgency of urination and often supra-pubic pain (Kunin 1987; Warren 1996). Cystitis has increased prevalence in patients fitted with catheters (Kunin 1987). Local periurinary infections have also been reported to be associated with catheterisation (Tribe & Silver 1969; Stover *et al.* 1991). These included infections such as urethritis, epididymitis, prostatitis, scrotal and prostatic abscesses (Warren 1991). Epididymitis and prostatitis, caused by reflux of infected urine into the prostatic and epididymal ducts, often occur simultaneously due to the contiguous nature of these structures (Kunin 1987).

Persistent infections of the bladder can lead to anatomical changes which allow the reflux of infected urine from the bladder into the ureters, where the bacteria can cause renal damage leading to pyelonephritis. (Warren *et al.* 1981). Pyelonephritis is an inflammation of renal membranes caused by infection, and acute pyelonephritis often occurs after catheterisation (Kunin 1987). Acute pyelonephritis can often be effectively controlled with standard chemotherapeutic agents, however in patients fitted with catheters hypertension, Gram-negative sepsis, and endotoxic shock can

occur (Kunin 1987). Warren *et al.* (1988) showed that renal inflammation was common among nursing home patients who died while undergoing long-term catheterisation. Postmortem evidence was also collected and revealed that the occurrence of pyelonephritis was significantly greater among patients who had died with their catheter in place (Warren *et al.* 1988).

Bacteraemia is also more prevalent in catheterised patients, and catheterisation has been reported to increase the risk of developing bacteraemia (Jepsen *et al.* 1982; Rudman *et al.* 1988; Muder *et al.* 1992). Rudman *et al.* (1988) examined the frequency of bacteraemia among 533 patients in a nursing home over the duration of 1 year. They found the urinary tract was the most frequent source of bacteraemia, and the 5% of patients that were catheterised at the start of the study experienced 40% of the Gram-negative bacteraemic episodes recorded. Other studies have found a high incidence of asymptomatic bacteraemia, but suggested that these may lead to more serious complications, such as endocarditis (Jewes *et al.* 1988).

A major complication during long-term catheterisation is the formation of crystalline deposits on the catheter surface (Getliffe & Mulhall 1991). Such deposits eventually obstruct the flow of urine and lead to a build up of infected urine in the bladder (Stickler 1996a,b). This can cause painful distension of the bladder, promotes leakage of urine around the catheter, and aids ascending urinary tract infection which can lead to episodes of pyelonephritis, septicaemia, and shock (Kunin 1987; Stickler & Zimakoff 1994; Stickler 1996a,b; Morris *et al.* 1997). The encrustation of the balloon and tip of the catheter can cause trauma to the urethra on withdrawal, and provide organisms with access to deeper tissues (Stickler & Zimakoff 1994; Stickler 1996b).

Kunin *et al.* (1987) classified nursing home patients fitted with long-term IUC as "blockers" and "non-blockers", with "blockers" defined as patients whose catheters became clogged or largely occluded. Of the population studied, over half were characterised as "blockers". C-UTIs are often asymptomatic and as such are frequently ignored until more serious complications arise (Kunin 1987; Warren 1996). Therefore, catheter blockage can have serious consequences if unnoticed, and is particularly dangerous in catheterised patients cared for at home where professional medical care is not immediately available (Stickler 1996b).

Crystalline deposits, termed infection stones, may also form in the urinary tract. They usually posses a similar crystalline structure and chemical composition to catheter encrustations (Clapham *et al.* 1990; Griffith *et al.* 1976; Cox & Hukins 1989). These stones can form in the bladder and in the renal tissue where they can lead to particularly serious complications. Stones that form in the kidney can obstruct the flow of urine, provide areas of colonisation for bacteria, and can eventually lead to pyelonephritis, renal abscesses and septicaemia (Stickler & Zimakoff 1994).

1.4 Biofilm formation

Studies of bacterial populations in natural aquatic habitats revealed the marked preference for surface associated growth displayed by these organisms. In the ecosystems studied more than 99.9% of bacteria have been suggested to grow as biofilms on a wide variety of surfaces (Donlan & Costerton 2002). Biofilm formation represents a survival strategy and cells associated with these communities behave differently than their planktonic counterparts. Biofilm associated bacteria exhibit an increased resistance to antimicrobial agents, are in a different physiological state, and are protected against predators and parasites (Costerton *et al.* 1987; Stickler 1996a; Sutherland *et al.* 1999; Donlan 2001; Donlan & Costerton 2002). Bacterial biofilms have recently been defined as a community of sessile cells that are irreversibly attached to a substratum or each other, embedded in a matrix of self generated extra cellular polymeric substances, and exhibit altered gene transcription and growth rate compared to planktonic cells (Donlan & Costerton 2002).

1.4.1 Attachment of cells to a surface

The formation of bacterial biofilms is thought to occur through a distinct sequence of events, which are summarised in Figure 1.4. Initially cells must come into contact with and adhere to the surface on which the biofilm will be formed. Several factors may influence attachment including characteristics of the surface, properties of the bacterial cell, and the presence of a conditioning film (Donlan 2002). The composition of the medium may also influence the attachment of cells, and studies have shown that an increase in nutrient concentration can lead to a greater number of cells adhering to a surface (Cowan *et al.* 1991). Other properties of the media such as pH, temperature, and ionic strength may also influence the ability of cells to attach to a surface (Donlan 2002).

Figure 1.4: The formation of bacterial biofilms.

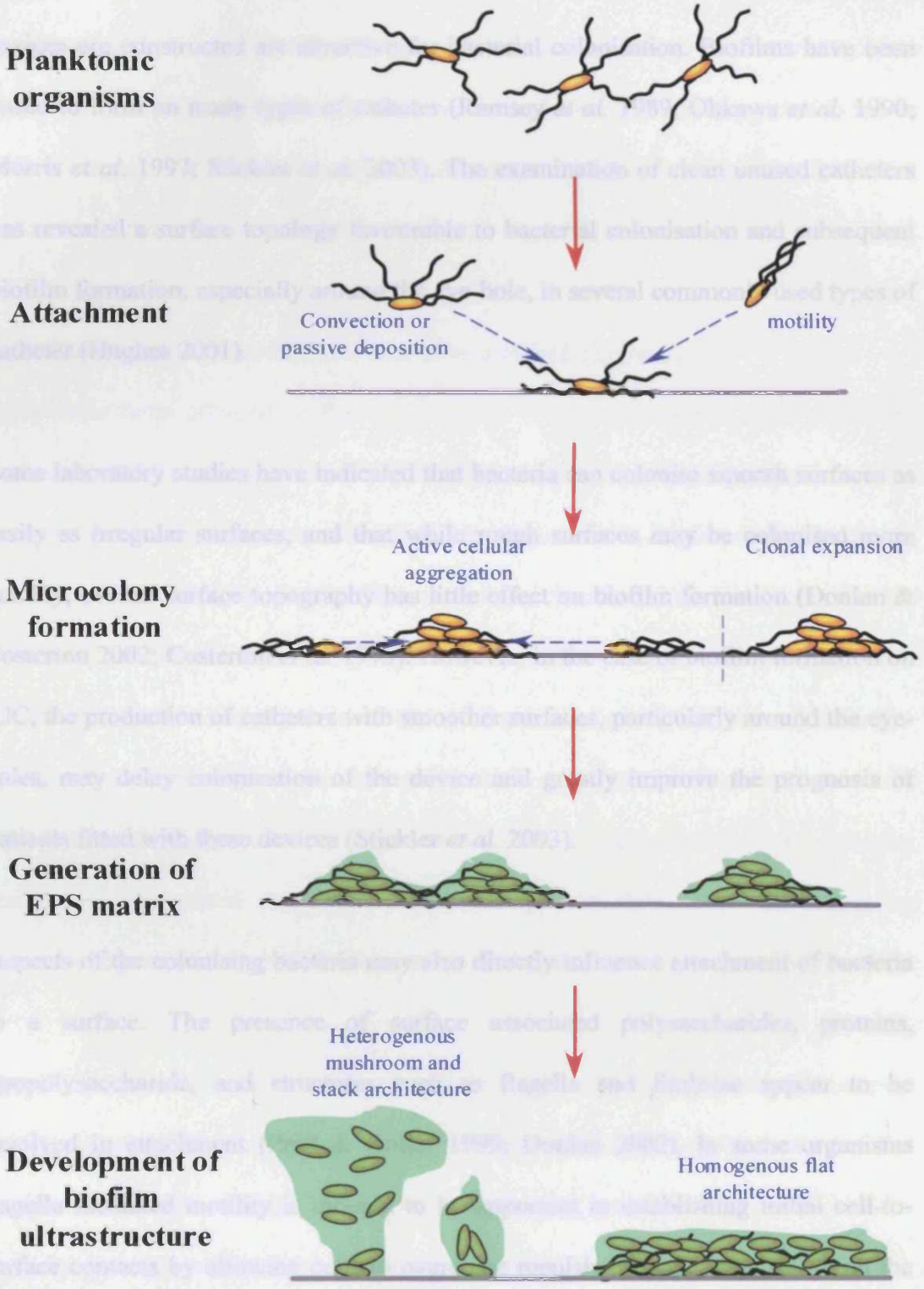

Characteristics of the surface to be colonised also have an effect on the attachment of bacteria, with rougher surfaces being generally more favourable to colonisation (Donlan 2002). In the case of urinary catheters, the materials from which these devices are constructed are attractive for bacterial colonisation. Biofilms have been found to form on many types of catheter (Ramsey *et al.* 1989; Ohkawa *et al.* 1990; Morris *et al.* 1997; Stickler *et al.* 2003). The examination of clean unused catheters has revealed a surface topology favourable to bacterial colonisation and subsequent biofilm formation, especially around the eye-hole, in several commonly used types of catheter (Hughes 2001).

Some laboratory studies have indicated that bacteria can colonise smooth surfaces as easily as irregular surfaces, and that while rough surfaces may be colonised more quickly, overall surface topography has little effect on biofilm formation (Donlan & Costerton 2002; Costerton *et al.* 1995). However, in the case of biofilm formation on IUC, the production of catheters with smoother surfaces, particularly around the eye-holes, may delay colonisation of the device and greatly improve the prognosis of patients fitted with these devices (Stickler *et al.* 2003).

Aspects of the colonising bacteria may also directly influence attachment of bacteria to a surface. The presence of surface associated polysaccharides, proteins, lipopolysaccharide, and structures such as flagella and fimbriae appear to be involved in attachment (Pratt & Kolter 1999; Donlan 2002). In some organisms flagella mediated motility is thought to be important in establishing initial cell-to-surface contacts by allowing cells to overcome repulsive forces associated with the surface (Pratt & Kolter 1999; Donlan 2002).

The formation of an organic conditioning film on the surface may enhance the adherence of the cell to a surface (Ohkawa *et al.* 1990; Donlan 2001; 2002). Studies of IUC removed from patients revealed the presence of a proteinacious layer, mainly composed of fibrinogen (Ohkawa *et al.* 1990). It is thought that this layer originates from injury to host tissues during fitting of the catheter, and was suggested to act as an adherent to which bacteria became attached and subsequently initiated biofilm formation (Ohkawa *et al.* 1990).

1.4.2 Development, architecture, and properties of biofilms

Once cells have adhered to the surface they begin to generate extra polymeric substances (EPS; Donlan 2001; 2002). EPS is composed mainly of polysaccharides, but may also include some proteins (Sutherland *et al.* 1999; Donlan 2001; Donlan & Costerton 2002; Donlan 2002). This exopolysaccharide matrix facilitates further development of the biofilm, strengthens attachment to the surface, and enhances cell-to-cell contacts (Stickler & McLean 1995; Sutherland *et al.* 1999; Donlan 2002). The production of EPS is also thought to perform a protective function, and cells embedded in the polysaccharide matrix of a biofilm are thought to be protected from various environmental stresses, such as changes in flow rate, and attack by bacteriophage or protozoa (Sutherland *et al.* 1999; Donlan & Costerton 2002).

The EPS matrix has also been suggested to play a role in the innate resistance of biofilms to the host immune system and antimicrobial agents. Cells in the biofilm could be shielded by the EPS matrix from antibodies, and other components of the immune system, such as polymorphonuclear leukocytes (Stickler & McLean 1995). The EPS may also protect cells against antimicrobial agents either by inhibiting diffusion of the agent through the biofilm, or by interacting directly with it to prevent

penetration of the biofilm (Sutherland *et al.* 1999). Biofilms of *Ps. aeruginosa*, exposed to concentration of tobramycin that greatly exceed the minimum inhibitory concentration for planktonic cells, showed only a 2-log reduction in cell number compared to a >8-log reduction in planktonic cells exposed to the same concentration (Anwar *et al.* 1992). However, it has been pointed out that increased resistance to antimicrobials in biofilm associated bacteria may also be a result of the cells altered physiological state and reduced growth rate (Williams *et al.* 1997).

After the initial attachment of cells, biofilm development proceeds through the formation of microcolonies. These are considered to be the basic structural units of biofilms (Donlan 2002; Donlan & Costerton 2002). Several mechanisms have been proposed for the development of microcolonies. It has been suggested that these units are formed by the aggregation of individual cells which migrate over the surface to form microcolonies (O'Toole & Kolter 1998a,b; Watnick & Kolter 1999; Pratt & Kolter 1999), or through the clonal expansion of individual cells that are attached (Tolker-Nielsen *et al.* 2000; Klausen *et al.* 2003). Clonal expansion is presumably the only method available to non-motile organisms but motile organisms may employ either strategy. For example, in mixed biofilms of *Ps. putida* and another *Pseudomonas* species, microcolony formation occurred initially through clonal expansion but as the biofilm matured intermixing of microcolonies proceeded via flagella driven motility (Tolker-Nielsen *et al.* 2000).

Communication between individual cells is also thought to be involved in the organisation of biofilm communities (McLean *et al.* 1997; Davies *et al.* 1998; Stickler *et al.* 1998a; Pratt & Kolter 1999). It has been suggested that genes responsible for the development of biofilms are regulated by quorum sensing

systems, which allow the expression of biofilm associated genes to be coupled to population density (Davies *et al.* 1998). The quorum sensing signal molecules, for example N-acyl homoserine lactones (AHLs) have been detected in biofilms that have formed in natural aquatic habitats, and on the surface of urethral catheters (McLean *et al.* 1997; Stickler *et al.* 1998a). In *Ps. aeruginosa* AHLs have been found to be involved in the development of biofilms. Mutants defective in production of two distinct AHLs were found to be reduced in the ability to form biofilms on a glass surface, and generated biofilms with an altered ultrastructure (Davies *et al.* 1998).

Observations from studies utilising flow chamber experiments and advanced microscopic techniques to examine the development of biofilms in real-time and *in situ*, have provided insights into the structure of mature biofilms. One of the most powerful techniques has been the use of confocal laser scanning microscopy which can generate three dimensional images of viable biofilms *in situ* without the destructive sampling techniques which inevitably alter the morphology of these biofilms (Donlan & Costerton 2002).

These studies indicated that the structure of mature biofilms is largely heterogeneous, and initial microcolonies were found to form structures resembling towers and mushrooms, separated by water channels (Costerton *et al.* 1995). It has been proposed that these water channels act as a primitive circulatory system, transporting nutrients throughout the biofilm and removing waste products (Costerton *et al.* 1995). Such observations have lead to the development of a generally accepted universal model of biofilm architecture, illustrated in Figure 1.5.

Figure 1.5: Illustration of the proposed universal structure of mature bacterial biofilms (modified from Pratt & Kolter 1999).

Depiction of a heterogeneous biofilm composed of bacterial populations enclosed in an abundant polysaccharide matrix to form "mushrooms" and "stacks". These structures are separated by fluid filled channels proposed to facilitate the dispersal of nutrients throughout the biofilm and remove waste products. This has been suggested to be the universal structure of mature biofilms (Costerton 2002).

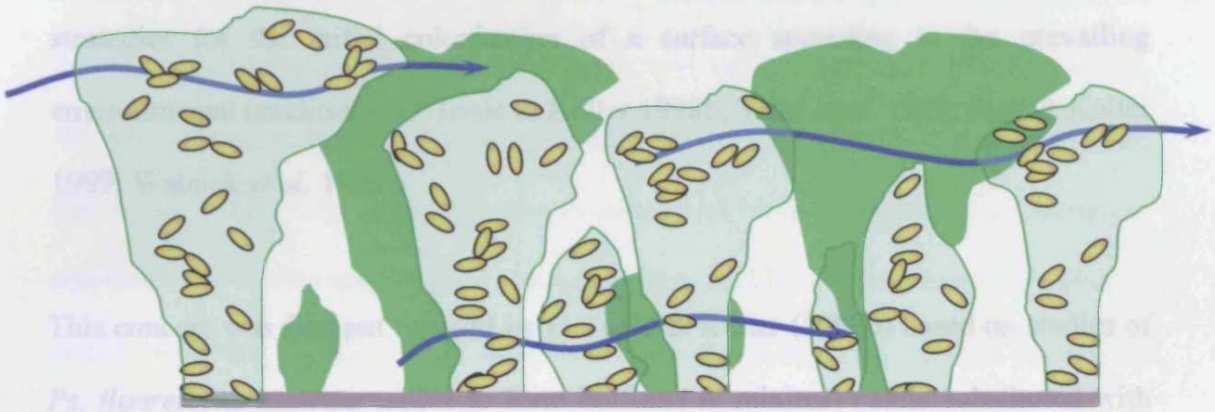

However, such studies were largely performed using *Ps. aeruginosa* biofilms in conditions of low nutrient availability, and as such the proposed universal model of biofilm architecture may only reflect a subset of organisms under specific conditions. Klausen *et al.* (2003) recently demonstrated that in *Ps. aeruginosa* PA01 architecture of the developed biofilm was dependant on the carbon source supplied. When glucose was utilised as the sole carbon source biofilms with the "classic" heterogeneous mushroom and stack architecture were formed, but a flat homogenous architecture was generated when glucose was substituted for either citrate, casamino acids, or benzoate as the sole carbon source.

Recent advances in molecular genetics have revealed that biofilm formation is a complex process, involving the co-ordinated expression of many genes, and in addition to the up-regulation of certain genes, biofilm formation is also thought to involve down regulation of genes (Pratt & Kolter 1999). Some studies also indicate that at least in some species of bacteria several distinct, but convergent genetic pathways for biofilm development exist, allowing these organisms to utilise alternate strategies for the initial colonisation of a surface according to the prevailing environmental conditions (O`Toole & Kolter 1998b; Vidal *et al.* 1998; Pratt & Kolter 1999; Watnick *et al.* 1999).

This concept was first put forward by O`Toole & Kolter (1998b) based on studies of *Ps. fluorescens* mutants unable to form biofilms in minimal media substituted with casamino acids. Analysis of biofilm formation in these mutants in minimal media containing high iron, citrate, or glutamate revealed several distinct classes of mutants which possessed the ability to form biofilms under differing environmental conditions, and indicated the presence of at least two distinct overlapping pathways of biofilm development in this organism. Additional evidence supporting the idea of multiple pathways of biofilm formation have come from studies with *E. coli* and *Vibrio cholerae* (Vidal *et al.* 1998; Watnick *et al.* 1999). In the case of *E. coli,* non-motile mutants which had gained the capability to form biofilms on PVC were found to over express a surface adhesin protein (Vidal *et al.* 1998). In *V. cholerae* the mannose sensitive haemagglutinin pilus was found to be necessary for colonisation of borosilicate glass but was not involved in adhesion to chitin (Watnick *et al.* 1999).

1.5 Formation of crystalline biofilms and blockage of urethral catheters

As discussed in the previous section, biofilm formation is ubiquitous and these communities establish themselves on many different surfaces in many environments. Implanted medical devices are no exception and biofilms have been identified on or in contact lenses, mechanical heart valves, central venous catheters, intrauterine devices, prosthetic joints, vocal prostheses, and urinary catheters (Donlan 2001). Biofilm formation poses particular problems in the treatment of device associated infections, which stem from the innate resistance of biofilm associated organisms to anti-microbial agents and the host immune system (Stickler & McLean 1995; Donlan 2002). Also the production of endo-toxins by Gram-negative biofilm associated bacteria can generate serious complications (Stickler & McLean 1997; Donlan 2002).

Organisms that cause C-UTI often establish biofilms on the surface of urinary catheters, (Ramsey *et al.* 1989; Ohkawa *et al.* 1990; Ganderton *et al.* 1992). Ohkawa *et al.* (1990) studied catheters removed from patients 7-16 days after insertion using electron microscopy, and found that 21 out of 28 catheters examined possessed bacterial biofilms. A similar study by Ganderton *et al.* (1992) revealed biofilms on 44 out of 50 catheters removed between 3 and 83 days after fitting, and the thickness of biofilms was found to vary considerably between catheters, ranging from cell monolayers to structures 400 cells deep. These biofilms may initially be composed of single species but the species diversity increases the longer the catheter remains in place (Clayton *et al.*1982). In the case of patients undergoing permanent or long-term catheterisation, the frequency with which catheters are changed may result in infected urine draining through the catheter for periods of up to three months (Stickler 1996a,b).

In addition to the difficulties biofilms pose to the treatment of C-UTI, the formation of biofilms represents a key process in the pathogenicity of these infections and the encrustation of IUC (Stickler 1996a,b). These biofilms become mineralised resulting in the formation of a crystalline structure, and it is the formation of these crystalline biofilms that induces one of the major complications associated with C-UTI, catheter blockage (Stickler *et al.* 1993; Getliffe & Mulhall 1991; Stickler 1996a). Therefore, the biofilm is responsible for the accumulation of crystalline deposits on the catheter surface, which eventually leads to obstruction of urine flow (Stickler *et al.* 1993; Getliffe & Mulhall 1991; Stickler 1996a). Figure 1.6 shows blocked and encrusted IUC.

The development of these crystalline biofilms is due to the presence of urease producing species in the catheterised urinary tract (Griffith *et al.* 1976; Mobley & Warren 1987; Kunin 1989; Stickler *et al.* 1993; Morris *et al.* 1997). The urease enzyme manufactured by these organisms hydrolyses urea present in the urine to produce ammonia and carbon dioxide, which generates a highly alkaline environment (Griffith *et al.* 1976; Stickler 1996b). Under such alkaline conditions calcium and magnesium phosphates precipitate out of solution and form crystals of struvite (magnesium ammonium phosphate) and hydroxyapatite (Hedelin *et al.* 1984; Cox & Hukins 1989). The morphology of these crystalline deposits has been investigated using electron microscopy, and were found to be composed of coffin shaped struvite crystals and amorphous hydroxyapatite (Cox & Hukins 1989). Figure 1.7 shows the morphology of crystals that encrust IUC.

Figure 1.6: Examples of blocked and encrusted IUC.
The images below provide examples of blocked and encrusted IUC, demonstrate total and partial occlusion of the lumen (**A, C**), crystalline deposits covering the balloon (**B**). Image **D** show a cross section through the eye-hole of a blocked IUC and shows that this has been completely sealed by crystalline material, as indicated by arrows. Images **A** and **B** are examples of catheters which have been removed from patients, while **C** and **D** were generated using *in vitro* bladder models.

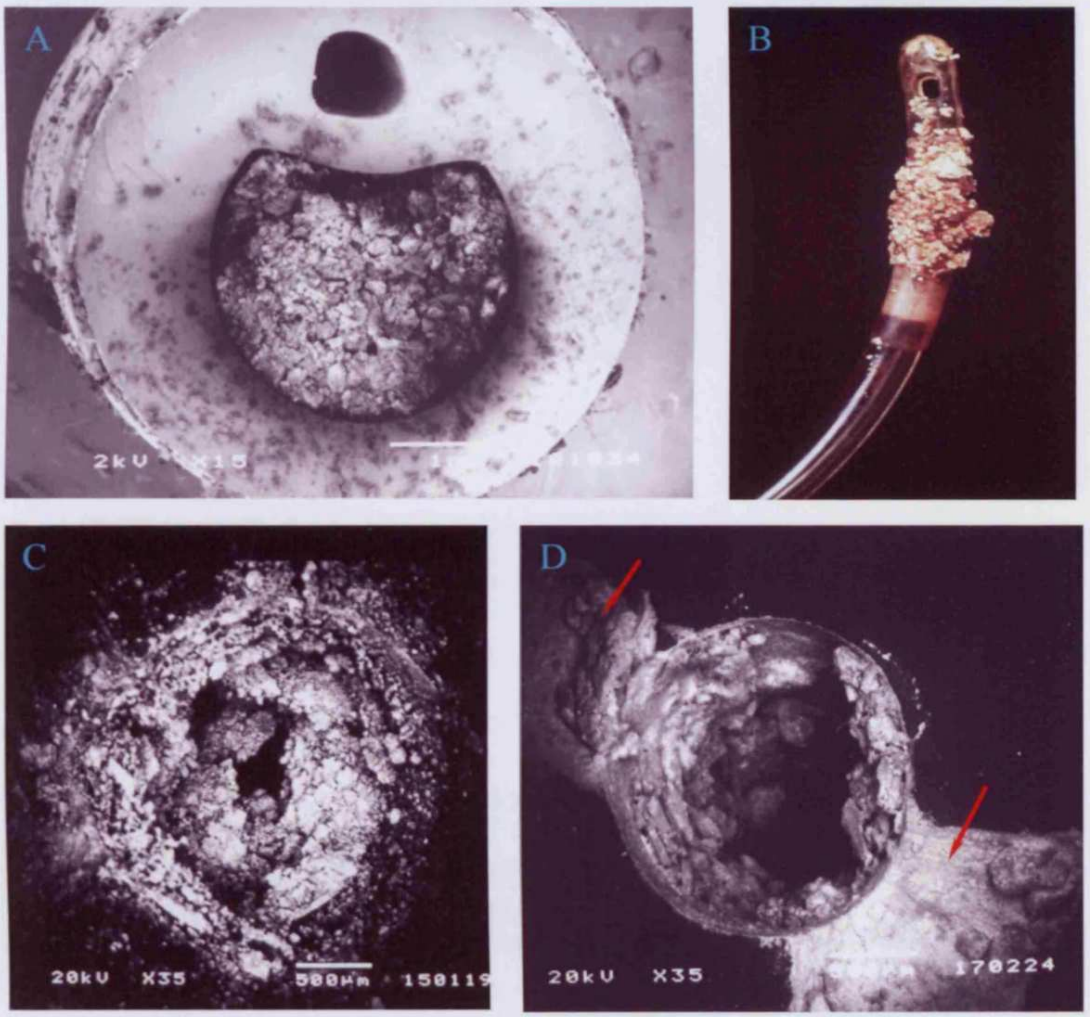

Images **A** and **B** were produced by Dr. D. J. Stickler. Image **C** was produced by Dr. N. Sabbuba. Image **D** was generated during this study.

Figure 1.7: Morphology of crystalline deposits on the surface of urethral catheters.

The scanning electron micrographs below illustrate the morphologies of the crystalline material formed on the surface of urethral catheters. Struvite crystals appear are large regular coffin shaped crystals (**A**) while the poorly crystalline material hydroxyapatite manifests as amorphous deposits (**B**). Bar = 100μm. Images were produced during this study.

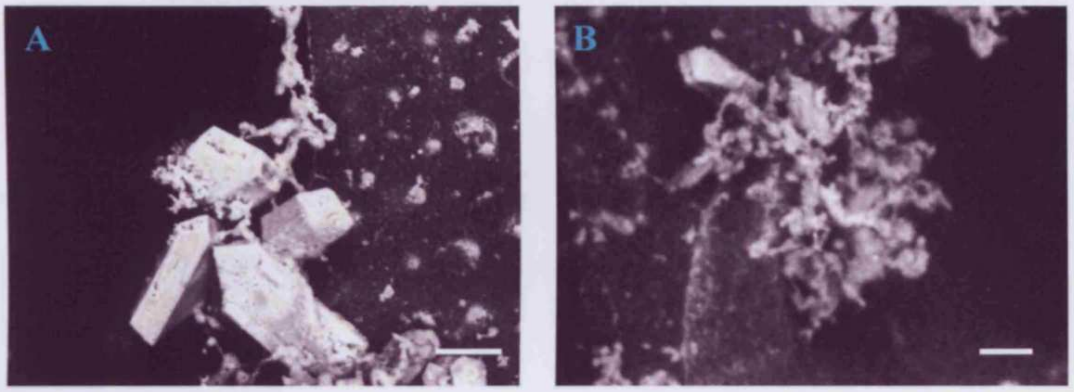

Despite the diversity of urease positive species associated with catheter blockage, studies have revealed that the predominant cause of catheter blockage is infection with *P. mirabilis* (Mobley & Warren 1987; Kunin 1989; Stickler *et al.* 1993; Stickler *et al.* 1998b). A study by Mobley & Warren (1987), in which weekly urine samples were taken from 32 long-term catheterised patients over the course of a year, found that the most commonly isolated urease producing species was *P. mirabilis,* which was significantly associated with the 67 blockages observed during the study. Kunin (1989) attempted to identify patients susceptible to catheter blockage but found no significant difference between "blockers", and "non-blockers" in terms of age, daily activities, mental status, or constituents of the urine which included protein, sodium, potassium, chloride, uric acid, calcium, and oxalate. However "blockers" were found to produce a more alkaline urine containing less urea, and were more frequently colonised by *P. mirabilis*.

Stickler *et al.* (1998b), investigated the role of other urease producing species in catheter blockage using an *in vitro* model of the catheterised urinary tract. Of the species tested (*P. mirabilis, P. vulgaris, K. pnuemoniae, E. coli, Ps. aeruginosa, Providencia stuartii,* and *Providencia rettgeri*), only *P. mirabilis, P. vulgaris*, and *Pv. rettgeri* were capable of causing blockage. However, since *P. mirabilis* is the most commonly isolated organism from blocked catheters, it was considered to be the predominant organism in crystalline biofilm formation and catheter blockage (Mobley & Warren 1987; Kunin 1989; Stickler *et al.* 1993; Stickler *et al.* 1998b).

Catheter colonisation and biofilm formation by *P. mirabilis* seems to begin with crystal growth (McLean *et al.* 1991), presumably driven by urease production from planktonic bacteria in urine of the catheter lumen or bladder. These crystals attach to catheter surfaces and facilitate colonisation by providing a surface to which planktonic bacteria can readily adhere and go on to establish biofilms (McLean *et al.* 1991; Morris *et al.* 1997). The developed biofilm itself can then become a highly alkaline microenvironment, which incubates growing crystals and may provide a buffering function against changes in the urine pH (McLean *et al.* 1991). The growth of crystals within the biofilm is enhanced and stabilised by the exopolysaccharide matrix of *P. mirabilis* biofilms, which is capable of binding magnesium and calcium ions (Clapham *et al.* 1990; Dumanski *et al.* 1994). Crystals suspended in the urine may also become trapped within the biofilm and incorporated into its structure.

Stickler (1996b) outlined the main factors influencing catheter encrustation: 1) Infection of the catheterised urinary tract by a urease producing species, primarily *P. mirabilis*; 2) Development of an organic conditioning film on the catheter surface; 3) Colonisation of the catheter by the urease producing species and subsequent biofilm

formation; 4) Elevation of the pH in the polysaccharide biofilm matrix through the hydrolysis of urea by urease; 5) attraction and binding of magnesium and calcium ions by the polysaccharide matrix, and 6) Gel stabilised crystal growth and formation of a crystalline biofilm structure.

1.6 Prevention of catheter associated UTI and catheter blockage

The complications induced by C-UTI have led to the development of a variety of methods for their control, which generally seek to prevent the acquisition of infection rather than treat retrospectively. The most effective strategy for preventing these infections is not to use the indwelling urethral catheter unless absolutely necessary (Warren 1991; Warren 1996). Where catheterisation is unavoidable the duration for which the patient is catheterised should be kept to a minimum, and care taken to maintain the integrity of the closed drainage system (Warren 1991). Handling and fitting catheters aseptically is also an important technique in prevention of C-UTI.

In patients undergoing short-term catheterisation the main weapon against these infections is proper maintenance of the closed drainage system, and strict hygiene procedures (Warren 1991). Unnecessary breaks in the closed drainage system should be avoided as this can greatly increase the incidence of bacteriuria. This was illustrated by Platt *et al.* (1983) who undertook a clinical trial to evaluate the effect of drainage bag disconnection on the frequency of C-UTI in hospital patients undergoing short-term catheterisation. The results indicated that among patients whose drainage bags were disconnected less frequently rates of infection and mortality were significantly lower.

1.6.1 Use of antimicrobial agents in closed drainage system and meatal cleansing

In order to cause C-UTI infecting organisms must first gain entry to the catheterised urinary tract. Methods to prevent this include the use of lubricating gels containing biocides such as chlorhexidine, or the direct instillation of antiseptics and antibiotics into the urethra (Stickler 1996a,b; Stickler 2002). Many studies have indicated that

bacteria may access the catheterised urinary tract at the junction between the exposed catheter and urethral meatus. Attempts to prevent organisms colonising this area from gaining entry include the use of intensive cleansing regimes, often with solutions of antimicrobial compounds such as chlorhexidine, and povidine-iodine (Burke *et al.* 1981; Southampton Infection Control Team 1982; Burke *et al.* 1983). Similar compounds have also been used to directly irrigate the bladder (Saint & Lipsky 1999). However, such strategies have been found to have little or no benefit in the prevention of C-UTI, and may potentially irritate the bladder or meatal area (Burke *et al.* 1981; Burke *et al.* 1983; Saint & Lipsky 1999).

The addition of biocides to the drainage bags of catheterised patients has also been used in an attempt to reduce the reservoirs of potential infection causing organisms that can accumulate here (Southampton Infection Control Team 1982). The relatively low frequency of the drainage bag as a source of infection means this method is of limited use in preventing C-UTI (Stamm 1991), but may in fact create additional problems by selecting for organisms, such as *P. mirabilis* (Stickler & Chawla 1987). Evaluation of the addition of chlorhexidine to the drainage bags of catheterised patients have shown no significant advantage to this practice (Gillespie *et al.* 1983), and has in at least one instance resulted in the emergence of chlorhexidine, and multi-drug resistant *P. mirabilis* as the dominant organism (Southampton Infection Control Team 1983).

An alternative way to deliver antimicrobial agents directly into the bladder was suggested by Bibby *et al.* (1995), who filled the retention balloon of Foley catheters with solutions containing antimicrobial compounds. Using an *in vitro* model

mandelic acid was shown to diffuse out into the medium when used to inflate the balloons. Recently Stickler *et al.* (2003) reported that inflating the balloons of all-silicone catheters with solutions of the biocide triclosan allowed catheters to drain freely for over seven days, when used in an *in vitro* model of the catheterised urinary tract infected with *P. mirabilis*.

1.6.2 Modification of the catheter surface

Another commonly employed tactic has been to alter the surface properties of the catheters to inhibit colonisation of the catheter surface. Catheters with surface coatings containing antimicrobial agents such as silver, or hydrophilic hydrogels have been used in attempts to prevent bacterial colonisation (Stickler 2002; Stamm 1991). Such strategies have become particularly relevant in the prevention of biofilm formation on the catheter surface.

It is unclear what contribution many of these devices may make to the prevention of C-UTI and catheter encrustation. Catheters containing antibiotics such as gentamicin and nitrofurazone have recently become available (Stickler 2002). It is possible that these types of catheter may be useful in inhibiting C-UTI over short periods but in long-term patients they may simply select for resistant organisms, such as the intrinsically nitrofurazone resistant *Ps. aeruginosa* and *P. mirabilis* (Stickler 2002). This is especially worrying in the case of front line antibiotics such a gentamicin. The use of such drugs will expose the highly complex microbial flora of the catheterised urinary tract to a steady selective pressure.

Catheters impregnated with silver have been claimed to be useful in the prevention of C-UTI (Lundberg 1986; Liedberg & Lundberg 1990). Liedberg & Lundberg (1990) found that catheters coated with silver alloy significantly reduced C-UTI after surgery compared to teflon-coated latex catheters. In contrast a larger study by Johnson *et al.* (1990) demonstrated little difference between rates of bacteriuria in patients fitted with silver-coated catheters and those fitted with standard catheters.

Although silver containing, and hydrogel-coated catheters are commercially produced and routinely used they appear to have little ability to prevent C-UTI or catheter encrustation (Morris *et al.* 1997; Darouchie 1999). Morris *et al.* (1997) evaluated the ability of 18 different types of catheter to resist encrustation by *P. mirabilis* using an *in vitro* model of the catheterised urinary tract. All types of catheter were found to be vulnerable to encrustation and blockage, with latex-based catheters blocking significantly faster than silicone devices (Morris *et al.* 1997). Other studies have indicated that hydrogel-coatings facilitate the migration of many organisms over catheter surfaces (Stickler & Hughes 1999; Sabbuba *et al.* 2002). Therefore, such coatings may enhance the ability of some species to migrate from the urethral meatus, along the catheter surface to the bladder and initiate bacteriuria.

1.6.3 Modulation of urinary pH

Control of catheter encrustation has also been attempted indirectly by methods which aim to maintain low urinary pH or inhibit the action of the urease enzyme (Stickler 1996b). Bladder washouts with acidifying agents or the lowering of urinary pH through dietary supplements (for example by the oral administration of ascorbic acid) have been used to control catheter blockage with little success (Stickler 1996b). Flow

cell studies of *P. mirabilis* biofilm development and crystal formation in artificial urine showed that acidification of the urine allowed dissolution of crystals in suspension but those trapped within the biofilm matrix were not dissolved (McLean *et al.* 1991). Urease inhibitors such as acetohydroxamic acid and flurofamide have been found to effectively reduce the pH of urine during *in vitro* experiments (Griffith *et al.* 1978), and inhibited stone formation when assessed in a controlled clinical trial (Williams *et al.* 1984). However the toxicity of these molecules prevents their oral administration and greatly limits their usefulness.

1.7 Virulence attributes of *Proteus mirabilis*

P. mirabilis is a Gram-negative, motile bacillus belonging to the family *Enterobacteriaceae*, and is closely related to *E. coli* and *Salmonella typhimurium* (Cowan & Steele 1993; Belas 1996). It is an opportunistic pathogen that primarily initiates infection in the complicated urinary tract. Individuals vulnerable to this organism include catheterised patients and those with structural abnormalities of the urinary tract (Mobley & Warren 1987; Warren 1996). *P. mirabilis* possesses a range of virulence attributes which are important in the pathogenesis of C-UTI (Mobley 1996; Coker *et al.* 2000).

Fortunately this organism is generally sensitive to the antibiotics commonly used to treat UTI, including ampicillin, gentamicin, chloramphenicol, and carbenicillin (Mobley 1996). However, it does have an intrinsic resistance to tetracycline and nitrofurazone (Mobley 1996; Stickler 2002). Recently isolates carrying a chromosomally encoded resistance to ampicillin have been reported (Bret *et al.* 1998).

1.7.1 Flagella, swimming and swarming

P. mirabilis expresses numerous flagella and displays two forms of flagella mediated motility: swimming in liquid media and swarming over solid surfaces. However, the role in virulence of flagella themselves or of either form of motility is unclear. Swimming motility or flagella themselves may be involved in the initial attachment of *P. mirabilis* to a surface, as has been implicated in other organisms (Pratt & Kolter 1998; O'Toole & Kolter 1998b; Pratt & Kolter 1999). It has been suggested that swarming may play a role in the colonisation of the urinary tract (Stickler & Hughes 1999; Belas 1996). Studies of mutants unable to generate flagella revealed that these

were reduced in virulence when tested in a murine model of urinary tract infection, but it was uncertain whether the lack of flagella themselves or the non-swimming, non-swarming phenotype of these mutants was responsible (Mobley 1996).

Mice infected with mutants specifically defective in swarming also showed a reduction in mortality, indicating that swarming is involved in the pathogenesis of these infections (Allison *et al.* 1994). In addition, swarming has been linked with an increased expression of virulence factors including urease and haemolysin. Invasion of kidney epithelial cells by *P. mirabilis* has been suggested to be accomplished primarily by swarmer cells rather than swimmer cells (Allison *et al.* 1992).

It has also been suggested that the ability of *P. mirabilis* to swarm rapidly over solid surfaces may play a role in the pathogenicity of this species in the catheterised urinary tract (Belas 1996; Stickler & Hughes 1999; Sabbuba *et al.* 2002). *P. mirabilis* is capable of migrating over several commonly used types of catheter, including those impregnated with silver (Stickler & Hughes 1999; Sabbuba *et al.* 2002). Stickler & Hughes (1999) suggested that swarming by *P. mirabilis* may allow the migration of this organism from the urethral meatus, along the surface of the catheter into the bladder. However, *P. mirabilis* has also been shown to be capable of migrating over the surfaces of catheters coated with hydrogels under conditions that inhibit swarming (Sabbuba *et al.* 2002). Therefore, it is likely that under certain conditions swimming motility may also be involved in colonisation of the catheterised urinary tract by this organism.

In contrast, some studies appear to indicate that swarming does not play a role in the pathogenesis of *P. mirabilis* UTI (Zunino *et al.* 1994; Legnani-Fajardo *et al.* 1996;

Jansen *et al.* 2003). A study in which the frequency of swarmer cells was assessed during experimental UTI in mice found that the predominant morphotype was the short swimmer cell (Jansen *et al.* 2003), while studies using non-swimming, non-swarming mutants of *P. mirabilis,* found these showed no reduction in ability to cause ascending UTI in mice (Legnani-Fajardo *et al.* 1996). In addition, a naturally occurring non-motile mutant of *P. mirabilis* has been reported to have been isolated from a patient suffering symptomatic UTI (Zunino *et al.* 1994). However, such studies do not consider the presence of a urinary catheter, and the potential role of swarming in the early stages of infection.

1.7.2 Urease

Production of urease is highly significant in blockage of urethral catheters and formation of infection stones by *P. mirabilis*. As discussed previously the hydrolysis of urea by the urease enzyme drives mineralisation of the biofilm leading to catheter blockage, and the formation of infection stones (Stickler *et al.* 1993; Mobley 1996; Stickler *et al.* 1998b). Several studies have also indicated that this enzyme is important for the colonisation of the kidney and induction of pyelonephritis (Mobley 1996; Johnson *et al.* 1993).

The *P. mirabilis* urease enzyme is a ~250 kDa cytoplasmic nickel-metalloenzyme, that it is expressed constitutively. However, the presence of urea can induce levels up to 25-fold greater than the normal basal level of expression (Mobley *et al.* 1995). Urea is thought to diffuse across the bacterial membrane where it increases urease expression and is hydrolysed. The ammonia generated then diffuses back out of the cell and elevates urinary pH (Mobley 1996).

The urease of *P. mirabilis* has been reported to be highly active, hydrolysing urea 6 – 10 times faster than that of other commonly isolated urease producing pathogens of the catheterised urinary tract (Mobley & Warren 1987). In addition, the positive, urea induced regulation of the *P. mirabilis* urease enzyme also appears important for its ability to encrust urinary catheters (Stickler *et al.* 1998b). The urease expression of other urinary tract pathogens may be induced by conditions which are not encountered in the urinary tract. For example, urease expression in *K. pneumoniae* is induced by nitrogen starvation which is unlikely to occur in the urinary tract (Mobley *et al.* 1995).

1.7.3 Pili and fimbriae

Adhesion to the catheter surface and urethral epithelium are thought to be of major importance in the initiation of C-UTI. *P. mirabilis* is known to express four distinct fimbriae: mannose-resistant *Proteus*-like (MR/P), *P. mirabilis* fimbriae (PMF), ambient-temperature fimbriae (ATF), and non-agglutinating fimbriae (NAF) (Mobley 1996). Of these structures the MR/P fimbriae has so far been the most strongly associated with virulence in *P. mirabilis*. Studies with mutants deficient in MR/P production have been found to be reduced in ability to colonise both the upper and lower urinary tract, and initiate pyelonephritis (Bahirani *et al.* 1994; Zunino *et al.* 2001). However, the role for these fimbriae in the colonisation of the catheterised urinary tract is unclear, but some similar structures in other pathogenic bacteria have been found to mediate attachment to abiotic surfaces (Pratt & Kolter 1999; Watnick *et al.* 1999).

1.7.4 Haemolysin, amino acid deaminase, and the polysaccharide capsule

Other virulence determinants of *P. mirabilis* include a haemolysin, amino acid deaminase, and potentially the bacterial polysaccharide capsule (Dumanski *et al.* 1994; Mobley 1996; Coker *et al.* 2000). Haemolysin has been suggested to be responsible for the tissue damage that *P. mirabilis* can cause, particularly during pyelonephritis where it is thought to facilitate the invasion of kidney epithelial cells (Coker *et al.* 2002). The role of the amino acid deaminase expressed by *P. mirabilis* is unclear, but it has been suggested that the urinary tract may be an iron limited environment, and that products of these enzymes constitute a novel iron acquisition system (Mobley 1996). The capsule of *P. mirabilis* may also be a potential virulence factor as it has been show to enhance the growth of crystals, encrustation, and blockage of catheters (Dumanski *et al.* 1994).

1.7.5 Metalloprotease and evasion of the host immune system

The metalloprotease ZapA is secreted by the majority of *P. mirabilis* isolates and as with other virulence factors its expression is co-ordinated with swarm cell differentiation (Mobley 1996; Walker *et al.* 1999). The ability of this enzyme to degrade human IgA and IgG antibodies has lead to the suggestion that ZapA helps *P. mirabilis* evade the host immune response (Walker *et al.* 1999). Studies have indicated that mutants unable to generate ZapA are attenuated in a mouse model of ascending UTI, and that ZapA may be part of a family of at least five proteins concerned with evasion of the host immune response (Walker *et al.* 1999).

In addition to the active degradation of antibodies by proteases such as ZapA, variation of antigenic surface structures is also thought to play a role in the evasion of host immune responses by *P. mirabilis* (Walker *et al.* 1999). One set of highly

antigenic surface structures involved in this process are the flagella filaments. *P. mirabilis* possesses three distinct copies of the gene encoding the main flagella subunit protein (flagellin), *flaA*, *flaB* and *flaC* (Belas 1994; Murphy & Belas 1999). Of these genes *flaA* is the main flagellin producing gene, while *flaB* and *flaC* are normally silent (Belas 1994). The fusion of the contiguous flagellin genes *flaA* and *flaB* to generate an antigenically distinct flagellin protein has been characterised, and suggested to play a role in antigenic variation of flagella and evasion of the immune system during infection (Murphy & Belas 1999). In addition to flagella the natural phase variable expression of surface structures such as the MR/P fimbriae are also thought to be involved in this aspect of *P. mirabilis* virulence (Bahirani *et al.* 1994).

1.8 Swarming by *Proteus mirabilis*

Swarming in *P. mirabilis* is a cyclic, multicellular behaviour, allowing rapid migration of cells over solid surfaces. It occurs in at least three distinct phases: 1) differentiation of swimmer cells to swarmer cells; 2) migration of swarmer cells over the surface and 3) consolidation. Initially swimmer cells that come into contact with a solid surface are induced to differentiate into swarmer cells. In liquid culture *P. mirabilis* exists as 1-2μm rods with up to 30 peritrichous flagella, but on contact with a solid surface it rapidly differentiates to form hyperflagellated, elongated, multi-nucleate, swarmer cells (Belas 1996; Fraser *et al.* 2000). Swarmer cells may be >80μm in length and possess 10^3 to 10^4 flagella per cell (Belas 1996).

Once fully differentiated, swarmer cells align along the edge of the colony to form multicelluar rafts which migrate over the surface away from the main colony. Migration is the result of co-ordinated multicellular behaviour by these groups of swarmer cells, and single swarmer cells are unable to swarm (Henrichsen 1972; Belas 1996). After migration has ceased swarmer cells begin to dedifferentiate and revert to vegetative cells. It is the cessation of migration and the reversion of swarmer cells to swimmer cells that constitutes the final phase of swarming, and is referred to as consolidation (Allison & Hughes 1991; Belas 1996). After the consolidation phase, the process begins again, and it is these successive periods of differentiation, migration and consolidation which leads to the terraced appearance of *P. mirabilis* colonies on agar plates. Figure 1.8 illustrates the temporal control of the *P. mirabilis* swarm cycle and the distinct phases involved in swarming.

Figure 1.8: Temporal control of the *P. mirabilis* swarm cycle.
Illustration of the temporal control of the *P. mirabilis* swarm cycle. In response to environmental stimuli swimmer cells are induced to differentiate into swarmer cells. Swarmer cells align to form multicellular rafts which migrate over the surface before consolidating and reverting to swimmer cells. This process is then repeated starting with differentiation. (Modified from Belas 1996).

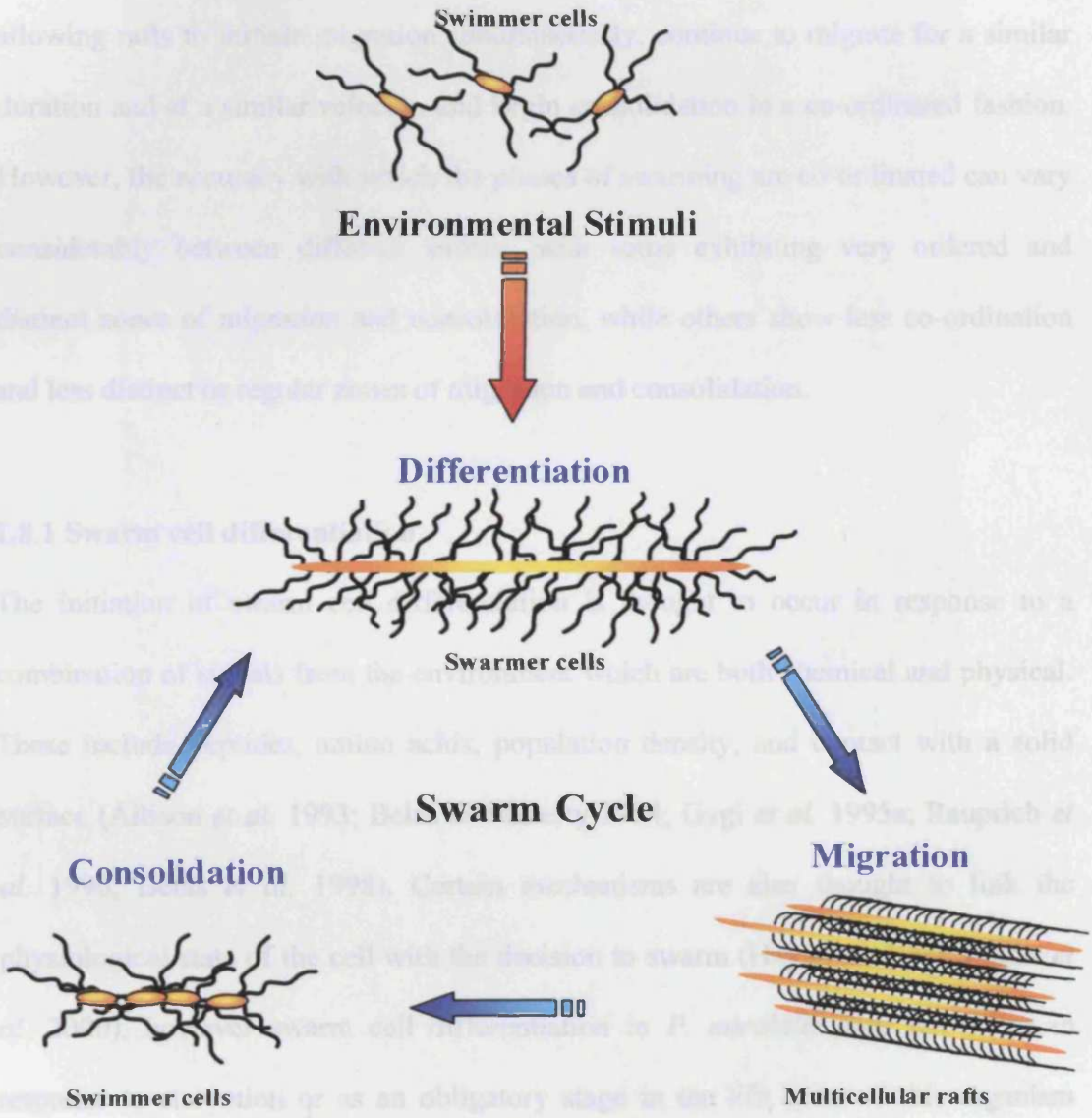

The events that comprise the *P. mirabilis* swarm cycle are tightly controlled requiring intercellular communication and co-ordinate expression of many genes (Belas 1996). This is reflected by the highly organised nature of the resulting *P. mirabilis* swarm, as regular zones of migration and consolidation (Figure 1.9). This also highlights the importance of intercellular communication during swarming, allowing rafts to initiate migration simultaneously, continue to migrate for a similar duration and at a similar velocity, and begin consolidation in a co-ordinated fashion. However, the accuracy with which the phases of swarming are co-ordinated can vary considerably between different strains, with some exhibiting very ordered and distinct zones of migration and consolidation, while others show less co-ordination and less distinct or regular zones of migration and consolidation.

1.8.1 Swarm cell differentiation

The initiation of swarm cell differentiation is thought to occur in response to a combination of signals from the environment which are both chemical and physical. These include peptides, amino acids, population density, and contact with a solid surface (Allison *et al.* 1993; Belas & Flaherty 1994; Gygi *et al.* 1995a; Rauprich *et al.* 1996; Belas *et al.* 1998). Certain mechanisms are also thought to link the physiological state of the cell with the decision to swarm (Hay *et al.* 1997; Fraser *et al.* 2000), however swarm cell differentiation in *P. mirabilis* does not occur in response to starvation or as an obligatory stage in the life cycle of this organism (Rauprich *et al.* 1996). Figure 1.10 depicts a swimmer cell and a swarmer cell, and lists some of the stimuli that may induce this transformation.

Figure 1.9: *P. mirabilis* swarming over agar surface.
An example of *P. mirabilis* swarming illustrating the terraced appearance of *P. mirabilis* colonies generated by the successive phases of differentiation, migration, and consolidation. The highly regular appearance of the migration and consolidation zones shows the highly organised nature of *P. mirabilis* swarming, and highlights the importance of intercellular communication. Image produced by B. V. Jones.

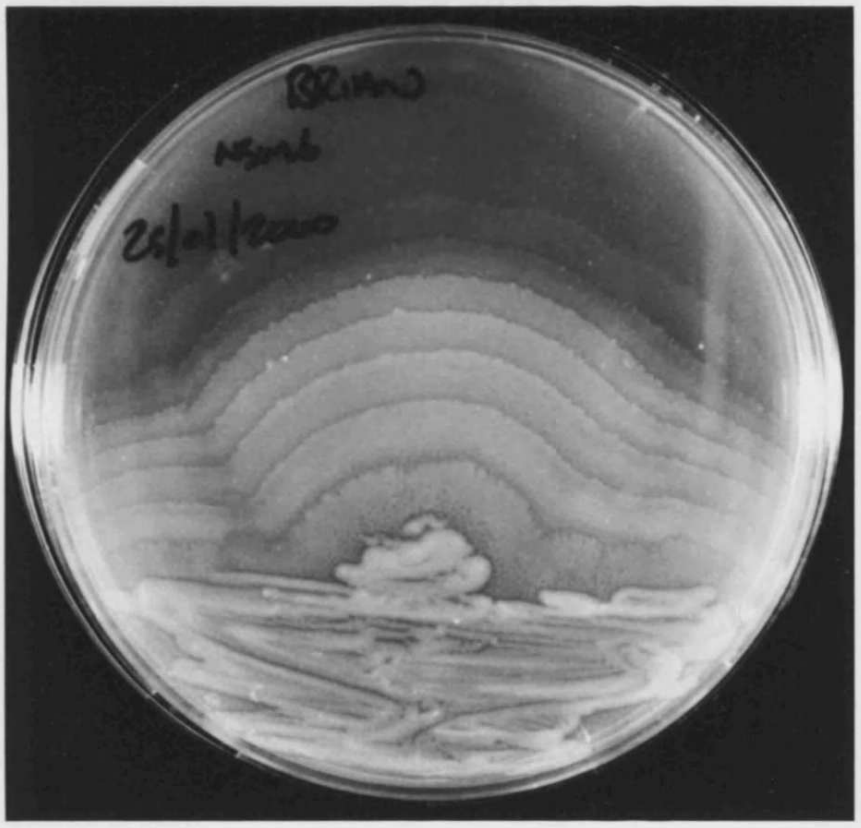

Figure 1.10: An example of a *P. mirabilis* swimmer cell and swarmer cell, and summary of the possible stimuli that may induce differentiation. **(Modified from Belas 1996).**

Images are negatively stained transmission electron micrographs of a *P. mirabilis* swimmer cell and part of a swarmer cell. Bar = 1μm. The text summarises known and potential stimuli that trigger differentiation, and the mechanisms by which these stimuli may be sensed or monitored. Images produced during this study.

Swimmer cell

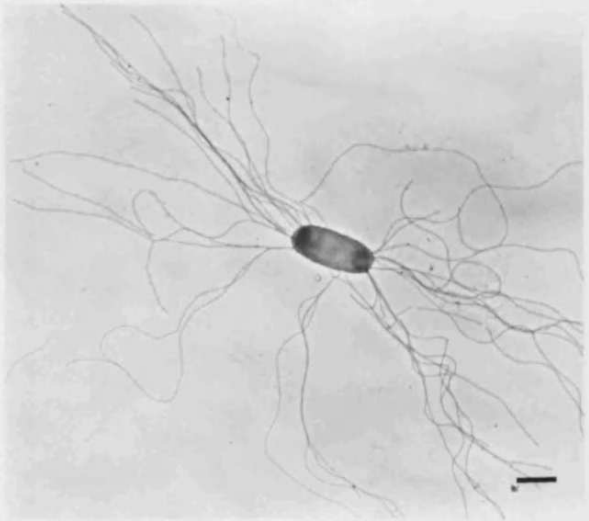

Stimuli that trigger differentiation

Swarmer cell

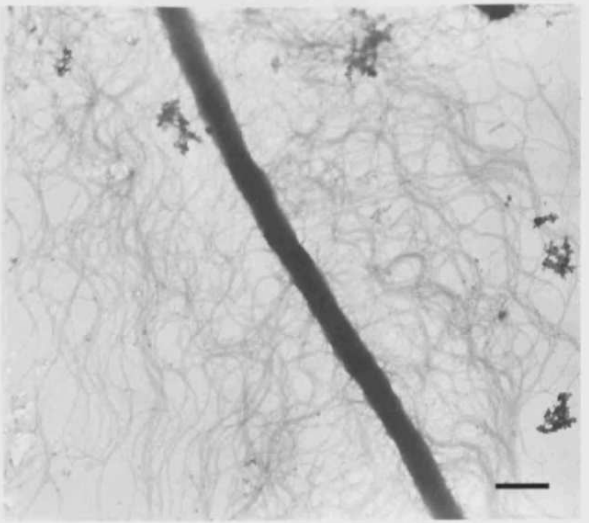

Contact with solid surface – Inhibition of flagella rotation
Population density – Quorum sensing, accumulation of toxic metabolites
Physiological status of the cell – Monitored by Lrp, other mechanisms
Other signals – Glutamine, peptides, others?

Allison *et al.* (1993) showed that the amino acid glutamine, was capable of initiating swarmer cell differentiation in *P. mirabilis* when incorporated into minimal media that did not support swarming. Glutamine analogues were able to block this effect highlighting the specificity of this signal. Furthermore swarmer cells were also found to exhibit a chemotactic attraction to glutamine, but this was not observed in swimmer cells, suggesting that this amino acid may not only induce swarming but also determine the direction of migration (Allison *et al.* 1993; Belas 1996). It has been postulated that the glutamine signal may be generated through the action of the *P. mirabilis* broad spectrum protease (Allison *et al.* 1992; Fraser *et al.* 2000).

This also raises the possibility that the glutamine signal may link swarming to pathogenesis. Invasion of kidney epithelial cells by *P. mirabilis* has been found to be carried out primarily by swarmer cells (Allison *et al.* 1993). Therefore, the degradation of host proteins may liberate glutamine or glutamine-containing peptides which initiate swarm cell differentiation, and promote invasion by directing swarming to sites of tissue damage.

Population density is also an important factor influencing the differentiation of *P. mirabilis* (Rauprich *et al.* 1996; Belas *et al.* 1998). The duration of the lag phase preceding the initiation of swarming has been shown to be dependent on the number of cells in the inoculum (Rauprich *et al.* 1996). The mechanism by which *P. mirabilis* determines population density has not been elucidated but several have been proposed. Lominski & Lendrum (1947) suggested that swarming may be linked to the build up of toxic metabolites that increase with population density, and the migration of *P. mirabilis* away from the colony reflected a negative chemotactic response to this. It was implied that accumulation of these toxic end products of

metabolism were also responsible for initiating swarm cell differentiation. However, a candidate molecule has yet to be identified and demonstrated to elicit this response (Belas 1996).

An alternative mechanism is that population density is monitored through a quorum sensing system (Fraser *et al.* 2000; Belas *et al.* 1998). This system relies on the synthesis of extra-cellular signal molecules, such as N-acyl homoserine lactones (AHLs). At certain threshold concentrations these can alter the transcription of target genes, thereby regulating a process in a cell density dependant manner (Bassler 1999). Therefore, quorum sensing could link the decision to initiate differentiation and swarming to the density of the population. This strategy has been characterised in other swarming bacteria, such as *Serratia liquefaciens* where AHLs have been shown to control the production of components important for swarming (Lindum *et al.* 1998). AHL production along with homologues of quorum sensing machinery for the Lux system have been identified in *P. mirabilis* (Schneider *et al.* 2002). Despite this they do not appear to play a role in differentiation or swarming (Fraser *et al.* 2000; Schneider *et al.* 2002). However, several distinct quorum sensing systems or languages have been characterised in Gram-negative bacteria (Bassler 1999), and their involvement in swarming has not been precluded.

Contact with a solid surface is a major trigger for swarm cell differentiation, and is perhaps the most extensively studied signal. The mechanism by which *P. mirabilis* senses contact with a solid surface is thought to be through the inhibition of flagella rotation, and there is much evidence to support this theory (Belas & Flaherty 1994; Belas 1994; Belas *et al.* 1995; Gygi *et al.* 1995a; Belas 1996; Fraser *et al.* 2000). Transfer to solid media, media of high viscosity, or tethering of flagella with

antibodies all inhibit normal flagella rotation and induce swarm cell differentiation (Belas 1994; Belas 1996). The flagella of swimmer cells are thought to function as tactile sensors, transducing signals regarding the viscosity of the surrounding medium into the cell, and thereby linking the expression of genes controlling swarm cell differentiation to the environmental conditions.

Further evidence supporting this concept has come from studies of defined mutants defective in aspects of flagella biosynthesis (Belas & Flaherty 1994; Belas *et al.* 1991a,b; Belas *et al.* 1995; Gygi *et al.* 1995a; Belas *et al.* 1996). Belas *et al.* (1991a,b) isolated numerous mini-Tn*5* mutants of *P. mirabilis* defective in swarming, and phenotypic analysis revealed that many unable to differentiate, possessed defects in flagella biosynthesis. Mutations in the *P. mirabilis* flagellin gene *flaA,* and other flagella assembly genes that disrupt the production of functional flagella have been associated with an inability to differentiate in *P. mirabilis* (Belas & Flaherty 1994; Belas *et al.* 1995; Gygi *et al.* 1995a; Gygi *et al.* 1997). Belas *et al.* 1995 investigated the genetic basis of defects in swarm cell differentiation among a group of transposon mutants defective in this aspect of swarming. Their study revealed that in a large number of these mutants the transposon had disrupted either structural or regulatory flagella biosynthesis genes, impairing flagella production.

In addition to controlling flagella biosynthesis the flagella master operon, *flhDC* is also thought to mediate the integration of various signals, and control several other aspects of differentiation, such as cell elongation and expression of virulence factors (Fraser *et al.* 2000; Fraser & Hughes 1999). Several signals that influence the decision to initiate swarm cell differentiation are thought to affect expression of the *flhDC* operon, including those that concern the cells' external environment (viscosity

of the media, population density etc.), and indicators of the physiological status of the cell (Belas & Flaherty 1994; Gygi *et al.* 1995a; Hay *et al.* 1997; Gygi *et al.* 1997; Dufour *et al.* 1998; Belas *et al.* 1998). These data reinforce the idea of flagella as vital structures in *P. mirabilis* swarm cell differentiation.

The mechanisms that link the physiological state of the cell with initiation of differentiation are not well understood, but the global transcriptional regulator, leucine responsive protein (Lrp) has been implicated (Hay *et al.* 1997). Mutants with disruptions in the *lrp* gene are capable of swimming motility but are unable to differentiate and swarm (Hay *et al.* 1997). Lrp is also known to be responsive to a variety of metabolites including amino acids, and is expressed at a higher level in differentiated swarmer cells compared to swimmer cells (Calvo & Matthews 1994; Fraser *et al.* 2000). Furthermore, Lrp has been shown to upregulate transcription of the flagella master operon *flhDC*, and artificial induction of *flhDC* transcription in *P. mirabilis lrp*$^-$ mutants results in hyperflagellation (Fraser *et al.* 2000). This indicates that Lrp may directly regulate flagella biosynthesis and other genes associated with swarm cell differentiation (Fraser *et al.* 2000).

Genes involved in synthesis of the cell wall peptidoglycan, and lipopolysaccharide (LPS) are also thought to be important for differentiation of swarmer cells. In the case of LPS several *P. mirabilis* mutants defective in LPS synthesis have been isolated and found to also lack the ability to differentiate (Belas 1996).

1.8.2 Multicellular migration and consolidation

As mentioned above swarming in *P. mirabilis* is a multicellular behaviour, and migration is mediated by organised groups of swarmer cells referred to as "rafts"

which move over the surface as a single unit. Figure 1.11 provides an example of a *P. mirabilis* multicellular raft. Several factors have been identified which are important for the migration of *P. mirabilis* rafts, including the synthesis of extracellular polysaccharides, LPS synthesis, and cellular alignment (Gygi *et al.* 1995b; Belas *et al.* 1995; Hay *et al.* 1999). The signals and mechanisms responsible for initiating migration, and controlling the duration and velocity are still unclear, although several have been proposed including glutamine (Lominski & Lendrum 1947; Williams *et al.* 1976; Williams & Schwarzhoff 1978; Belas *et al.* 1991b; Belas 1996; Fraser *et al.* 2000).

Initiation of migration, like differentiation, is related to population density (Rauprich *et al.* 1996), and subsequent consolidation may also be regulated by similar mechanisms (Lominski & Lendrum 1947; Belas *et al.* 1991b; Belas 1996). For example, the accumulation of toxic waste products in the colony may trigger migration when threshold levels are reached (Lominski & Lendrum 1947). In this scenario the concentration of these molecules decreases with distance from the centre of the colony. As rafts migrate away from the colony the concentration of these molecules decreases and no longer present a stimulus for migration. At this point cells cease swarming and initiate consolidation (Lominski & Lendrum 1947).

The duration of migration in *P. mirabilis* has also been attributed to the depletion of a stored energy source which is utilised by swarmer cells (Williams & Schwarzhoff 1978). Once swarming migration has been initiated swarmer cells do not require an

Figure 1.11: Example of a multicellular raft of swarmer cells.
Phase contrast micrograph of a multicellular raft of *P. mirabilis* swarmer cells migrating over LB agar. Image produced during this study.

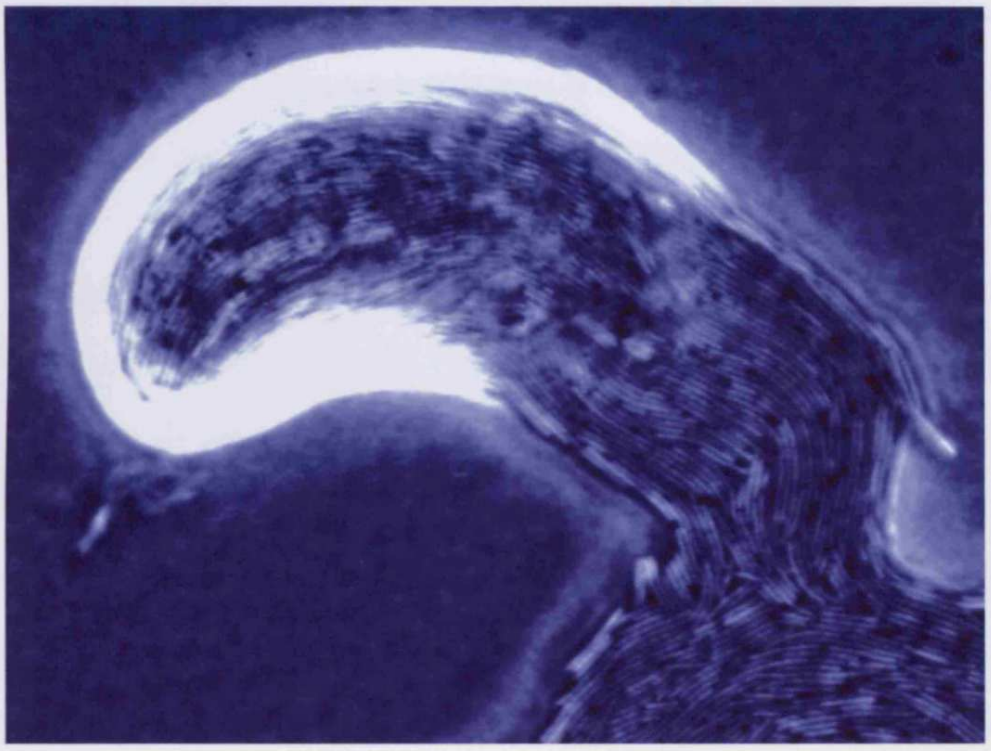

external energy source, and it has been suggested that they generate the energy necessary for swarming through the fermentation of a stored energy source (Williams *et al.* 1976; Williams & Schwarzhoff 1978). It has been proposed that the periodicity of migration and consolidation is a consequence of the depletion of this energy source, which triggers consolidation in order to replenish reserves of this fuel before swarming can continue (Williams & Schwarzhoff 1978).

It has also been suggested that the initiation of migration, its duration, and the subsequent onset of consolidation are genetically determined (Belas *et al.* 1991b; Belas 1996). These events may be controlled by a quorum sensing or similar system through specific extra cellular signal molecules which are synthesised and destroyed in a cyclic manner to stimulate periods of migration and consolidation (Belas 1996). Mutants that display enhanced swarming behaviour have been characterised and the disrupted genes found to be homologous to a membrane sensor histidine kinase, which indicates that this gene may function as a sensor of external environmental conditions (Belas *et al.* 1998).

This gene was designated *rsbA* for regulator of swarming behaviour, and it was proposed that the enhanced swarming phenotype of this mutant resulted from the production of a truncated protein (rather than a nonsense mutation) that removed the negative regulation that this gene imposed upon migration. However, while the control of migration by a quorum sensing type system seems likely, the signal molecules and associated apparatus have yet to be identified and demonstrated to control multicellular migration in *P. mirabilis*.

Migration has also been suggested to be controlled solely by the population dynamics within the *P. mirabilis* colony using a mathematical model of *P. mirabilis* swarming, in which migration and consolidation are dependant on the age of swarm cells and the density of the population (Esipov & Shapiro 1998). In this model there is a minimum age at which swarm cells may initiate migration, and the model also assumes that a minimum number of capable swarmer cells must be present before migration begins. There is also a maximum age for swarmer cells and when this is reached cells cease migration and initiate consolidation.

Other factors have been identified which directly affect the ability of *P. mirabilis* swarmer cells to move over solid surfaces. Gygi *et al.* (1995b) demonstrated the importance of the abundant polysaccharide matrix through which *P. mirabilis* swarmer cells migrate. Mutants defective in the production of this polysaccharide capsule were found to differentiate normally but were unable to migrate over an agar surface. This polysaccharide matrix is thought to act as a surfactant lubricating the passage of swarmer cells (Gygi *et al.* 1995b), and may extract water from the underlying surface (Rauprich *et al.* 1996). In addition to facilitating migration, this polysaccharide matrix is also thought to be important for maintaining cell-cell contacts, and facilitating the passage of intercellular signals (Gygi *et al.* 1995b). Surface associated LPS has also been implicated in the migration of *P. mirabilis*, and several non-swarming mutants exhibit defects in LPS synthesis (Belas *et al.* 1995).

The importance of multicellular raft formation and the close alignments of cells within these formations was highlighted by Hay *et al.* (1999). In this study a motile but non-swarming mutant of *P. mirabilis* was isolated and found to generate swarmer cells with abnormal morphology. The disrupted locus was designated *ccmA* for

curved cell morphology, and it was suggested that the inability of these curved cells to form the close alignments (observed in wild type multicellular rafts) was responsible for the defect in swarming motility. Therefore, cell morphology and organisation also appear to be crucial for *P. mirabilis* swarm cell migration.

1.9 Molecular genetic approaches to elucidate the role of swarming in blockage of urethral catheters

Analysis at the molecular genetic level has become a powerful approach to the elucidation of mechanisms by which bacteria accomplish many processes (Hensel & Holden 1996; Chaing *et al.* 1999). For example, genes involved in virulence of pathogenic organisms (Isberg & Falkow 1985; Mahan *et al.* 1993; Hensel *et al.* 1995; Mahenthiralingam *et al.*1998); colonisation of plant roots by leguminous bacteria (Leigh *et al.* 1985; Leigh & Walker 1994); bacterial biofilm formation (Pratt & Kolter 1998; O'Toole & Kolter 1998a,b; Vidal *et al.* 1998; Watnick *et al.* 1999); aspects of *P. mirabilis* swarming (Belas *et al.* 1998; Belas 1996; Gygi *et al.* 1995a,b; Belas *et al.* 1991a,b); genes involved in bacterial resistance to antimicrobial agents (Codling 2004); and studies aimed at resolving regulation of gene expression (Totten *et al.* 1990), have all been studied using molecular genetic methods.

1.9.1 Molecular genetic approaches to the study of virulence

The molecular genetic approach to the study of bacterial virulence can draw upon many powerful techniques which fall into several broad categories: expression based methods, gene transfer methods, genomic comparison, and mutation based methods (Hensel & Holden 1996; Chaing *et al.* 1999). Each class of strategy offers distinct advantages and disadvantages compared to other approaches that may be used (Table 1.1). The problems associated with their application to elucidate the role of swarming in catheter encrustation by *P. mirabilis* are also listed. While a particular method may appear to offer the best chance of acquiring the desired information, factors such as availability of genetic systems, availability of sequence data, knowledge of genes involved in a virulence attribute, and availability of suitable organisms for cloning, ultimately decide the strategy that will be employed.

Table 1.1: Advantages and disadvantages of molecular genetic approaches in the study of bacterial virulence and their application to *P. mirabilis*. Modified from Hensel & Holden (1996).

Category	Advantages	Disadvantages	Application to the study of *P. mirabilis* swarming during catheter encrustation
Expression based	Can identify genes specifically induced during infection. Broadly applicable. Can identify many putative virulence genes in one experiment.	Requires additional experiments to verify role in virulence. Discriminates against genes expressed outside of infection model. Promoter fusion systems require a molecular genetic system for the pathogen. Annotated genome sequence data required for microarrays.	Highly likely that *in vitro* expressed genes involved. Annotated sequence data not available. Limited genetic system.
Gene transfer Methods	Cloning of genes facilitates identification and sequencing. Can use host infection model as positive screen.	May miss traits involving more than one gene. Requires related organism which does not exhibit any traits of interest. Requires molecular genetic system and additional experiments to verify role of genes.	Swarming results from co-ordinated expression of many genes. Related organisms for cloning exhibit some traits of interest such as swarming. Limited genetic system.
Genome Comparison	No genetic system required. Rapid cloning of identified genes possible.	Requires related organism which does not exhibit any traits of interest. Requires additional experiments to verify role of genes.	Related organisms, such as *E. coli*, exhibit traits of interest such as biofilm formation and adherence to catheter surfaces.
Directed Mutation Based Methods	Can be used to clarify role in virulence	Knowledge of genes involved in virulence required, including sequence data.	Many genes involved in swarming unidentified
Random Mutation Based Methods	**Chemical/UV:** Easy and generally applicable. Require no previous knowledge of genes involved. **Transposon:** Require no previous knowledge of genes involved. Generally give single mutation per genome. Direct tagging of genes aids identification and cloning. Signature-tagged mutagenesis allows for simultaneous screening of many mutants. Can link unexpected genes with an attribute.	May cause more than one mutation per genome. Cloning of gene difficult or impossible. Requires additional experiments to verify role in virulence. May exhibit non-random preferential insertion at hot-spots. Insertional mutagenesis system required. Requires additional experiments to verify single random inserts and role of mutated genes. E.g. complementation studies	Need to be able to easily clone and identify genes disrupted. Single mutation required. Delivery of transposon can be difficult. "Hot spot" could limit number of genes disrupted.

In the case of *P. mirabilis* and the use of such methods to study the role of swarming in colonisation and blockage of urethral catheters, mutation based approaches are the most suited. These strategies have been successfully applied to the study of bacterial virulence and swarming in a variety of species, including *P. mirabilis*, and are generally the most popular and successful approaches for the genetic analysis of bacterial virulence (Belas *et al.* 1991a,b; Gygi *et al.* 1995a,b; Hensel & Holden 1996).

These approaches can be divided into two groups, directed mutagenesis and random mutagenesis, each offering a different set of advantages and disadvantages (Hensel & Holden 1996; Chiang *et al.* 1999). Directed mutagenesis is often employed as a proof of function test in studies utilising methods such as genome comparison or gene transfer, which require verification of the role of any putative virulence genes identified (Groisman *et al.* 1993; Wigfield *et al.* 2002).

However, where sequence data is available directed mutagenesis alone can be used to elucidate the roles of suspected virulence genes in the pathogenicity of an organism (Mahenthiralingam *et al.* 1998). This method is well suited to clarify the role of genes suspected to be involved in virulence, but can only be used where the gene has already been identified and characterised, and sequence data is available. These requirements limit the overall usefulness of this method and make it unsuitable for the investigation of the role of swarming in *P. mirabilis* pathogenicity.

In contrast, random mutagenesis methods, particularly transposon-based mutagenesis, are ideally suited to this investigation. Such strategies do not require any previous knowledge of the genes involved in a putative virulence attribute or

pathogenicity factor, and can generally be applied to most organisms (Hensel & Holden 1996; de Lorenzo & Timmis 1994). Another major advantage offered by random mutagenesis, is the potential to generate a diverse range of mutants deficient or enhanced in almost any ability; this allows the function in pathogenicity of a virulence attribute or phenotype to be established. The limited molecular genetic systems in *P. mirabilis*, the current lack of a genome sequence, the absence of a suitable surrogate organism or strain for genomic comparison methods, and the fact that many of the genes involved in swarming remain unidentified and/or uncharacterised all favour random mutational strategies.

1.9.2 Random mutagenesis based methods

In random mutation based methods the key to the identification of genes involved in a process is the generation of mutant organisms, and the subsequent selection of individuals which are attenuated, altered, or enhanced in ability or phenotype (Belas *et al.* 1991a,b; Hensel *et al.* 1995; Chiang & Mekalanos 1998). Figure 1.12 illustrates the basic principles of random mutagenesis strategies. Specialised screens are required to identify mutants with the desired phenotype, and the invention and implementation of such screens is often the limiting factor in mutagenesis strategies. Fortunately swarming in *P. mirabilis* is a highly visible phenotype and screening for attenuation or inhibition of swarming is straightforward. For example, Belas *et al.* (1991b) isolated swarming-deficient transposon mutants of *P. mirabilis* using a simple screening procedure based on an inability to swarm over LB agar.

There are two general approaches to the generation of random mutants, chemical based methods, and transposon based mutagenesis strategies (de Lorenzo & Timmis 1994; Hensel & Holden 1996). The creation of random mutants can be accomplished

Figure 1.12: General strategy for the identification of virulence genes by random mutagenesis based strategies.

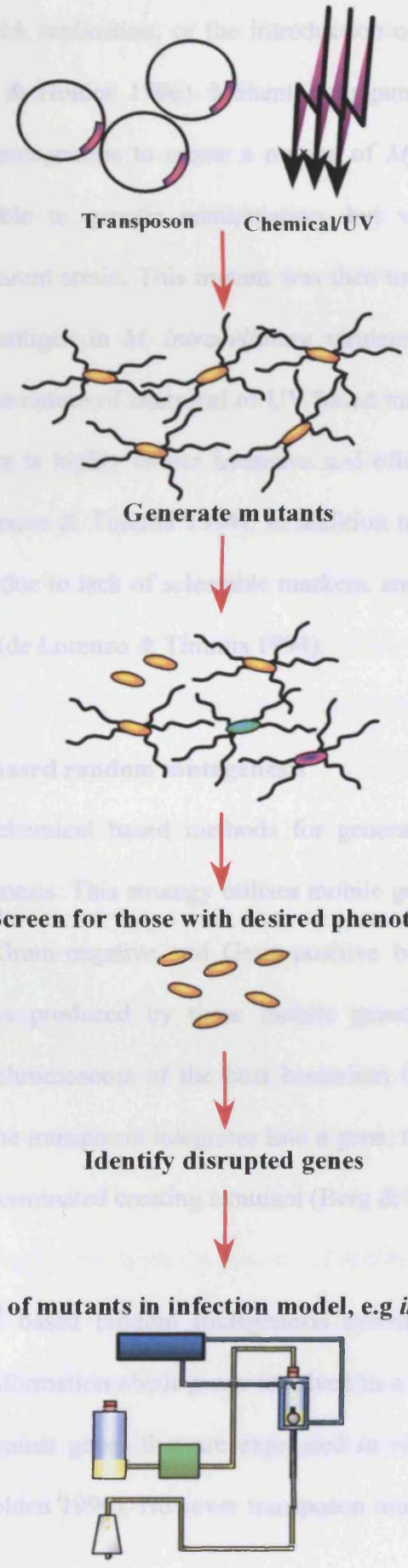

with compounds such as nitrosguanidine (NTG), which cause mutations by interfering with DNA replication, or the introduction of random mutations by UV irradiation (Hensel & Holden 1996). Mahenthiralingam *et al.* (1998), successfully used NTG based mutagenesis to create a mutant of *Mycobacterium intracellulare* which was amenable to genetic manipulation, but which retained the virulent phenotype of the parent strain. This mutant was then used to investigate the role of the 19 kilodalton antigen in *M. intracellulare* virulence by directed mutagenesis. However, due to the nature of chemical or UV based mutagenesis, the identification of inactivated genes is highly labour intensive and often extremely difficult if not impossible (de Lorenzo & Timmis 1994). In addition to this the initial isolation of mutants is difficult due to lack of selectable markers, and mutants are likely to carry multiple mutations (de Lorenzo & Timmis 1994).

1.9.3 Transposon based random mutagenesis

An alternative to chemical based methods for generation of random mutants is transposon mutagenesis. This strategy utilises mobile genetic elements which occur naturally in both Gram-negative and Gram-positive bacteria (Sherrat 1989). The transposase enzyme produced by these mobile genetic elements mediates their insertion into the chromosome of the host bacterium (Berg 1989; Kleckner 1989; Sherratt 1989). If the transposon integrates into a gene, that gene is usually disrupted and its expression terminated creating a mutant (Berg & Berg 1983).

As with chemical based random mutagenesis systems, transposon mutagenesis requires no prior information about genes involved in a virulence attribute and does not discriminate against genes that are expressed *in vitro* (de Lorenzo & Timmis 1994; Hensel & Holden 1996). However transposon mutagenesis also offers several

major advantages over chemical mutagenesis, including easier identification of mutants through selectable markers, and the ability to quickly clone and identify disrupted genes (de Lorenzo & Timmis 1994).

Transposons frequently carry genes which confer a selectable phenotype on the host organism, such as resistance to an antibiotic (Berg 1989; Kleckner 1989). In the case of wild type transposon Tn*5*, resistance to the antibiotics kanamycin, bleomycin and streptomycin are conferred on the host (Berg 1989), while Tn*10* confers resistance to tetracycline (Kleckner 1989). This can be utilised to easily identify transposon mutants which can then be processed using a specialised screen to identify those with the desired phenotype. Further characterisation of the disrupted gene is facilitated by the presence of the transposon, which effectively "tags" the gene with a known DNA sequence that can be exploited to determine its identity (de Lorenzo & Timmis 1994). In addition, transposons generally insert only once per genome, eliminating the problem of multiple mutations which is a major drawback associated with chemical mutagenesis (de Lorenzo & Timmis 1994).

The properties of transposons have been exploited by molecular biologists to develop powerful and highly versatile mutagenesis systems that incorporate some of the most desirable features of random mutagenesis and directed mutagenesis methods (Berg & Berg 1983; de Lorenzo & Timmis 1994; Hensel & Holden 1996). Transposons of Gram-negative bacteria have been the subject of much study and modification, and as a result transposon mutagenesis systems for Gram-negative species are the most developed (Hensel & Holden 1996). Of the transposon mutagenesis systems now available, those based on derivatives of Tn*5* and Tn*10* elements are among the most

widely used, and Tn*5* in particular has been widely used in a range of Gram-negative bacteria (Simon *et al.* 1989; Merriman & Lamont 1993; de Lorenzo *et al.* 1998).

The widespread use of Tn*5* for mutagenesis and cloning has resulted in the generation of many distinct Tn*5* elements and delivery systems, designed to fulfil a variety of demands (Simon *et al.* 1989; de Lorenzo *et al.* 1990; Herrero *et al.* 1990; Merriman & Lamont 1993; Hensel *et al.* 1995; Hansen *et al.* 1997). Modifications include the incorporation of reporter genes such as *lacZ*; the generation of Tn*5* elements with alternative selectable markers (Simon *et al.* 1989; Herrero *et al.* 1990); the production of Tn*5* based elements which facilitate cloning of DNA flanking transposon inserts (Merriman & Lamont 1993); and the development of transposable elements that eliminate some of the disadvantages associated with the use of wild type based transposons (de Lorenzo & Timmis 1994).

Wild type transposons are: large and difficult to handle often containing unwanted or inappropriate resistance genes; have a general lack of useful restriction sites, making cloning of disrupted genes potentially difficult; possess an active transposase gene making insertions unstable and inhibiting additional transposon mutagenesis; and the large repeated sequences at the ends also serve to promote genetic rearrangements in the host DNA (Kleckner *et al.* 1991; Hensel & Holden 1996; de Lorenzo *et al.* 1998). Transposon mutagenesis can be further complicated by problems with delivery of the transposon to the target organism (Herrero *et al.* 1990; de Lorenzo *et al.* 1998). Early delivery systems often relied on specialised host/phage interactions; in *E. coli* delivery was often accomplished by the use of defective phage λ and as such was only applicable to *E. coli* (Herrero *et al.* 1990; Kleckner *et al.* 1991). Plasmid based

suicide vectors were also available, but lacked versatility and were still not a widely applicable system (Herrero *et al.* 1990; Kleckner *et al.* 1991).

Herrero *et al.* (1990) and de Lorenzo *et al.* (1990) addressed these problems with the construction of a set of modified genetic elements based on Tn*5* and Tn*10*, and a widely applicable delivery system. The resulting constructs were named mini-transposons due to their reduced size (de Lorenzo *et al.* 1998). The name mini-transposon has now come to refer to a collection of artificially modified genetic elements based on Tn*5* and Tn*10*, which exhibit reduced length compared to the wild type elements (de Lorenzo *et al.* 1998). The modifications to wild type Tn*5* elements essentially generated a set of streamlined Tn*5*, lacking many of the disadvantages associated with wild type transposons, and designed for use in a wide range of Gram-negative bacteria. Mini-transposons possess single selectable markers, which can be chosen to suit the requirements of the study; lack an active transposase gene enhancing insertion stability; and are less likely to induce genomic rearrangements.

The construction of a widely applicable delivery system for mini-Tn*5* transposons resulted in the pUT plasmid, a suicide based delivery system (Herrero *et al.* 1990; de Lorenzo & Timmis 1994; de Lorenzo *et al.* 1998). The pUT vector contains the R6K origin of replication which requires the π protein product of the *pir* gene, and can only replicate in hosts producing this protein (Herrero *et al.* 1990; de Lorenzo & Timmis 1994). In addition to this the delivery vector also contains the RP4 derived *ori*T which allows for broad host range conjugal transfer of the plasmid, and a Tn*5* transposase gene which drives transposition of the mini-Tn*5* element (de Lorenzo & Timmis 1994). The pUT delivery vector was based on the suicide delivery vector pGP704, which also employs an R6K based π dependant replication system, and has

been used as a more general delivery system for transposon mutagenesis (Miller & Mekalanos 1988; de Lorenzo & Timmis 1994).

The pUT vector can be maintained in a host which produces the π protein, such as an *E. coli* λpir lysogen, and introduced to target organisms by conjugal transfer (Herrero *et al.* 1990; de Lorenzo & Timmis 1994). When in the new host the pUT vector is unable to replicate and is lost, but exists long enough to allow transposition of the mini-transposon it carries (de Lorenzo & Timmis 1994). The presence of the transposase gene on the plasmid external to the mini-Tn*5* element means that this is also lost with the pUT vector so cannot mediate further transposition, resulting in a stable insertion (de Lorenzo & Timmis 1994). Furthermore, the transposase gene is also responsible for generating a protein that results in immunity to subsequent rounds of transposon mutagenesis with similar elements. Therefore the loss of the transposase gene with the pUT vector also eliminates this problem (de Lorenzo & Timmis 1994).

Transposon mutagenesis has already been successfully applied to the study of processes relevant to the pathogenicity of *P. mirabilis* in the catheterised urinary tract. The most notable of these include the identification of genes involved in biofilm formation of *E. coli* and *Ps. aeruginosa* (O'Toole & Kolter 1998a,b; Pratt & Kolter 1998); and in the elucidation of mechanisms involved in swarming by *P. mirabilis* (Gygi *et al.* 1995a,b; Belas 1996; Hay *et al.* 1997; Belas *et al.* 1998). For example, Hay *et al.* (1997) described a non-swarming *P. mirabilis* mutant generated by transposon mutagenesis which was lacking in a global transcription regulator; while Gygi *et al.* (1995b) utilised transposon mutagenesis to highlight the role of capsular polysaccharide production in *P. mirabilis* swarming. The application of this

strategy in the current study will hopefully help elucidate the role of swarming in colonisation of the catheterised urinary tract and encrustation of catheters by *P. mirabilis*, and could potentially identify novel genes involved in both swarming and the pathogenicity of this organism.

1.10 Aims

The general aim of this study was to elucidate the role of swarming in the pathogenesis of *P. mirabilis* C-UTI. In particular, the contribution of swarming to colonisation of the catheterised urinary tract, and development of crystalline biofilms on urinary catheters was investigated. This study also aimed to identify novel genes involved in *P. mirabilis* swarming and pathogenesis. Specific aims are outlined below:

- Evaluate and optimise transposon based mutagenesis systems for use with clinical isolates of *Proteus mirabilis* from C-UTI, and generate defined mutants deficient in swarming.

- Assess the role of swarming in attachment to catheter biomaterials and biofilm formation by *P. mirabilis*.

- Assess the contribution of swarming to the blockage and encrustation of urinary catheters by *P. mirabilis*.

- To investigate the role of swarming in colonisation of the catheterised urinary tract by *P. mirabilis*.

- Identify genes involved in swarming and the encrustation of urinary catheters by *P. mirabilis*.

- Elucidate the function of genes involved in swarming and/or catheter encrustation.

Chapter 2: Materials & Methods

2.1 Materials

2.1.1 Chemicals and culture media

Chemicals used in this study, were obtained from either Fisher Scientific (Loughborough, UK) or Sigma Chemical Company (Poole, UK). EM grade chemicals for electron microscopy sample preparation were obtained from AGAR Scientific (Stanstead, UK). Antibiotics were obtained from Sigma Chemical Company or ICN (Basingstoke, UK). Culture media was purchased from Oxoid LTD (Basingstoke, UK), and all media was sterilised by autoclaving before use.

2.1.2 Enzymes and PCR reagents

Restriction enzymes were obtained from either New England Biolabs (Hertfordshire, UK), or Promega UK (Southampton, UK). T4 DNA ligase and Ligation buffer was supplied by Promega UK. All PCR reagents including *Taq* DNA polymerase were purchased from Qiagen (Crawley, UK). Oligonucleotide primers were synthesised by MWG Biotech-AG (Ebersberg, Germany).

2.1.3 Bacteria

Table 2.1 lists bacterial strains used in this study, along with their source and main features.

2.1.4 Plasmids and transposons

Properties, functions, and sources of plasmids and transposable elements utilised in this study are outlined in Table 2.2. Plasmid pUTmini-Tn*5*Km2 vector map is presented in Figure 2.1. Plasmid pB4 was generated from pOT182 as described in section 2.9.3.

Table 2.1: Bacterial strains used in this study

Strain	Comment	Source
Proteus mirabilis		
B1, B2, B3, B4, B5, B6.	Recent clinical isolates from encrusted indwelling urethral catheters.	Dr N. Morris and Dr. S. Sabbuba , Cardiff School of Biosciences, Cardiff University
U6450	Wild type strain – uropathogenic isolate.	Gygi *et al.* (1995a)
U6450 *flhA*⁻	Non-swimming, non-swarming mutant of U6450. Flagellin export protein gene *flhA* disrupted by Tn*5phoA* transposon.	Gygi *et al.* (1995a)
G33, G37, NS63, G64, G77, NS77, G78, PS92, G93	Swarming-deficient mini-Tn*5*Km2 mutants of strain B4.	This Study
BVJ12, BVJ14, BVJ15	Mini-Tn*5*Km2 mutants, unaffected in swarming. Control mutants for effects of mini-Tn*5*Km2 on swarming.	This Study
Escherichia coli		
SM10	Used to maintain and deliver plasmid pOT182	Promega, Southampton, UK
S17.1	λpir lysogen, produces π protein which allows replication of plasmids with R6K origin of replication. Used to maintain and deliver plasmid pUTmini-Tn*5*Km2, and constructs based on plasmid pB4.	Microscience Ltd., Wokingham, UK
VCS257	Used to maintain cosmid library	Provided with Giga Pack III XL *in vitro* Packaging kit - Stratagene, Netherlands.
10418	Sensitive to most antibiotics. Control strain for MICs and disc testing	Promega, Southampton, UK
JM109	Standard cloning strain. Obtained as frozen competent cells.	Promega, Southampton, UK

Table 2.2: Plasmids and transposable elements used in this study.

Plasmid/ Transposon	Selectable Markers [a]	Comment/Use	Source
Plasmids			
pOT182	Amp^R, Tc^R, Cm^R, Gm^R, *lacZ*	Suicide delivery vector carrying transposonTn*5*-OT182. P15A replication origin. Maintained in *E. coli* SM10.	Merriman & Lamont (1993)
pUTMini-Tn*5*Km2	Km^R, Amp^R	Suicide delivery vector pUT, carrying transposon mini-Tn*5*Km2. R6K replication origin. Only replicates in *pir+* host. Maintained in *E. coli* S17.1λ*pir*.	de Lorenzo & Timmis (1994)
pSCOSPA1	Amp^R, Gm^R	Cosmid vector for construction of genomic DNA libraries.	Sokol *et al.* (1999)
pUC18	Amp^R	Standard cloning vector	Promega, Southampton, UK
pB4	Gm^R, Cm^R	Derivative of pOT182 lacking transposon Tn*5*-OT182. P15A replication origin. Replicates in *P. mirabilis*. Maintained in *E. coli* S17.1λ*pir*.	This Study
Transposons			
Tn*5*-OT182	Amp^R, Tc^R, *lacZ*	Modified Tn*5* element carrying selectable markers for use in random Tn mutagenesis. Delivered on suicide vector pOT182. Has ColE1 origin of replication to facilitate cloning of flanking DNA. (Merriman & Lamont 1993)	Merriman & Lamont (1993)
Mini-Tn*5*Km2	Km^R	Modified Tn*5* element, reduced in size, and carrying selectable markers for use in random Tn mutagenesis. Transposase (*tnp)* gene provided on pUT delivery vector, external to mini-Tn*5*Km2. (de Lorenzo & Timmis 1994)	de Lorenzo & Timmis (1994)

a - ^{R}: denotes resistance to respective antibiotic. *lacZ*: Complete or partial *E. coli* β-galactosidase gene.

Figure 2.1: Suicide delivery vector pUT carrying transposon mini-Tn5Km2 (plasmid pUTmini-Tn5Km2).

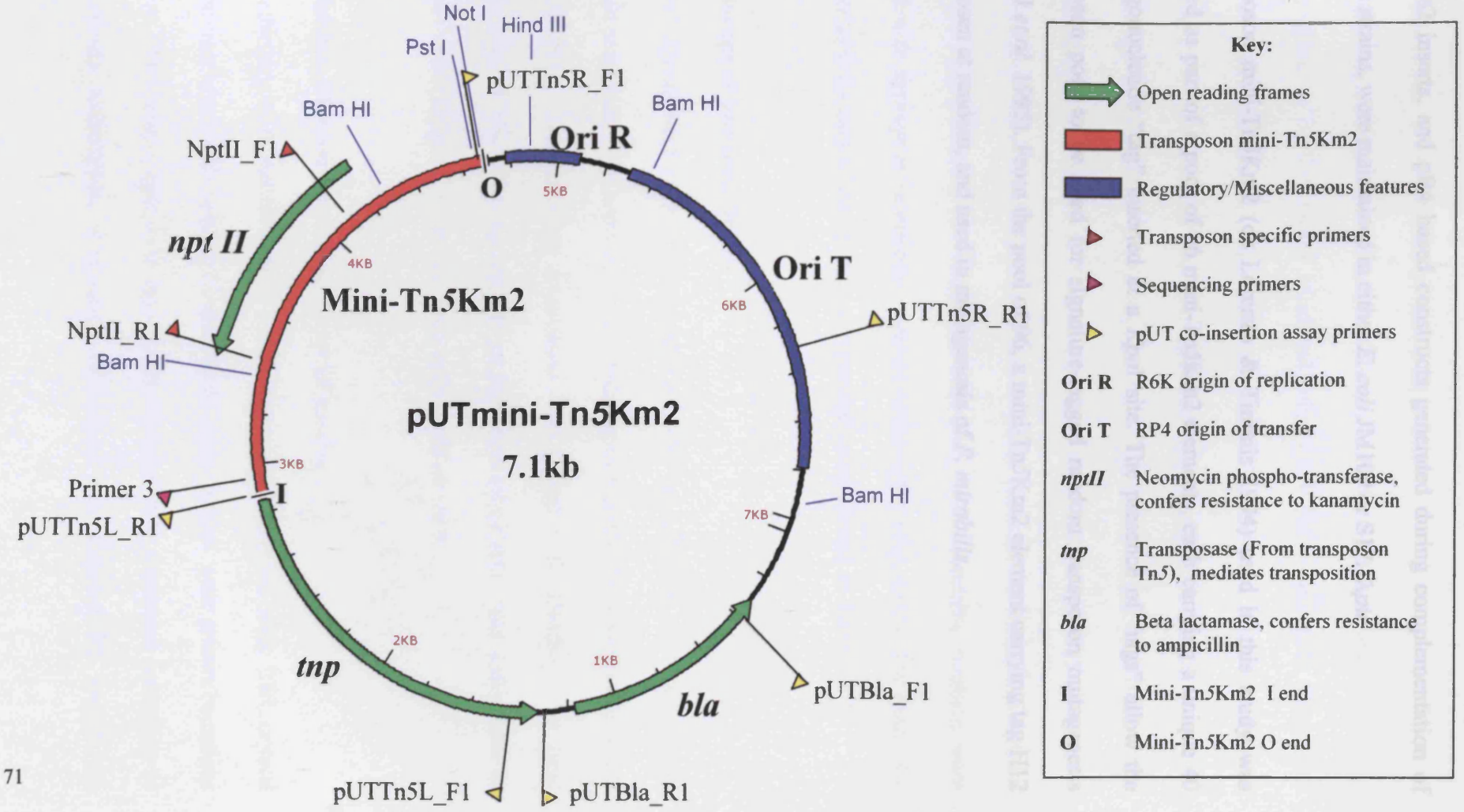

All pUC18 based constructs generated during sub-cloning of DNA flanking mini-Tn*5*Km2 inserts, and pB4 based constructs generated during complementation of mutant strains, were maintained in either *E. coli* JM109 or S17.1λ*pir*.

Transposon mini-Tn*5*Km2 (de Lorenzo & Timmis 1994) used in this study was obtained as part of a pool of 96 mini-Tn*5*Km2 elements, each carrying a unique 40 bp oligonucletide "tag" inserted at a *Kpn*I site. The presence of "tags" allow the transposon pool to be used for signature-tagged random transposon mutagenesis (Hensel *et al.* 1995). From the pool of 96, a mini-Tn*5*Km2 element carrying tag H12 was chosen at random, and used in mutagenesis of *P. mirabilis*.

2.2 General microbiology methods

2.2.1 Culture and manipulation of bacterial strains

All bacterial strains were grown in Luria-Bertani (LB) broth (Sambrook *et al.* 1989) with aeration, or on LB media solidified with 1.5% (w/v) agar (LB agar), and incubated overnight at 37°C unless otherwise stated. Isolation of single colonies of swarming *P. mirabilis* strains was accomplished using dry MacConkey agar without salt (Oxoid). Sterile 14 ml polypropylene tubes (Becton Dickinson, Oxford, UK) were used for liquid cultures of 5 ml and under. Liquid cultures of 5-25 ml volume were grown in sterile 50 ml polypropylene tubes (Becton Dickinson). Bacterial strains carrying plasmids, or transposon insertions, with selectable markers were cultured with appropriate antibiotic selection unless otherwise stated. The antibiotic selection used for each plasmid and transposon are summarised in Table 2.3.

2.2.2 Storage of bacterial strains

Bacterial strains were cultured overnight at 37°C on LB agar with appropriate antibiotic selection. Cells were harvested with a sterile swab and resuspended in LB broth (2 ml). The resulting suspension was mixed with DMSO to a final concentration of 8% (v/v). An aliquot of this mixture (2 ml) was transferred to cryogenic vials (Nalgene, Hereford, UK), and stored at -80°C.

2.2.3 Identification/verification of bacterial species

Species identity of *P. mirabilis* or *E. coli* isolates was confirmed using BBL crystal non-fermenter/enteric ID system (Becton Dickinson). Strains were grown overnight on LB or MacConkey agar with appropriate selection then processed according to manufacturers instructions. Production of indole was assessed by inoculating

Table 2.3: Antibiotic selection used for cultivation of strains carrying plasmids or transposons.

Organism/Plasmid/Insert	Antibiotic Selection
Escherichia coli	
pOT182	Tc 20 μg/ml
pUTKm	Km 30 μg/ml
pB4 (and related constructs)	Gm 10 μg/ml
pUC18 (and related constructs)	Amp 100 μg/ml
pSCOSPA1	Gm 10 μg/ml
Proteus mirabilis	
pB4 (and related constructs)	Gm 20 μg/ml
Tn*5*-OT182	Tc 200 μg/ml
Mini-Tn*5*Km2	Km 30 μg/ml

bacterial cells onto filter paper saturated with indole reagent (Becton Dickinson). Production of oxidase was assessed using oxidase test sticks (Oxoid).

2.2.4 Enumeration of bacterial cells by viable cell count

Concentrations of *P. mirabilis* cells grown in artificial or human urine were established by serial dilution in phosphate buffered saline, (PBS, Fisher Scientific) and culture on MacConkey agar. Dilutions of the original culture ranging from 10^0 to 10^{-7}were prepared. Three 10 µl drops of each dilution were inoculated onto a designated area of a dry MacConkey agar plate, and plates prepared in triplicate. Drops were allowed to dry, and plates incubated overnight at 37°C. Dilutions giving between 3 and 30 colonies per drop were counted and used to calculate the number of viable cells in the original culture, expressed in cfu/ml.

2.2.5 Antibiotic sensitivity testing

The sensitivity of *P. mirabilis* strains to various antibiotics commonly used to treat urinary tract infections was tested using methods obtained from the British Society for Antimicrobial Chemotherapy (BSAC, www.bsac.org.uk). Antibiotics and concentrations at which they were tested are summarised in Table 2.4. Antibiotics were chosen to reflect agents and concentrations commonly used to treat urinary tract infections, as recommended by BSAC (www.bsac.org.uk). Antibiotic sensitivity assays were performed in triplicate for each strain tested. *E. coli* 10418, which is sensitive to all antibiotics used, was included in each replicate test as a negative control.

Table 2.4: Antibiotics and concentrations used for antibiotic sensitivity testing.

Antibiotic	Concentration (μg)
Ciprofloxacin	1
Nalidixic Acid	30
Fosfomycin	200
Nitrofurantoin	200
Trimethoprim	2.5
Cephalexin	30
Ampicillin	25

Strains to be tested were grown overnight on LB agar, and used to prepare cell suspensions in sterile deionised water. Cell density was adjusted to equal the 0.5 McFarland standard (Sigma). Dry, Iso-sensitest agar (Oxoid) plates were inoculated with the suspensions by swabbing in three directions, to generate confluent bacterial growth. Plates were allowed to dry at room temperature, but used within 15 min of inoculation. Discs containing antibiotics at desired concentrations (Mast Pharmaceuticals, Beadle, UK) were distributed evenly onto the surface of the plate, and no more than four discs were used per plate. Plates were incubated overnight at 37°C, and the diameter of any zones of inhibition measured.

2.2.6 Minimum inhibitory concentration

The minimum inhibitory concentration (MIC) of the various antibiotics used was assessed. Approximate MICs were determined using methods modified from Mackie & McCartney (1989) from the results of three replicate experiments for each test strain. Approximate MICs were determined for cell grown in both liquid media (LB broth) and on solid media (MacConkey agar):

LB Broth: LB broth (5 ml), containing various concentrations of the antibiotic being tested were prepared. These were inoculated with 10 µl of an overnight starter culture, of the test strain, diluted 1:20 in LB broth. Cultures for were incubated overnight at 37°C with aeration.

MacConkey Agar: MacConkey agar plates containing various concentrations of the antibiotic to be tested were prepared, and dried overnight at room temperature. Plates were inoculated with overnight cultures of test strains. Three drops, (10 µl) of

undiluted culture, and dilutions of 10^{-2}, 10^{-4}, and 10^{-6} in LB broth were used. Drops were allowed to dry and plates were incubated overnight at 37°C.

For both types of media, controls were included in each replicate. These consisted of: (i) uninoculated media without antibiotics, (ii) uninoculated media with antibiotics for each concentration tested, (iii) inoculated media without antibiotics. The approximate MIC was taken as the lowest concentration that inhibited bacterial growth.

2.2.7 Statistical analysis and reproducibility

All experiments were performed in triplicate, and data is presented as the mean values. Where appropriate the standard deviation of the mean is also given. Significant differences between means were assessed using two sample t-tests at the 95% confidence interval where appropriate. The null hypothesis for these tests was of no significant difference between means tested. Relationships between variables were investigated by calculating the Pearson correlation coefficient where appropriate. The significance of relationships indicated by the correlation coefficients were assessed at the 95% confidence interval using critical values for correlation coefficients calculated by Fry (1993). All statistical analysis was carried out using Minitab version 10.3 (Minitab Inc, PA, USA).

2.3 General molecular biology methods

2.3.1 DNA gel electrophoresis

DNA fragments were separated using the Sub-Cell GT range of electrophoresis cells (Biorad, Hemel Hempstead, UK), and Power Pak 200 power supply units (Biorad). Separation of DNA fragments was carried out according to standard protocols (Sambrook *et al.* 1989). Fragments larger than ~8 kb were separated on 1% (w/v) agarose gels, while fragments below ~8 kb were separated using 1.5% (w/v) agarose gels, at 60-100 V. DNA was stained by immersing gels in TBE buffer (5.4 g/L Tris, 2.75 g/L Boric acid, 1 mM EDTA) supplemented with ethidium bromide (0.5 μg/ml), and incubation at room temperature for 15-30 min. DNA fragments were viewed a Gene Genius gel documentation system (Syngene, Cambridge, UK). A 1 kb molecular size standard (Helena Biosciences, Sunderland, UK) was included in all gels.

2.3.2 PCR

PCR reactions were carried out in 0.2 ml thin walled PCR tubes within a Flexigene thermal cycler (Techne, Cambridge, UK). Primers were combined and diluted to create stock solutions containing specific primer sets of both forward and reverse primers. Primers were combined at a concentration of 10 pmol per primer, 1:1 ratio forward:reverse.

Individual reactions were composed of 2.5 μl of 10X PCR buffer (containing 15 mM $MgCl_2$), 5 μl Q solution, 0.5 μl dNTPs, 0.2 μl *Taq* DNA polymerase, and 1.4 μl of primer stock solution. The final reaction contained 1.5 mM $MgCl_2$, and if required

additional $MgCl_2$ was added before reactions were brought to a final volume of 23 µl with sterile deionised water.

Each reaction was inoculated with 2 µl of template DNA dissolved in sterile deionised water. A negative control was included in each set of reactions to assess purity of reagents, and consisted of reaction mixture with 2 µl of sterile deionised water substituted for template DNA. Reactions were carried out using the following cycling conditions:

Initial denaturation - 95°C for 5 min

30 cycles of:

Primer specific anneal temperature for 45 s

72°C for 1 min

94°C for 30 s

Final extension - 72°C for 5 min,

Final hold - 4°C overnight.

The primer specific anneal temperature was varied according to the melting temperature (Tm) of the different primer combinations used. Table 2.5 summarises primer combinations used, the respective annealing temperature, and expected products of amplification. After completion, PCR products were visualised by gel electrophoresis (section 2.13). Primer sequence information is provided in Table 2.6.

Table 2.5: Summary of PCR primer combinations, annealing temperatures, and amplified products.

Primer Set[a]		AT[b](°C)	Product[c]
F R	NPT2_F1 NPT2_R1	61	676 bp segment of mini-Tn*5*Km2 *nptII* gene. (See Fig 2.1)
F R	P2 P4	49	60 bp product, containing 40 bp H12 "tag" from mini-Tn*5*Km2
F R	TetA1 TetA2	48	523 bp segment of *tetA* gene from Tn*5*-OT182
F R	pUTTn5L_F1 pUTTn5L_R1	51	1462 bp portion of pUTKm flanking I end of mini-Tn*5*Km2. (See Fig 2.1)
F R	pUTTn5R_F1 pUTTn5R_R1	51	1459 bp portion of pUTKm flanking O end of mini-Tn*5*Km2. (See Fig 2.1)
F R	pUTBla_F1 pUTBla_R1	51	1036 bp portion of pUTKm and most of *Bla* gene. (See Fig 2.1)
F R	AnsA_F1 AnsA_R1	50	464 bp of DNA downstream of Mini-Tn5Km2 insert in *P. mirabilis* G78*
F R	PST_F1 PST_R1	50	476 bp of DNA downstream of Mini-Tn5Km2 insert in *P. mirabilis* G64*
F R	GLT_F1 GLT_R1	50	439 bp of DNA downstream of Mini-Tn5Km2 insert in *P. mirabilis* G37*
F R	FlhA_F1 FlhA_R1	50	140 bp of DNA downstream of Mini-Tn5Km2 insert in *P. mirabilis* NS63*
F R	SurA_F2 SurA_R1	50	380 bp of DNA downstream of Mini-Tn5Km2 insert in *P. mirabilis* G93*
S	Primer 3	60	Mini-Tn*5*Km2 specific primer used to sequence DNA flanking I end of transposon. (See Fig 2.1)

[a]F - Forward primer; R - Reverse primer; S - Sequencing primer

[b]**AT** - Annealing temperature

[c] *nptII* - Neomycin phospho-transferase, confers resistance to kanamycin; *Bla* - Beta-lactamase, confers resistance to ampicillin; *tetA* - Tetracycline resistance protein, confers resistance to tetracycline.

* Swarming-deficient mutant

Table 2.6: Primer sequences

Primer	Sequence (5'-3')
NPT2_F1	CTTGCTCGAGGCCGCGATTAAATT
NPT2_R1	TTCCATAGGATGGCAAGATCCTGG
P1	TACCTACAACCTCAAGTC
P2	TACCCATTCTAACCAAGC
pUTTn5L_F1	GTTCGCTTGCTGTCCATA
pUTTn5L_R1	GCCAGATCTGATCAAGAG
pUTTn5R_F1	GCCGCACTTGTGTATAAC
pUTTn5R_R1	AGCGGATGGCTGATGAAA
pUTBla_F1	CGTTCATCCATAGTTGCC
pUTBla_R1	GGAAGCCCTGCAAAGTAA
TetA_F1	GTGAAACCCAACATACC
TetA_R1	GAAATTGAGGCCGTTCAC
PST_F1	CGCTCTCTTTTGGTAGTT
PST_R1	GAGGAAGATGTTTGAGAC
AnsA_F1	GCTGCACATCCGATTAAT
AnsA_R1	TCATAACCACTGATCACC
GLT_F1	CGGTGATGCATATTGTCT
GLT_R1	GAAAGGCTGTTCAAATGC
SurA_F2	GCAAGCTGTTTAGCAAAG
SurA_R1	AGAAAATACCGCATCAGG
FlhA_F1	TGCAAAACCTGTTGCCAG
FlhA_R1	CACCAAACCAGTGTTGTG
Primer3	CGGATTACAGCCGGATCCCCG

2.3.3 Restriction digest of DNA

Restriction digests were set up according to manufacturer's instruction (Promega), and were composed of 3 µl of 10 X restriction buffer, 1 µl of 10 X BSA, ~1-3 µg DNA (as 5-10 µl of an aqueous DNA solution), and 5 units of restriction enzyme. Sterile deionised water was added to give a final volume of 30 µl. Reagents were mixed thoroughly, and digests incubated overnight at 37°C. Products of digestion were visualised by gel electrophoresis.

2.3.4 Purification of plasmid DNA from *P. mirabilis* strains

Plasmid DNA from *P. mirabilis* was purified by alkaline lysis mini-prep with phenol and chloroform extraction (Sambrook *et al.* 1989). Strains were grown overnight in 3 ml of LB broth and 1.5 ml of culture transferred to a sterile micro-centrifuge tube. Cells were harvested by centrifugation (1 min at 10,000 *g*) and the supernatant discarded. Cells were resuspended in 100 µl of TE_1 buffer (10 mM Tris-Cl pH 8, 1 mM EDTA) by pipetting, and 200 µl of alkaline lysis buffer (1% w/v SDS, 0.2 M NaOH) was added to each tube. Contents were mixed by gentle inversion, and incubated at room temperature for 5 min.

After cell lysis, 150 µl of 3 M potassium acetate (pH 5.5) was added, mixed by inversion, and tubes incubated on ice for 10 min. The resulting precipitate was removed by addition of 500 µl of phenol, mixed vigorously, centrifuged (10,000 *g* for 3 min), and the upper aqueous phase transferred to a high yield micro-centrifuge tube (coated to enable a high degree of nucleic acid recovery, supplied by Fisher Scientific). This extraction step was repeated using 500 µl of chloroform. DNA was then precipitated by addition of 3 volumes of ice-cold 100% ethanol (~1 ml) and

incubation at -20°C for 30 min. Plasmid DNA was harvested by centrifugation at 10,000 *g* for 15 min, and the supernatant discarded. The resulting pellets were washed in 500 µl of 70% (v/v) ethanol, then dried under vacuum for 15-20 min. Dry pellets of plasmid DNA were dissolved in 30-50 µl of TE_1 buffer, or sterile deionised water, containing RNaseA (1 µg/ml). Dissolved plasmid DNA was incubated at 37°C for 15 min to allow degradation of RNA, and stored at -20°C until required.

2.3.5 Purification of plasmid DNA from *E. coli* strains

Plasmid DNA was purified from *E. coli* strains using Wizard SV Plus Minipreps - DNA Purification System (Promega, UK). Cells from 5-10 ml of overnight culture were harvested and processed according to manufacturers protocol for purification using centrifuge. All centrifugation steps were performed at 13,000 rpm (10,000 *g*) in a Genofuge micro centrifuge (Techne, Cambridge, UK). Plasmid DNA was eluted in 30-50 µl of sterile deionised water.

2.3.6 Purification of bacterial chromosomal DNA

Cells from overnight LB broth cultures (5 ml) were harvested by centrifugation (1600 *g* for 15 min). The supernatant was discarded and cells evenly resuspended in 200 µl TE_{10} buffer (10 mM Tris-Cl pH 8, 10 mM EDTA). To lyse cells, 2.8 ml of lysis buffer (1% w/v SDS, 50 mM Tris-Cl pH 8, 50 mM EDTA, 1 mg/ml Pronase) was added and cell suspensions incubated at 37°C, with gentle rocking, for 4 hours. After lysis, 1 ml of saturated ammonium acetate was added, mixed thoroughly, and tubes incubated at room temperature for 1 hour to allow precipitation of protein and polysaccharide.

After precipitation of cellular debris, 4 ml of chloroform was added to each tube, mixed by vigorous shaking, and debris removed by centrifugation (1600 *g* for 15 min). The upper aqueous phase was transferred to fresh tubes. If necessary, centrifugation and collection of this upper aqueous phase was repeated until 2-3 ml had been acquired. DNA was precipitated by addition of ice-cold ethanol (9 ml), which was mixed by inverting tubes.

The precipitated DNA was harvested by centrifugation (1600 *g* for 10 min), and transferred to a hi-yield micro-centrifuge tube containing 70% (v/v) ethanol (1 ml). Tubes were centrifuged (10,000 *g* for 1 min) and supernatant discarded. DNA pellets were then dried under vacuum for 15-20 min, and dissolved in 500 µl of sterile deionised water, or TE_1 buffer containing RNaseA (1 µg/ml). DNA solutions were incubated at 37°C for 1 hour to allow degradation of RNA, and stored at -20°C until required.

2.3.7 Purification of DNA

A QIAquick PCR purification kit (Qiagen) was used to purify DNA fragments and vectors (under 10 kb) from restriction digests, PCR, and other reaction mixtures. Purification was performed according to manufacturer's protocol for purification using a micro-centrifuge. Fragments were eluted in 30-50 µl of sterile deionised water, and stored at -20°C until required.

DNA fragments over 10 kb, were purified by chloroform extraction and ethanol precipitation. DNA solutions were supplemented with 1/3rd volume of saturated ammonium acetate, and brought to a final volume of 200-300 µl by addition of

sterile deionised water. Chloroform (200 µl) was added and tubes shaken vigorously. Tubes were centrifuged (10,000 *g* for 1 min) and the upper aqueous phase removed to a fresh high yield micro-centrifuge tube. DNA was precipitated by addition of 3 volumes of 100% ethanol and incubated at -20°C for 1 hour. Precipitated DNA was collected by centrifugation (10,000 *g* for 30 min), and supernatant discarded. DNA pellets were washed in 70% (v/v) ethanol (500 µl), dried under vacuum, then dissolved in 30-50 µl of sterile deionised water.

2.3.8 Transfer of plasmids to *P. mirabilis*.

Plasmid vectors were introduced to *P. mirabilis* strains by conjugal transfer. Matings were set up between either *E. coli* S17.1λ*pir* or SM10 carrying the plasmid (donor strains) and a *P. mirabilis* recipient strain. Matings were performed according to a modification of the method used by Lewenza *et al.* (1999).

The *E. coli* donor strain and *P. mirabilis* recipient strain were grown overnight in LB broth (3 ml). Cultures were centrifuged (1600 *g* for 10 min), the supernatant discarded, and cells resuspended in sterile PBS (2 ml). A 1 ml aliquot of the *E. coli* suspension was transferred to a sterile micro-centrifuge tube, and cells recovered by centrifugation (6000 *g* for 1 min). The supernatant was discarded, and cells resuspended in PBS (100 µl). An aliquot (100 µl) of the *P. mirabilis* cell suspension was mixed with the *E. coli* suspension, and centrifuged at 6000 *g* for 1 min. The supernatant was discarded, and the cells resuspended in 100 µl PBS. This final suspension was dropped onto nitrocellulose filters (0.2 µm pore size, Whatman, Maidstone, UK) resting on LB agar containing 10 mM $MgSO_4$. Drops were allowed to dry at room temperature before overnight incubation at 37°C.

Filters were removed to a sterile 14 ml tube and cells resuspended in 1 ml PBS by vortexing. Aliquots (100 µl) of this suspension were spread over MacConkey agar supplemented with PMX (60 units/ml), to eliminate *E. coli* donor strains, and containing antibiotic selection appropriate to plasmid used (see Table 2.2).

2.3.9 Generation of competent *E. coli* cells for transformation

E. coli strains were cultured overnight on LB agar, and used to inoculate two 25 ml aliquots of LB broth in sterile 50 ml polypropylene tubes (Becton Dickinson). Cultures were grown for ~3 hours at 37°C with aeration, then incubated on ice for 15 min. Cells were harvested by centrifugation (1600 *g* for 10 min), and the supernatant discarded. Tubes were placed in an inverted position on absorbent material for 1 min to allow all traces of media to drain away. Each pellet was then resuspended in 5 ml of an ice-cold 0.1 M $CaCl_2$ solution. Cell suspensions were again centrifuged (1600 *g* for 10 min) and cells resuspended in 500 µl of ice-cold 0.1 M $CaCl_2$ solution. Aliquots (100 µl) of this cell suspension were transferred to chilled, sterile micro-centrifuge tubes, and snap frozen by immersion in liquid nitrogen. Competent cells were stored at -80°C until required.

2.3.10 Generation of electro-competent *E. coli* cells

Electro-competent *E. coli* were generated as described in section 2.3.9. However, an ice-cold 10% (v/v) glycerol solution was used in place of the 0.1 M $CaCl_2$ solution. Aliquots of electro-competent cells were snap frozen by immersion in liquid nitrogen and stored at -80°C until required.

2.3.11 Transformation of *E. coli* strains

An aliquot of competent cells was thawed slowly on ice. An aliquot (10 µl) of aqueous plasmid solution was transferred to a chilled 14 ml snap top tube (Becton Dickinson). Competent cells (100 µl) were added, and the mixture incubated on ice for 15 min. Care was taken to keep pippeting to a minimum. Cells were then incubated in a water bath at 42°C for 45 s, then incubated on ice for a further 2 min. Cells were suspended in 900 µl of pre-warmed SOB broth (20 g/L Tryptone, 5 g/L Yeast extract, 0.5 g/L NaCl) containing 10 mM $MgCl_2$, and the resulting suspension incubated at 37°C with aeration for 2 hours. Transformed *E. coli* were identified by spreading aliquots (100 µl) over selective LB or MacConkey agar plates containing antibiotic appropriate to the plasmid being transformed (see Table 2.2).

2.3.12 Electroporation of *E. coli* strains

Electro-competent *E. coli* strains were electroporated using Genepulser electroporation cuvettes (Biorad) with a 0.2 cm gap. A Genepulser electroporation system equipped with a Genepulser capacitance extender module (Biorad) was utilised. An electroporation cuvette, containing ~1 µg of plasmid DNA in a maximum volume of 5 µl, was cooled on ice for 10 min. Aliquots of frozen electro-competent *E. coli* were thawed on ice, and 100 µl transferred to the cuvette. The contents of the cuvettes were electroporated at 1.8 kV, 200 Ω resistance, and 25 µF capacitance. Immediately after electroporation, 900 µl of SOB broth containing 10 mM $MgCl_2$ was added. The resulting suspension was transferred to a sterile tube, and incubated at 37°C for 1 hour. Transformed cells were selected by spreading aliquots (100 µl) of the cell suspension over LB agar plates containing antibiotic selection appropriate to the plasmid being transformed (See Table 2.2).

2.3.13 Ligations

All solutions of DNA used in ligations were purified using a QIAquick PCR purification kit (Qiagen), and dissolved in sterile deionised water. Ligation buffer (10X) was stored as 1 µl aliquots, at -20°C in 0.2 ml PCR tubes until required, and thawed (on ice) before use.

Ligations were performed in 0.2 ml PCR tubes, and reaction mixtures consisted of: 1 µl 10X ligation buffer, 1 µl of vector DNA solution (~100-300 ng DNA linearized with appropriate restriction enzyme), 3 units of T4 ligase (in a volume of 1 µl), and 4-7 µl of target DNA solution (~500 ng – 1 µg DNA). If required, sterile deionised water was added to give a final volume of 10 µl. Tubes were centrifuged briefly, and incubated at 4°C overnight. Ligations were either transformed (section 2.3.11) or electroporated (section 2.3.12) into a suitable *E. coli* host strain.

2.3.14 Dephosphorylation of linearized plasmid vectors.

To prevent re-circularisation of plasmid vectors during ligations, terminal phosphate groups were removed from linearized vectors using shrimp alkaline phosphatase (SAP), (Promega). Digested vectors were purified using a QIAquick PCR purification kit (Qiagen) and DNA quantified at 320 nm using a Gene Quant spectrophotometer (Pharmica). SAP was added at a concentration of 1 unit/µg vector DNA, and SAP buffer added to give a final volume of 30-50 µl. The resulting mixture was incubated at 37°C for 15 min, and then at 65°C for 15 min to inactivate SAP. Vector DNA was used without further processing.

2.4 Pulsed field gel electrophoresis

Total genomic DNA from *P. mirabilis* parental strains, and putative transposon mutants, was immobilised in agarose gel and digested with *Not*I restriction enzyme. Fragments were then separated by pulsed field gel electrophoresis (PFGE). PFGE was performed as described by Sabbuba *et al.* (2003).

2.4.1 Immobilisation of total genomic DNA in agarose plugs

Strains were grown overnight in 3 ml of LB broth, and cells were recovered by centrifugation (1600 *g* for 10 min). Supernatant was discarded, and cells were resuspended in 500 µl of SE buffer (75 mM NaCl, 25 mM EDTA). The suspension was then centrifuged (6000 *g* for 10 min), supernatant discarded, and cells resuspended in 400 µl SE buffer. Optical density of the resulting suspensions was adjusted to 1.0 by addition of SE buffer. Optical density was measured in semi-micro cuvettes (Fisher Scientific) using a Helios$^{\gamma}$ UV-Vis spectrophotometer (Unicam, Cambridge, UK), at a wavelength of 620 nm, against a blank of SE buffer. The remainder of the diluted sample was retained as a sterile cell suspension.

The bases of plug moulds (Biorad) were sealed with adhesive tape and secured to a clean plastic tray. An aliquot (300 µl) of the cell suspension, was incubated at 45°C in a water bath, then mixed thoroughly with 300 µl of molten plug mould agarose (2% w/v agarose in SE buffer, held at 45°C to maintain fluidity). The cell-agarose mixture was then used to fill plug moulds, and allowed to set. The tray was covered and incubated at 4°C for 15 min to allow plugs to set completely.

Cells immobilised in agarose were digested to liberate genomic DNA, which remained immobilised in the agarose plugs. Solidified plugs were ejected into 5 ml of PEN buffer (0.5 M EDTA, 1% w/v N-lauryl sarcinose, 1 mg/ml pronase, pH 9.6), and incubated overnight at 37°C with mixing by gentle rocking. PEN buffer was removed and plugs were suspended in 12 ml of TE_1 buffer, and incubated at room temperature with gentle agitation for 1 hour. This step was performed five times before plugs were finally suspended in 5 ml TE buffer and stored at 4°C until required.

2.4.2 Restriction digest of immobilised DNA

A sterile glass cover slip was used to cut 2 mm slices from agarose plugs containing immobilised genomic DNA (section 2.4.1). Plug slices were transferred to sterile eppendorfs containing 150 µl digestion mixture. Digestion mixtures were composed of: 15 µl of 10X restriction buffer, 15 µl 10X BSA, 10 units *Not*I restriction endonuclease (in a volume of 1 µl), 119 µl sterile deionised water. Tubes were centrifuged briefly to ensure slices were immersed in digestion mixture and incubated overnight at 37°C.

2.4.3 Fragment separation

Separation of DNA fragments was performed using a CHEF-DR II pulsed field gel electrophoresis system (Biorad). The gel tank was filled with 2.4 L of TBE buffer. TBE buffer was pre-cooled to 14°C, and maintained at this temperature for the duration of fragment separation by circulation through a refrigeration unit.

The gel was cast using 100 ml of 1.2% (w/v) agarose in TBE buffer, and allowed to set for 30 min before the comb was removed. Slices of agarose plugs containing genomic DNA were removed from the digest mixture and loaded into the wells of the gel. Molecular size markers, consisting of Lambda DNA (Biorad) were prepared according to manufacturer's instructions, and loaded into desired wells. Wells were then filled with plug sealing agarose (1.2% w/v agarose in TBE buffer), to seal in plugs, and the gel positioned in the gel tank. Separation of fragments was performed at 6 V/cm with switching times of 1-3 s for 8 hours followed by 30-70 s for 16 hours. Gels were then stained and viewed as in section 2.13.

2.5 Southern hybridisation

2.5.1 Transfer of DNA to positively charged membranes (squash blot)

DNA fragments were separated by gel electrophoresis (section 2.3.1), or pulsed field gel electrophoresis (section 2.4), and transferred from the agarose gel to a positively charged nylon membrane. Gels were washed briefly in TE_1 buffer, and unused segments removed, along with the bottom right hand corner to allow orientation. Gels were immersed in 200 ml of denaturing solution (0.5 M NaOH, 1.5 M NaCl) and incubated at room temperature for 15-20 min with gentle agitation.

Four pieces of quick draw paper (Sigma) were cut to the size of the gel and wetted in denaturing buffer. Gels were placed face down onto three layers of the wet blotting paper. A positively charged nylon membrane (Roche) was cut to the size of the gel, labelled on one side and carefully placed onto the back of the gel so that the labelled side, or DNA side, was in direct contact with the gel. Care was taken to ensure that the membrane did not overhang the edge of the gel, and any air bubbles were removed. The fourth piece of wet quick draw paper was placed on top of the nylon membrane, and six additional layers were cut to the size of the gel and positioned on top.

The remaining denaturing buffer was poured into the bottom of the tray and a heavy weight placed on top of the completed squash blot. Care was taken to ensure that the weight was distributed as evenly as possible over the squash blot. Blots were incubated overnight at room temperature, to allow transfer of DNA. After transfer, the nylon membrane was placed in equilibration buffer (0.5 M Tris-Cl pH8, 1.5 M NaCl) for 1-5 min with gentle agitation, and rinsed with 2 X SSC buffer (17.53 g/L

NaCl, 8.82 g/L sodium citrate, pH7.0). DNA was fixed to the membrane by exposure to UV light for 3 min.

2.5.2 Generation of digoxygenin labelled nucleic acid probes

Digoxygenin (DIG) labelled probes were generated by the general PCR reaction outlined in section 2.3.2, using primers specific to the sequence of interest. However, in these reactions, standard dNTPs were replaced by DIG-labelled dNTPs (Roche). DIG-labelled probes were visualised by gel electrophoresis, to verify product size and ensure PCR was successful. Individual PCR reactions containing DIG probes were stored at -20°C until required, and used without further processing.

2.5.3 Hybridisation of digoxygenin labelled probes to target sequences

DNA bound to nylon membranes was probed using DIG labelled nucleic acid probes, specific to the sequence of interest. Membranes were wetted with TE_1 buffer and placed in hybridisation tubes (Fisher Scientific), with the DNA side facing the interior of the tube containing. DIG Easy Hyb buffer (20 ml) (Roche) was added and tubes were incubated at hybridisation temperature, with continuous rotation in a hybridisation oven (Stuart Scientific, Redhill, UK). The hybridisation temperature (HT) for each probe was calculated using the following formula:

$$HT = Tm - 20°C$$

$$Tm = 49.82 + (0.41 \times G+C\%) - (600/L)$$

Where Tm = Melting temperature, G+C% = G+C content of probe, and L = Probe length. However, the calculated hybridisation temperature was often adjusted in subsequent experiments to optimise probe hybridisation and detection.

DIG labelled probes (Section 2.5.2) were thawed and incubated in a boiling water bath for 10 min, then cooled on ice for 1 min. An aliquot of probe (10 µl) was mixed thoroughly with 500 µl of DIG Easy Hyb buffer and transferred into the hybridisation tube. Tubes were then incubated overnight at hybridisation temperature with continuous rotation.

2.5.4 Chemiluminescent detection of digoxygenin labelled probes

DIG labelled probes, bound to homologous target sequences on nylon membranes, were detected using a commercially available kit for the detection of DIG labelled probes by chemiluminescence (Roche). This contained anti-DIG antibodies conjugated to the enzyme alkaline phosphotase (anti-DIG-AP fragments), membrane blocking reagent to prevent non-specific antibody binding, and alkaline phosphatase substrate CSPD. Washing buffer, blocking solution, and antibody solution were constituted using maleic acid buffer (0.1 M Maleic acid, 0.15 M NaCl, pH7.5).

After probe hybridisation, probes not bound to homologous sequences were removed by washing membranes twice for 15 min in 20 ml of 2X sodium chloride sodium citrate (SSC) washing solution (17.53 g/L NaCl, 8.82 g/L sodium citrate, 0.1% w/v SDS), then twice for 15 min in 20 ml of 0.1X SSC washing solution (0.877 g/L NaCl, 0.441 g/L sodium citrate, 0.1% w/v SDS). These washes were carried out at a temperature 10°C above the hybridisation temperature. All further washes were carried out at room temperature.

Membranes were then rinsed in 100 ml washing buffer (maleic acid buffer pH7.5, 0.3% w/v Tween 20) for 1 min. Membranes were then incubated in 100 ml blocking

solution (maleic acid buffer, 10% w/v blocking reagent) (Roche) for 30 min, to prevent non-specific antibody binding. This was followed by a 30 min wash in antibody solution (20 ml), which consisted of anti-DIG-AP fragments (Roche) diluted 1:10,000 in blocking solution. Finally membranes were washed twice for 15 min in washing buffer. Membranes were then equilibrated by immersion in 20 ml of detection buffer (0.1 M Tris-HCl, 0.1 M NaCl, pH9.5) for 2-5 min.

2.5.5 Visualisation

Equilibrated membranes were placed on a plastic sheet, DNA side up. An aliquot (1 ml) of the alkaline phosphatase substrate CSPD, diluted 1:100 in detection buffer, was distributed evenly over the surface of the membrane. A second plastic sheet was placed over the membrane, excess liquid and air bubbles removed, and the edges sealed with cling film to create development folder. Development folders were then incubated for at 37°C for 15-30 min, to allow the reaction to begin. Antibodies bound to DIG labelled probes were visualised by exposure of development folders to Kodak X-ray film (Sigma) in an autoradiogram cassette, at 37°C. X-ray film was exposed for 30 min-1 hour, before films were developed using standard Kodak developing and fixing solutions (Sigma), according to manufacturer's protocols. Exposure time varied with individual experiments, and all exposure and development of X-ray film was carried out in a dark room.

2.6 Mutagenesis of *P. mirabilis*

2.6.1 Random transposon mutagenesis.

P. mirabilis strain B4 was subjected to random transposon mutagenesis with either Tn*5*-OT182 or mini-Tn*5*Km2 (Table 2.2). Each suicide delivery vector was transferred to *P. mirabilis* strain B4 by conjugation, according to the method described in section 2.3.7. Trans-conjugants harbouring transposon inserts were selected on MacConkey agar containing polymixin (PMX) (60 units/ml) to eliminate *E. coli* donor strains, and either Tc (200 μg/ml) to select for Tn*5*-OT182, or Km (30 μg/ml) to select for mini-Tn*5*Km2.

Several trans-conjugant *P. mirabilis* colonies were selected at random and sub-cultured on MacConkey agar with appropriate antibiotic selection. These were confirmed as *P. mirabilis* using the BBL Crystal Enteric/Non-fermenter ID system, and used in subsequent experiments to evaluate success of mutagenesis (Section 2.6.2, 2.6.3, and 2.6.4).

2.6.2 Loss of plasmid delivery vector

pOT182: To verify loss of the pOT182 suicide delivery vector, plasmid DNA was extracted from the trans-conjugants selected after mutagenesis, and compared to pOT182 plasmid DNA purified from *E. coli* SM10 by gel electrophoresis.

pUT: Loss of the pUT delivery vector was confirmed by *Bam*HI digest of plasmid DNA, extracted from the trans-conjugants selected after mutagenesis. Products of digestion were compared to *Bam*HI digested pUT (purified from *E. coli* S17.1λ*pir*)

by gel electrophoresis (Section 2.3.1). In addition, mutants were also confirmed as sensitive to Amp (100 μg/ml).

2.6.3 Confirmation of transposon insertion

Trans-conjugants were screened to confirm presence of the transposon. Presence of a transposon, in each of the selected trans-conjugants, was identified by PCR using primers specific to each transposon. Primers NPTII_F1, NPTII_R1 (Table 2.3) were used to confirm presence of mini-Tn*5*Km2, while primers TetA1, TetA2 (Table 2.3) were used for Tn*5*-OT182. Template DNA for PCR reactions was prepared by homogenising a small amount of growth from an LB agar plate in 10 X PCR buffer (20 μl), and incubating in a boiling water bath for 10 min to lyse cells. PCR products were visualised by gel electrophoresis and compared to control reactions performed on purified pOT182, or pUTmini-Tn*5*Km2.

2.6.4 Verification of single random insertion

To confirm single, random insertion of both transposons (Tn*5*-OT182, and mini-Tn*5*Km2) total genomic DNA was extracted from the trans-conjugants selected after mutagenesis, and digested with restriction enzyme *Not*I. Fragments were separated by pulsed field gel electrophoresis (Section 2.4), and analysed by southern hybridisation using digoxygenin labelled probes specific to the appropriate transposon (Section 2.5). Tn*5*-OT182 specific probes were generated from plasmid pOT182 template DNA using primers TET_A1, TET_A2 (Table 2.4), while mini-Tn*5*Km2 specific probes were generated from plasmid pUTmini-Tn*5*Km2 template DNA using primers P2, P4 (Table 2.4).

2.6.5 Isolation of swarming-deficient mutants

Following mutagenesis with mini-Tn*5*Km2, 1000 distinct *P. mirabilis* trans-conjugant colonies were picked off MacConkey agar plates, and stabbed into the centre of LB agar plates solidified with 0.7% (w/v) agar. Plates were incubated overnight at 37°C, and mutants deficient in swarming were identified by their inability to spread over the surface of the agar plates (Figure 2.2). Mutants were sub-cultured on LB agar before being stored at -80°C until required. As a control for a spontaneous non-swarming phenotype, 1000 wild type *P. mirabilis* colonies were also screened in the same way.

Figure 2.2: Isolation of swarming-deficient mutants

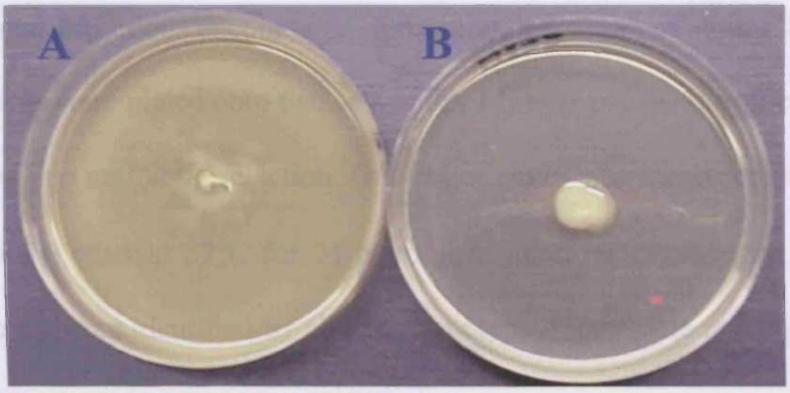

A: *P. mirabilis* wild type (Strain B4), **B:** Non-swarming mini-Tn*5*Km2 mutant

2.6.6 Identification of pUT co-insertion

Swarming deficient mutants were screened for co-insertion of portions of the pUT delivery vector. Co-insertion was identified using a PCR based screen and a plate based assay.

PCR based screen: Three sets of primers were designed to amplify different portions of the pUT plasmid: (i): PUTTn5L_F1, PUTTn5L_R1 (ii) PUTTn5R_F1, PUTTn5R_R1 (iii) PUTBla_F1, PUTBla_R1. Details of the regions amplified by the

primer sets are given in Table 2.4, and illustrated in Figure 2.1. PCR products were visualised by gel electrophoresis, and compared to products amplified from pUT plasmid DNA, purified from *E. coli* S17.1*λpir*. Negative control reactions contained wild type genomic DNA as the template.

Plate based assay: Co-insertion of portions of the pUT plasmid, containing the β-lactamase producing *bla* gene, were identified by growth on LB agar containing Amp (100 μg/ml).

2.6.7 Stability of swarming-deficient mutants.

The phenotypic stability of swarming deficient mutants was assessed under a range of environmental conditions encountered during routine culture of strains. Swarming deficient mutants were plated onto two sets of dry LB agar plates, in triplicate. These plates contained no antibiotic selection. One set of plates was incubated at 37°C for 72 hours, and the other at 37°C for 24 hours then room temperature for 48 hours. Unstable mutants were identified by altered phenotype or complete reversion to wild type phenotype.

2.6.8 Urease assay

Urease activity of swarming deficient mutants was measured using a protocol modified from Creno *et al.* (1970). *P. mirabilis* strains were cultured for 4 hours in 5 ml LB broth supplemented with urea (0.1% w/v). Cells were harvested by centrifugation (1600 *g* for 10 min), the supernatant discarded, and pellets resuspended in 2.5 ml of ice-cold sodium phosphate buffer (0.1 M sodium phosphate, 10 mM EDTA. pH7.3). Total protein in cell suspensions was determined using a Micro Protein Determination kit (Sigma) according to manufacturer's instructions.

To measure urease activity, 200 µl of cell suspension was added to 800 µl of reaction buffer (50 mM urea, 0.1 M sodium phosphate), mixed thoroughly and incubated at 37°C for 10 min. The addition of phenol sodium nitroprusside solution (2 ml) (0.5% phenol w/v, 0.025% w/v sodium nitroprusside) was used to terminate the reaction. Colour development was initiated by addition of sodium hypochlorite solution (2 ml) (0.2% w/v sodium hydroxide, 0.21% w/v sodium hypochlorite). These mixtures were incubated at 56°C for 5 min. Colour change was measured against a blank containing 200 µl of sodium phosphate buffer instead of cell suspension, at 626 nm using a Helios$^{\gamma}$ UV-Vis spectrophotometer (Unicam). Urease activity was expressed as mM urea hydrolysed/min/mg protein. Urease activity was calculated using a standard curve of ammonium chloride solutions ranging in concentration from 0.01 mM to 10 mM.

2.6.9 Assessment of swimming and swarming activities.

Swarming motility was characterised on LB agar (1.5% w/v agar). Plates were dried overnight at room temperature, then for 15 min in a laminar flow cabinet with the lids removed. A 10 µl drop of overnight culture was inoculated onto the centre of each plate. The drops were allowed to soak into the agar at room temperature, and then the plates were incubated for 8 hours at 37°C. To assess swimming motility, 2 µl drops of overnight culture were stabbed into the centre of LB agar plates solidified with 0.3% (w/v) agar, and plates incubated for 6 hours at 37°C. The distance migrated on both types of agar from the point of inoculation was measured. The swimming and swarming ability of each mutant was expressed as a percentage of that of the wild type motility.

2.7 Electron microscopy

2.7.1 Demonstration of flagella production and structure

Flagella of wild type *P. mirabilis* and mutants were visualised by negative staining of swimmer cells and examination by transmission electron microscopy (TEM). Strains were grown in LB broth overnight at 37°C with aeration. For mutant strains LB broth was supplemented with Km (30 μg/ml). Formavar coated copper grids were floated on a drop of overnight culture for 1 min. Grids were then washed three times by floating on drops of sterile deionised water for 30 s. Finally cells were negatively stained by floating the grids on a drop of 1% uranyl acetate for 1 min. Samples were then viewed using a Philips TEM208 transmission electron microscope.

2.7.2 Scanning electron microscopy of swarm fronts

Swarm fronts of mutants and wild type *P. mirabilis* were fixed *in situ* on LB agar using vapour fixation. *P. mirabilis* strain B4 was grown in LB broth while mutant strains were cultured in LB broth supplemented with Km (30 μg/ml). Cultures were incubated overnight at 37°C with aeration. Aliquots (10 μl) of overnight cultures of test strains were inoculated onto the centre of the LB agar plates and incubated at 37°C to allow swarming. Plates were removed during active migration of swarm fronts and suspended face down over 10 ml of an aqueous solution containing 12.5% EM grade glutaraldehyde (Agar Scientific, Stanstead, UK), and 8% paraformaldehyde (Agar Scientific), in a sealed staining dish for 18-24 hours at room temperature. After vapour fixation, blocks of agar (1 cm^2) supporting a section of the swarm front were cut from the plates using a sterile scalpel. Blocks were stained by immersion in aqueous osmium tetroxide (1% w/v) (Agar Scientific) for 1 hour, and

dehydrated in a series of ethanol solutions before critical point drying. The dehydrated blocks were then sputter coated with gold and swarm fronts viewed using a Philips XL20 scanning electron microscope.

2.7.3 Transmission electron microsocopy of swarm fronts

Swarm fronts of *P. mirabilis* strain B4 were prepared by *in situ* vapour fixation as for SEM observations. The agar blocks supporting swarm fronts were post fixed by immersion in aqueous osmium tetroxide (1% w/v), then dehydrated in a series of ethanols (70%, 90%, 2 x 100% v/v). Dehydrated blocks were "cleared" by immersion in propylene oxide twice for 15 min, and infiltrated with Araldite embedding resin for 30 hours with agitation at room temperature. Blocks were then embedded in resin, which was polymerised by incubation at 60°C for 24 hours. Thin sections (80 nm thick) were cut from embedded blocks using a Reichart Ultracut microtome and diamond knife. The thin sections were collected on uncoated copper grids, and stained by immersion in aqueous uranyl acetate (2% w/v) for 10 min, then Reynold's lead citrate for 5 min. Samples were viewed using a Philips TEM208 transmission electron microscope.

2.8 Construction of B4 genomic DNA library.

2.8.1 Partial digest of B4 genomic DNA

Total genomic DNA was extracted from *P. mirabilis* B4 using the method described in section 2.3.6, and dissolved in sterile deionised water. A bulk digestion mix was prepared, consisting of: 120 µl restriction buffer, 12 µl 100X BSA, 300 µl of a genomic DNA solution (~90 µg *P. mirabilis* B4 DNA), and 768 µl of sterile deionised water. The bulk digestion mix was distributed between nine micro-centrifuge tubes (200 µl in tube 1, 100 µl in tubes 2-9).

To the first tube only, 2 µl of a *Sau* 3A solution (0.1 units/µl) was added, and mixed thoroughly. An aliquot of the mixture in tube 1 (100 µl) was transferred to tube 2, and mixed thoroughly. This step was repeated for tubes 3-8 to create a series of doubling dilutions. Tube 9 served as a control for the quality of DNA, and was not provided with enzyme. The resulting digestion mixtures were incubated at 37°C for 1 hour. A small aliquot of the products were visualised by gel electrophoresis (1% w/v agarose gel). During visualisation the remainder of the digests were stored at -20°C. Digests showing desired level of digestion were immediately purified using methods described in section 2.3.7, and dissolved in sterile deionised water.

2.8.2 Ligation of *Sau* 3a fragments into pSCOSPA1

Cosmid vector pSCOSPA1 was digested with restriction enzyme *Bam*HI, and products purified using a QIAquick PCR purification kit (Qiagen). Ligations were set up, consisting of: 3 units T4 ligase, 2 µl of 10X ligation buffer, 7 µl of pSCOSPA1 DNA (~ 1 µg), 10 µl *Sau* 3a digested *P. mirabilis* B4 DNA (~1-3 µg). Ligations were incubated overnight at 4°C.

2.8.3 Packaging of cosmid library

Products generated by ligations described in section 2.8.2, were packaged into bacteriophage λ capsids using the Gigapack III XL *in vitro* packaging kit (Stratagene). An aliquot of packaging extract was thawed quickly, and combined with ligation products (4 µl). The resulting mixture was incubated at room temperature for 2h. Following incubation, 500 µl of SM buffer (NaCl 5.8g/L, $MgSO_4.7H_2O$ 2.0g/L, 50mM Tris-Cl pH7.5, 0.01% w/v gelatin), and chloroform (20 µl) was added and mixed gently. Debris and chloroform were removed by brief centrifugation (10,000 *g* for 1 min), and the supernatant, containing packaged cosmid DNA, was removed to a fresh tube. This was then used for transfection of *E. coli* VCS257.

2.8.4 Transfection of packaged library to *E. coli* VCS257

E. coli VCS257 was grown overnight on LB agar, and used to inoculate 3 ml of LB broth supplemented with maltose (0.2% w/v) and $MgSO_4$ (10 mM). Cultures were grown for 4 hours at 37°C with aeration. Cells were recovered by centrifugation (1600 *g* for 10 min), and resuspended in a solution of 10 mM $MgSO_4$. The optical density of this suspension was adjusted to 0.5-1.0 (λ600 nm) with 10 mM $MgSO_4$ solution, using a Helios$^{\gamma}$ UV-Vis spectrophotometer (Unicam). The resulting suspension was used immediately. Packaged cosmid DNA (5 µl) was mixed with 45 µl of the cell suspension, and incubated at room temperature for 30 min. The suspension was then supplemented with LB broth (200 µl) and incubated at 37°C for 1 hour. During incubation, tubes were agitated every 15min. Aliquots of neat suspension (100 µl) and dilutions (1:10, 1:100, and 1:1000 in LB broth) were spread

over LB agar plates with containing Gm (10 μg/ml), and incubated overnight at 37°C.

2.8.5 Organisation and storage of library.

Individual *E. coli* VCS287 colonies carrying cosmids were inoculated into the wells of 96 well tissue culture plates, containing LB broth (100 μl per well) supplemented with Gm (10 μg/ml). A total 1056 colonies were picked into eleven tissue culture plates. Plates were incubated overnight at 37°C with aeration, then wells were supplemented with a sterile 40% (v/v) glycerol solution (100 μl). Contents of wells were mixed thoroughly, and plates were stored at -80°C until required.

2.9 Identification of disrupted genes, and complementation of swarming-deficient mutants

2.9.1 Cloning of disrupted genes

The cloning and sequencing strategy, for the identification of disrupted genes, is illustrated in Figure 2.3. Total genomic DNA was extracted from swarming deficient mutants as described in section 2.3.6, and dissolved in sterile deionised water. Extracted DNA was digested with restriction enzyme *Pst*I (Section 2.3.3). Complete digestion was verified by gel electrophoresis (Section 2.3.1), and DNA purified using a QIAquick PCR purification kit (Qiagen). This solution was used to set up ligations according to section 2.3.13, containing 4 µl of digested genomic DNA (~500 ng DNA), and 1 µl of *Pst*I digested pUC18 (~100 ng DNA). The resulting ligation products were transformed into *E. coli* JM109 (see section 2.3.9). Clones containing pUC18 with desired inserts were selected on LB agar containing Km (30 µg/ml).

The resulting colonies were sub-cultured in LB broth (3 ml) supplemented with Km (30 µg/ml), and plasmids purified using a Wizard SV Plus miniprep kit (Promega). The presence of inserts, composed of mini-Tn*5*Km2 segments plus flanking chromosomal DNA, in purified plasmids was confirmed by PCR (Section 2.3.2) using mini-Tn*5*Km2 specific primers NptII_F1, NptII_R1 (Table 2.4, 2.5), and digestion of constructs with *Pst*I (Section 2.3.3). Products were visualised by gel electrophoresis (Section 2.3.1), and compared to products from PCR reactions and digests performed on non-recombinant pUC18.

Figure 2.3: Identification of genes disrupted by mini-Tn*5*Km2.

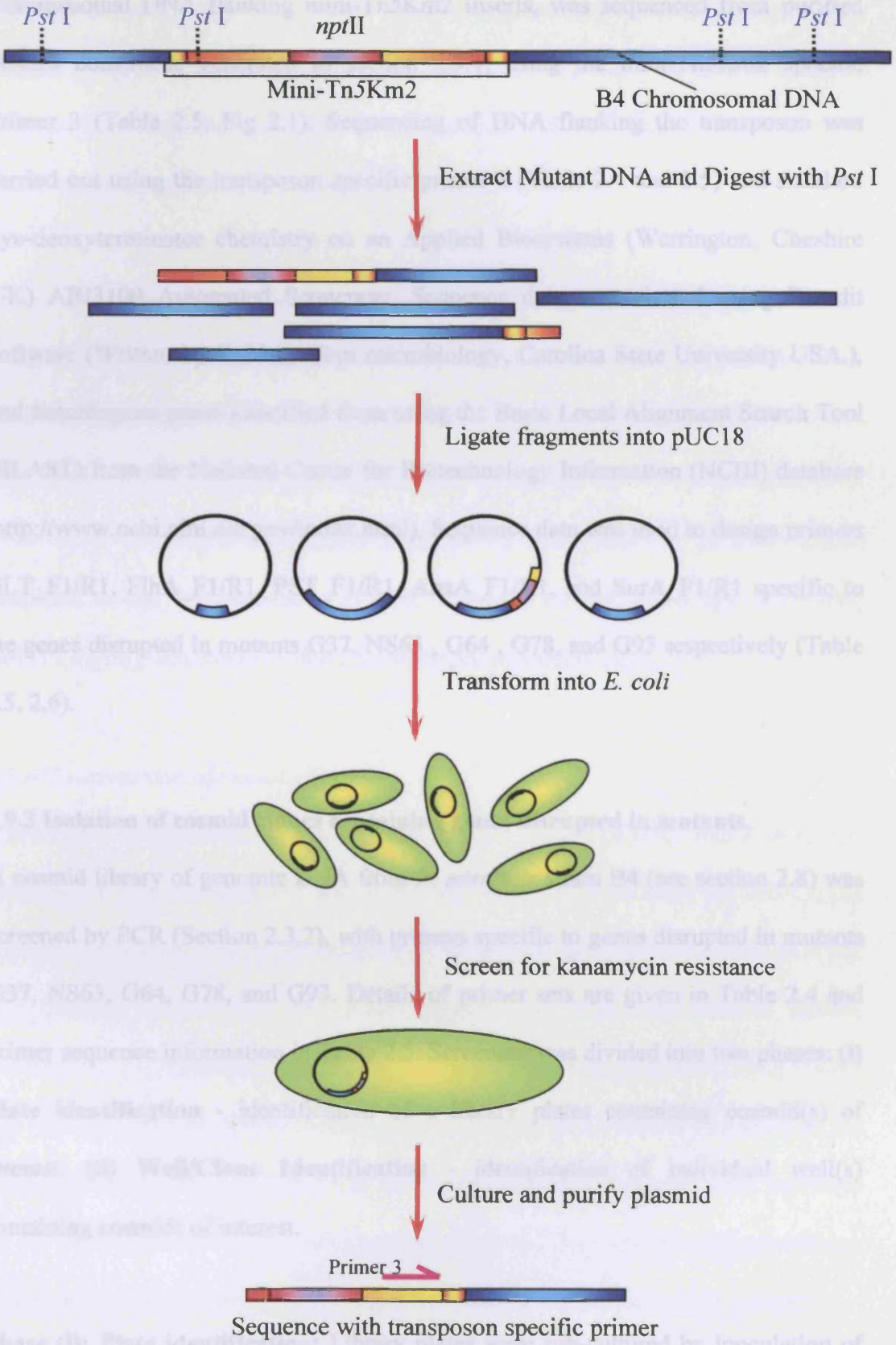

2.9.2 Sequencing and identification of disrupted genes

Chromosomal DNA flanking mini-Tn*5*Km2 inserts, was sequenced from purified pUC18 constructs, generated in section 2.9.1, using the mini-Tn*5*Km2 specific Primer 3 (Table 2.5, Fig 2.1). Sequencing of DNA flanking the transposon was carried out using the transposon specific primer 3 (Table 2.4 and 2.5) and standard dye-deoxyterminator chemistry on an Applied Biosystems (Warrington, Cheshire UK) ABI3100 Automated Sequencer. Sequence data was viewed using Bioedit software (Written by T. Hall, Dept microbiology, Carolina State University USA.), and homologous genes identified from using the Basic Local Alignment Search Tool (BLAST) from the National Centre for Biotechnology Information (NCBI) database (http://www.ncbi.nlm.nih.gov/index.html). Sequence data was used to design primers GLT_F1/R1, FlhA_F1/R1, PST_F1/R1, AnsA_F1/R1, and SurA_F1/R1 specific to the genes disrupted in mutants G37, NS63 , G64 , G78, and G93 respectively (Table 2.5, 2.6).

2.9.3 Isolation of cosmid clones containing genes disrupted in mutants.

A cosmid library of genomic DNA from *P. mirabilis* strain B4 (see section 2.8) was screened by PCR (Section 2.3.2), with primers specific to genes disrupted in mutants G37, NS63, G64, G78, and G93. Details of primer sets are given in Table 2.4 and primer sequence information in Table 2.5. Screening was divided into two phases: **(i) Plate identification** - identification of a library plates containing cosmid(s) of interest. **(ii) Well/Clone Identification** - identification of individual well(s) containing cosmids of interest.

Phase (i): Plate identification: Library plates were sub-cultured by inoculation of duplicate 96 well plates, containing LB broth (100 µl per well) supplemented with

Gm (10 μg/ml). Replica plates were incubated overnight at 37°C with aeration. The contents of each plate were divided into 2 pools, and the cosmids purified using Wizard SV plus mini-prep kit (Promega). These cosmid pools were used as template DNA in individual PCR reactions (Section 2.3.2) with each primer set, to identify plates containing cosmid clones of interest.

Phase (ii): Well/Clone identification: Plates identified as containing clones of interest were sub-cultured as in phase (i), and individual wells screened by PCR (Section 2.3.2) to identify cosmids of interest. Template DNA was prepared from individual wells. An aliquot of culture (5 μl) from each well was mixed with 10 X PCR buffer (20 μl), and incubated in a boiling water bath for 10 min. Clones identified as carrying cosmids of interest were sub-cultured on LB agar containing Gm (10 μg/ml), and stored at -80°C as described in section 2.2.2.

2.9.4 Construction of vector pB4

Vector pB4 was constructed to enable transfer and cloning of DNA into *P. mirabilis* strain B4. It is a derivative of plasmid pOT182 which does not carry the Tn*5*-OT182 transposon (Figure 2.4). Construction was performed as follows: Plasmid pOT182 was purified from *E. coli* SM10 and digested with restriction enzyme *Bam*H1 (Section 2.3.3). Digestion generated two fragments consisting of Tn*5*-OT182 (11264 bp), and the vector backbone (7316 bp) containing the p15A origin of replication, the RP4 origin of transfer, Gm, and Cm resistance cassettes. Fragments were separated by gel electrophoresis on 1% (w/v) agarose (Section 2.3.1), and the vector backbone fragment purified by gel extraction using a QIAquick Gel Extraction kit (Qiagen).

Figure 2.4: Map of vector pB4

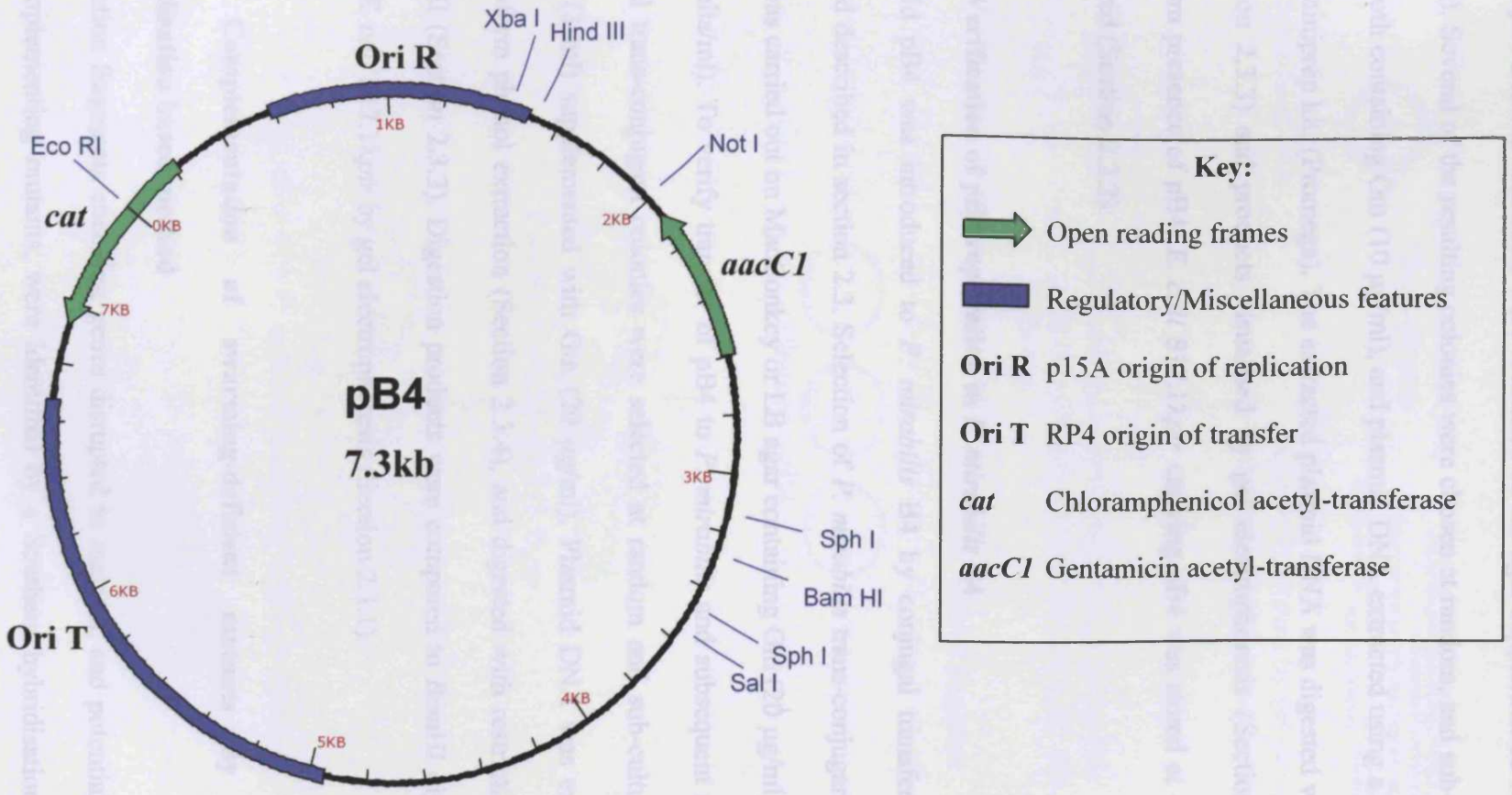

The purified fragment was re-circularised by ligation, and transformed into *E. coli* S17.1λ*pir*. Desired constructs were identified on LB agar supplemented with Gm (10 μg/ml). Several of the resulting colonies were chosen at random, and sub-cultured in LB broth containing Gm (10 μg/ml), and plasmid DNA extracted using a Wizard SV plus miniprep kit, (Promega). The extracted plasmid DNA was digested with *Bam*HI (Section 2.3.3) and products visualised by gel electrophoresis (Section 2.3.1) to confirm presence of pB4. *E. coli* S17.1λ*pir* carrying pB4 was stored at -80°C until required (Section 2.2.2).

2.9.5 Verification of pB4 replication in *P. mirabilis* B4

Plasmid pB4 was introduced to *P. mirabilis* B4 by conjugal transfer using the method described in section 2.3. Selection of *P. mirabilis* trans-conjugants carrying pB4 was carried out on MacConkey or LB agar containing Gm (20 μg/ml) and PMX (60 units/ml). To verify transfer of pB4 to *P. mirabilis* and subsequent replication, several trans-conjugant colonies were selected at random and sub-cultured in LB broth (3 ml) supplemented with Gm (20 μg/ml). Plasmid DNA was extracted by chloroform phenol extraction (Section 2.3.4), and digested with restriction enzyme *Bam*HI (Section 2.3.3). Digestion products were compared to *Bam*HI digested pB4 from *E. coli* S17.1λ*pir* by gel electrophoresis (Section 2.3.1).

2.9.6 Complementation of swarming-deficient mutants by Southern hybridisation based method

Restriction fragments encoding genes disrupted in mutants, and potentially capable of complementing mutants, were identified by a Southern hybridisation approach (illustrated in Figure 2.5). Cosmid clones containing genes disrupted in swarming

Figure 2.5: Complementation of swarming-deficient mutants by Southern hybridisation based method.

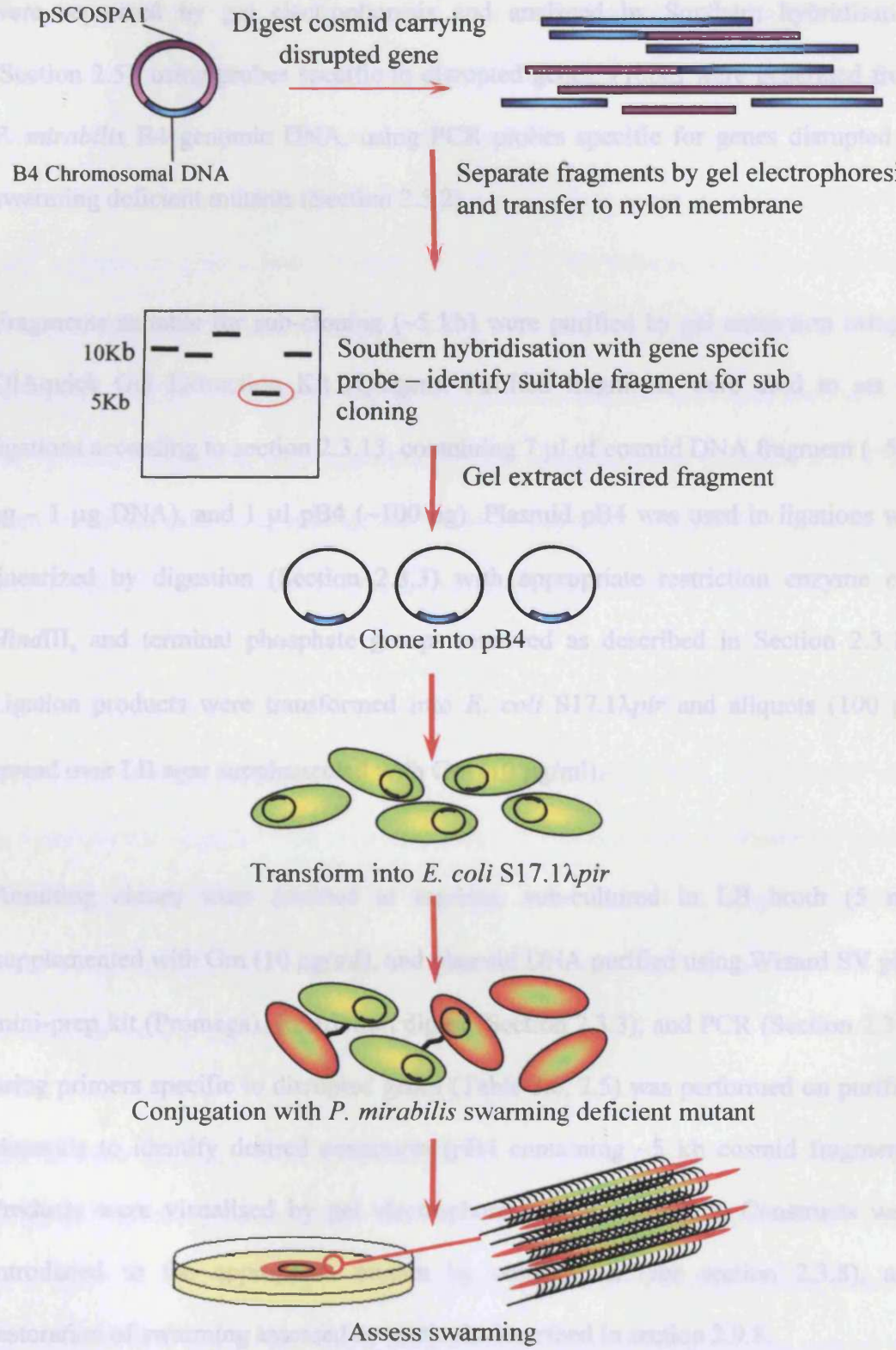

deficient mutants were purified with Wizard SV Plus miniprep kits, and digested with restriction enzymes *Sal*I, *Nco*I, *Not*I, *Hind*III, and *Xba*I (Section 2.3.3). Products were separated by gel electrophoresis and analysed by Southern hybridisation (Section 2.5), using probes specific to disrupted genes. Probes were generated from *P. mirabilis* B4 genomic DNA, using PCR probes specific for genes disrupted in swarming deficient mutants (Section 2.5.2).

Fragments suitable for sub-cloning (~5 kb) were purified by gel extraction using a QIAquick Gel Extraction Kit (Qiagen). Purified fragments were used to set up ligations according to section 2.3.13, containing 7 µl of cosmid DNA fragment (~500 ng – 1 µg DNA), and 1 µl pB4 (~100 ng). Plasmid pB4 was used in ligations was linearized by digestion (Section 2.3.3) with appropriate restriction enzyme e.g. *Hind*III, and terminal phosphate groups removed as described in Section 2.3.14. Ligation products were transformed into *E. coli* S17.1λ*pir* and aliquots (100 µl) spread over LB agar supplemented with Gm (10 µg/ml).

Resulting clones were selected at random, sub-cultured in LB broth (5 ml) supplemented with Gm (10 µg/ml), and plasmid DNA purified using Wizard SV plus mini-prep kit (Promega). Restriction digest (Section 2.3.3), and PCR (Section 2.3.2) using primers specific to disrupted genes (Table 2.6, 2.5) was performed on purified plasmids to identify desired constructs (pB4 containing ~5 kb cosmid fragment). Products were visualised by gel electrophoresis (Section 2.3.1). Constructs were introduced to the appropriate mutant by conjugation (see section 2.3.8), and restoration of swarming assessed by methods described in section 2.9.8.

2.9.7 Complementation of swarming-deficient mutants using *Sau* 3A partial digestion method

Complementation of mutants by the *Sau* 3A partial digest approach is illustrated in Figure 2.6. Cosmid clones of interest were purified using a Wizard SV Plus miniprep kit and digested with restriction enzyme *Sau* 3A by a modification of protocols described in section 2.8.1. The bulk digestion mixture reagents were combined at $1/6^{th}$ volume, to give a final volume of 200 µl. This mixture was then distributed between nine micro-centrifuge tubes (30 µl in tube 1, 20 µl in tubes 2-9), and provided with *Sau* 3A as described in section 2.8.1. Digests were incubated at 37°C for 45 min. Fragments were separated by gel electrophoresis (Section 2.3.1), and from reactions exhibiting appropriate levels of digestion, fragments 4-6 kb in size were purified by gel extraction using QIAquick Gel Extraction kit (Qiagen).

Purified fragments were used to set up ligations containing 7 µl of purified cosmid fragments (~500 ng – 1 µg DNA), and 1 µl pB4 (~100ng DNA). Plasmid pB4 used in ligations was digested with *Bam*HI (Section 2.3.3) and terminal phosphate groups removed from linearised plasmid as described in section 2.3.14. Ligation products were transformed into *E. coli* S17.1λ*pir*, and aliquots (100 µl) spread over LB agar containing Gm (10 µg/ml).

The plasmid constructs were transferred to the appropriate mutant by a modification of the conjugation protocols described in section 2.3.8. The colonies from five plates of *E. coli* S17.1λ*pir*, transformed with ligations, were harvested and resuspended in LB broth (5 ml). The *E. coli* suspension, and an overnight culture of the appropriate mutant were then processed according to section 2.3.8, but 500 µl of the *E. coli*

Figure 2.6: Complementation of swarming deficient-mutants by *Sau 3A* based method.

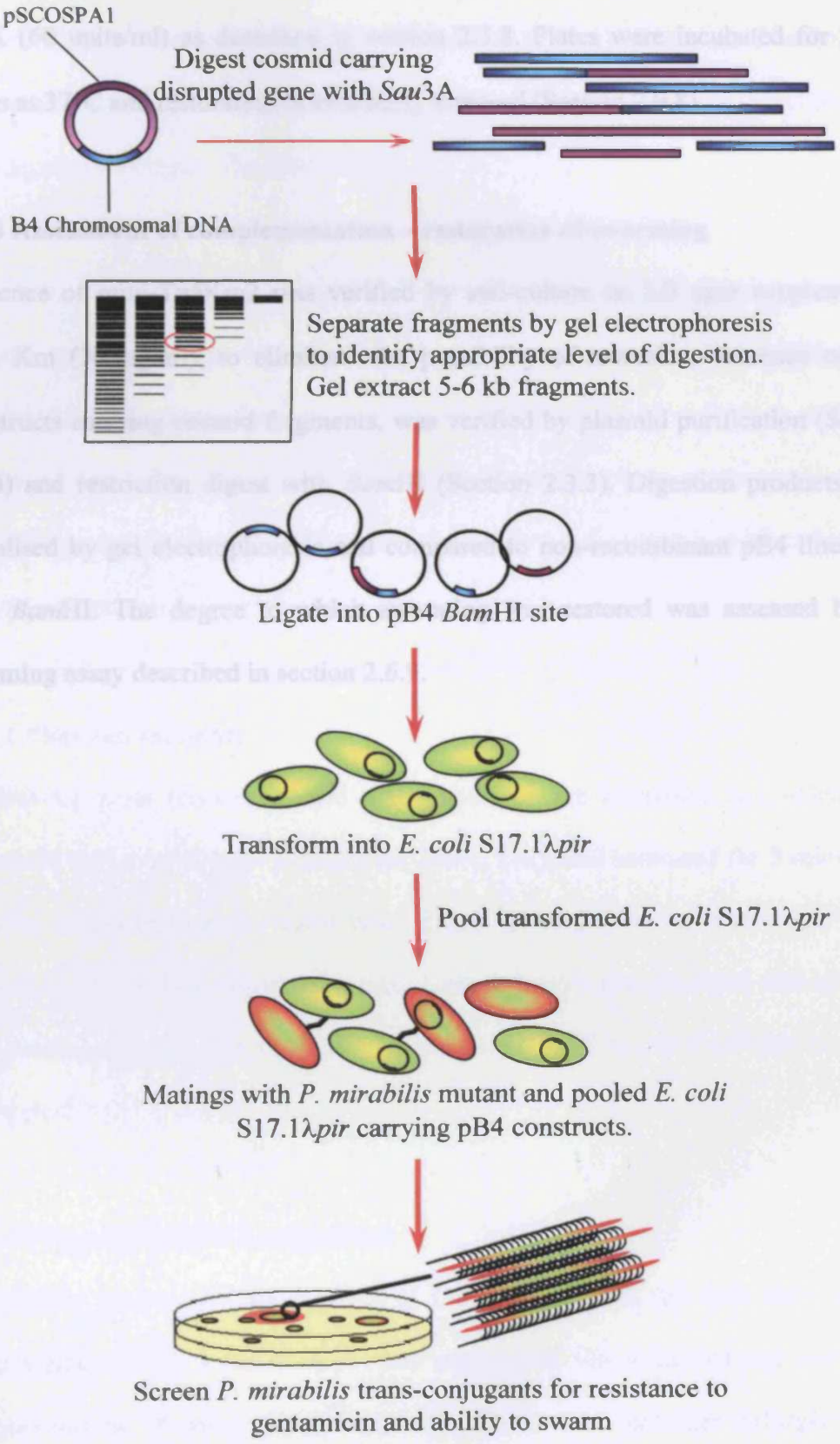

suspension was mixed with 100 µl of the *P. mirabilis* mutant suspension in the final step. Trans-conjugants were spread over LB agar supplemented with Gm (20 µg/ml), PMX (60 units/ml) as described in section 2.3.8. Plates were incubated for 24-48 hours at 37°C and restoration of swarming assessed (Section 2.9.8).

2.9.8 Assessment of complementation – restoration of swarming

Presence of mini-Tn*5*Km2 was verified by sub-culture on LB agar supplemented with Km (30 µg/ml), to eliminate the possibility of reversion. Presence of pB4 constructs carrying cosmid fragments, was verified by plasmid purification (Section 2.3.4) and restriction digest with *Bam*HI (Section 2.3.3). Digestion products were visualised by gel electrophoresis and compared to non-recombinant pB4 linearized with *Bam*HI. The degree to which swarming was restored was assessed by the swarming assay described in section 2.6.9.

2.10 Parallel plate flow chamber

The ability of *P. mirabilis* strain B4 and swarming deficient mutants, to adhere to silicone surfaces, was assessed using a parallel plate flow cell system. The flow cell chamber was purchased from the Laboratory for Materia Technical, University of Groningen, Groningen, The Netherlands.

The flow cell chamber is illustrated in Figure 2.7. The chamber was composed of a nickel coated brass base and lid, which house two glass plates separated by teflon spacers. The base and lid are secured by 14 screws and rubber O-rings to form a watertight seal. Cell deposition was monitored using a phase contrast microscope with a long working distance objective lens. The flow cell system was assembled and run in a constant temperature room maintained at 37°C.

2.10.1 Flow cell assembly

A glass top plate (uncoated), and teflon spacers were immersed in a solution of Decon 90 (2% v/v) (Decon laboratories, Hove, UK), and sonicated for 5 minutes at 60 kHz. Plates and spacers were then washed thoroughly in hot water, and rinsed once in methanol, then deionised water. A glass, bottom plate, (coated with silicone) was positioned in the base of the flow chamber and the flow cell assembled as shown in Figure 2.7.

2.10.2 Preparation of test suspension

Test strains were grown overnight in of LB broth (15 ml), and cells harvested by centrifugation (1600 *g* for 15 min). The supernatant was discarded and cells were resuspended in 15 ml of phosphate buffer (di-sodium hydrogen orthophosphate 11.357 g/L, potassium di-hydrogen orthophosphate 2.722 g/L, pH 7.4). The

Figure 2.7: Parallel plate flow chamber

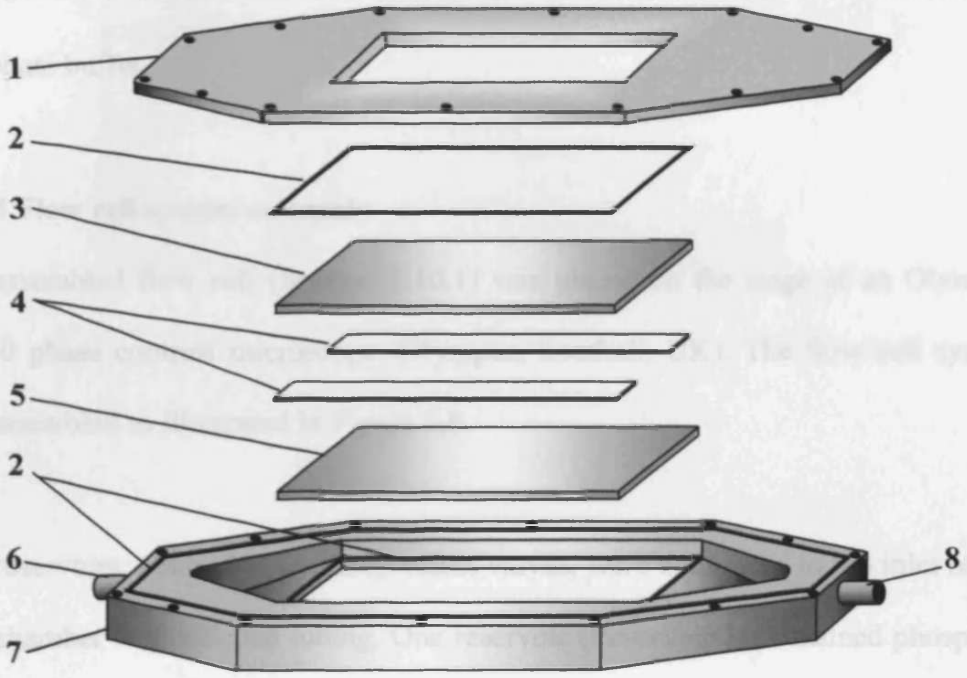

Key:

1: Flow chamber lid

2: Rubber O-rings

3: Glass top plate

4: Teflon Spacers

5: Glass bottom plate (Coated with test material)

6: Flow chamber inlet

7: Flow chamber base

8: Flow chamber outlet

resuspended cells were then sonicated for 20 s at 60 kHz, to break up cell aggregates. Cells were quantified using a haemocytometer (Mod-Fuch's Rosethal, Fisher UK), and adjusted to a final concentration of 3 x 10^8 cells/ml, in a final volume of 250 ml phosphate buffer.

2.10.3 Flow cell system assembly

The assembled flow cell (Section 2.10.1) was placed on the stage of an Olympus BX-40 phase contrast microscope (Olympus, Southall, UK). The flow cell system was assembled as illustrated in Figure 2.8.

Two reservoirs, controlled by independent valves, were connected to the inlet of the flow chamber with silicone tubing. One reservoir (Reservoir 1) contained phosphate buffer, while the other (Reservoir 2) contained the bacterial test suspension. Liquid discharged from the flow chamber outlet was passed to a third reservoir, from which media was re-circulated to the main reservoir via a peristaltic pump (Watson-Marlow). To remove air from the system, phosphate buffer from reservoir 1 was flushed through the system for 15-20 min.

The microscope was equipped with an ultra long working distance objective (LC-ACH x 40 PH, Olympus), and a green interference filter (Olympus, 43 IF550-W45) to improve resolution. The microscope was also equipped with a VC600 CCD video camera (Video Control Ltd), fixed with a camera mount adapter. Images were viewed using a Vista KVM14 monitor (Norbain SDL, Wokingham, UK). Images were captured in TIFF format using a monochrome frame grabber (Mach Series DT3155, Data Translation Ltd), installed in an IBM compatible Pentium II PC.

Figure 2.8: Illustration of the parallel plate flow chamber system.

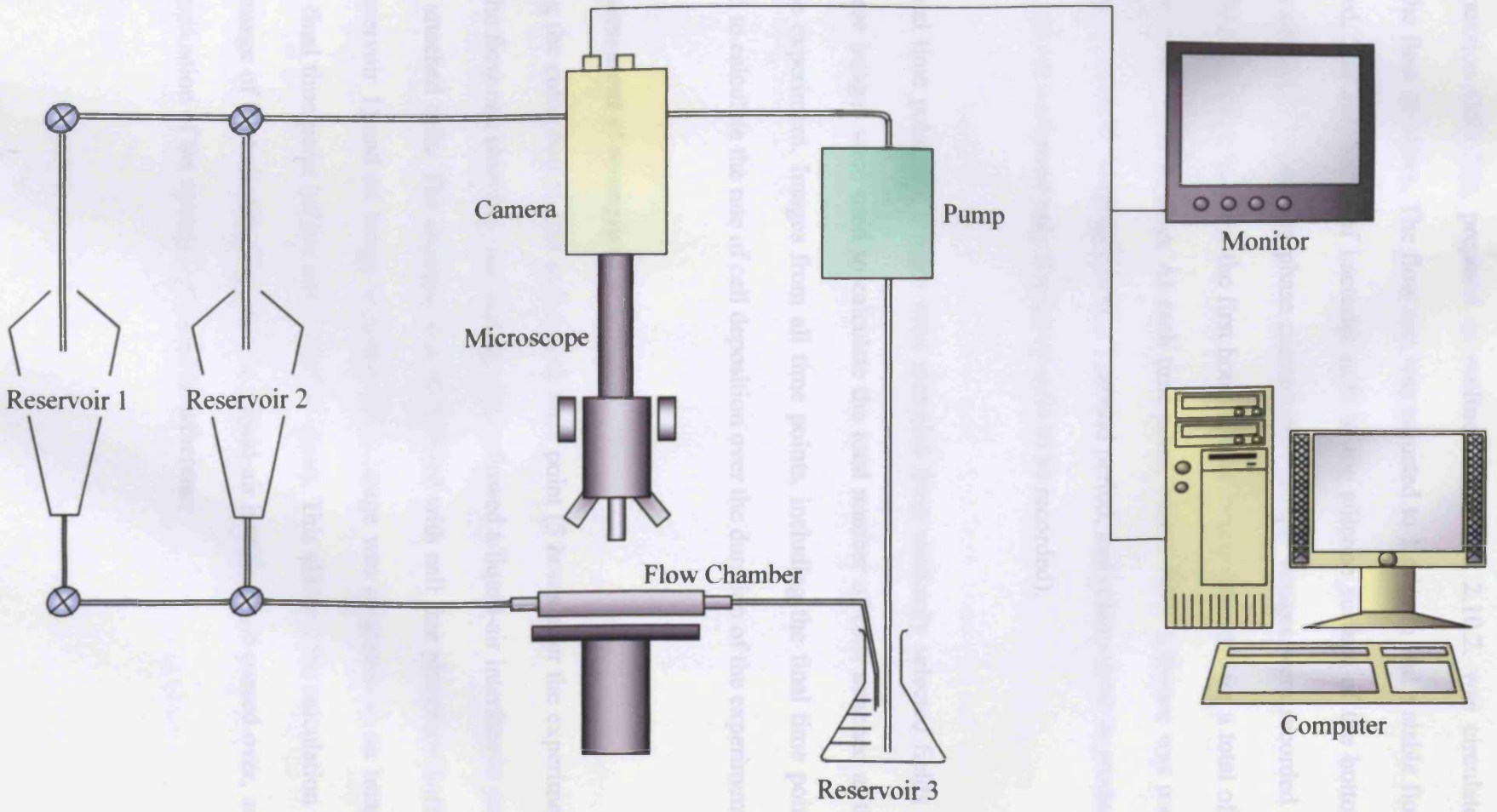

2.10.4 Assessment of *P. mirabilis* adherence to silicone

Test suspension (250 ml), prepared as outlined in section 2.10.2, was circulated through the flow chamber. The flow rate was adjusted to 1 ml/min and a stable flow established. The adherence of bacterial cells to the silicone surface of the bottom plate was observed directly by phase contrast microscopy. Images were recorded at 10 min, 30 min, and 1 hour for the first hour, then at hourly intervals for a total of 5 hours after flow cell activation. At each time point, Vision XXL software was used to recorded a series of 30 images over a 1 second period, and collate these to produce a final image (this allowed only stationary cells to be recorded).

At the final time point, six images were recorded from randomly selected fields of view. These images were used to calculate the total number of cells attached at the end of the experiment. Images from all time points, including the final time point, were used to calculate the rate of cell deposition over the duration of the experiment.

2.10.5 Assessment of strength of adherence

Following the collection of data at the final time point (5 hours after the experiment began), the flow cell chamber was drained. This allowed a liquid-air interface to pass over the attached cells. The chamber was then filled with cell free phosphate buffer (from Reservoir 1) and an image recorded. This image was compared to an image from the final time point (of the same field of view). This allowed the calculation of the percentage of bacteria attached after the liquid-air interface had passed over, and gave an indication of the strength of bacterial adherence.

2.11 Models of infection

2.11.1 Catheter bridge models

The ability of the swarming deficient mutants to migrate over the surfaces of urethral catheters was assessed using the simple model described by Stickler & Hughes (1999). Plates of 1.5% LB agar were dried and 0.8 cm wide channels were cut across their centres. Aliquots (10 µl) of 4 hours cultures of test strains, grown in LB broth, were inoculated at the edge of the channel. After the inocula had dried into the agar, sections (1 cm) of all-silicone, or hydrogel-coated latex catheters (Bard, Crawley, UK) were placed as bridges between the agar blocks, adjacent to points of inoculation. As a control, one point of inoculation on each plate was not provided with a catheter bridge, and the corresponding area of the opposing agar block isolated by a 0.5 cm channel (Figure 2.8). Plates were incubated at 37°C for 24 hours, and migration across

2.11.2 *In vitro* bladder models

An *in vitro* model of the catheterised urinary tract (Stickler *et al.* 1995) was used to assess the ability of swarming deficient mutants to form crystalline biofilms, and block all-silicone urethral catheters (Figure 2.9). Bladder models consisted of glass containers surrounded by a water jacket, with an outlet from the interior chamber of the vessel (Figure 2.9). A section (10 cm) of silicone tubing attached to the outlet of the model and served as the urethra. Each strain was tested in triplicate, and the time taken for catheters to become completely obstructed recorded. The pH of media in models, and the number of viable cells at model activation and time of blockage, was also measured.

Figure 2.9: An example of a catheter bridge model.
P. mirabilis swarming over 1 cm sections of hydrogel-coated latex catheter. Image kindly provided by Dr. N Sabbubba.

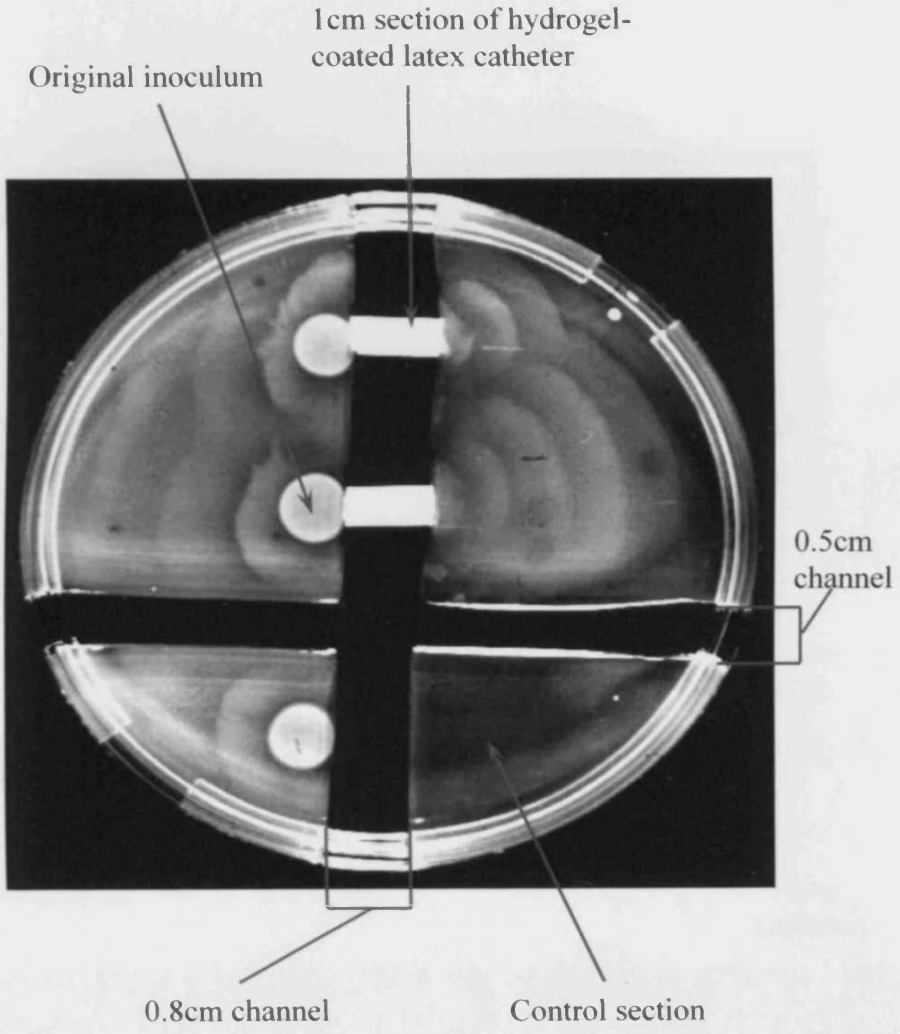

Figure 2.10: Illustration of an *in vitro* bladder model.
Arrows indicate flow of liquid through system: yellow = flow of urine, blue = flow of water for maintaining temperature of model at 37°C

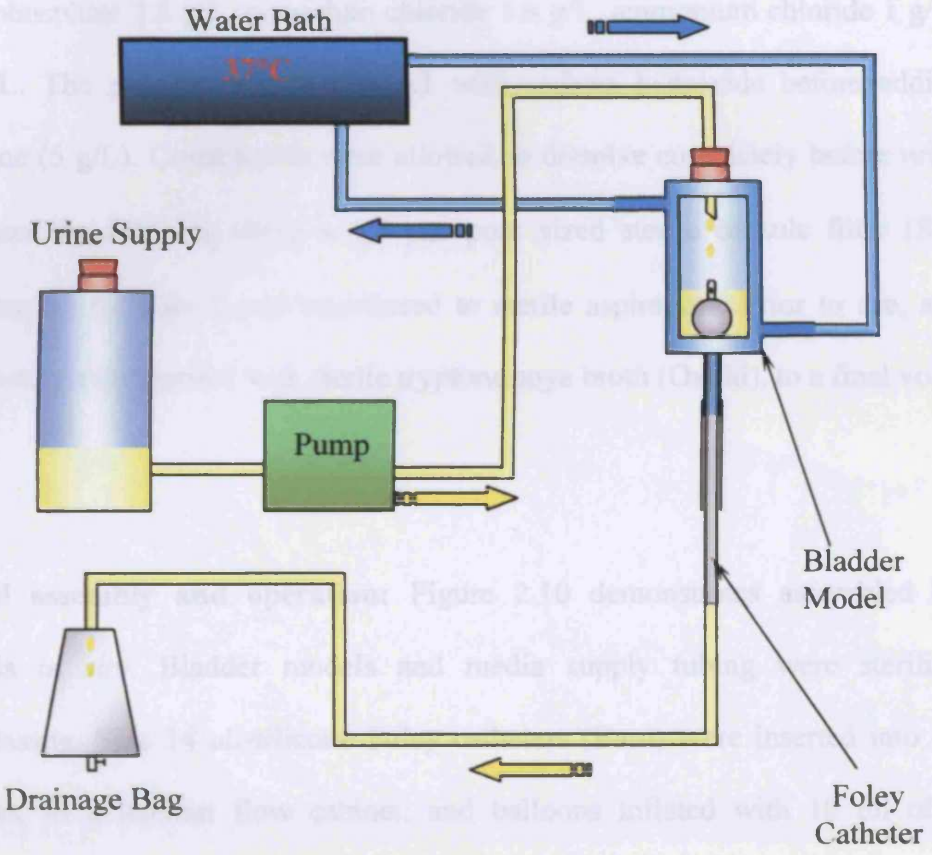

Preparation of artificial urine: Artificial urine was synthesised by dissolving the following in sterile deionised water: Di-sodium sulphate 2.3 g/L, calcium chloride (dihydrate) 0.65 g/L, magnesium chloride (hexahydrate) 0.65 g/L, sodium chloride 4.6 g/L, tri-sodium citrate 0.65 g/L, sodium oxalate 0.02 g/L, potassium di-hydrogen orthophosphate 2.8 g/L, potassium chloride 1.6 g/L, ammonium chloride 1 g/L, urea 25 g/L. The pH was adjusted to 6.1 with sodium hydroxide before addition of gelatine (5 g/L). Constituents were allowed to dissolve completely before urine was sterilised by filtration using a 0.2 μm pore sized sterile capsule filter (Satorius, Goettingen, Germany), and transferred to sterile aspiratiors. Prior to use, artificial urine was supplemented with sterile tryptone soya broth (Oxoid), to a final volume of 1 g/L.

Model assembly and operation: Figure 2.10 demonstrates assembled bladder models *in situ*. Bladder models and media supply tubing were sterilised by autoclaving. Size 14 all-silicone Foley catheters (Bard) were inserted into bladder models, in a laminar flow cabinet, and balloons inflated with 10 ml of sterile deionised water and drainage bags (Bard) were connected to catheters. The water jackets of models were supplied from a circulating water bath set at 37°C, via silicone tubing (0.5 cm bore, Fisher).

Media supply tubing (0.1 cm bore all-silicone, Fisher) was connected to aspirators containing artificial urine, and to bladder models. Models were supplied with media via a peristaltic pump (Watson & Marlow, Falmouth, UK), and filled until media began to drain through catheters (~20 ml). Models were inoculated with log phase cultures of test strain, grown in artificial urine without antibiotic selection, by substituting an aliquot (10 ml) of media in models for an equal volume of culture.

Figure 2.11: An example of *in vitro* bladder models *in situ*

Key:

1: Bladder models

2: Aspirators containing urine supply

3: Peristaltic pump

4: Media supply tubing

5: Drainage tube

6: Drainage Bags

7: Water supply tubing

8: "Urethra" (silicon tubing)

9: Water bath

10: Foley catheter

The viable cell count of the inoculum was calculated using the method described in section 2.2.4. Models were activated 1 h after inoculation, and were supplied with media at a constant flow rate of 0.5 ml/min. Prior to activation a 1 ml aliquot of culture was removed from each model and used to measure the pH in models at time of activation. Upon blockage of catheters, the number of viable cells in each model was calculated (Section 2.2.4), and the pH of media in the model measured.

Chapter 3: Results

3.1 Characterisation of *P. mirabilis* clinical isolates

Several recent clinical isolates of *Proteus mirabilis*, which had been acquired from blocked or encrusted indwelling urethral catheters, were obtained for use in this study. The suitability of the six isolates, designated B1, B2, B3, B4, B5, and B6, for the investigation of catheter blockage using a molecular genetic approach was evaluated.

3.1.1 Confirmation of species identity of clinical isolates

In order to confirm that the recent clinical isolates obtained for this study were *P. mirabilis*, the identity of each isolate was tested using a BBL crystal enteric/non-fermenter ID system. Oxidase and indole production was assessed separately. The results of these tests confirmed that all clinical isolates were *P. mirabilis*.

3.1.2 Antibiotic disc testing and approximate MICs

The activity of a range of antibiotics, commonly used to treat urinary tract infection, was assessed against the *P. mirabilis* clinical isolates B1-B6, by antibiotic disc testing (Section 2.2.5). Approximate minimum inhibitory concentrations for chloramphenicol, tetracycline, gentamicin, and kanamycin were established in both solid and liquid media (Table 3.2 and 3.3). These antibiotics were chosen as they reflect common selectable markers for genetic manipulation. This allowed identification of any isolates with antibiotic resistance profiles that could be problematic in subsequent procedures. The results of the disc testing are presented in Table 3.1, and MIC data is presented in Tables 3.2, and 3.3.

Antibiotic disc testing showed that the *P. mirabilis* clinical isolates, B1, B3, B4, B5, and B6 were sensitive to all antibiotics tested (Table 3.1). Isolate B2 was found to be

Table 3.1: Results of antibiotic disc testing on *P. mirabilis* clinical isolates B1 – B6.

	Size of inhibition zone for strain/isolate[a]						
Antibiotic	**B1**	**B2**[b]	**B3**	**B4**	**B5**	**B6**	**10418**
Ciprofloxacin (1 µg/ml)	35.33 ± 0.76	28.67 ± 0.76	35.33 ± 0.29	35.67 ± 0.76	34.33 ± 0.29	33.00 ± 1.00	34.00 ± 0.87
Nalidixic acid (30 µg/ml)	25.67 ± 1.76	24.00 ± 0.50	24.33 ± 0.76	22.67 ± 1.04	23.00 ± 0.87	23.67 ± 0.76	30.3 ± 0.29
Fosfomycin (200 µg/ml)	39.00 ± 0.5	0.00	43.67 ± 7.42	42.67 ± 1.04	39.67 ± 0.29	39.33 ± 1.04	29.67 ± 0.76
Trimethoprim (2.5 µg/ml)	26.33 ± 1.15	0.00	23.00 ± 1.32	24.67 ± 0.29	21.00 ± 1.50	19.00 ± 0.50	29.00 ± 0.87
Cephalexin (30 µg/ml)	16.67 ± 1.04	20.67 ± 3.51	17.00 ± 1.50	19.00 ± 1.32	20.33 ± 0.76	21.00 ± 0.50	21.67 ± 0.87
Ampicillin (25 µg/ml)	36.00 ± 1.00	0.00	33.67 ± 1.15	32.33 ± 0.76	36.00 ± 1.32	35.33 ± 1.61	31.00 ± 0.87

[a] Values indicate diameters of inhibition zones in mm, for *P. mirabilis* clinical isolates B1-B6, and *E. coli* control strain 10418, and represent the means of three replicate experiments. Values following ± indicate the standard deviation of the mean. Zone diameters were measured according to BSAC guidelines for *P. mirabilis*, and interpreted in relation to break point values provided by BSAC, to identify resistance.

[b] Values highlighted in red indicate resistance to an antibiotic at the tested concentration.

Table 3.2: Approximate MICs of chloramphenicol, tetracycline, gentamicin, and kanamycin, against *P. mirabilis* clinical isolates B1-B6 grown in LB broth.

	Approximate MIC of *P. mirabilis* isolates (μg/ml)					
Antibiotic	**B1**	**B2**	**B3**	**B4**	**B5**	**B6**
Chloramphenicol	10	20	15	15	20	15
Tetracycline	120	>120	>120	120	110	110
Gentamicin	10	10	>25	20	15	10
Kanamycin[a]	ND	ND	ND	20	ND	ND

[a] **ND = Not determined**

Table 3.3: Approximate MICs of chloramphenicol, tetracycline, gentamicin, and kanamycin, against *P. mirabilis* clinical isolates B1-B6 grown on MacConkey agar.

	Approximate MIC of *P. mirabilis* isolates (μg/ml)					
Antibiotic	**B1**	**B2**	**B3**	**B4**	**B5**	**B6**
Chloramphenicol	40	80	40	40	40	40
Tetracycline	120	140	120	140	120	120
Gentamicin	40	20	20	20	20	20
Kanamycin [a]	ND	ND	ND	20	ND	ND

[a] **ND = Not determined**

resistant to ampicillin (25 μg/ml), trimethoprim (2.5 μg/ml), and fosfomycin (200 μg/ml). The *P. mirabilis* clinical isolates generally possessed similar approximate MICs to tetracycline (Table 3.2, and 3.3), but more variation was present in MICs to chloramphenicol and gentamicin. In general clinical isolates also showed increased MICs to all antibiotics when used in MacConkey agar (Table 3.3).

3.1.3 Detection of plasmids in *P. mirabilis* clinical isolates

The *P. mirabilis* clinical isolates B1-B6 were screened for the presence of plasmids, which could interfere with mutagenesis and other genetic manipulations. Detection of plasmids in these isolates was carried out by purification and visualisation of any plasmid DNA present in the clinical isolates (Section 2.3.4, and 2.3.1). The results of the initial plasmid screens indicated that only *P. mirabilis* isolate B2 harboured a plasmid, which was designated pB2 (Figure 3.1). *Eco*RI restriction digest confirmed isolate B2 carried a large plasmid, >25 kb in size (Figure 3.1).

3.1.4 Transfer of plasmids to *P. mirabilis* clinical isolates

The ability to transform *P. mirabilis* clinical isolates by both electroporation (Section 2.3.12) and conjugal transfer of plasmids (Section 2.3.8) was assessed. All isolates were tested with the exception of B2. Attempts were made to introduce plasmid pUC18, a narrow host range *E. coli* cloning vector, by electroporation. Introduction pOT182, a mobilisable transposon donor vector, (carrying Tn*5*-OT182), was attempted by both electroporation and conjugal transfer from an *E. coli* donor strain. None of the clinical isolates tested could be transformed by electroporation. However, pOT182 was successfully introduced to isolates B3 and B4 by conjugal transfer, and both isolates produced trans-conjugant colonies on MacConkey agar selective for Tn5-OT182 (tetracycline 200 μg/ml, and polymixin 60 units/ml).

Figure 3.1: Detection of plasmids in *P. mirabilis* clinical isolates B1-B6

Plasmid DNA was purified from *P. mirabilis* clinical isolates B1-B6 and visualised by gel electrophoresis to determine if any natural plasmids were present in these isolates (A). Any plasmids detected were also analysed by restriction digest (B).

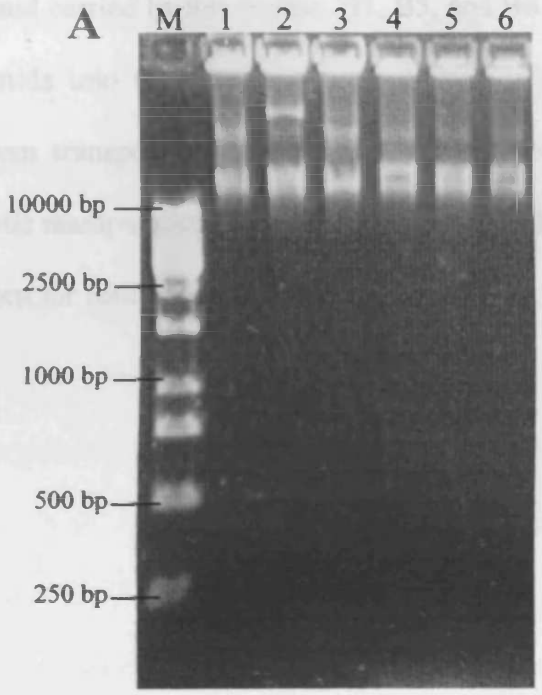

A: Initial screen for presence of plasmids in *P. mirabilis* clinical isolates revealed isolate B2 harboured a plasmid, designated pB2.

M, 1 kb molecular size standard.
1–6, Plasmid DNA purified from *P. mirabilis* clinical isolates B1 – B6 respectively

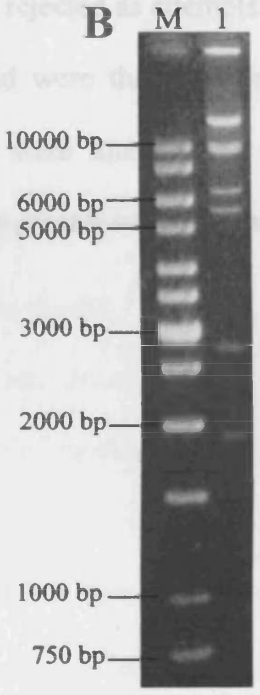

B: Gel electrophoresis of plasmid pB2 digested with *Eco*RI restriction enzyme.

M, 1 kb molecular size standard.
1, products of pB2 *Eco*RI digest.

3.1.5 Selection of *P. mirabilis* isolate for mutagenesis

Of the clinical isolates, ultimately only B4 was selected for further study. Isolate B2 was rejected on the basis of the altered antibiotic resistance profile, and the large pB2 plasmid carried by this isolate. B1, B5, and B6 were rejected as attempts to introduce plasmids into these isolates were unsuccessful, and were therefore unsuitable for random transposon mutagenesis. Both B3 and B4 were found to be amenable to genetic manipulation, but B4 was observed to have a greater swarming ability so was chosen for further study.

3.2 Mutagenesis of *P. mirabilis* strain B4

Two transposon based mutagenesis systems were evaluated for the generation of mutants from *P. mirabilis* strain B4 (Section 2.6.1). These were the mini-Tn*5*Km2 transposon delivered using the pUT suicide delivery vector (de Lorenzo & Timmis 1994), and the Tn*5*-OT182 transposon delivered using the pOT182 suicide delivery vector (de Lorenzo & Timmis 1994).

3.2.1 Introduction of transposons to *P. mirabilis* strain B4

The delivery vectors carrying the transposons were introduced to *P. mirabilis* B4 by conjugation from *E. coli* donor strains, using the mating method described in Section 2.3.8. Both transposon systems generated trans-conjugant colonies on media selective for *P. mirabilis* harbouring the mini-Tn*5*Km2 transposon (kanamycin 30 μg/ml, polymixin 60 units/ml) and transposon Tn*5*-OT182 (tetracycline 200 μg/ml, polymixin 60 units/ml).

The presence of each transposon, in randomly selected trans-conjugants, was confirmed by PCR amplification of transposon specific sequences (the Tn*5*-OT182 tetracycline resistance gene *tetA1*, and the mini-Tn*5*Km2 kanamycin resistance gene *nptII*). These trans-conjugants were verified as *P. mirabilis* using the BBL crystal ID system. PCR primers TetA1,A2 (Table 2.5 and 2.6) were used to confirm the presence of transposon Tn*5*-OT182 in nine trans-conjugants (designated BVJ1-9) from pOT182 matings. Mini-Tn*5*Km2 was confirmed in all eight trans-conjugants (designated BVJ10-17) tested using primers NPT2_F1,R1 (Table 2.5 and 2.6). The results obtained for each PCR assay are presented in Figure 3.2 and illustrate that the transposon delivery vectors (noted above) could be used to successfully introduce their respective transposons into *P. mirabilis* B4 by conjugal transfer.

Figure 3.2: PCR confirmation of transposons Tn*5*-OT182, and mini-Tn*5*Km2 in *P. mirabilis* trans-conjugants.

Trans-conjugants BVJ1-9 were used to verify successful transfer of transposon Tn*5*-OT182 into *P. mirabilis* strain B4, by PCR with primers TetA1,A2 (A). Successful transfer of mini-Tn*5*Km2 into *P. mirabilis* B4 was verified by PCR with primers NPT2_F1,R1, using trans-conjugants BVJ10-17 (B).

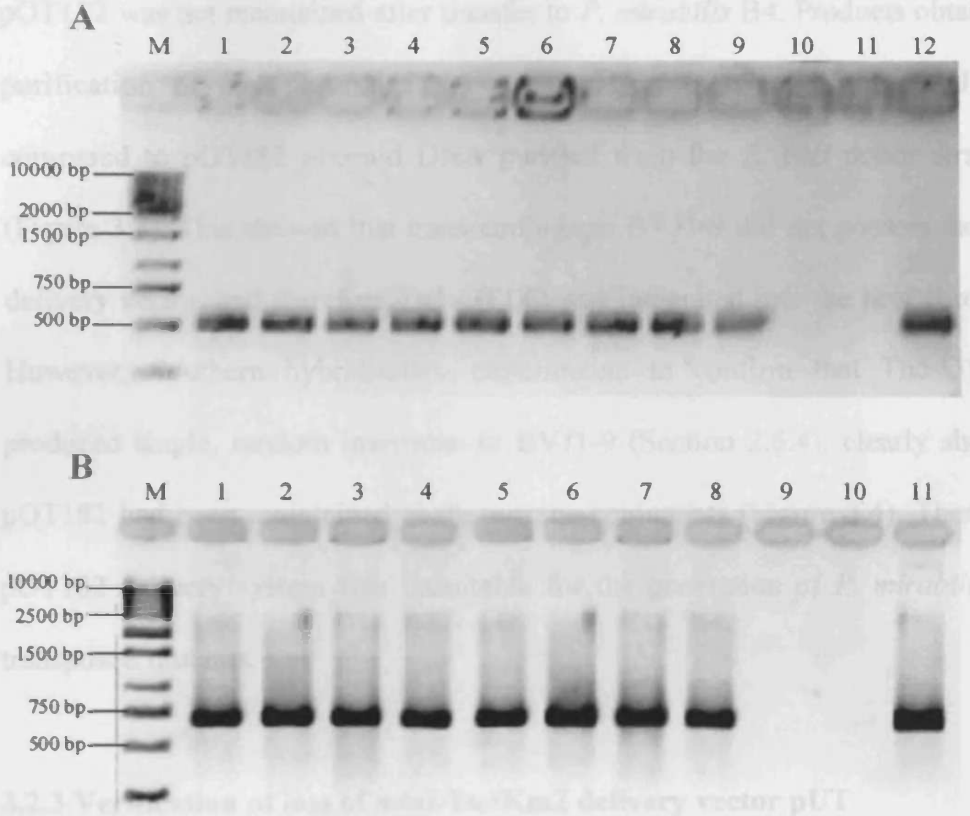

A: results of PCR on trans-conjugants BVJ1-9 with primers TetA1,A2
M, 1 kb molecular size standard
1-9, Trans-conjugants **BVJ1-9** respectively
10, *P. mirabilis* wild type strain **B4**
11, Negative control (Sterile deionised water)
12, Positive control (**pOT182** DNA purified from *E. coli* donor strain SM10)

B: results of PCR on trans-conjugants BVJ10-17 with primers NPT2_F1,R1
M, 1 kb molecular size standard
1-8, Trans-conjugants **BVJ10-17** respectively
9, *P. mirabilis* wild type strain **B4**
10, Negative control (Sterile deionised water)
11, Positive control (**pUTmini-Tn*5*Km2** DNA purified from *E. coli* donor strain S17.1λ*pir*)

3.2.2 Verification of loss of Tn*5*-OT182 delivery vector

Trans-conjugants BVJ1-9, which had been used to confirm presence of Tn*5*-OT182 in *P. mirabilis* (Section 3.2.1), were also used to confirm that the delivery vector pOT182 was not maintained after transfer to *P. mirabilis* B4. Products obtained from purification of any plasmid DNA contained in trans-conjugants BVJ1-9 were compared to pOT182 plasmid DNA purified from the *E. coli* donor strain SM10 (Figure 3.3). This showed that trans-conjugants BVJ1-9 did not possess the pOT182 delivery vector, and therefore Tn*5*-OT182 was integrated into the host chromosome. However, Southern hybridisation experiments to confirm that Tn*5*-OT182 had produced single, random insertions in BVJ1-9 (Section 2.6.4), clearly showed that pOT182 had been maintained in these trans-conjugants (Figure 3.4). Therefore, the pOT182 delivery system was unsuitable for the generation of *P. mirabilis* random transposon mutants.

3.2.3 Verification of loss of mini-Tn*5*Km2 delivery vector pUT

Trans-conjugants (designated BVJ10-17), which had been used to confirm presence of mini-Tn*5*Km2 in *P. mirabilis* (Section 3.2.1), were also used to confirm that the delivery vector pUT was not maintained after transfer to *P. mirabilis* B4. As with pOT182, absence of the delivery vector in BVJ10-17 would indicate successful mutagenesis of *P. mirabilis* B4 with this transposon.

Products obtained from purification of any plasmid DNA present in trans-conjugants BVJ10-17 were digested with *Bam*HI restriction enzyme, and compared to *Bam*H1 digested pUTmini-Tn*5*Km2 plasmid DNA purified from the *E. coli* donor strain S17.1λ*pir* (Figure 3.5). *Bam*H1 digests were utilised to increase the sensitivity of the assay, and avoid false negative results such as those obtained during assays for the

Figure 3.3: Screen for loss of pOT182 delivery vector in Tn*5*-OT182 positive trans-conjugants BVJ1-9.

Possible replication of delivery vector pOT182 in *P. mirabilis* trans-conjugants BVJ1-9 was assessed. Presence of transposon Tn*5*-OT182 had been confirmed in these trans-conjugants (Figure 3.2), and visualisation of products obtained from purification of plasmid DNA indicated that the delivery vector pOT182 had not been maintained.

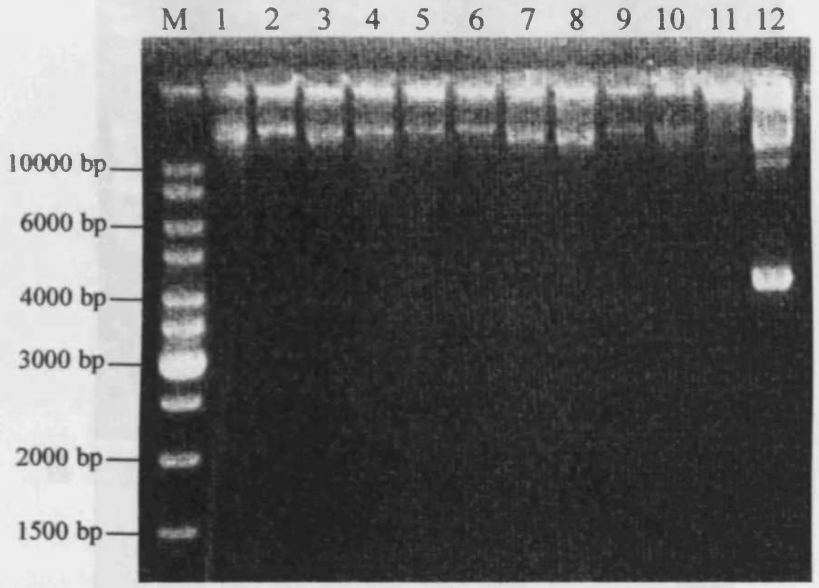

M, 1 kb molecular size standard.
1-9, Products of plasmid purification from trans-conjugants **BVJ1-9**
10, Products of plasmid purification from wild type strain **B4**
11, Products of plasmid purification wild type strain **B5**
12, Plasmid **pOT182** (carrying Tn*5*-OT182) purified from *E. coli* donor strain SM10

Figure 3.4: Assessment of single, random insertion of transposon Tn5-OT182 in trans-conjugants BVJ1-9.

The generation of single, random inserts in the chromosomes of trans-conjugants BVJ1-9 by transposon Tn5-OT182, was assessed by Southern hybridisation. The results of these experiments show that the delivery vector pOT182 had been maintained in these trans-conjugants.

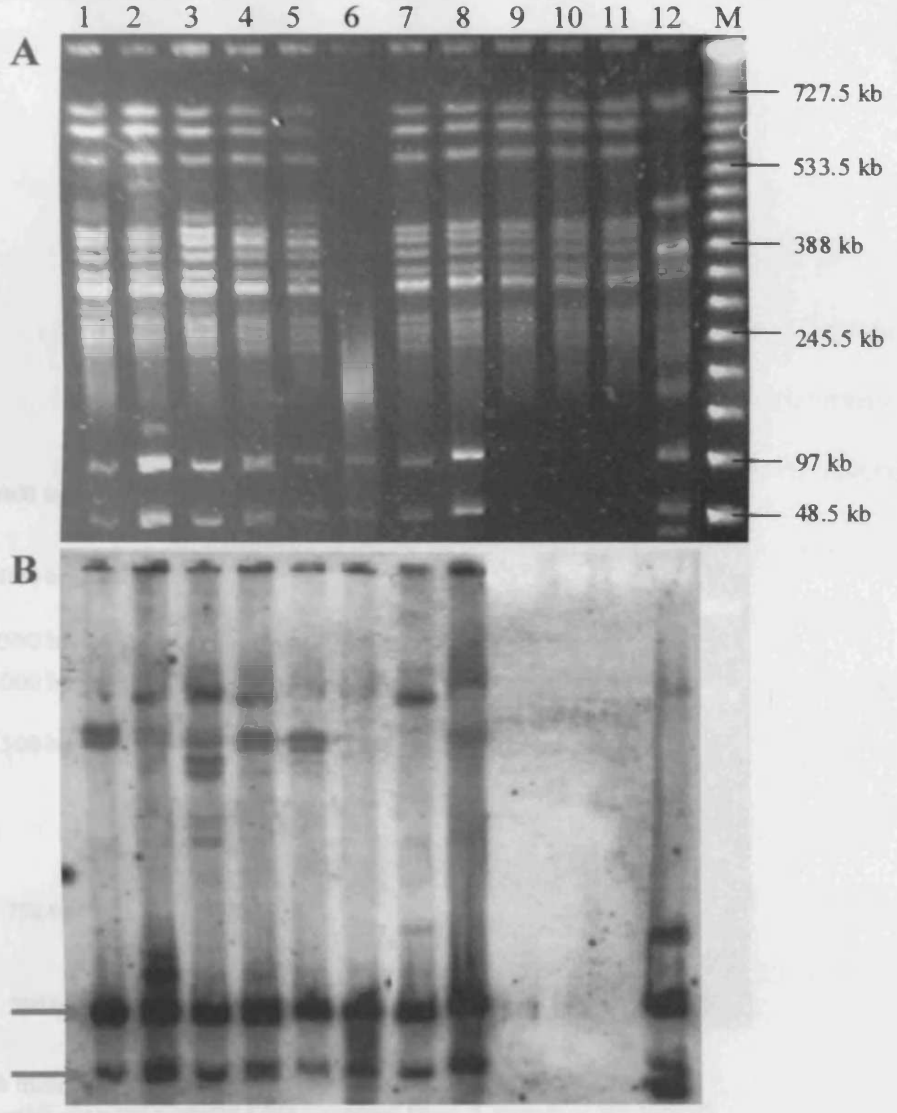

A: Total genomic DNA was extracted form trans-conjugants BVJ1-9 and digested with *Not*I. Fragments were separated by pulsed field gel electrophoresis (Section 2.4).

B: Separated fragments were transferred to a nylon membrane and analysed by Southern hybridisation using Tn5-OT182 specific probes. Arrows indicate maintained pOT182.

M, 1 kb molecular size marker.
1-9, genomic DNA extracted from trans-conjugants **BVJ1-9**
10, genomic DNA extracted from *P. mirabilis* strain **B4**
11, genomic DNA extracted from *P. mirabilis* Strain **B5**
12, genomic DNA extracted from **pOT182** ***E. coli*** **donor strain SM10**

Figure 3.5: Screen for maintenance of pUT delivery vector in mini-Tn*5*Km2 positive trans-conjugants BVJ10-17.

Replication of delivery vector pUT in *P. mirabilis* was assessed using trans-conjugants BVJ10-17, in which the presence of mini-Tn*5*Km2 had been confirmed (Figure 3.2). Visualisation of *Bam*HI digested plasmid DNA purified from these trans-conjugants, indicated that the delivery vector pUT had not been maintained.

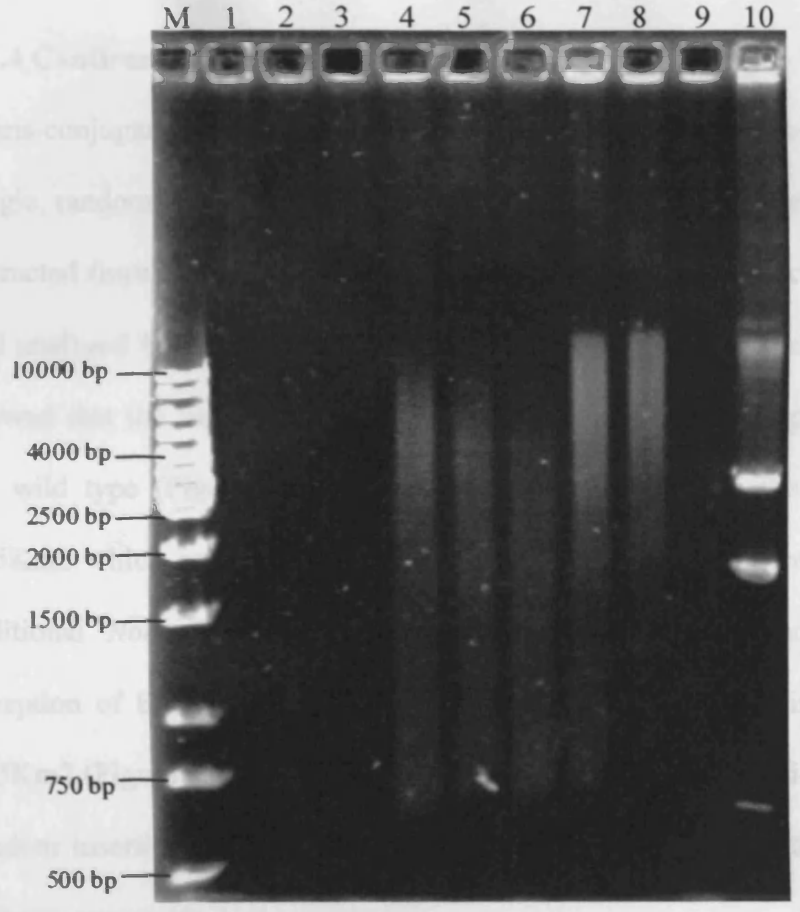

M, 1 kb molecular size standard.
1–8, *Bam*HI digested plasmid DNA, purified from *P. mirabilis* **BVJ10-17**
9, *Bam*HI digested plasmid DNA, purified from *P. mirabilis* wild type strain **B4**
10, *Bam*H1 digested **pUTmini-Tn*5*Km2** DNA, purified from *E. coli* S17.1λ*pir*

loss of pOT182 (Section 2.3.2). The results clearly show that the delivery vector pUT was not maintained in the trans-conjugants BVJ10-17 (Figure 3.5). Therefore, transposon mini-Tn*5*Km2 and the pUT delivery vector could be used to successfully generate *P. mirabilis* B4 transposon mutants.

3.2.4 Confirmation of single, random mini-Tn*5*Km2 insertion in *P. mirabilis* B4

Trans-conjugants BVJ10-17 were also used to ensure that mini-Tn*5*Km2 produced single, random inserts in the *P. mirabilis* chromosome. *Not*I digested genomic DNA extracted from BVJ10-17, was separated by pulsed field gel electrophoresis (PFGE) and analysed by Southern hybridisation with mini-Tn*5*Km2 specific probes. PFGE showed that the trans-conjugants exhibited an altered banding pattern compared to the wild type (Figure 3.6). These alterations were due to the presence of mini-Tn*5*Km2 which carries a unique *Not*I restriction site, and therefore introduced an additional *Not*I site into the chromosomes of the trans-conjugants. With the exception of BVJ16, all trans-conjugants tested harboured a single copy of mini-Tn*5*Km2 (Figure 3.6). These experiments also indicated that mini-Tn*5*Km2 exhibited random insertion in *P. mirabilis* B4 (Figure 3.6). In addition, the loss of the pUT delivery vector was also confirmed.

Figure 3.6: Assessment of single, random insertion of mini-Tn*5*Km2 transposon in trans-conjugants BVJ10-17.

The generation of single, random inserts in the chromosomes of trans-conjugants BVJ1-9 by mini-Tn*5*Km2, was assessed by Southern. The results of these experiments show that mini-TnIKm2 inserts at random in the *P. mirabilis* chromosome, and can be used to generate mutants with single transposon inserts.

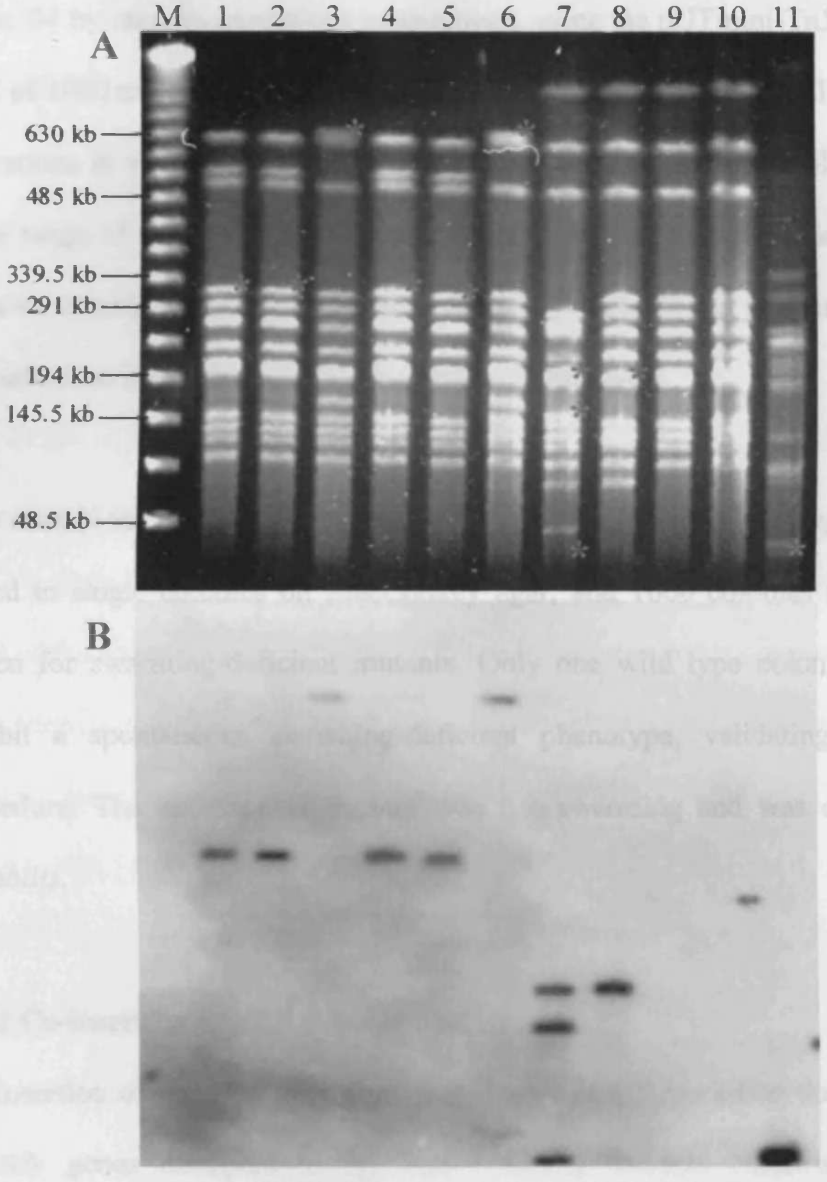

M, Molecular size marker.
1-8, genomic DNA extracted from trans-conjugants **BVJ10-17**
9, genomic DNA extracted from *P. mirabilis* strain **B4**
10, genomic DNA extracted from *P. mirabilis* Strain **B5**
11, genomic DNA extracted from **pUTmini-Tn*5*Km2 *E. coli* donor strain S17.1λ*pir***

A: Total genomic DNA, extracted form trans-conjugants BVJ10-17, was digested with *Not*I and fragments separated by pulsed field gel electrophoresis (Section 2.4). *indicates fragments carrying mini-Tn*5*Km2, identified by Southern hybridisation (**B**).

B: Separated fragments were transferred to a nylon membrane and analysed by Southern hybridisation using mini-Tn*5*Km2 specific probes.

3.3 Isolation and characterisation of swarming deficient mutants

3.3.1 Isolation of swarming deficient mutants

Stable swarming deficient mutants were successfully generated from *P. mirabilis* strain B4 by random transposon mutagenesis, using the pUTmini-Tn*5*Km2 system. A total of 1000 mutants were screened for swarming deficiencies, and 150 mutants with alterations in swarming phenotype were identified. The mutants isolated exhibited a wide range of swarming phenotypes. These included a complete inability to swarm (non-swarmers), reduced migration (poor-swarmers), altered swarming pattern, and perturbations in the temporal control of the swarm cycle.

As a control for the isolation of swarming deficient mutants, wild type strain B4 was plated to single colonies on MacConkey agar, and 1000 colonies subjected to the screen for swarming-deficient mutants. Only one wild type colony was found to exhibit a spontaneous swarming-deficient phenotype, validating the screening procedure. The spontaneous mutant was non-swarming and was confirmed as *P. mirabilis*.

3.3.2 Co-insertion of pUT delivery vector

Co-insertion of the pUT delivery vector was initially identified during attempts to identify genes disrupted in the non-swarming mutants NS68 and NS70. The sequence of DNA flanking the transposon in both these mutants was analysed using the BLASTN search tool, and was found to be homologous to pUTmini-Tn*5*Km2. NS68 and NS70 were also found to be resistant to ampicillin (100 μg/ml), indicating the presence of the pUT *bla* gene (confers resistance to ampicillin, Figure 2.1) in these mutants.

Total genomic DNA from mutants NS68, and NS70 was analysed by southern hybridisation using a mini-Tn*5*Km2 specific probe. DNA was digested with *Pst*I and *Sal*I restriction enzymes and compared to digested DNA from two swarming-deficient mutants (NS104, and NS117), which had shown no resistance to ampicillin (100 μg/ml), and the pUTmini-Tn*5*Km2 plasmid. This revealed that segments of the pUT delivery vector (extending at least as far as the *Pst*I restriction site) had integrated into the host chromosome contiguous with the mini-Tn*5*Km2 transposon (Figure 3.7).

The extent of pUT co-insertion was further investigated using the PCR based assay, described in Section 2.6.6. Details of the primer sets used are listed in Tables 2.5, and 2.6. Both NS68 and NS70 possessed a segment of the plasmid DNA flanking the I end of the transposon (designated pUTTn5I), and a segment containing the pUT *bla* gene (designated pUTBla). NS68 was also found to contain a segment of the pUT plasmid flanking the O end of the transposon (designated pUTTn5O). Mutants NS104, NS117, were confirmed to be negative for pUT co-insertion. The results of the PCR based assay for the non-swarming mutants NS68, NS70, NS104 and NS117, and the regions of the pUT plasmid amplified during the assay, are shown in Figure 3.8.

3.3.3 **Frequency of pUT co-insertion in swarming-deficient mutants**

The frequency of pUT co-insertion among swarming deficient mutants was investigated using both PCR and plate based assays (Section 2.6.6). Thirty swarming-deficient mutants were selected at random and screened for pUT co-insertion by the PCR based assay. The results of the PCR screening showed that all mutants positive for pUT co-insertion possessed segments of the plasmid flanking

Figure 3.7: Identification of pUT co-insertion in swarming-deficient mutants NS68, NS70.

Southern hybridisation with mini-Tn5Km2 specific probes of pUTmini-Tn5Km2, and genomic DNA from swarming deficient mutants NS68, NS70, NS104, and NS117, digested with *Pst*I* and *Sal*I*. Bands illustrate pUT co-insertion in ampicillin resistant mutants NS68 and NS70, and lack of pUT co-insertion in ampicillin sensitive mutants NS104, and NS117.

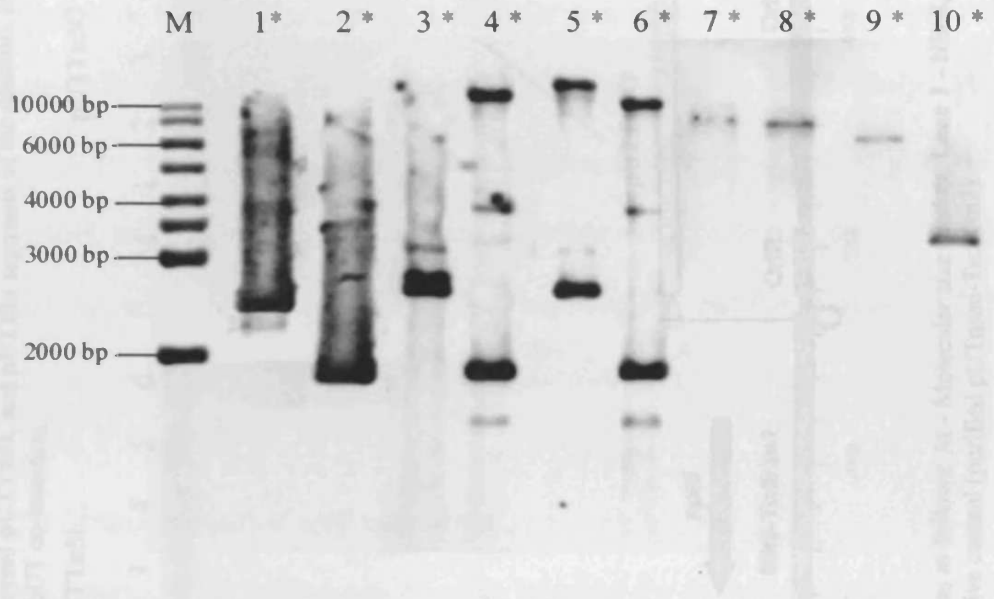

M , 1 Kb molecular size standard
Lane 1*-2*, pUTmini-Tn5Km2 DNA.
Lane 3*-4*, NS68 genomic DNA.
Lane 5*-6*, NS70 genomic DNA.
Lane 7*-8*, NS104 genomic DNA.
Lane 9*-10*, NS117 genomic DNA.

* *Pst*I digest
* *Sal*I digest

Figure 3.8: Regions of pUT plasmid amplified, and results obtained from PCR based pUT co-insertion assay in mutants NS68 and NS70.
Investigation of the extent of pUT co-insertion in mutants NS68 and NS70. Both mutants possessed pUTTn5I, and pUTBla segments of the plasmid. In NS68 the pUTTn5O segment of pUT was also present. Mutants NS104 and NS117 were confirmed as negative for pUT co-insertion.

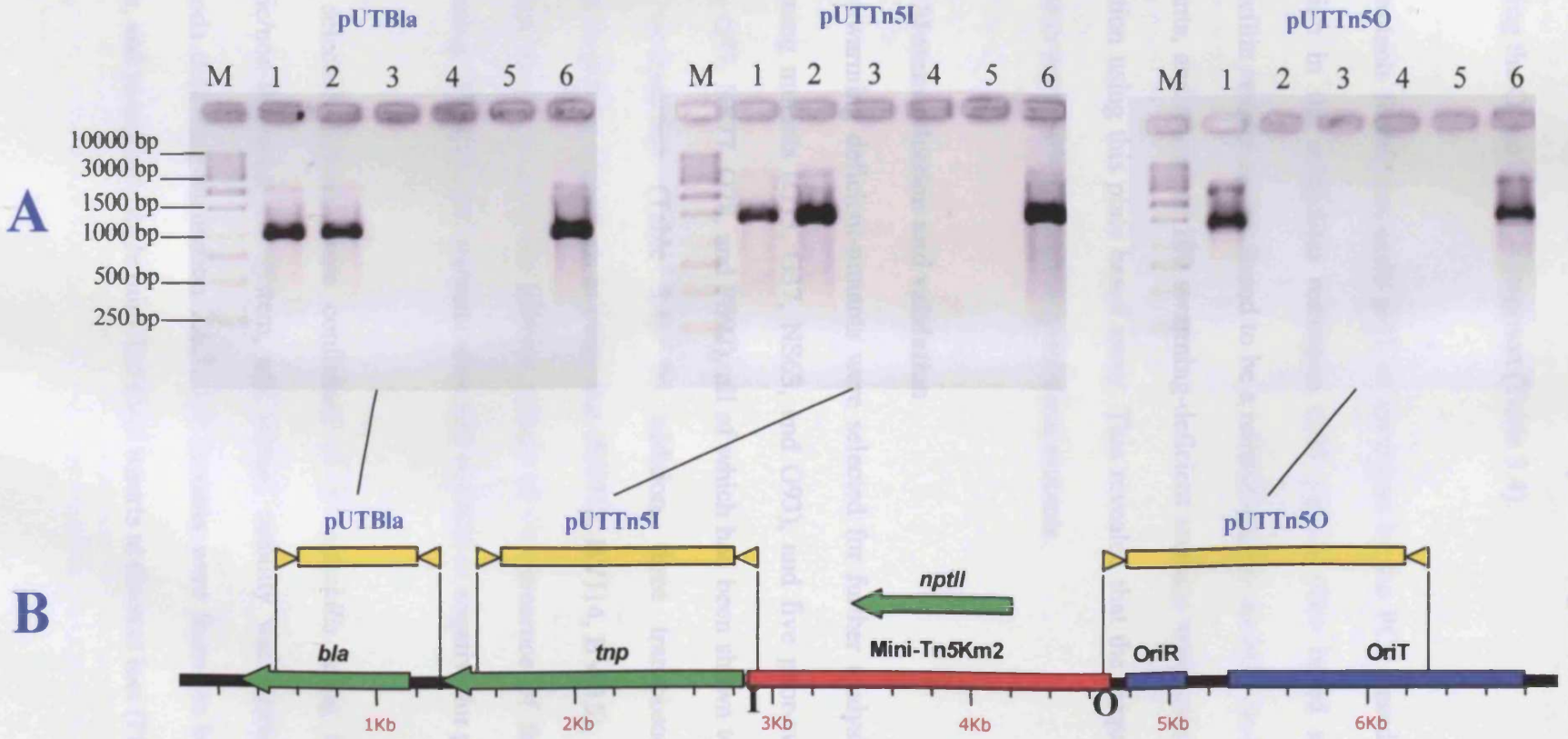

A : Results of PCR based pUT co-insertion assay.
Gel loading order was identical for all PCR reactions shown in this example. Loading order was as follows: **M** - Molecular size marker, **Lane 1** - NS68, **Lane 2** - NS70, **Lane 3** - NS104, **Lane 4** - NS117, **Lane 5** - Negative control (sterile deionised water), **Lane 6** - Positive control (purified pUTmini-Tn*5*Km2).

B : Linear map of pUT delivery vector carrying transposon mini-Tn*5*Km2.
➡ - Open reading frames. ▬ - Mini-Tn*5*Km2 transposon. ▶ - PCR primers for pUT co-insertion assay. ▭ - Regions of pUT amplified during PCR based co-insertion assay. ▬ - Regulatory regions. **OriT** - RP4 origin of transfer. **OriR** - R6K origin of replication. ***nptII*** - Neomycin phospho-transferase, confers kanamycin resistance. ***tnp*** - Transposase (from transposon Tn*5*), mediates transposition. ***bla*** - β-Lactamase, confers resistance to ampicillin. **I** - Mini-Tn*5*Km2 I end. **O** - Mini-Tn*5*Km2 O end.

the I end of the transposon, and segments containing the *bla* gene (Table 3.4). Only two of the selected mutants were found to possess segments of the pUT, plasmid flanking the O end of the transposon (Table 3.4).

All mutants found to contain pUT co-insertions by the PCR based assay were also positive in the ampicillin resistance (100 μg/ml) plate based assay. Therefore, ampicillin resistance was found to be a reliable marker for pUT co-insertion in these mutants, and a total of 100 swarming-deficient mutants were screened for pUT co-insertion using this plate based assay. This revealed that the frequency of pUT co-insertion was ~30% in swarming-deficient mutants.

3.3.4 Mutant selection and validation

Nine swarming deficient-mutants were selected for further analysis: the four non-swarming mutants (G33, G37, NS63, and G93), and five poor-swarming mutants (G64, G77, NS77, G78, and PS92), all of which had been shown to be negative for pUT co-insertion (Table 3.4). In addition, three transposon mutants that demonstrated no alterations in swarming (BVJ12, BVJ14, BVJ15), were included as controls to assess possible adverse effects of the presence of the transposon on swarming. These control mutants were also verified as negative for pUT co-insertion.

The selected mutants were confirmed as *P. mirabilis* using the BBL crystal enteric/non-fermenter ID system, and mutant stability was assessed according to methods described in section 2.6.7. All mutants were found to be phenotypically stable, and possessed single mini-Tn*5*Km2 inserts at discreet loci (Figure 3.9).

Table 3.4: Frequency of pUT co-insertion in swarming-deficient mutants.

The ability to detect pUT co-insertion based on resistance to ampicillin (100 μg/ml) was assessed by analysing 30 randomly selected swarming-deficient mutants by the PCR based assay, and a plate assay.

Mutant	PCR assay[a]			Plate assay[b]
	pUTBla	PUTTn5I	PUTTn5O	
G1	+	+	-	R
G2	+	+	-	R
NS3	-	-	-	S
NS6	-	-	-	S
G10	+	+	-	R
NS10	-	-	-	S
G14	+	+	+	R
G16	+	+	-	R
G20	-	-	-	S
NS21	+	+	-	R
G33	-	-	-	S
G37	-	-	-	S
NS44	+	+	-	R
NS58	-	-	-	S
NS63	-	-	-	S
G64	-	-	-	S
NS68	+	+	+	R
NS69	+	+	-	R
NS70	+	+	-	R
NS77	-	-	-	S
G77	-	-	-	S
G78	-	-	-	S
PS92	-	-	-	S
G93	-	-	-	S
NS104	-	-	-	S
NS109	+	+	-	R
NS116	+	+	-	R
NS117	-	-	-	S
NS119	-	-	-	S
NS123	-	-	-	S

[a] Results of PCR assay for co-insertion of pUT segments. **pUTBla** – Regions of the pUT plasmid containing the β-lactamase resistance gene (*bla*). **pUTTn5I** – Region of pUT plasmid flanking the I end of mini-Tn*5*Km2, containing transposase gene (*tnp*). **pUTTn5O** – Region of pUT plasmid flanking the O end of mini-Tn*5*Km2. Regions of the pUT plasmid amplified are illustrated in Figure 3.8.

[b] Results of plate based pUT co-insertion assay, using resistance to ampicillin (100 μg/ml) as an indicator for pUT co-insertion. R denotes resistance to ampicillin (100 μg/ml). S denotes sensitivity to ampicillin.

Figure 3.9: Confirmation of single, random, mini-Tn*5*Km2 integration in stable swarming-deficient mutants, and control mutants.

Southern hybridisation with mini-Tn*5*Km2 specific probes, of *Pst*I digested genomic DNA from stable transposon mutants (swarming deficient and control mutants) selected for further study. Bands indicate presence of the transposon, and show each mutant possessed a single transposon insert, and that insertion was random. *P. mirabilis* wild type strain B4 was included as a negative control.

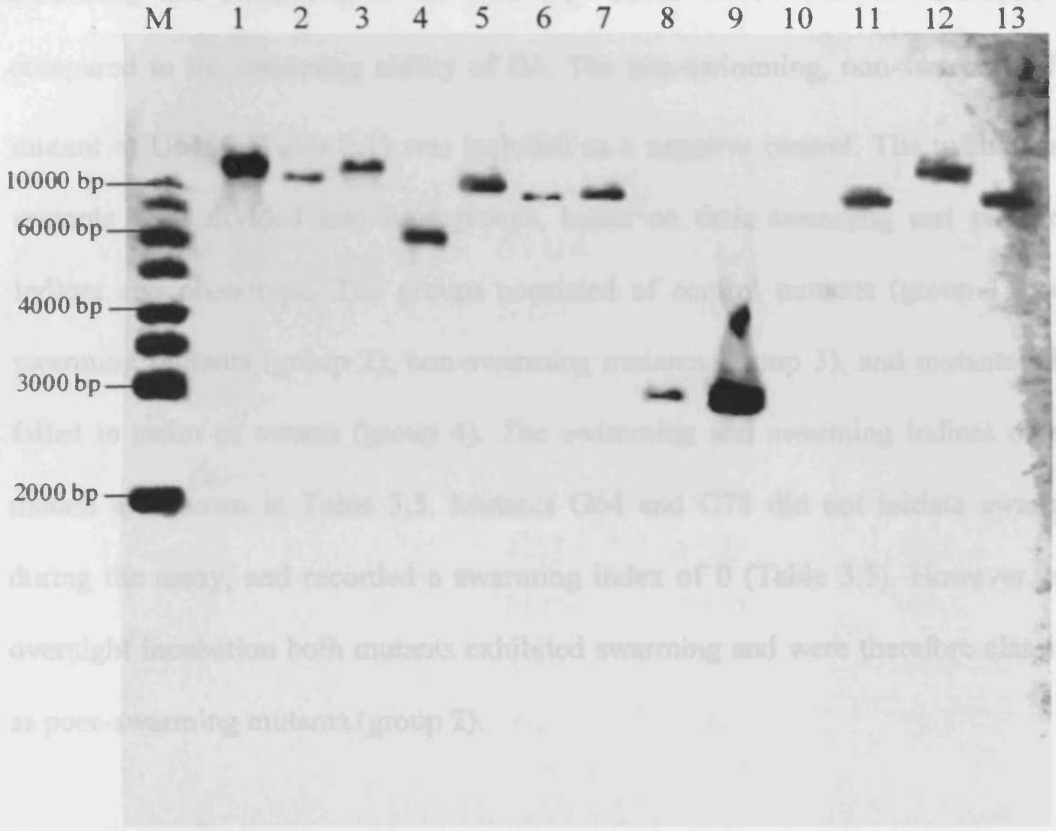

M, 1 Kb molecular size standard
1, Non-swarming mutant **G33** (Group 3)
2, Non-swarming mutant **G37** (Group 3)
3, Non-swarming, non-swimming mutant **NS63** (Group 4)
4, Poor-swarming mutant **G64** (Group 2)
5, Poor-swarming mutant **NS77** (Group 2)
6, Poor-swarming mutant **G77** (Group 2)
7, Poor-swarming mutant **G78** (Group 2)
8, Non-swarming mutant **G93** (Group 3)
9, Poor-swarming mutant **PS92** (Group 2)
10, *P. mirabilis* wild type strain **B4**
11, Control mutant **BVJ12** (Group 1)
12, Control mutant **BVJ14** (Group 1)
13, Control mutant **BVJ15** (Group 1)

3.3.5 Swimming and swarming ability

The ability of the selected mutants (including control mutants) to swarm over and swim through LB agar was tested, and compared to the wild type parent strain B4. Swarming and swimming in the wild type strain U6450 was also assessed and compared to the swarming ability of B4. The non-swimming, non-swarming *flh*A$^-$ mutant of U6450 (Table 2.1) was included as a negative control. The twelve stable mutants were divided into four groups, based on their swarming and swimming indices and phenotype. The groups consisted of control mutants (group 1), poor-swarming mutants (group 2), non-swarming mutants (group 3), and mutants which failed to swim or swarm (group 4). The swimming and swarming indices of each mutant are shown in Table 3.5. Mutants G64 and G78 did not initiate swarming during the assay, and recorded a swarming index of 0 (Table 3.5). However, after overnight incubation both mutants exhibited swarming and were therefore classified as poor-swarming mutants (group 2).

3.3.6 Periodicity of the swarm cycle

The periodicity of the swarming cycle in the control mutants (Figure 3.10), and the poor-swarming mutants G77, NS77, and PS92 (Figure 3.11) was also investigated. Data collected during assessment of swarming ability in the mutants (Section 2.6.9) was used to calculate the migration velocity (mm/hour) for each time point during the assay. Swarm cycle periodicity could not be assessed in the poor-swarming mutants G78 or G64 as these mutants failed to swarm within the duration of the assay.

Table 3.5: Assessment of swarming and swimming ability of *P. mirabilis* wild type strain B4 and transposon mutants.

The swarming and swimming abilities of the swarming-deficient and control mutants were assessed, and related to the wild type strain B4.

Group	Strain	Swarming[a] Index	Swimming[a] Index
Wild Type	**B4**	**100**	**100**
	U6450	64.41	64.6
Group1: Control mutants	BVJ14	167.8	100
	BVJ12	110.1	100
	BVJ15	105	95.5
Group 2: Poor-swarming mutants	NS77	16.95	74.6
	G77	15.25	86.1
	PS92	10.17	106.1
	G78	0	36.9
	G64	0	28.5
Group 3: Non-Swarming mutants	G93	0	42.30
	G37	0	40
	G33	0	32.3
Group 4: Non-swimming, non-swarming mutants	NS63	0	0
	U6450 *flhA*⁻	0	0

[a] Swimming and swarming indices were calculated for each strain, and represent a percentage of the wild type strain **B4** motility, including the wild type strain **U6450**.

Figure 3.10: Periodicity of the swarm cycle in *P. mirabilis* wild type strain B4 and control mutants BVJ12, BVJ14, and BVJ15.
The temporal control of the swarm cycle in control mutants was compared to the wild type strain B4. Data obtained during assessment of swarming ability was converted to represent the velocity of migration (mm/hour) at each time point.

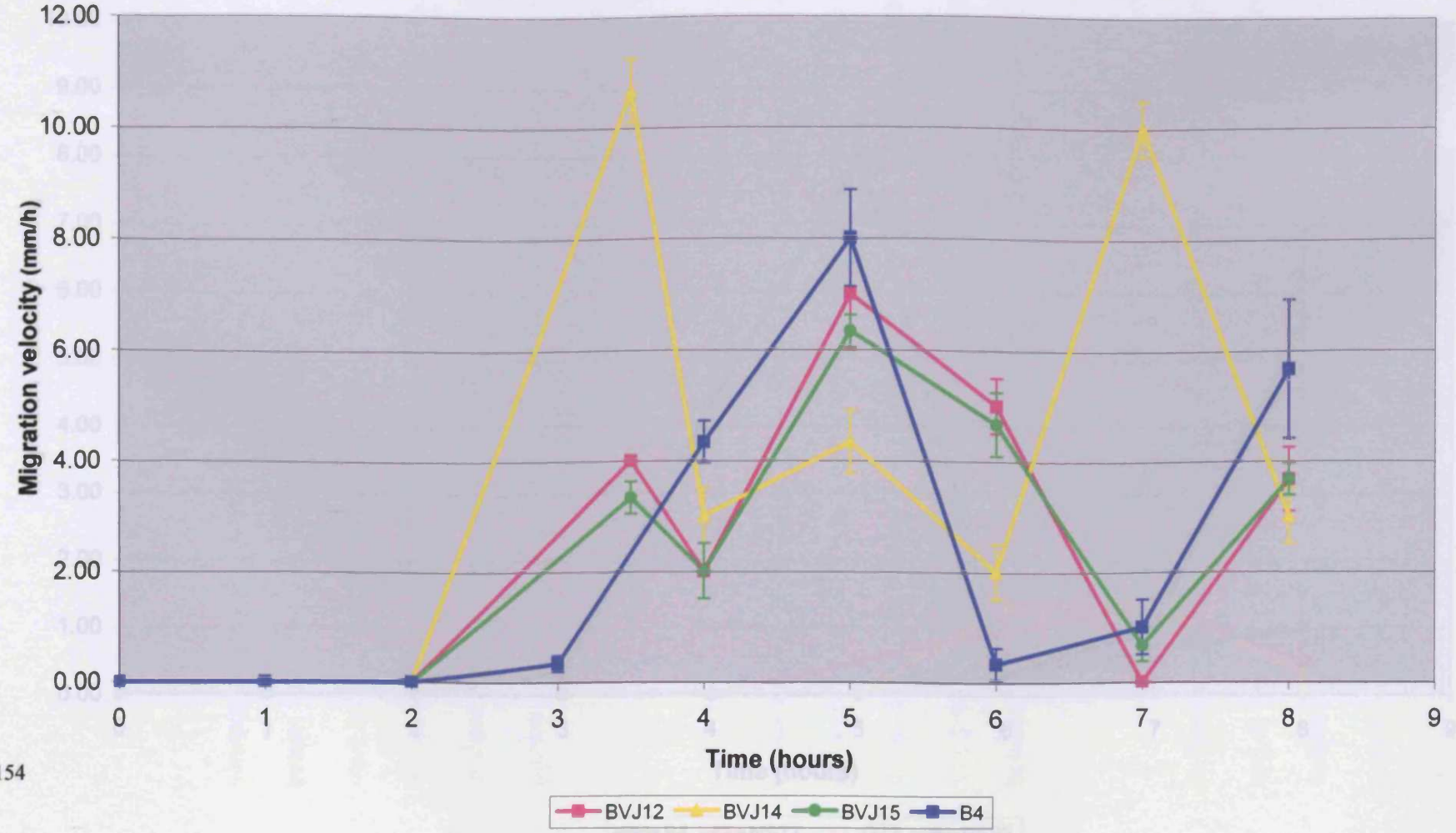

Figure 3.11: Periodicity of the swarm cycle in *P. mirabilis* wild type strain B4 and poor-swarming mutants NS77, G77, and PS92.
The temporal control of the swarm cycle in the poor-swarming mutants NS77, G77, and PS92 (Group 2) was compared to the wild type strain B4. Data obtained during assessment of swarming ability was converted to represent the velocity of migration (mm/hour) at each time point

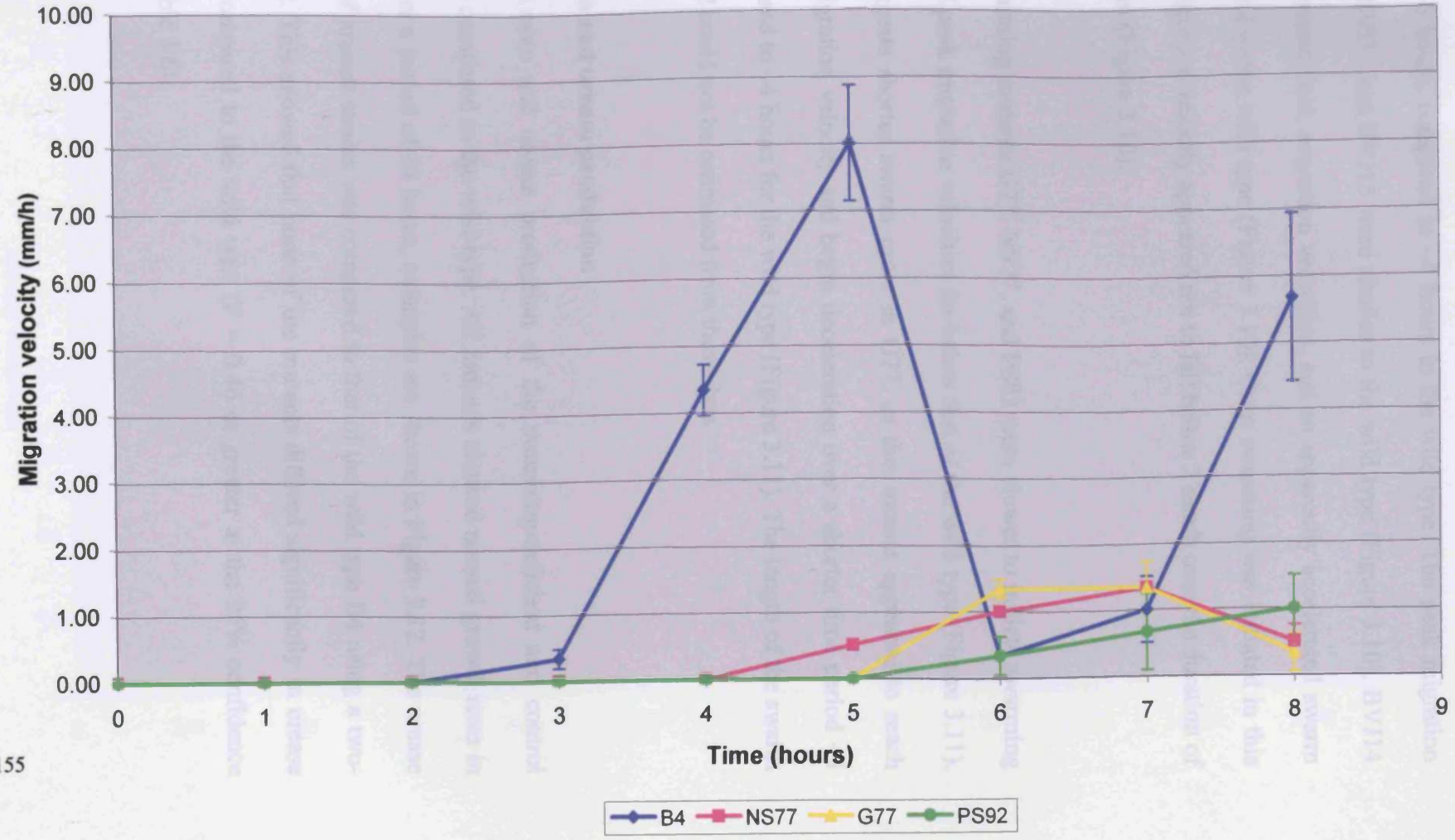

Control mutants BVJ12 and BVJ15 displayed higher initial migration velocities and slower deceleration than the wild type. The swarm cycle also appeared to be extended to ~5 hours, compared to ~4 hours in the wild type. The peak migration velocities of BVJ12 and BVJ15 were similar to the wild type (Figure 3.10). BVJ14 exhibited increased peak migration velocities, and an apparently accelerated swarm cycle compared to the wild type (Figure 3.10). Once swarming was initiated in this mutant the migration velocity appeared not to fall below 2 mm/h over the duration of the experiment (Figure 3.10).

The poor-swarming mutants G77, NS77, and PS92 were slower to initiate swarming and exhibited peak migration velocities far below that of the wild type (Figure 3.11). The data suggests shorter swarm cycle in G77, as this mutant appeared to reach maximum migration velocity and begin deceleration over a shorter time period ~3 hours, compared to ~4 hours for the wild type (Figure 3.11). The length of the swarm cycle in PS92 could not be estimated from these data.

3.3.7 **Growth and urease production**

The growth rates and urease production of the swarming-deficient and control mutants was compared to the wild type. All mutants showed normal growth rates in LB broth over a period of 24 hours, examples are shown in Figure 3.12. The urease production of mutant strains was compared to that of the wild type B4 using a two-sample t-test. This showed that none of the mutants differed significantly in urease production compared to the wild type ($P = 0.46$ or greater at the 95% confidence interval) (Table 3.6).

Figure 3.12: Examples of growth curves from *P. mirabilis* wild type strain B4, and transposon mutants grown in LB broth.

The growth curves presented here represent the wild type strain B4, and examples obtained for mutants from different groups; BVJ14 (control mutant, Group 1), G78 (poor-swarming mutant, Group 2), G37 (non-Swarming mutant, Group 3), and NS63 (Non-swarming, non-swimming mutant, Group 4).

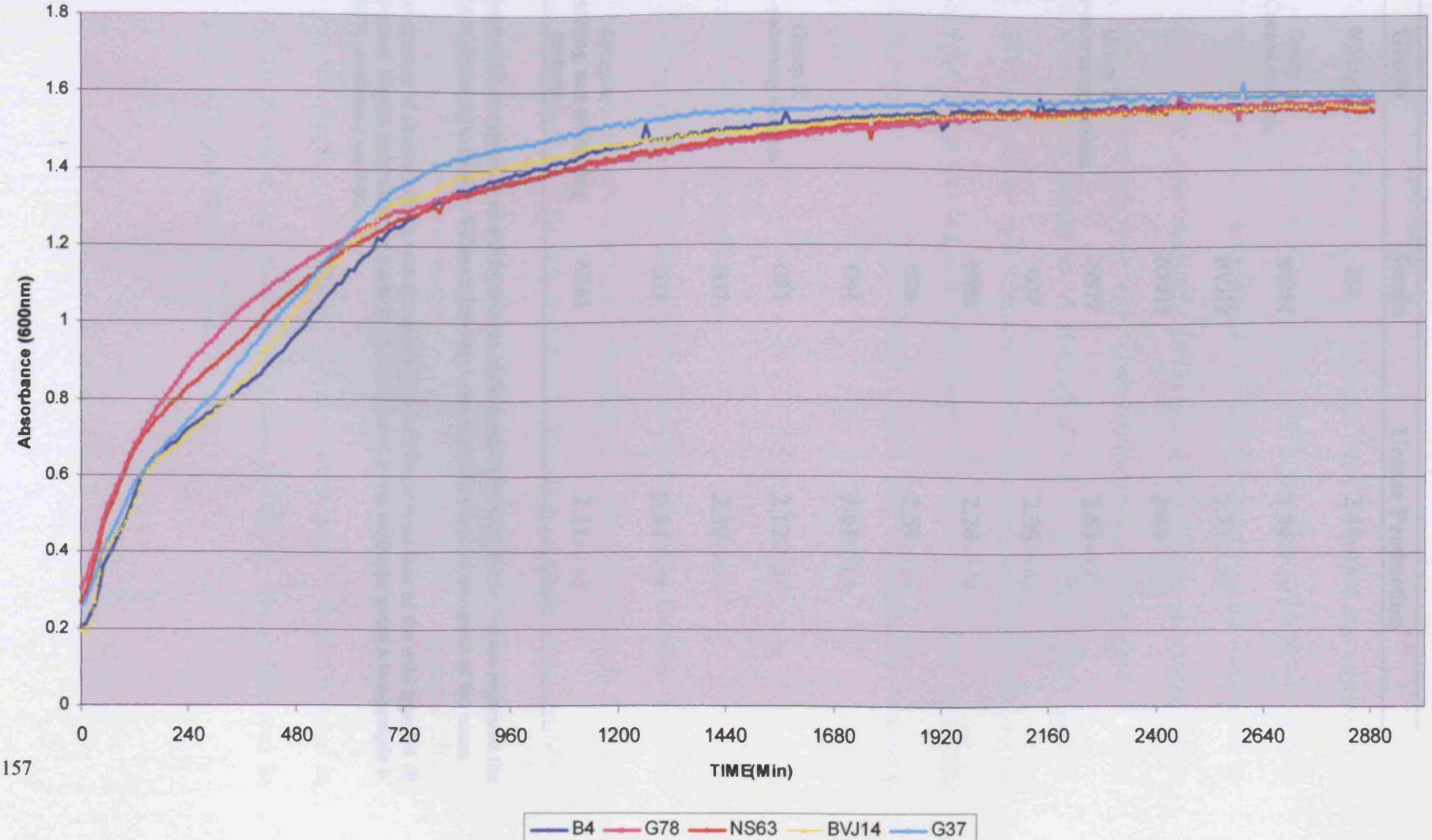

Table 3.6: Assessment of urease production by wild type strain B4, control mutants, and swarming-deficient mutants.

Group	Strain	Urease Production[a,b]
Wild type	B4	2.48±0.07
Group 1: Control mutants	BVJ14	3.39±1.41
	BVJ12	2.72±1.20
	BVJ15	3.64±1.22
Group 2: Poor-swarming mutants	NS77	2.69±0.72
	G77	2.36±0.62
	PS92	2.26±0.74
	G78	2.59±0.68
	G64	2.61±0.65
Group 3: Non-swarming mutants	G93	2.12±0.41
	G37	2.39±0.95
	G33	2.94±0.78
Group 4: Non-swarming, non-swimming mutants	NS63	2.11±0.40

[a] Urease production is expressed as millimols urea hydrolysed/ min/ mg protein. Values represent the means form triplicate experiments. Values following ± represent the standard deviation of the mean.

[b] Urease production of mutant strains was not significantly different from that of the wild type B4 (P =0.46 or greater). Urease production of mutants was compared to the wild type using a two-sample t-test at the 95% confidence interval.

3.4 Identification of disrupted genes, and complementation of swarming-deficient mutants

Genes disrupted in swarming-deficient mutants were identified by cloning, and sequencing of *P. mirabilis* chromosomal DNA flanking transposon inserts. Complementation studies were undertaken to confirm that the genes inactivated by the transposon inserts were responsible for the swarming-deficient phenotypes of the mutants. Mutants were supplied with intact copies of disrupted genes *in trans*, expressed from native promoters. A cosmid library of genomic DNA from *P. mirabilis* wild type strain B4 was screened for cosmid clones containing intact copies of the disrupted genes, and segments sub-cloned into vector pB4. These constructs were then introduced into the appropriate mutant, and restoration of swarming assessed.

3.4.1 Identification of disrupted genes

To identify genes disrupted in swarming deficient mutants, DNA flanking the mini-Tn*5*Km2 insertions was sub-cloned into the plasmid vector pUC18 (Table 2.2), and sequenced using primer 3 (Fig 2.1, Table 2.5). Homologous genes were identified from the NCBI database using the BLASTX search tool (Basic Local Alignment Search Tool X, http://www.ncbi.nlm.nih.gov/index.html) which translates DNA sequences in all six reading frames then identifies homologous peptide sequences in the database. The identity and function of genes homologous to those disrupted in each mutant are provided in Table 3.7. Attempts to identify genes disrupted in mutants BVJ12, G33, and PS92 were unsuccessful.

Table 3.7: Identification and putative function of genes disrupted in swarming-deficient and control mutants.
The sequence data of DNA flanking the transposon inserts in swarming-deficient, and control mutants was analysed using the BLASTX search tool (http://www.ncbi.nlm.nih.gov/index.html) to identify genes homologous to those disrupted in the mutants, and establish a putative function of the disrupted genes.

Group	Strain[a]	Identity and putative function of disrupted gene	% Sequence identity	E-value
Group 1: Control mutants	BVJ14	CjrC from *E. coli* – Outer membrane protein involved in Colicin Js sensitivity.	70%	4e-25
	BVJ12	No data	-	-
	BVJ15	FliS from *Salmonella enterica* serovar Typhimurium- Cytosolic flagellin export chaperone.	78%	2e-11
Group 2: Poor-swarming mutants	NS77	YdcM from *E. coli* - hypothetical protein / putative virulence factor	84%	6e-46
	G77	No Homologies	-	-
	PS92	No data	-	-
	G78[+]	AnsA from *E. coli* - Cytoplasmic L-asparaginase	81%	2e-36
	G64[+]	Putative polysaccharide transport protein from *S. enterica* serovar Typhimurium	80%	5e-17
Group 3: Non-swarming mutants	G93[-]	SurA from *S. enterica* serovar Typhimurium - Survival protein precursor; encodes a peptidyl-prolyl-cis-trans isomerase.	70%	5e-13
	G37[-]	WbdN form *E. coli* - Putative glycosyl transferase	58%	3e-08
	G33	No data	-	-
Group 4: Non-Swarming, non swimming mutants	NS63[+]	FlhA from *P. mirabilis* – Flagella biosynthesis	97%	1e-40

[a] Mutants marked with + or – identify those for which complementation studies were undertaken. + successful complementation, – complementation was unsuccessful.

3.4.2 Design of mutant specific PCR primers and screening of cosmid library

Five of the nine original swarming-deficient mutants generated in this study (Section 3.3.4) were selected for complementation. These were the poor-swarming mutants G78 and G64 (Group 2), the non-swarming mutants G37 and G93 (Group 3), and the non-swarming, non-swimming mutant NS63 (Group 4). Sets of PCR primers specific to the genes disrupted in each mutant were designed using the sequence data of DNA flanking the transposon inserts. These primer sets were used to generate DIG labelled probes specific to genes disrupted in the mutants, and screen a cosmid library of B4 genomic DNA. The primer sets associated with each mutant are given in Table 3.8 (details of each primer set are provided in Tables 2.5 and 2.6), and an example of PCR reactions are provided in Figure 3.13. Several clones were identified for each mutant (Table 3.8), and an example of the results obtained form the library screening procedure is shown in Figure 3.14.

3.4.3 Construction of vector pB4 and assessment of effect on mutant phenotype

Plasmid pB4 was constructed in order to introduce sub-cloned segments of the isolated cosmids into the appropriate mutant. This vector was derived from plasmid pOT182 that had been shown to replicate in *P. mirabilis* strain B4 (Section 3.2.2), by removal of the Tn*5*-OT182 transposon. This resulted in a vector that could be easily introduced to *P. mirabilis* by conjugal transfer using the mating method described in section 2.3.8. Replication of pB4 in *P. mirabilis* B4 was confirmed, and found to have no effect on the stability of the swarming-deficient mutants.

Table 3.8: Primer sets specific to genes disrupted in mutants, and cosmid clones isolated from B4 cosmid library.

Primer sets relevant to each mutant were used to screen the B4 cosmid library by PCR. Several cosmid clones, which potentially contained intact copies of disrupted genes, were identified using each primer set.

Strain	Primer set[a]	Cosmids isolated[b]
G37	GLT_F1 GLT_R1	pCOSGLT1 pCOSGLT2
NS63	FlhA_F1 FlhA_R1	pCOSFLHA1 pCOSFLHA2 pCOSFLHA3*
G64	PST_F1 PST_R1	pCOSPST2 pCOSPST3* pCOSPST4
G78	AnsA_F1 AnsA_R1	pCOSANSA1 pCOSANSA2*
G93	SurA_F2 SurA_R1	pCOSSURA1 pCOSSURA2 pCOSSURA3

[a] Details of primers, including expected products of amplification, and sequence data, are provided in Tables 2.5 and 2.6

[b] Lists the cosmids clones identified with each primer set, and used in subsequent attempts to complement the associated swarming-deficient mutants.

* Denotes the cosmid clone used to successfully complement relevant mutant

Figure 3.13: Products of PCR reactions with primer sets used for screening of B4 cosmid library.

PCR reactions with the primer sets were optimised using purified genomic DNA from *P. mirabilis* wild type strain B4. Below are examples of typical PCR reactions performed on dilutions of B4 genomic DNA.

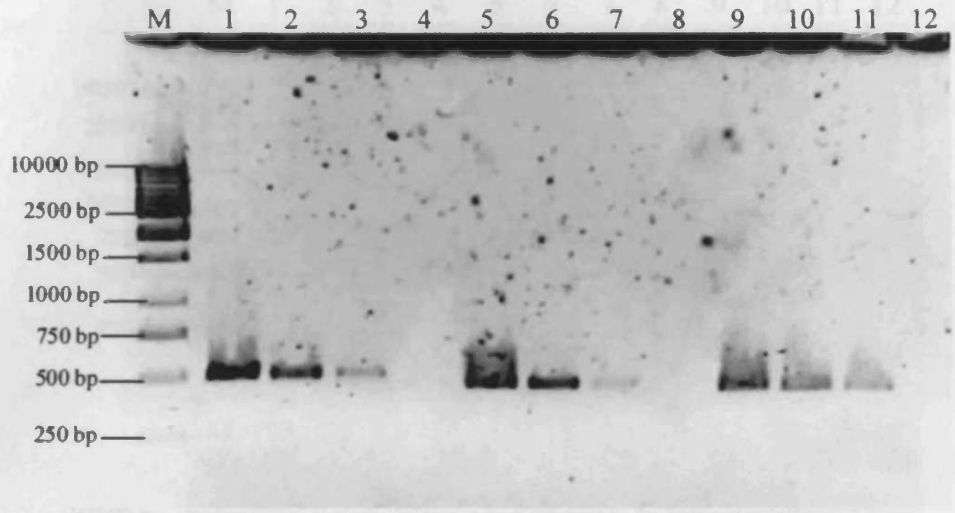

M, 1 kb molecular size standard

1-3, Products from PCR reactions with primers PST_F1,R1, using 1:10, 1:100, and 1:1000 dilutions of B4 DNA respectively.
4, PST_F1,R1 negative control (Sterile deionised water).

5-7, Products from PCR reactions with primers AnsA_F1,R1, using 1:10, 1:100, and 1:1000 dilutions of B4 DNA respectively.
8, AnsA_F1,R1 negative control (Sterile deionised water).

9-11, Products from PCR reactions with primers GLT_F1,R1, using 1:10, 1:100, and 1:1000 dilutions of B4 DNA respectively.
12, GLT_F1,R1 negative control (Sterile deionised water).

Figure 3.14: Screening of B4 cosmid library with primers specific to genes disrupted in swarming-deficient mutants.

An example of cosmid library screening with primers AnsA_F1,R1, to identify cosmid clones potentially carrying intact copies of the gene disrupted in swarming-deficient mutants. Lane 4 and Lane 18 indicate cosmid clones identified as potentially carrying intact copies of the a*nsA* gene.

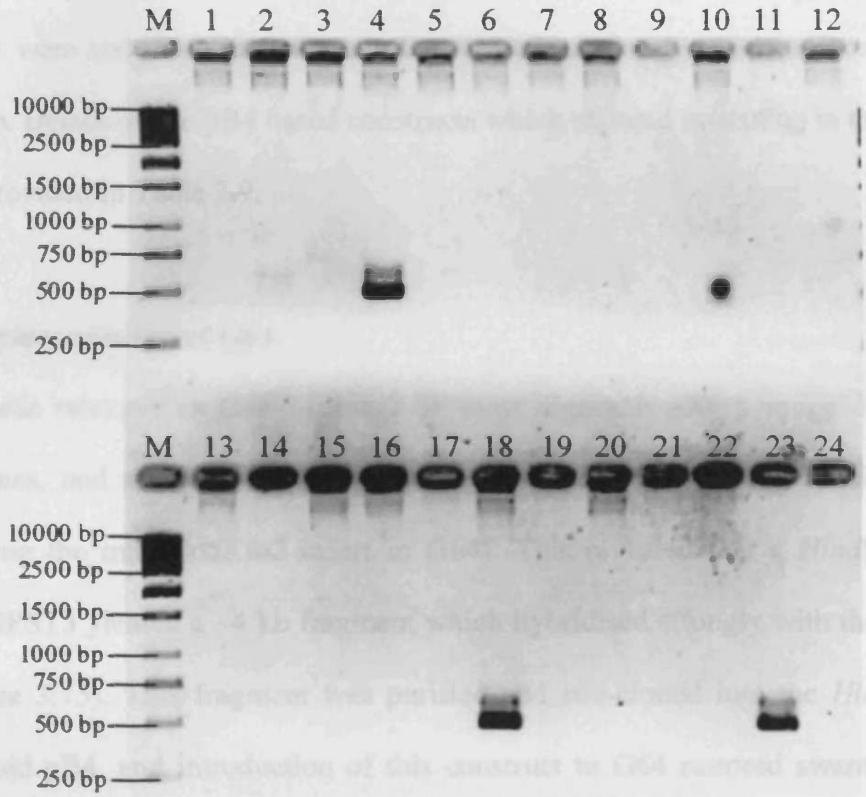

M, 1 kb molecular size standard
1-22, Purified cosmid DNA from distinct clones
23, Positive control (Purified genomic DNA form *P. mirabilis* B4)
24, Negative control (Sterile deionised water)

3.4.4 Complementation of swarming-deficient mutants

The poor-swarming mutants G64, and G78, and the non-swimming non-swarming mutant NS63 were successfully complemented. Attempts to complement the non-swarming mutants G37 and G93 were unsuccessful. Mutant G64 was complemented using a Southern hybridisation approach (section 2.9.6), while mutants G78 and NS63 were complemented through the *Sau* 3A partial digestion approach (Section 2.9.7). Details of the pB4 based constructs which restored swarming in these mutants are provided in Table 3.9.

Complementation of G64

Cosmids relevant to G64 (Table 3.8) were digested with a range of restriction enzymes, and analysed by Southern hybridisation (using probes specific to DNA flanking the mini-Tn*5*Km2 insert in G64). This revealed that a *Hind*III digest of pCOSPST3 yielded a ~4 kb fragment which hybridised strongly with the G64 probe (Figure 3.15). This fragment was purified and sub-cloned into the *Hind*III site of plasmid pB4, and introduction of this construct to G64 restored swarming. Figure 3.16 shows results of assays to confirm the presence of this construct (designated pB4PST3) in G64 exhibiting restored swarming ability.

Complementation of NS63 and G78

Restriction enzyme *Sau* 3A, at a range of concentrations, was used to digest cosmid clones relevant to mutants NS63 and G78. An example of products obtained from these digests is shown in Figure 3.17. Fragments ~5-6 kb in size were gel purified from cosmids exhibiting desired levels of digestion, and sub-cloned into the *Bam*H1 site of vector pB4. When the resulting constructs were introduced to the appropriate mutant, colonies exhibiting a swarming phenotype were generated, indicating that

Table 3.9: Summary of pB4 based constructs which restore swarming in mutants NS63, G64, G78, and U6450 *flhA*⁻.

Construct	Strain(s) Complemented	Positive for disrupted gene by PCR[a]	Description
pB4PST3	G64	Yes	Plasmid pB4 carrying a ~4 kb *Hind*III fragment from pCOSPST3. Generated by Southern hybridisation approach
pB4ANSA2	G78	Yes	Plasmid pB4 carrying a ~5-6 kb *Sau* 3A fragment from pCOSANSA2. Generated by the *Sau* 3A partial digest approach
pB4FLHA3	NS63, U6450 *flhA*⁻	No	Plasmid pB4 carrying a ~5-6 kb *Sau* 3A fragment from pCOSFLHA3. Generated by the *Sau* 3A partial digest approach

[a] PCR assays were performed using the primer sets associated with each mutant, listed in Table 3.8, on the appropriate construct.

Figure 3.15: Identification of fragments from pCOSPST3, suitable for sub-cloning into pB4.

Southern hybridisation, with probes specific to DNA flanking the transposon insert in G64, was used to identify fragments of cosmid clone pCOSPST3 (Table 3.9) suitable for sub-cloning into vector pB4.

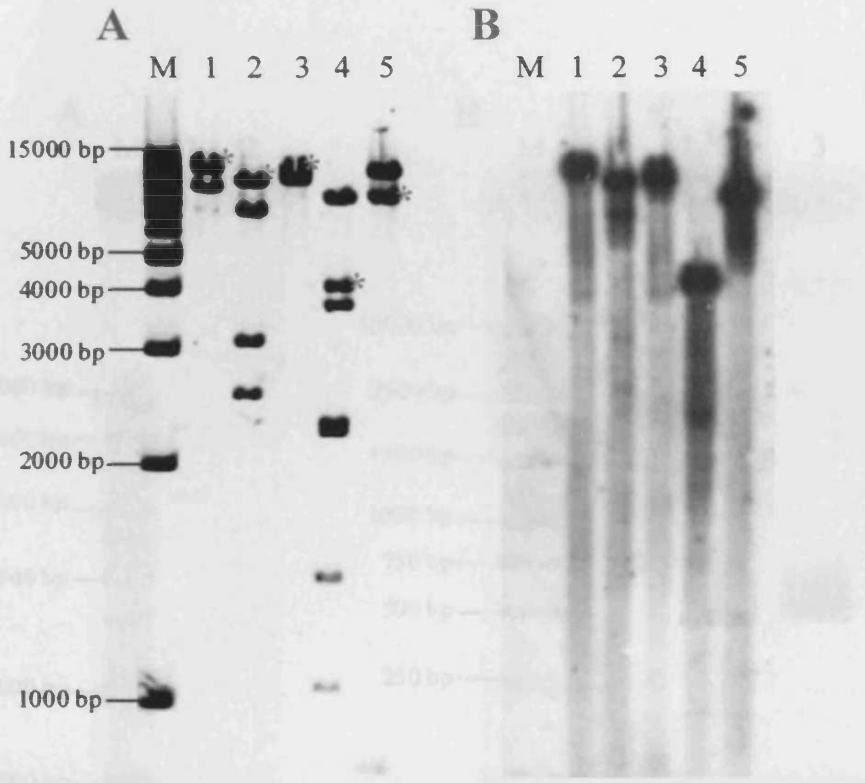

M, 1 kb molecular standard
1, *Sal*I digest of pCOSPST3
2, *Nco*I digest of pCOSPST3
3, *Xba*I digest of pCOSPST3
4, *Hind*III digest of pCOSPST3
5, *Sac*I digest of pCOSPST3

A: Restriction digests of cosmid clone pCOSPST3. *indicates fragments identified by Southern hybridisation (**B**). *Hind*III digests generated a ~4 kb fragment suitable for sub-cloning.

B: Southern hybridisation of digested clones with probes specific to DNA flanking transposon insert in G64.

Figure 3.16: Analysis of construct pB4PST3 extracted from mutant G64 with restored swarming ability.

The pB4 based construct capable of restoring swarming in mutant G64 (pB4PST3, Table 3.9), was extracted from G64 restored in swarming, and analysed. Presence of the *Hind*III fragment from pCOSPST3 was confirmed by *Hind*III digest (A). Plasmid pB4PST3 was also confirmed as possessing the DNA sequence flanking the transposon insert in G64, by PCR using primers PST_F1,R1 (B).

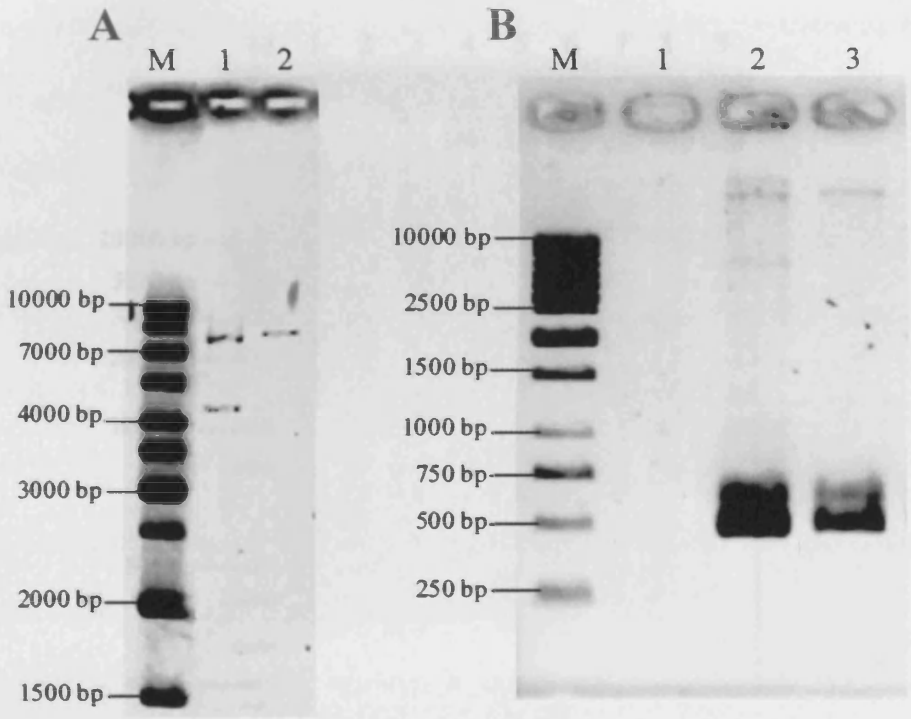

A: *Hind* III digest of pB4PST3 extracted from mutant G64 with restored swarming ability, and pB4 purified from *E. coli* JM109.

M, 1 kb molecular size standard
1, *Hind*III digested pB4PST3
2, *Hind*III digested pB4

B: PCR with primers PST_F1,R1 on plasmid pB4PST3, and B4 genomic DNA.

M, 1 kb molecular size standard
1, negative control (sterile deionised water)
2, pB4PST3
3, B4 genomic DNA

Figure 3.17: An example of *Sau* 3A partial digests of cosmid clones for complementation of swarming-deficient mutants.

For complementation using the *Sau* 3A partial digestion approach, purified cosmid clones were digested with a range of concentrations of restriction enzyme *Sau* 3A. Fragments ~5-6 kb in size were then purified from digests exhibiting desired levels of digestion. The example below shows *Sau* 3A partial digestion of pCOSFLHA3. Fragments were purified from Lane 1, and successfully used to restore swarming in mutant NS63 (Table 3.9).

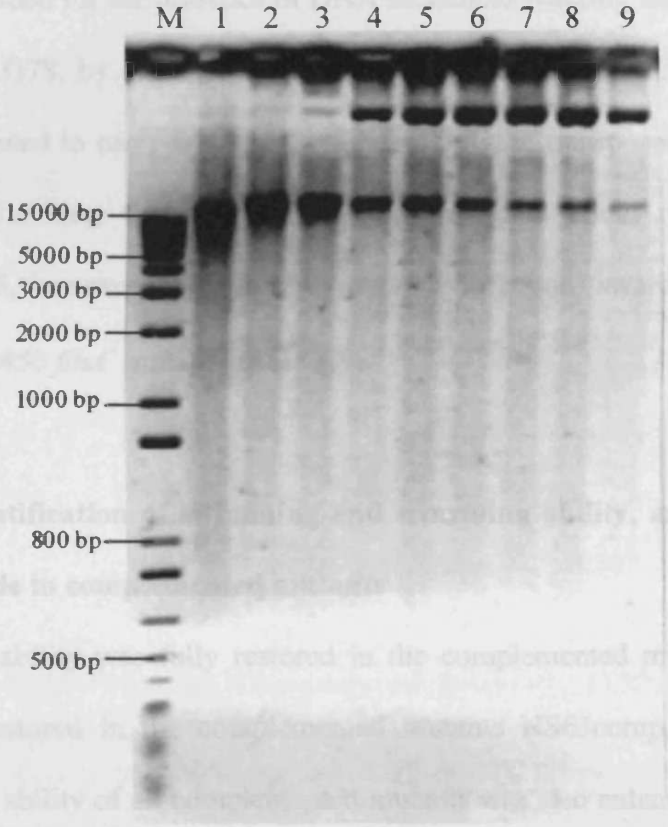

M, 1 kb molecular size standard
1-8, pCOSFLHA3 digested with decreasing concentrations of *Sau* 3A
9, undigested pCOSFLHA3

mutants had been successfully complemented. The presence of these constructs was confirmed in several complemented NS63 and G78 colonies (Figure 3.18).

Swarming was restored in mutants NS63 and G78 by the introduction of pB4 based constructs designated pB4FLHA3 and pB4ANSA2 respectively. These constructs were examined for the presence of DNA sequences flanking the transposon inserts in NS63 and G78, by PCR with primer sets listed in Table 3.8. Plasmid pB4ANSA2 was confirmed to carry DNA sequence flanking the transposon insert in G78. DNA sequence flanking the transposon insert in NS63 could not be confirmed on pB4FLHA3, however, this plasmid was able to restore swarming when introduced into the U6450 *flhA*$^{-}$ mutant (Table 3.9).

3.4.5 Quantification of swimming and swarming ability, and periodicity of the swarm cycle in complemented mutants

Swarming ability was fully restored in the complemented mutants G64comp, and partially restored in the complemented mutants NS63comp, and G78comp. The swimming ability of all complemented mutants was also enhanced, compared to that of their un-complemented counterparts (Table 3.10). The temporal control of the swarm cycle in the complemented mutants was compared to that of the wild type strain B4. The duration of the swarm cycle NS63comp and G78comp was similar to that of the wild type (~4h), although initiation of migration was delayed in these mutants (Figure 3.19). The complemented mutant G64comp appeared to exhibit an accelerated swarming cycle, with a shorter period of migration (~2-3h) compared to the wild type (~4h). In this mutant migration was initiated sooner than in the wild type, with each successive phase of migration reaching a higher peak migration velocity than the previous phase (Figure 3.19).

Figure 3.18: Analysis of constructs pB4ANSA2 and pB4FLHA3, extracted from mutants G78 and NS63 with restored swarming ability.

The pB4 based constructs capable of restoring swarming in mutants G78 (pB4ANSA2, Table 3.9), and NS63 (pB4FLHA3, Table 3.9), were extracted mutants with and analysed. *Bam*HI digests of pB4ANSA2 (A), and pB4FLHA3 (B), were used to confirm presence of the *Sau* 3A fragments from pCOSANSA2, and pCOSFLHA3 respectively. Plasmid pB4ANSA2 was also confirmed as possessing the DNA sequence flanking the transposon insert in G78, by PCR using primers AnsA_F1,R1(A).

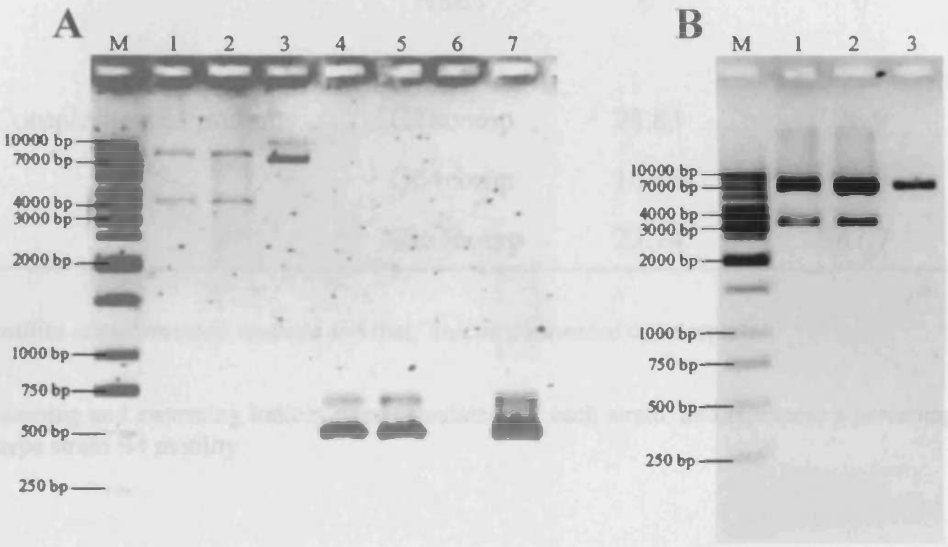

A: Products of *Bam*HI digest, and PCR reactions with primers PST_F1,R1 on pB4ANSA2.

M, 1kb molecular size standard
1-2, ***Bam*HI** digested **pB4ANSA2** (purified from distinct G78 colonies with restored swarming ability)
3, ***Bam*HI** digested **pB4** purified from *E. coli* JM109
4-5, **PCR** products for reactions on **pB4ANSA2** (purified from distinct G78 colonies with restored swarming ability)
6, **PCR** negative control (sterile deionised water)
7, **PCR** positive control (**B4** genomic DNA)

B: Products of *Bam*HI digest of pB4FLHA3.

M, 1 kb molecular size standard
1-2, ***Bam*HI** digested **pB4FLHA3** (purified from distinct NS63 colonies with restored swarming ability)
3, ***Bam*HI** digested **pB4** purified from *E. coli* JM109

Table 3.10: Swimming and swarming abilities of complemented mutants.

Mutant Type[a]	Strain	Swarming[b] Index	Swimming[b] Index
Un-complemented mutants	G78	0	36.9
	G64	0	28.5
	NS63	0	0
Complemented mutants	G78comp	28.83	76.9
	G64comp	105.8	52.3
	NS63comp	23.74	47.7

[a] Identifies complemented mutants and their un-complemented counterparts.

[b] Swimming and swarming indices were calculated for each strain, and represent a percentage of the wild type strain B4 motility.

Figure 3.19: Analysis of swarm cycle periodicity in complemented mutants NS63comp, G64comp, and G78comp.
The temporal control of the swarm cycle in complemented mutants NS63comp, G64comp, and G78comp (Group 2) was compared to the wild type strain B4. Data obtained during assessment of swarming ability was converted to represent the velocity of migration (mm/hour) at each time point

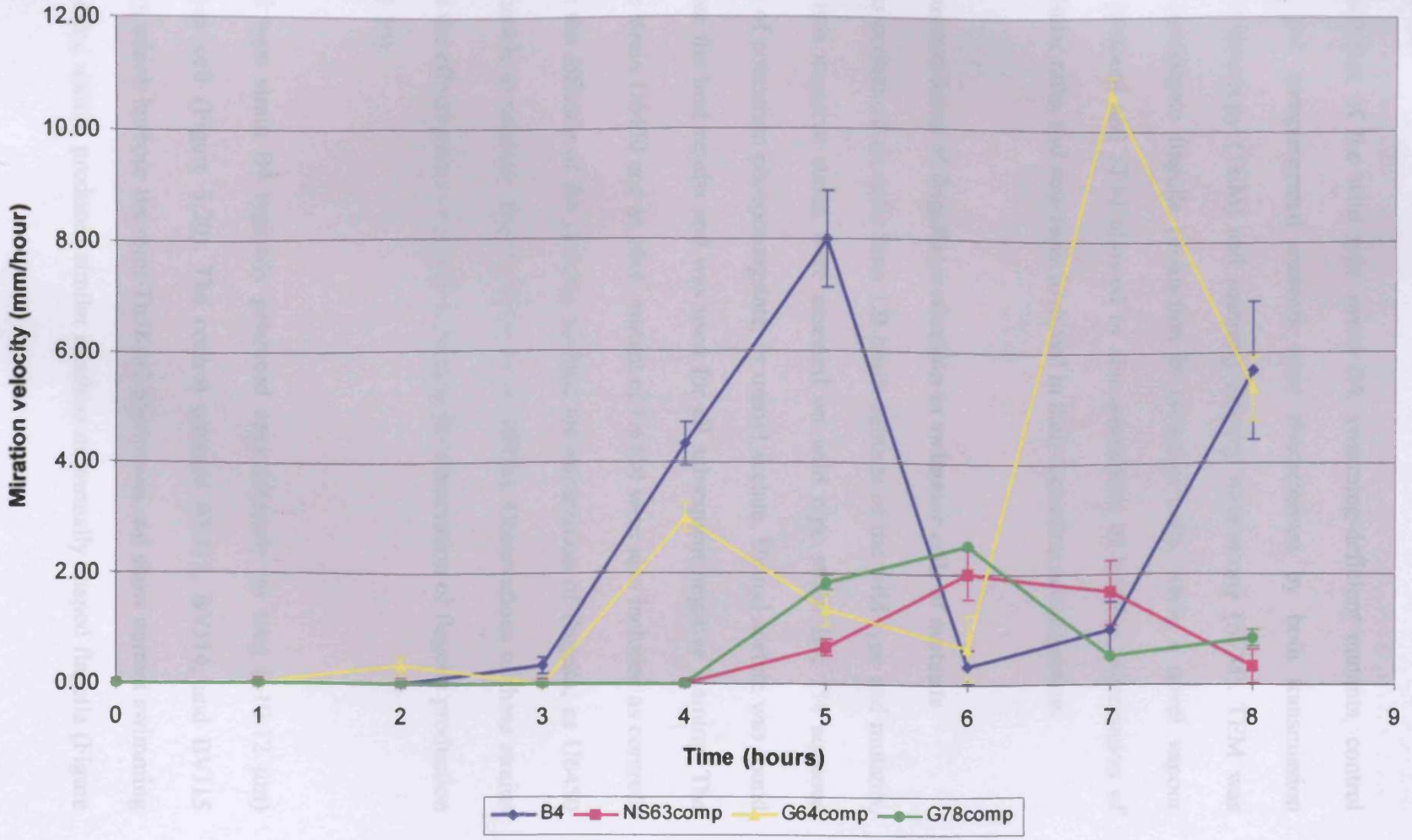

3.5 Characterisation of swarming-deficient mutants by electron microscopy

The phenotypes of the wild type strain B4, swarming-deficient mutants, control mutants, and complemented mutants were characterised by both transmission electron microscopy (TEM) and scanning electron microscopy (SEM). TEM was used to investigate flagella production in swimmer cells, while a novel vapour fixation protocol and SEM allowed *in situ* assessment of cellular organisation of multi-cellular rafts, and structures involved in their formation and migration.

3.5.1 Demonstration of flagella production in swimmer cells of mutants

TEM was performed on cells from LB broth cultures of the wild type and mutants. Initially two negative stains were assessed on wild type strain B4; 1% aqueous solutions of potassium phospotungstate, or uranyl acetate. Uranyl acetate was found to generate the best results and was used for all subsequent negative staining. The wild type strain U6450 and an *flhA*$^-$ mutant of U6450 were also included as controls to assess the efficacy of the staining method for observation of flagella, as U6450 *flhA*$^-$ is unable to produce flagella (Gygi *et al.* 1995a). Observations of these strains validated the effectiveness of negative staining for observation of flagella production (Figure 3.20).

The wild type strain B4 typically produced approximately 30 long (~10-12 μm) flagella per cell (Figure 3.20). The control mutants BVJ12, BVJ14, and BVJ15 (Group 1), which harbour the mini-Tn*5*Km2 transposon and show normal swimming and swarming ability, produced similar numbers of normally shaped flagella (Figure 3.20).

Figure 3.20: Demonstration of flagella production and phenotype in *P. mirabilis* wild type strains and control mutants.

TEM observations of flagella production in wild type *P. mirabilis* strains and mutants. Micrographs are as follows: **U6450** - wild type strain. **U6450 *fla*A⁻** - U6450 mutant incapable of flagella production (Group 4). **B4** - wild type strain used to generate swarming-deficient mutants. **BVJ12, BVJ14, BVJ15** - transposon containing control mutants of B4 with normal swarming and swimming ability (Group 1). **Bar = ~1 μm.**

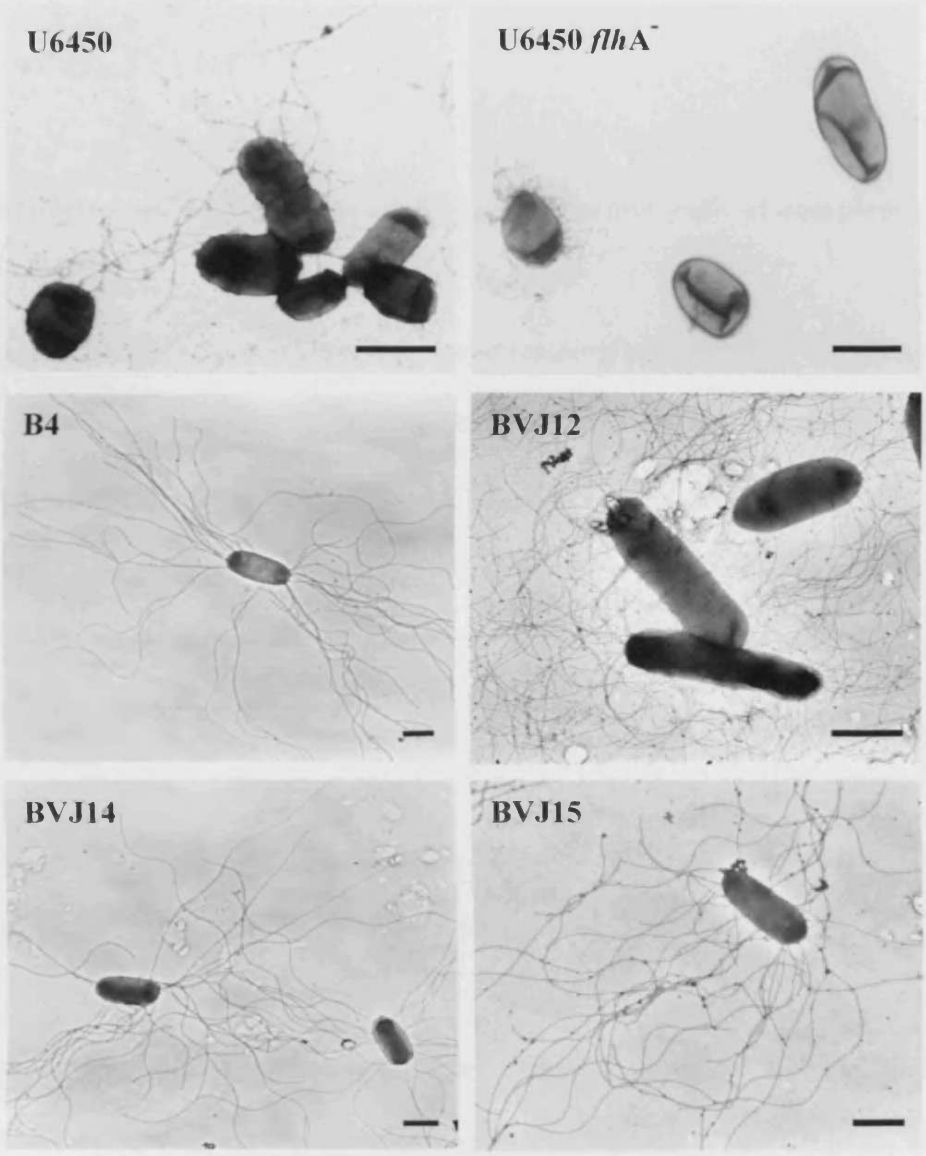

All mutants deficient in swarming produced fewer flagella (~0-11) than the wild type, and several appeared to produce abnormal flagella (Figure 3.21). The defects observed included alterations in flagella shape (G78, Figure 3.21), decreased length of flagella (G64, Figure 3.21), and dissociation of flagella filaments from cells (G37, Figure 3.21). No flagella were observed on the non-swarming, non-swimming mutant NS63 (Figure 3.21).

3.5.2 Demonstration of flagella production in swimmer cells of complemented mutants

Complementation of the non-swimming, non-swarming mutant NS63 (NS63comp), resulted in restoration of flagella production in this mutant. The abnormal flagella observed in mutants G64 and G78 (Figure 3.21) were not evident in their complemented counterparts G64comp and G78comp (Figure 3.22). Flagella of normal length were generated by G64comp while G78comp produced flagella exhibiting a less distorted morphology than those produced by G78. However, the shape of the flagella filaments synthesised by G78comp were less curved and appeared straighter than those of the wild type (Figure 3.22). All complemented mutants produced fewer flagella filaments than the wild type (Figure 3.22).

3.5.3 Scanning electron microscopy of swarm fronts

Swarm fronts of the wild type and mutants were observed using SEM. Swarm fronts were fixed *in situ*, during active migration on agar, by vapour fixation. Cells of the wild type strains B4 and U6450 appeared aligned to form multi-cellular rafts of parallel cells (Figure 3.23). Cells at the swarm front were elongated and hyper-flagellated, which is consistent with previous observations of *P. mirabilis* swarmer cells (Allison *et al.* 1993; Gygi *et al.* 1995a; Belas 1996).

Figure 3.21: Demonstration of flagella production and phenotype in swarming-deficient mutants.

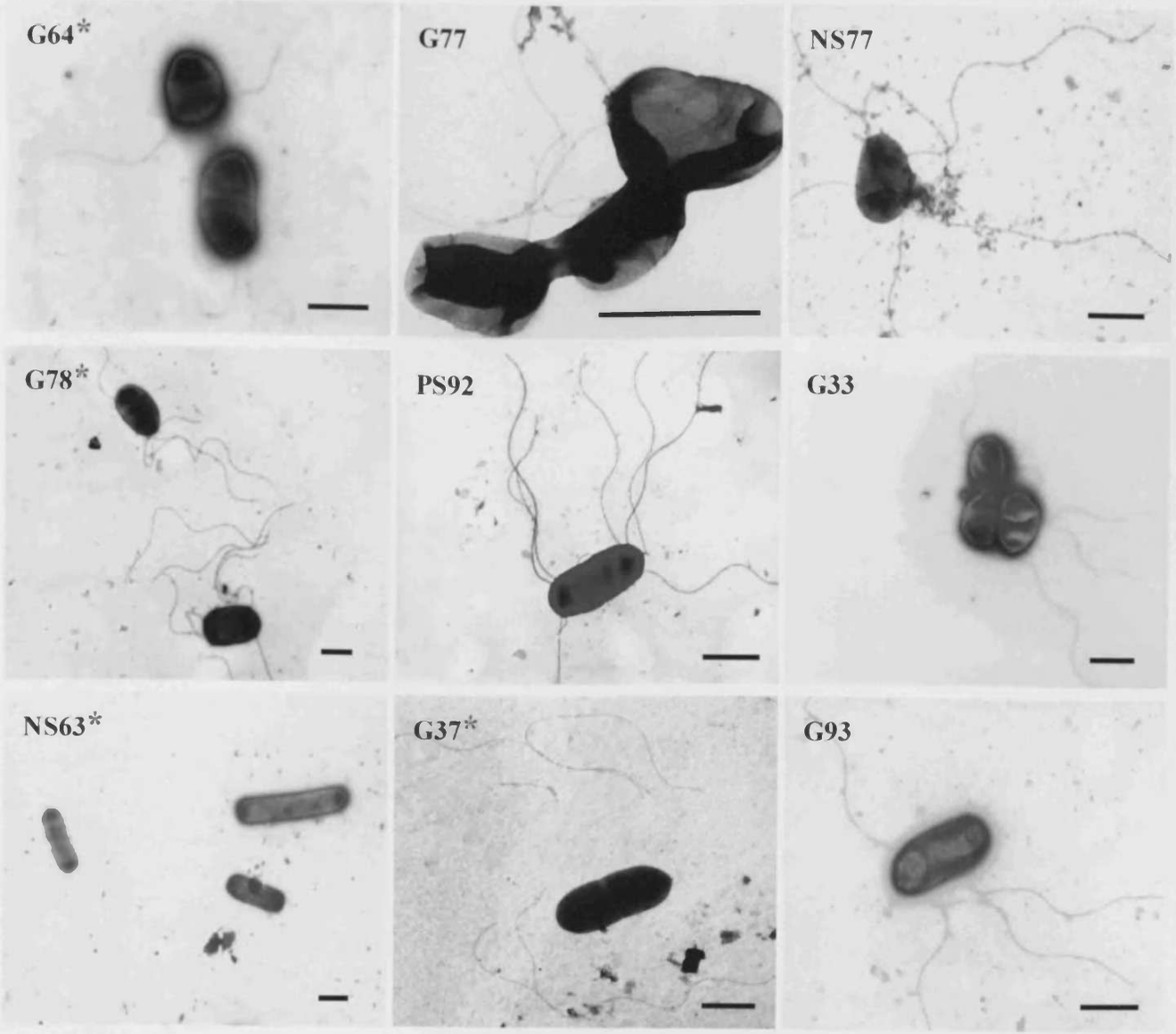

TEM observations of flagella production in swarming deficient mutants. Micrographs are as follows:

Poor-swarming mutants (Group 2) -**G64***, **G77, NS77, G78*, PS92.**

Non-swarming mutants (group 3) - **G33, G37*, G93.**

Non-swimming, non-swarming mutants (group 4) - **NS63*.**

* Denotes mutants that produce abnormal flagella compared to the wild type.

* Denotes mutants unable to produce flagella.

Bar = ~1 μm.

Figure 3.22: Flagella production and shape in complemented mutants.
Flagella production, and shape of flagella filaments was analysed in the complemented mutants (NS63comp, G64comp, G78comp) by negative staining of swimmer cells and TEM. **Bar = ~1 μm**

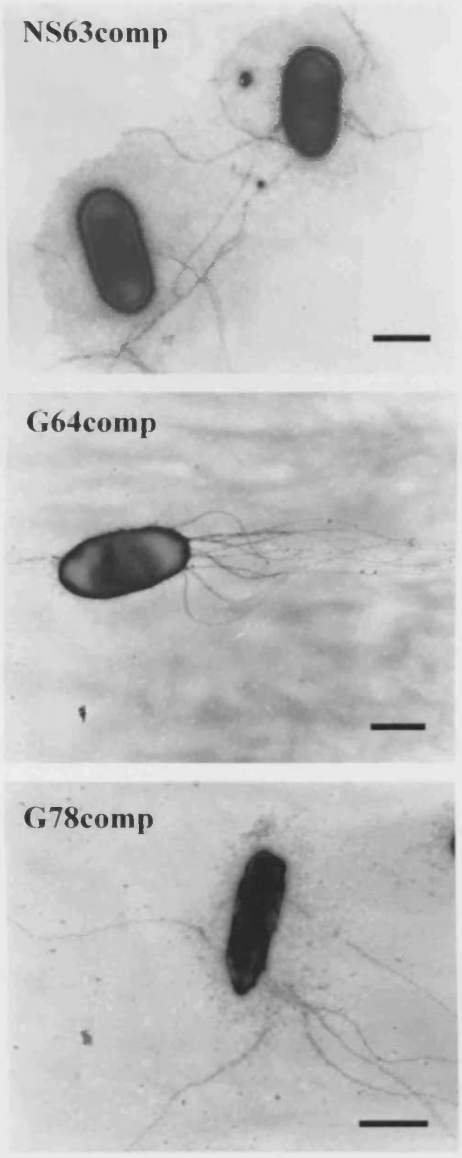

However, *in situ* vapour fixation also revealed a completely novel aspect of the *P. mirabilis* swarming cycle. Observations of these wild type strains showed that the flagella filaments of *P. mirabilis* are highly organised during migration, and appear to be interwoven in phase, to form helical connections between adjacent swarmer cells (Figure 3.23). The control mutants were comparable to the parent strain B4, and formed rafts of parallel, hyper-flagellated, elongated swarmer cells, with helical connections produced between adjacent cells (Figure 3.24).

The poor-swarming mutant G64 also exhibited helical connections, but these structures were less evident in all other poor-swarming mutants (Group 2), and flagella filaments appeared less organised (Figure 3.25). Helical connections were not observed on the non-swarming mutants (Group 3), or non-swarming, non-swimming mutants (Group 4) (Figures 3.26, and 3.27). The elongated, hyper-flagellated swarmer cells seen in the wild type, were not formed by non-swarming mutants (Figure 3.26), or the non-swarming, non-swimming mutant U6450 *flhA*$^{-}$ (Figure 3.27). The non-swarming, non-swimming mutant NS63 however, retained the ability to produce elongated cells (Figure 3.27). A summary of the observations on the swarm fronts of all strains is presented in Table 3.11.

3.5.4 Scanning electron microscopy of swarm fronts from complemented mutants

SEM observations of swarm fronts of complemented mutants revealed that formation of helical connections was restored in NS63comp and G78comp, while G64comp displayed no change in its ability to create these structures (Figure 3.28).

Figure 3.23: SEM observations of wild type *P. mirabilis* B4, and U6450 swarm fronts.

Swarm fronts were fixed *in situ*, by vapour fixation, during active migration on LB agar. Both wild type strains produced multicellular rafts of elongated, hyper-flagellated swarmer cells, and flagella filaments were interwoven in phase to form helical connections between adjacent cells. **Bar = ~1 μm**.

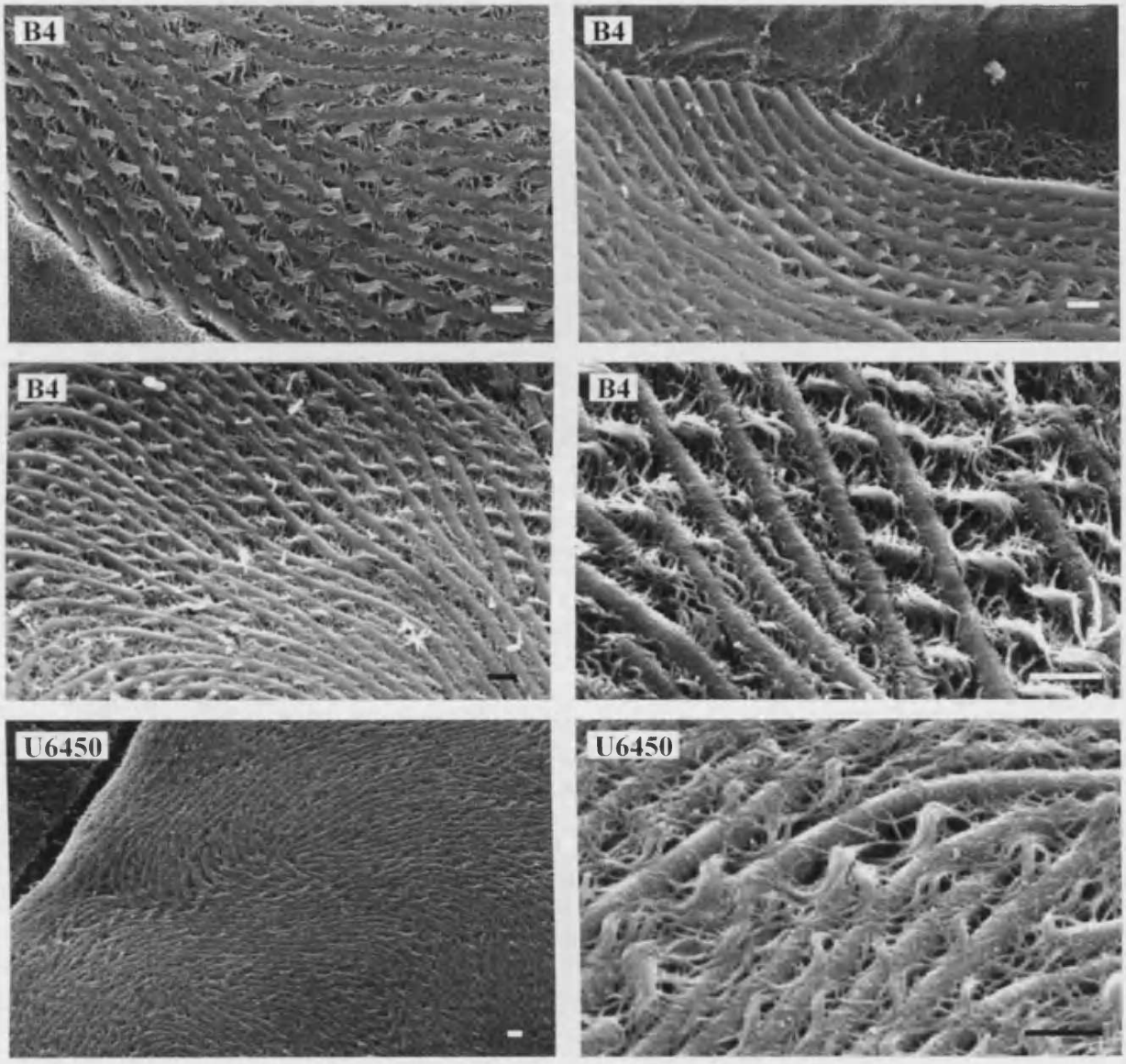

Figure 3.24: SEM observations of control mutant (group 1) swarm fronts.
SEM observations of swarm fronts of transposon containing control mutants **BVJ12**, **BVJ14**, and **BVJ15** with wild type or above swarming ability (Group 1). Swarm fronts were fixed *in situ*, by vapour fixation, during active migration on LB agar. Formation of multicellular rafts, and generation of the helical connections observed in the parent strain B4, was unaltered in the control mutants. **Bar = ~1 μm.**

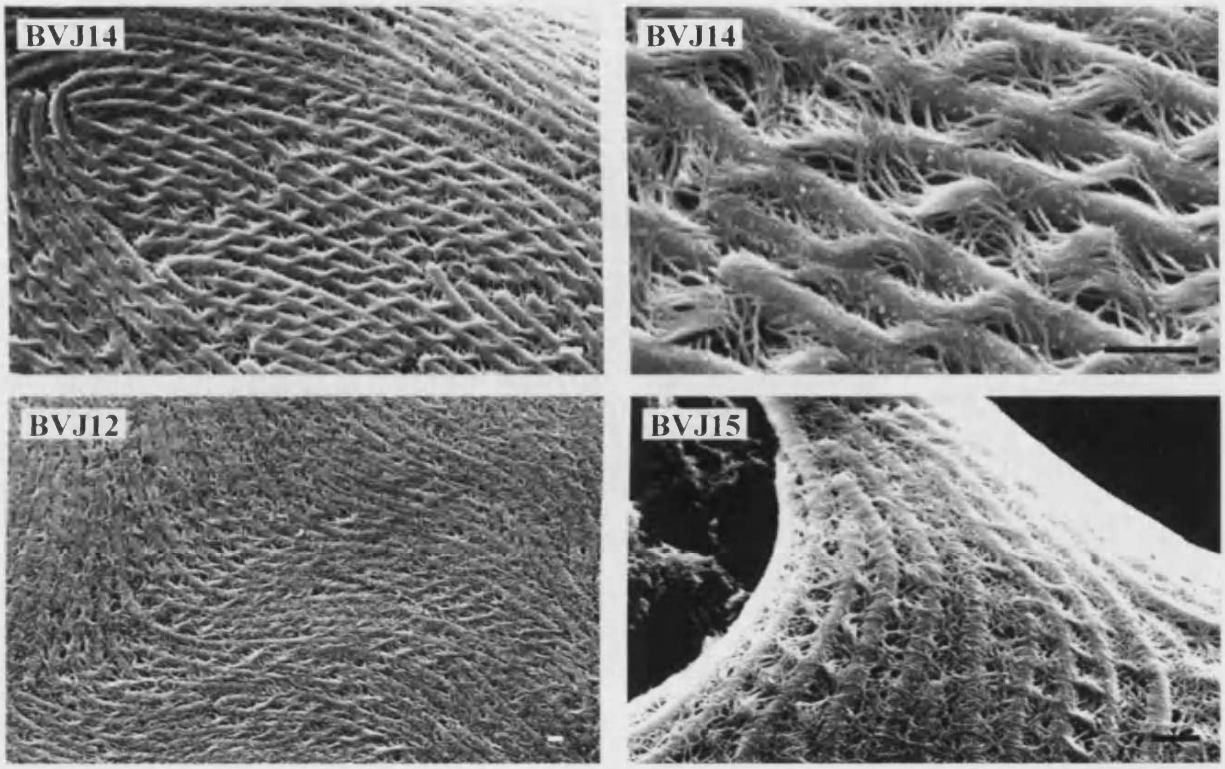

Figure 3.25: SEM observations of swarm fronts of poor-swarming mutants (group 2). SEM observations of swarm fronts of wild type *P. mirabilis* poor-swarming mutants (Group 2). Swarm fronts were fixed *in situ*, by vapour fixation, during active migration on LB agar. **G64** generated helical connections but these structures were less evident in all other poor-swarming mutants (**G77, NS77, G78, PS92**). Poor-swarming mutants **G77** and **PS92** were also defective in cellular organisation. **Bar = ~1 μm.**

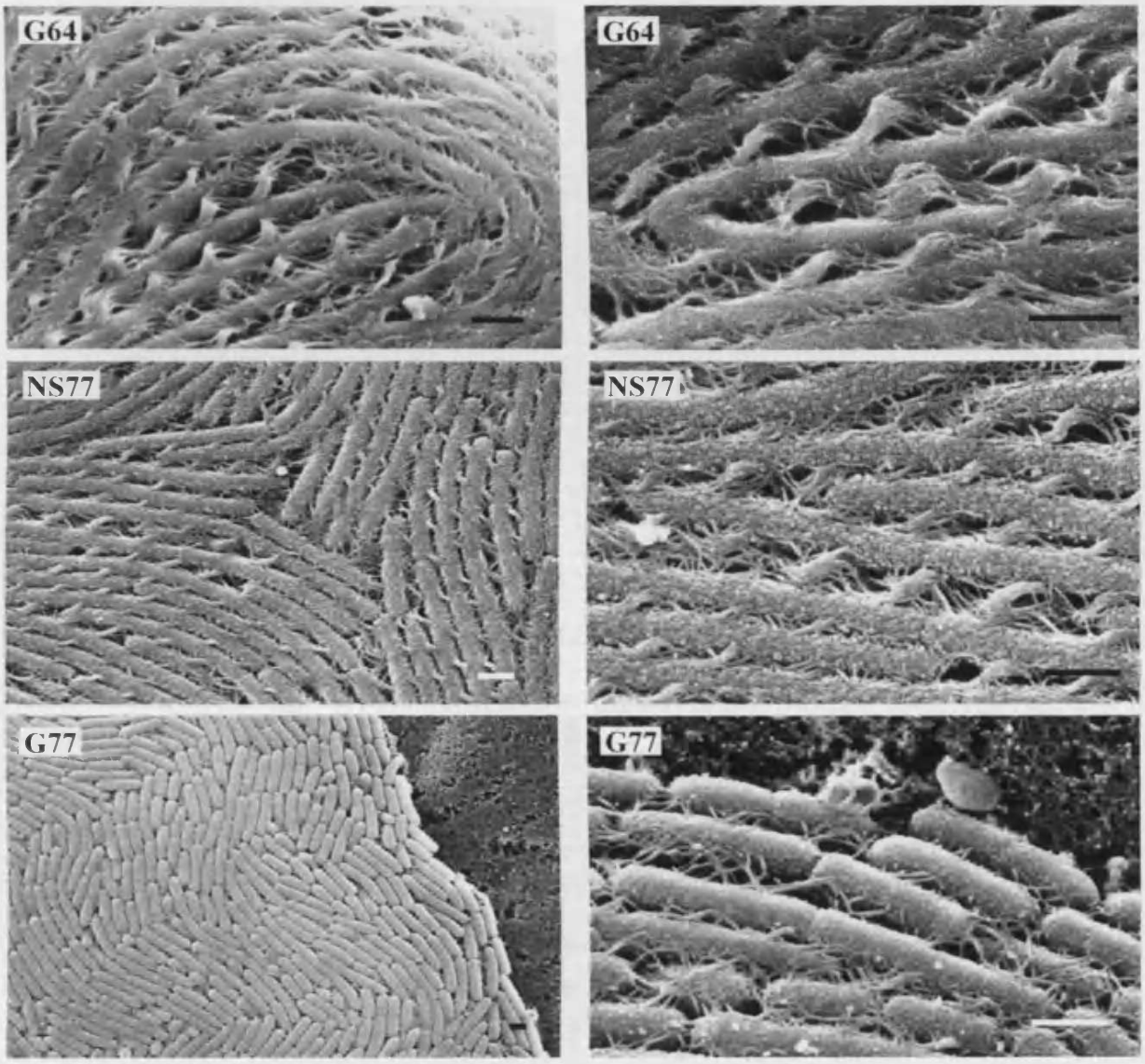

Figure 3.25 continued on page 183.

Figure 3.25 continued.

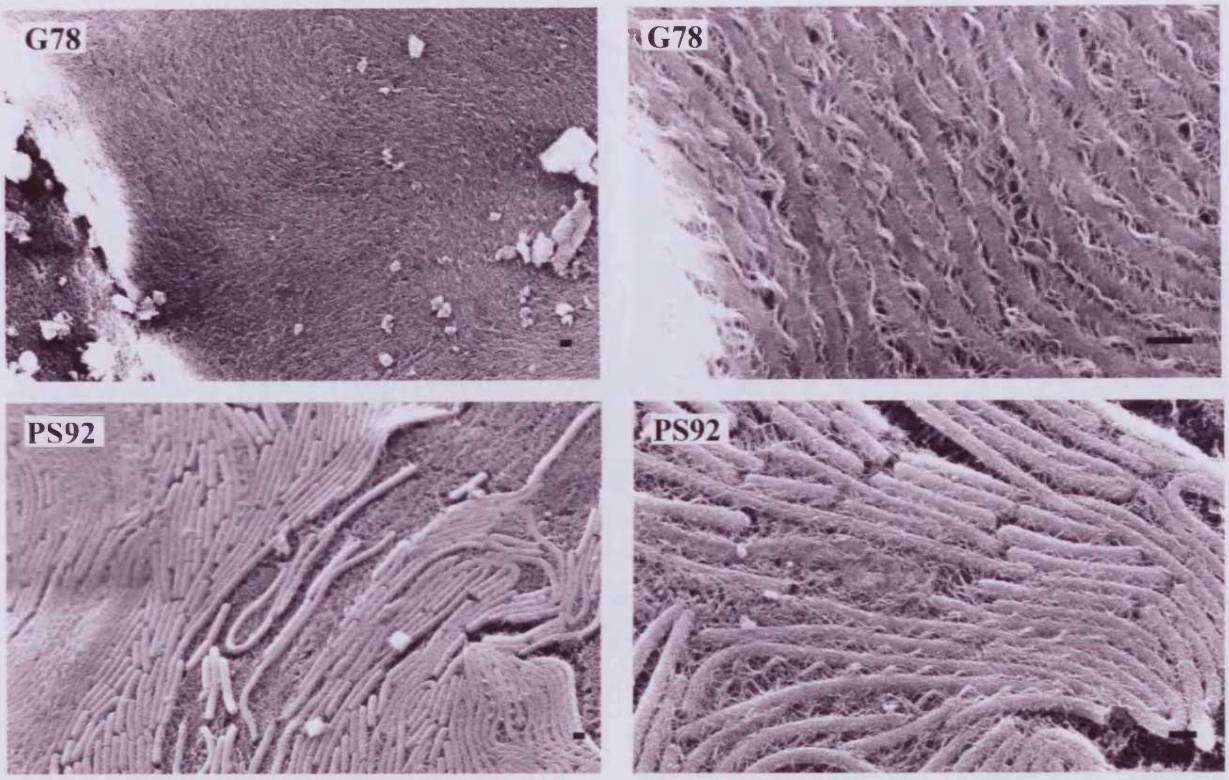

Figure 3.26: SEM observations of non-swarming mutants (group 3).
Swarm fronts were fixed *in situ*, by vapour fixation, on LB agar. Non-swarming mutants failed to differentiate and no helical connections were observed. Mutants **G33**, and **G93** exhibited some evidence of cellular organisation at the colony boundary. **Bar = ~1 μm**.

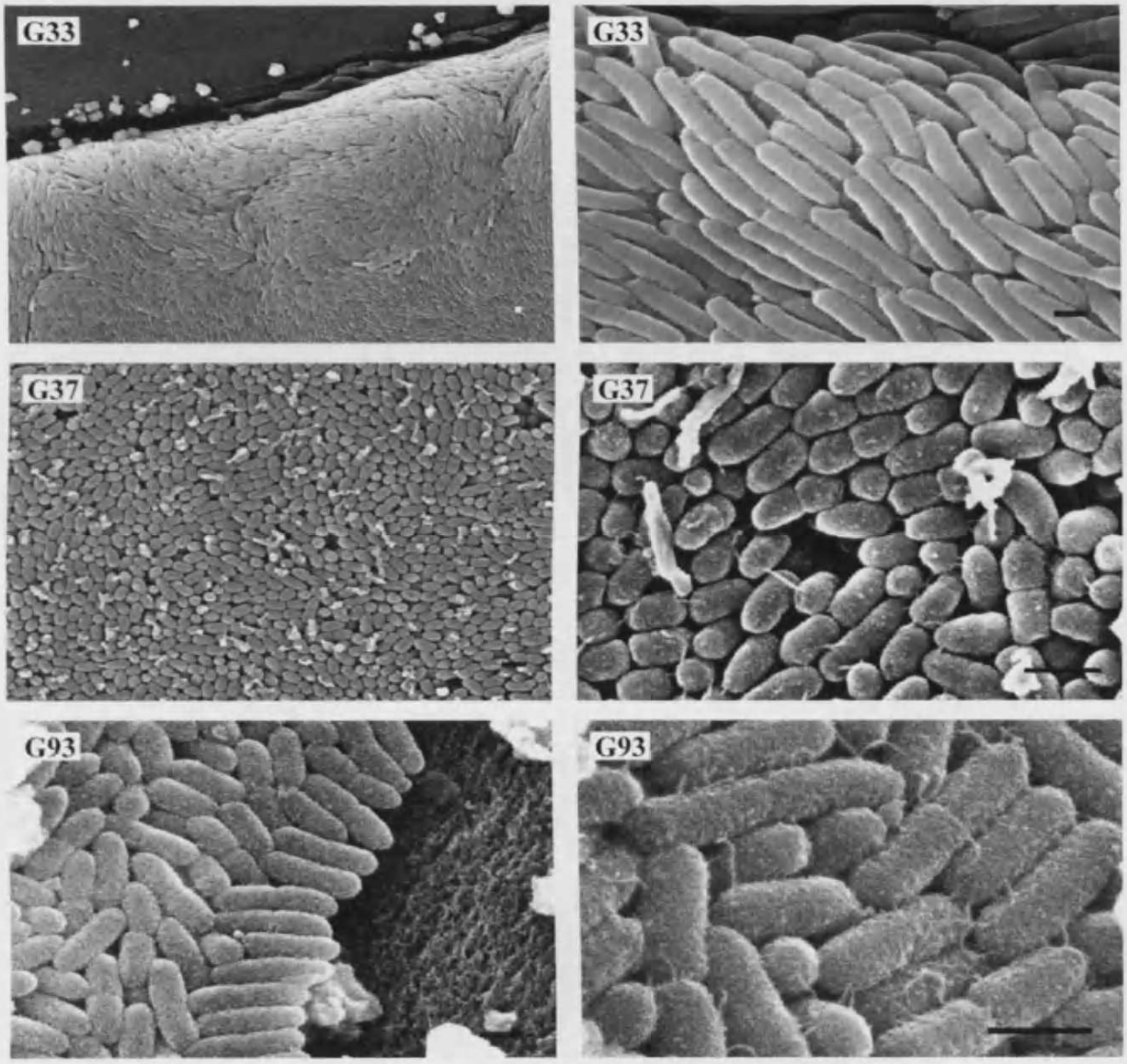

Figure 3.27: SEM observations of non-swarming, non-swimming mutants (group 4).
Swarm fronts were fixed *in situ*, by vapour fixation, on LB agar. No helical connections were observed on these mutants. **NS63** generated elongated cells and which showed evidence of alignment. **Bar = ~1μm.**

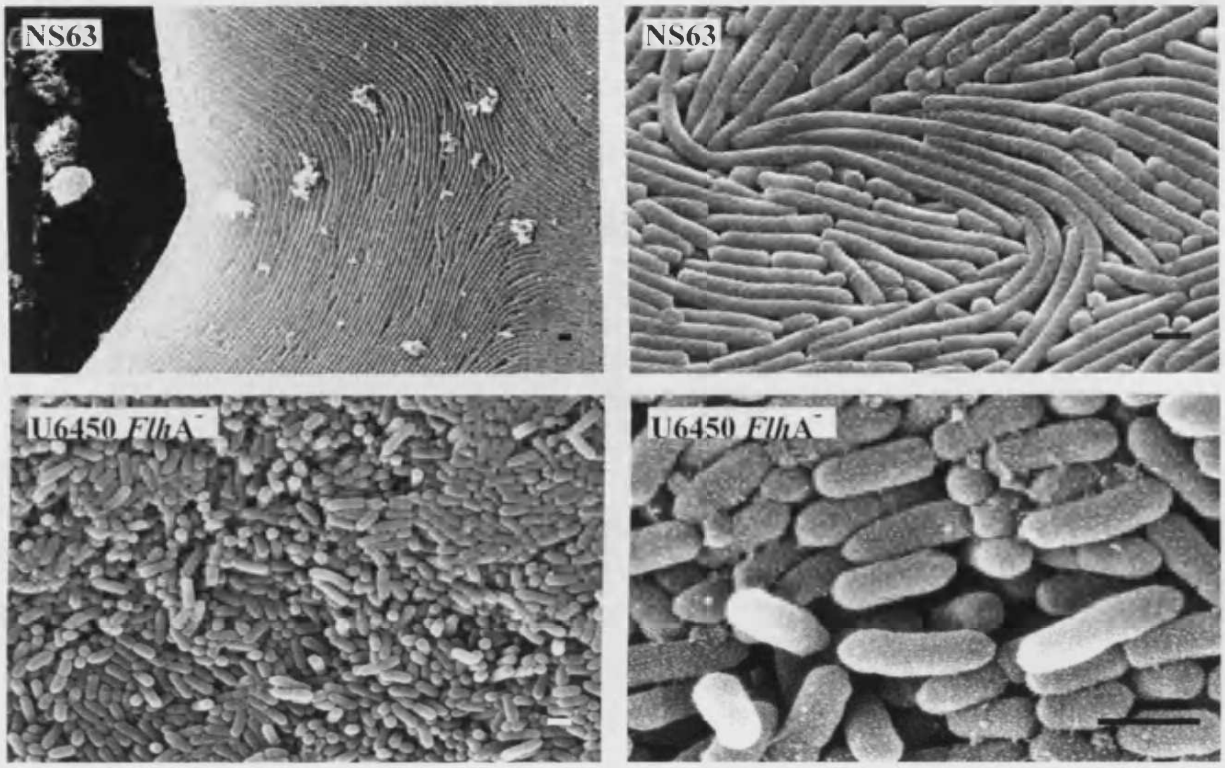

Table 3.11: Summary of SEM observations on *P. mirabilis* swarm fronts, fixed *in situ* on agar.

Group/Figure	Strain	Organisation of Flagella Filaments	Cellular Organisation at Swarm Fronts
Wild type Figure 3.23	B4, U6450	Flagella filaments are localised between adjacent cells, and interwoven to form regular helical connections.	Cells are elongated, similar in length, and organised into rafts of parallel swarmer cells.
Group 1: Control mutants Figure 3.24	BVJ12, BVJ14, BVJ15	As wild type	As wild type
Group 2: Poor-swarming mutants Figure 3.25	NS77	Helical connections formed but were composed of fewer flagella filaments than those observed in the wild type	As wild type
	G77	Evidence of vestigial helical connections, but flagella organisation greatly reduced.	Cells lack the organisation seen in the wild type swarm fronts. Cell length reduced.
	PS92	Helical connections formed but not uniformly throughout swarm front.	Large variation in cell length at swarm front. Cells formed poorly organised rafts, and were unable to maintain formation.
	G78	Flagella filaments were organised and interwoven but do not form a regular helical pattern.	Cells organised into rafts, but were closer together than cells in wild type swarm fronts.
	G64	As wild type	As wild type
Group 3: Non-swarming mutants Figure 3.26	G37	No helical connections formed, but some short flagella filaments visible	No elongation or cellular organisation.
	G33	No helical connections formed, no visible flagella filaments.	Cells exhibit slight elongation. Cells have a mucoid appearance and show some alignment.
	G93	No helical connections formed, but some flagella filaments visible	Cells exhibit slight elongation and some alignment at the colony boundary.
Group 4: Non-swimming, Non-swarming mutants Figure 3.27	NS63	No helical connections formed, no visible flagella filaments.	Large variation in cell length, with some extensively elongated cells. Elongated cells appear to align.
	U6450 *FlhA*$^-$	No helical connections formed, no visible flagella filaments.	No elongation or cellular organisation.

Figure 3.28: SEM observations of swarm fronts of complemented mutants.
The ability of the complemented mutants (NS63comp, G64comp, and G78comp) to generate helical connections during migration was assessed using in situ vapour fixation and SEM. This showed varying degrees of helical connection formation in all complemented mutants.

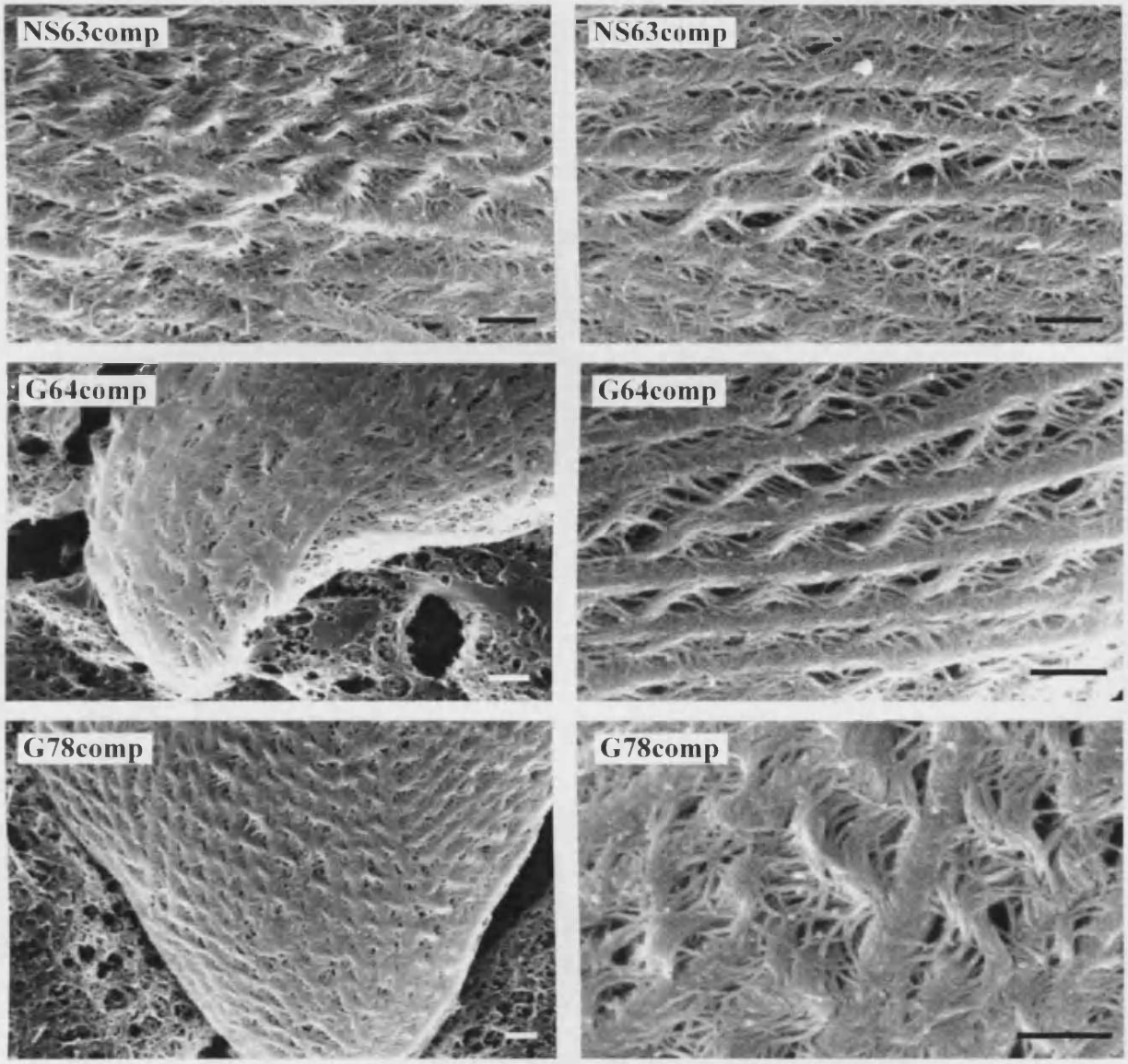

3.5.5 Transmission electron microscopy on B4 swarm fronts

The nature of flagella organisation during migration of swarmer cells was also investigated using TEM. Thin sections cut through wild type swarm fronts, fixed *in situ* during active migration on agar were observed. Micrographs of both transverse sections (TS) and longitudinal sections (LS) are presented in Figure 3.29. The TS sections confirmed that flagella filaments are tightly interwoven during migration, and are localised between adjacent cells in the monolayer of swarmer cells. Observations of the LS section revealed that the flagella filaments are interwoven in a criss-cross pattern.

Figure 3.29: TEM on thin sectioned swarm fronts of wild type *P. mirabilis* strain B4, fixed *in situ* during active migration on agar.

TEM observation of a longitudinal section **(A)**, and a transverse section **(B)** through wild type swarm front during migration over agar. The swarm front was fixed *in situ* by vapour fixation. Arrows indicate flagella filaments **(f)**, agar surface **(a)**, and cells **(c)**. Longitudinal section **(A)** shows flagella filaments interweaving in a criss-cross pattern, with and against the direction of migration. Transverse section shows flagella filaments are mainly localised between adjacent cells during migration.
Bar = ~300 nm.

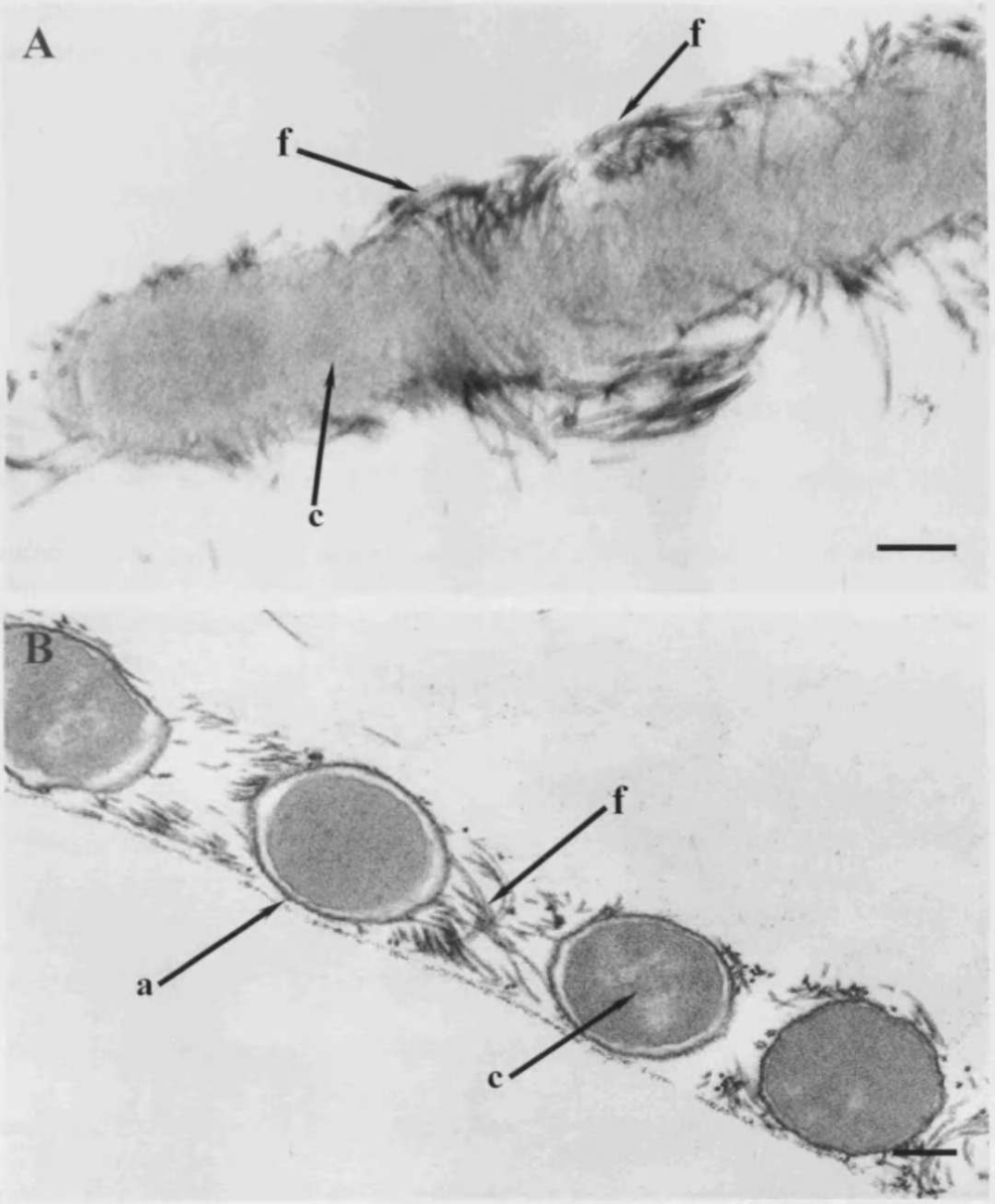

3.6 Parallel plate flow chamber results

The adherence of *P. mirabilis* strain B4 to silicone was compared to that of the non-swarming mutants (G37, NS63, and G93), poor swarming mutants (G64 and G78), and the control mutants (BVJ12, BVJ14, and BVJ15). Attachment was assessed in phosphate buffer at a flow rate of 1 ml/min, using a parallel plate flow chamber and phase contrast microscopy (Section 2.10).

3.6.1 Deposition rates of wild type and mutant *P. mirabilis* strains onto silicone

Data from triplicate experiments was used to calculate the rate at which cells of each test strain were deposited onto a silicone surface, over a period of 5 hours. A sequence of images demonstrating deposition of wild type cells onto silicone over 5 hours is presented in Figure 3.30, as an example of the data obtained from flow chamber experiments. The deposition rates of non-swarming, poor-swarming, and control mutants respectively, compared to the wild type strain B4 are shown in Figures 3.31, 3.32, and 3.33.

Non-swarming and poor-swarming mutants generally deposited more cells than the wild type over the duration of the experiments, but initially showed lower levels of deposition than the wild type (Figures 3.31, and 3.32). In non-swarming mutants, rates of deposition exceeded that of the wild type within 30 min (Figure 3.32), and remained above wild type deposition rates. The deposition rates of poor-swarming mutants exceeded the wild type deposition rate after 60 min (Figure 3.32), and were then maintained above wild type levels. In contrast, control mutants BVJ12 and BVJ14 demonstrated lower rates of deposition throughout the duration of the experiments when compared to the wild type (Figure 3.33). BVJ15 exhibited rates similar to that of the wild type (Figure 3.33).

Figure 3.30: Adhesion of *P. mirabilis* wild type strain B4 to silicone
A sequence of images captured from a flow chamber experiment with *P. mirabilis* strain B4. Images show deposition of cells onto the silicone-coated glass bottom plate of the flow chamber over 5 hours.

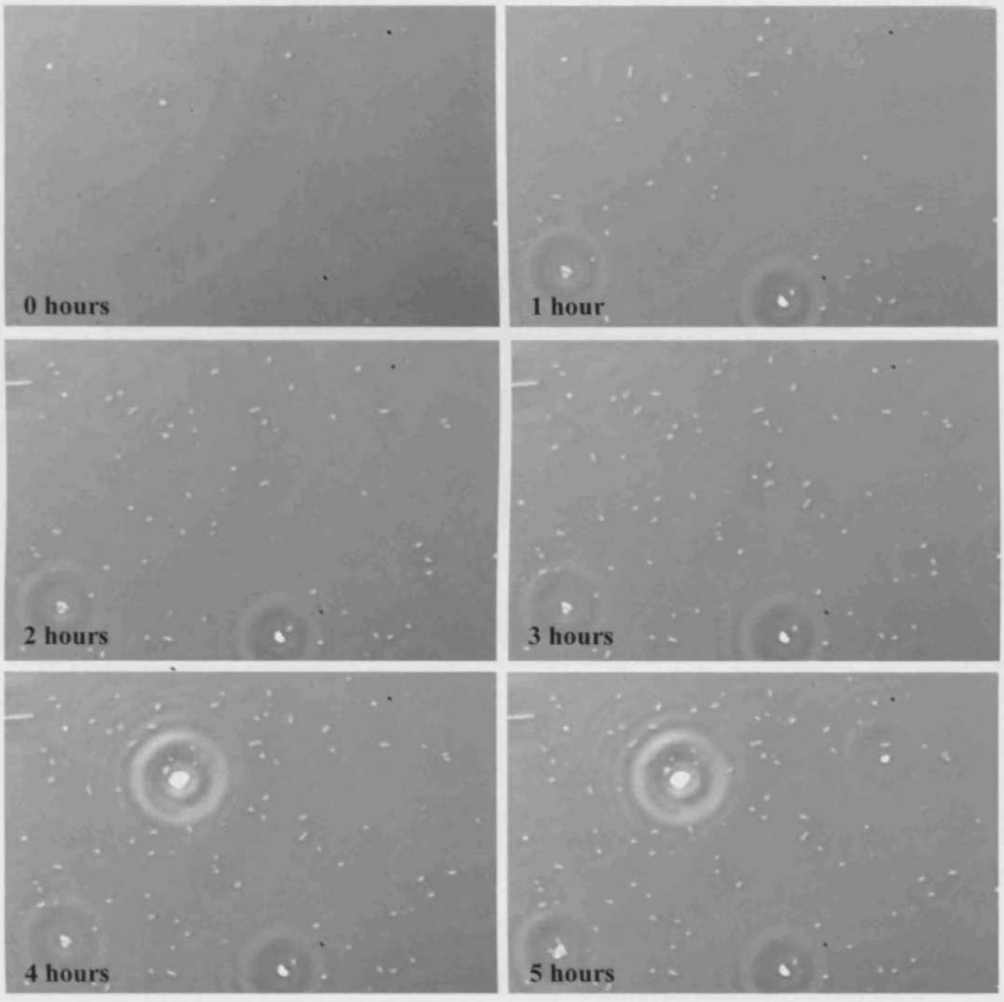

Figure 3.31: Adhesion of *P. mirabilis* wild type strain B4, and non-swarming mutants G37, NS63, and G93 to silicone.

The deposition rates of the wild type strain B4, and the non-swarming mutants G37, NS63, and G93, onto a silicone-coated glass plate in a parallel plate flow chamber (described in Section 2.10). The data shows the number of cells attached in one field of view (0.014 mm) at each time point, and represents the mean of three replicate experiments. Error bars show the standard error of the mean.

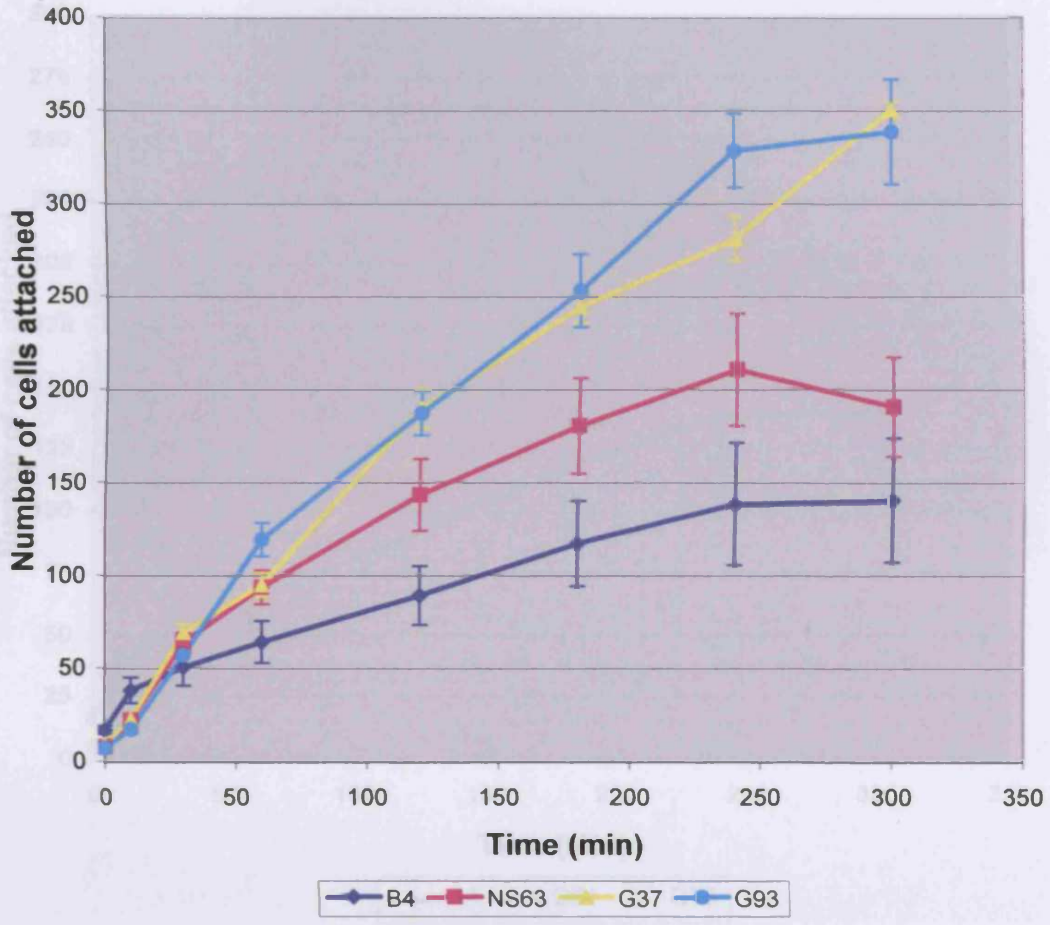

Figure 3.32: Adherence of *P. mirabilis* wild type strain B4 and poor-swarming mutants G64, and G78 to silicone.

The deposition rates of the wild type strain B4, and the poor-swarming mutants G64, and G78 onto a silicone coated glass plate in a parallel plate flow chamber (described in Section 2.10). The data shows the number of cells attached in one field of view (0.014 mm) at each time point, and represents the mean of three replicate experiments. Error bars show the standard error of the mean.

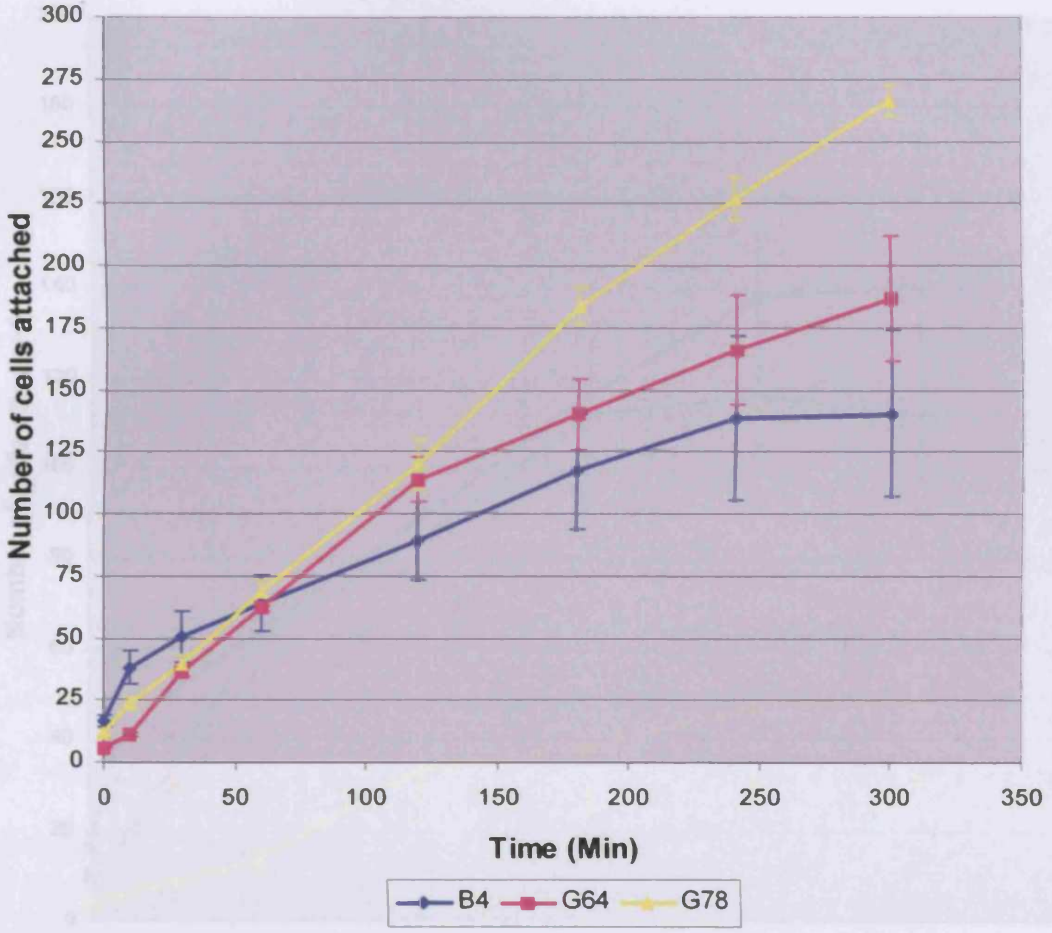

Figure 3.33: Adherence of *P. mirabilis* wild type strain B4, and control mutants BVJ12, BVJ14, and BVJ15 to silicone.

The deposition rates of the wild type strain B4, and control mutants BVJ12, BVJ14, and BVJ15, onto a silicone-coated glass plate in a parallel plate flow chamber (described in Section 2.10). The data indicates the number of cells attached in one field of view (0.014 mm) at each time point, and represents the mean of three replicate experiments. Error bars show the standard error of the mean

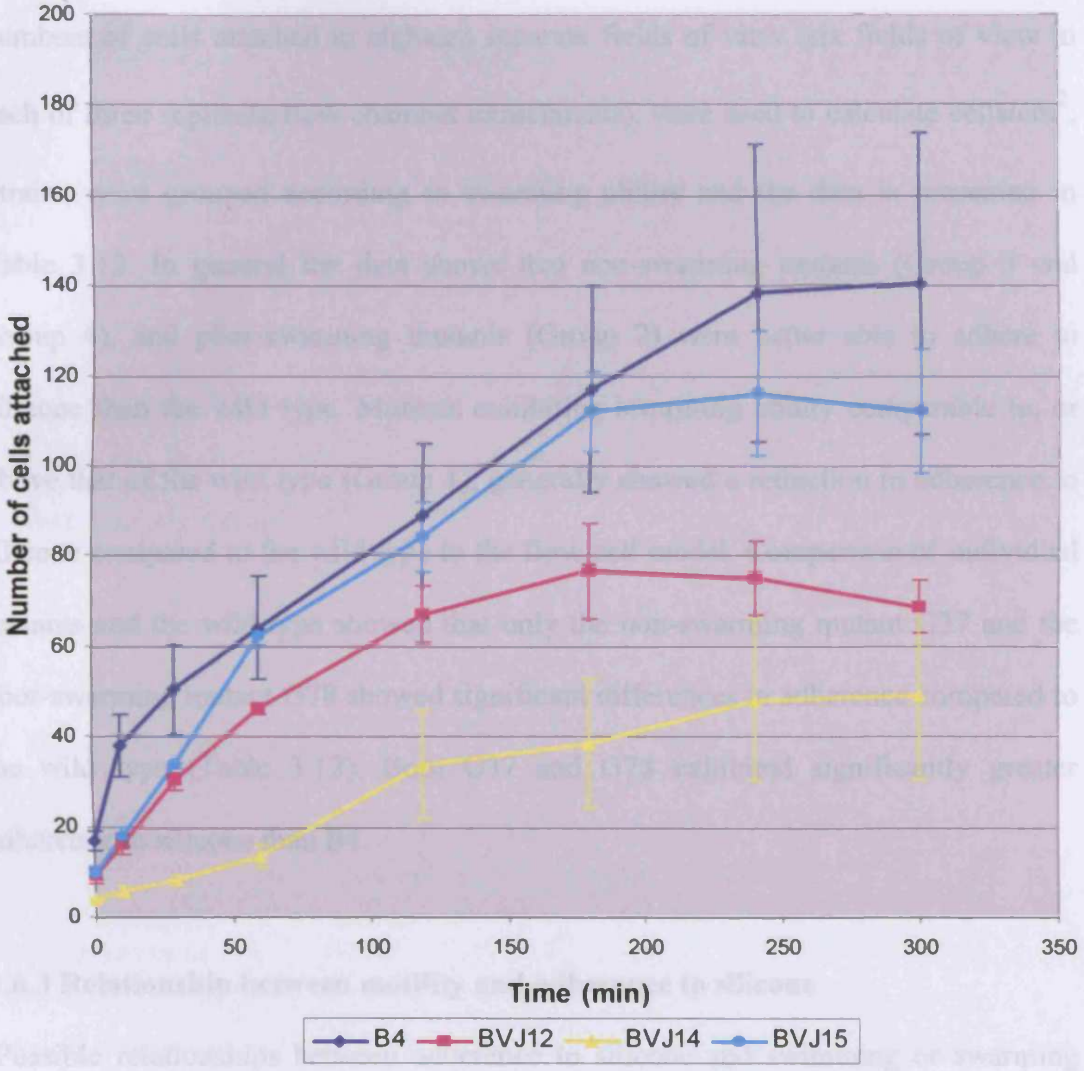

3.6.2 Ability of wild type, swarming-deficient, and control mutants to adhere to silicone

The overall ability of the wild type and mutant strains to adhere to silicone was assessed by calculating the number of cells attached per cm^2 after 5 hours. The numbers of cells attached in eighteen separate fields of view (six fields of view in each of three replicate flow chamber experiments), were used to calculate cells/cm^2. Strains were grouped according to swarming ability and the data is presented in Table 3.12. In general the data shows that non-swarming mutants (Group 3 and Group 4), and poor-swarming mutants (Group 2) were better able to adhere to silicone than the wild type. Mutants exhibiting swarming ability comparable to, or above that of the wild type (Group 1), generally showed a reduction in adherence to silicone compared to the wild type in the flow cell model. Comparison of individual mutants and the wild type showed that only the non-swarming mutant G37 and the poor-swarming mutant G78 showed significant differences in adherence compared to the wild type (Table 3.12). Both G37 and G78 exhibited significantly greater adherence to silicone than B4.

3.6.3 Relationship between motility and adherence to silicone

Possible relationships between adherence to silicone and swimming or swarming ability were also assessed. To evaluate any such relationships strains were ranked by their ability to adhere to silicone (cells/cm^2 after 5 hours, Table 3.12) and the swimming and swarming indices plotted. Figure 3.34 shows the swimming and swarming indices of all test strains when ranked by their ability to adhere to silicone. The analysis indicated that as swarming and swimming ability increases, adherence to silicone decreases. The relationship between these motilities and adherence to

Table 3.12: Ability of *P. mirabilis* wild type strain B4 and swarming-deficient mutants to adhere to silicone.

The overall ability of the test strains to adhere to silicone, in the parallel plate flow chamber, was assessed by calculating the number of cells attached per cm^2 after 5 hours.

Group	Strain	Cells/cm^2[a]	Significantly different to B4[b]
Wild type	B4	$8.28 \times 10^4 \pm 1.41 \times 10^4$	-
Group 1: Control mutants	BVJ14	$3.06 \times 10^4 \pm 7.22 \times 10^3$	No (P 0.18)
	BVJ12	$5.68 \times 10^4 \pm 1.44 \times 10^3$	No (P 0.41)
	BVJ15	$6.64 \times 10^4 \pm 2.14 \times 10^3$	No (P 0.60)
Group 2: Poor-swarming mutants	G78	$1.67 \times 10^5 \pm 4.28 \times 10^3$	Yes (P 0.046)
	G64	$1.26 \times 10^5 \pm 1.47 \times 10^4$	No (P 0.35)
Group 3: Non-swarming mutants	G93	$2.14 \times 10^5 \pm 3.37 \times 10^4$	No (P 0.15)
	G37	$2.12 \times 10^5 \pm 1.32 \times 10^4$	Yes (P 0.029)
Group 4: Non-swarming, non-swimming mutants	NS63	$1.25 \times 10^5 \pm 1.72 \times 10^4$	No (P 0.39)

a Values show the number of cells attached per cm^2 after 5 hours, and represent the means of three replicate experiments. Values following ± show the standard error of the mean.

b A two-sample T-test was used to compare the mean cells/cm^2 of the wild type to that of each mutant, at the 95% confidence level. Figures in parentheses are the P values obtained for each test.

Figure 3.34: Relationship between swarming and swimming ability and adherence to silicone.

To investigate any possible relationship between adherence to silicon and swimming or swarming ability, test strains were ranked according to ability to adhere to silicone in ascending order (Table 3.12), and swimming and swarming indices plotted.

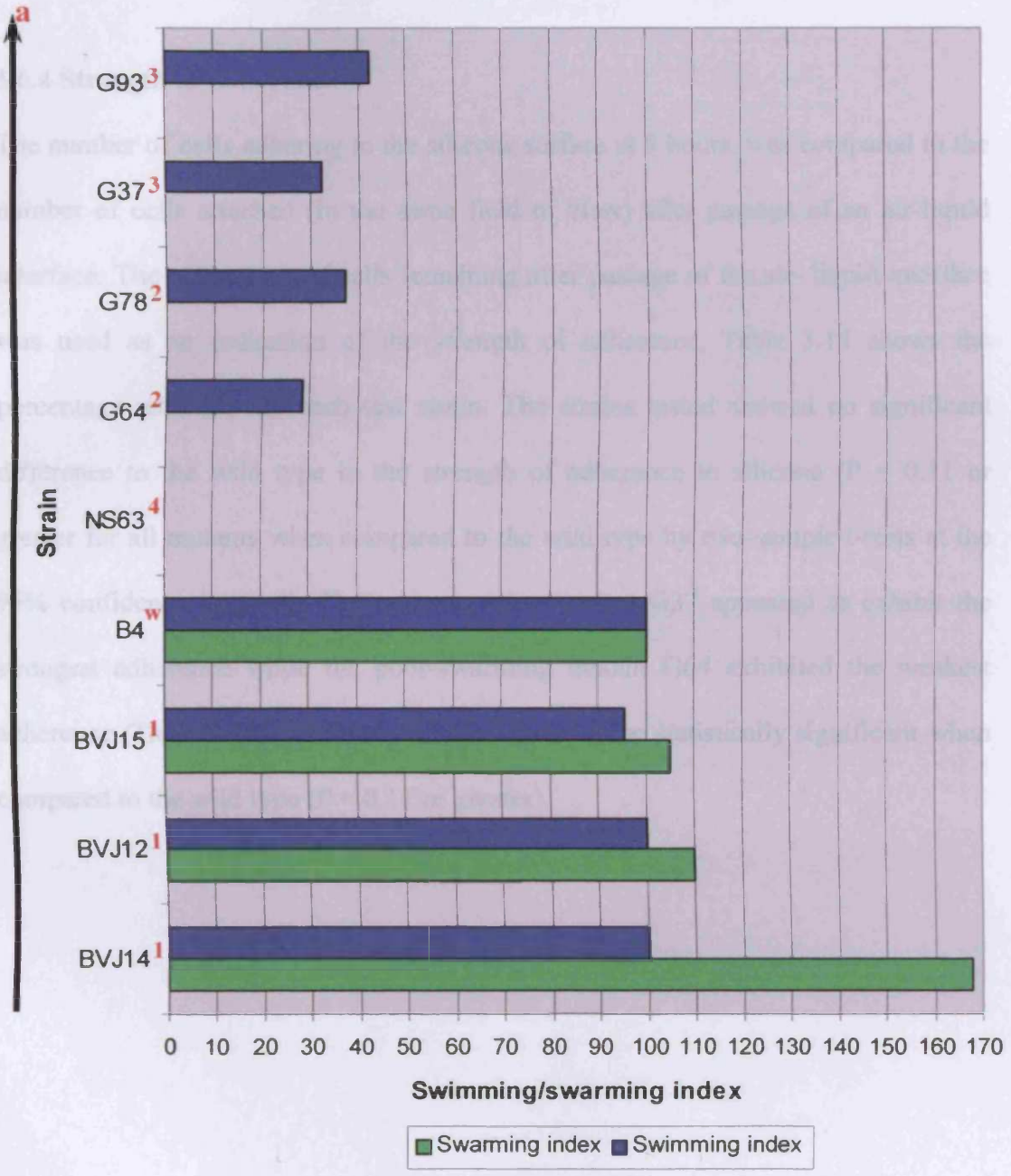

a, Arrow denotes increasing adherence to silicone in the parallel plate flow chamber (Table 3.12).
w, *P. mirabilis* wild type strain
1, Group 1 mutants: control mutants wild type or above swarming ability.
2, Group 2 mutants: Poor-swarming.
3, Group 3 mutants: Non-swarming.
4, Group 4 mutants: Non-swarming, non-swimming.

silicone was also examined by calculating correlation coefficients. The correlation coefficients are presented in Table 3.13, and indicate a strong negative correlation between both types of motility and adherence to silicone.

3.6.4 Strength of adherence

The number of cells adhering to the silicone surface at 5 hours, was compared to the number of cells attached (in the same field of view) after passage of an air-liquid interface. The percentage of cells remaining after passage of the air- liquid interface was used as an indication of the strength of adherence. Table 3.14 shows the percentage retention for each test strain. The strains tested showed no significant difference to the wild type in the strength of adherence to silicone ($P = 0.11$ or greater for all mutants when compared to the wild type by two-sample t-tests at the 95% confidence interval). The non-swarming mutant G37 appeared to exhibit the strongest adherence while the poor-swarming mutant G64 exhibited the weakest adherence (Table 3.14). Neither result was found to be statistically significant when compared to the wild type ($P = 0.11$ or greater).

Table 3.13: Analysis of the relationship between swimming and swarming ability and adherence to silicone.

Factors Compared	Correlation Coefficient[a]	Explanation
Adherence (cells/cm^2) vs Swarming index	-0.88	Indicates a very **strong negative correlation** between adherence and swarming ability
Adherence (cells/cm^2) vs Swimming index	-0.729	Indicates **strong negative correlation** between adherence and swimming ability

[a] All correlation coefficients were significant at the 95% confidence level, as assessed using critical coefficient values presented by Fry (1993).

Table 3.14: Strength of adherence of *P. mirabilis* wild type strain B4, and mutant strains to silicone.

The strength of adherence of each test strain to silicone, in the parallel plate flow chamber, was assessed by comparing the number of cells attached before and after the passage of an air-liquid interface.

Group	Strain	Retention[a,b]
Wild type	B4	38.48 ± 8.15
Group 1: Control mutants	BVJ14	30.64 ± 0.88
	BVJ12	42.52 ± 7.80
	BVJ15	34.81 ± 9.62
Group 2: Poor-swarming mutants	G78	31.08 ± 6.83
	G64	18.63 ± 2.36
Group 3: Non-swarming mutants	G93	23.34 ± 7.92
	G37	63.49 ± 9.40
Group 4: Non-swarming, non-swimming mutants	NS63	40.78 ± 7.68

[a] Values show the percentage of cells still attached after the passage of an air-liquid interface. Data represents the mean of three replicates, and figures following ± show the standard deviation of the mean.

[b] None of the mutants tested showed significant differences in strength of adherence when compared to the wild type (P = 0.11 or greater). Strains were compared using a two-sample T-test at the 95% confidence interval.

3.6.5 Biofilm architecture of *P. mirabilis* wild type and mutants on silicone

Figures 3.35-3.43 show images from flow chamber experiments with B4 and mutants strains after 5 hours. Elongated cells of the wild type strain B4 were found to adhere to the silicone surface (Figure 3.35). Adherence of elongated cells was also observed in flow chamber experiments with the control mutant BVJ12 (Figure 3.36) and the non-swarming mutant NS63, which appeared to deposit mainly elongated cells (Figure 3.43).

All of the strains tested showed evidence of micro-colony formation and cellular aggregation in flow chamber experiments, but ability to form these structures varied greatly. The wild type strain B4 produced large groups of cells but also adhered as single cells (Figure 3.35), as did mutants G78 and BVJ15 (Figures 3.39, and 3.38). Cells of control mutants BVJ12 and BVJ14 appeared to generate large cellular aggregates, with few cells attached outside these formations (Figures 3.36, and 3.37). The non-swarming mutant G37 exhibited increased aggregation compared to the wild type, and attached predominantly as small groups of cells (Figure 3.42). In contrast, aggregation of cells was less evident in the non-swarming mutant G93 (Figure 3.41), and the poor swarming mutant G64 (Figure 3.40).

Figure 3.35: Structure of *P. mirabilis* strain B4 biofilm on silicone after 5 hours.
Adherence of *P. mirabilis* wild type strain B4, to silicone–coated glass after 5 hours in parallel plate flow chamber. Cells were observed using phase contrast microscopy, and images **A-C** represent separate fields of view (0.014 mm) captured from three replicate experiments.

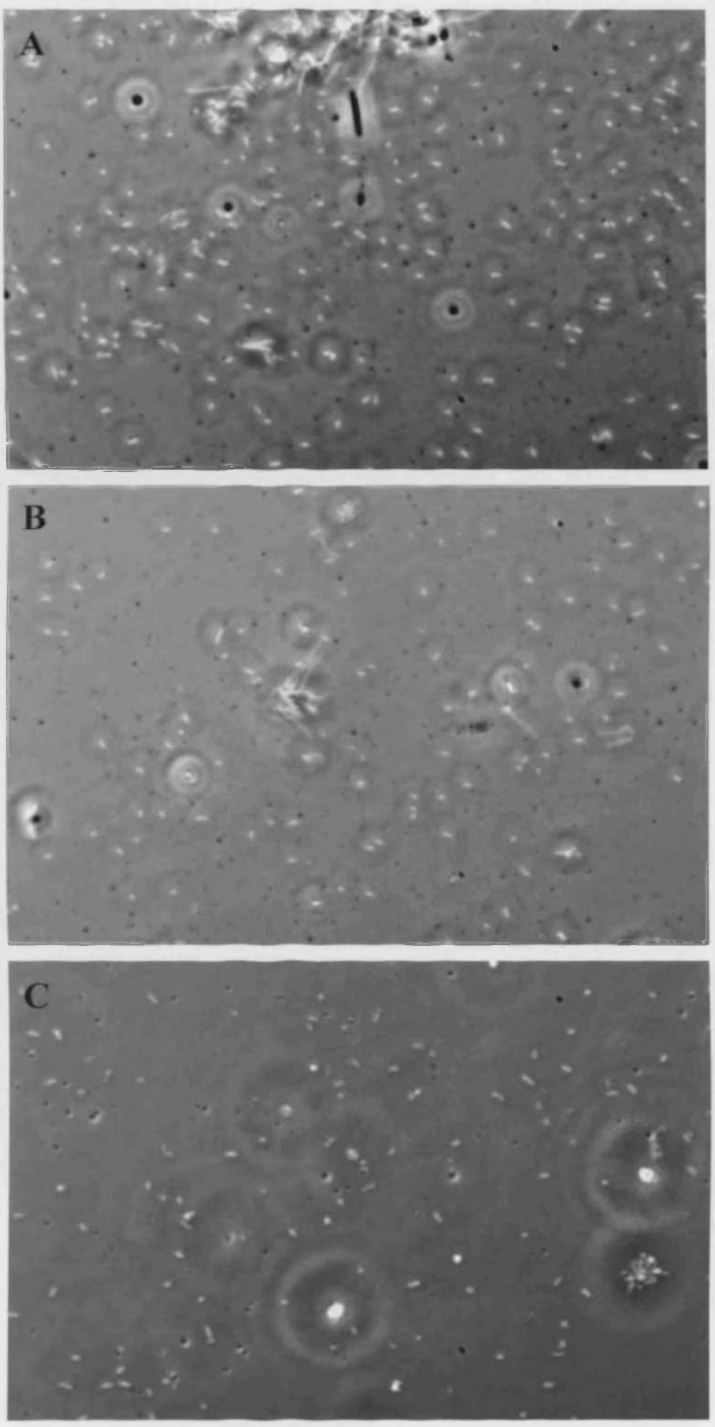

Figure 3.36: Structure of *P. mirabilis* strain BVJ12 biofilm on silicone after 5 hours.

Adherence of *P. mirabilis* control mutant BVJ12, to silicone–coated glass after 5 hours in parallel plate flow chamber. Cells were observed using phase contrast microscopy, and images **A-C** represent separate fields of view (0.014 mm) captured from three replicate experiments.

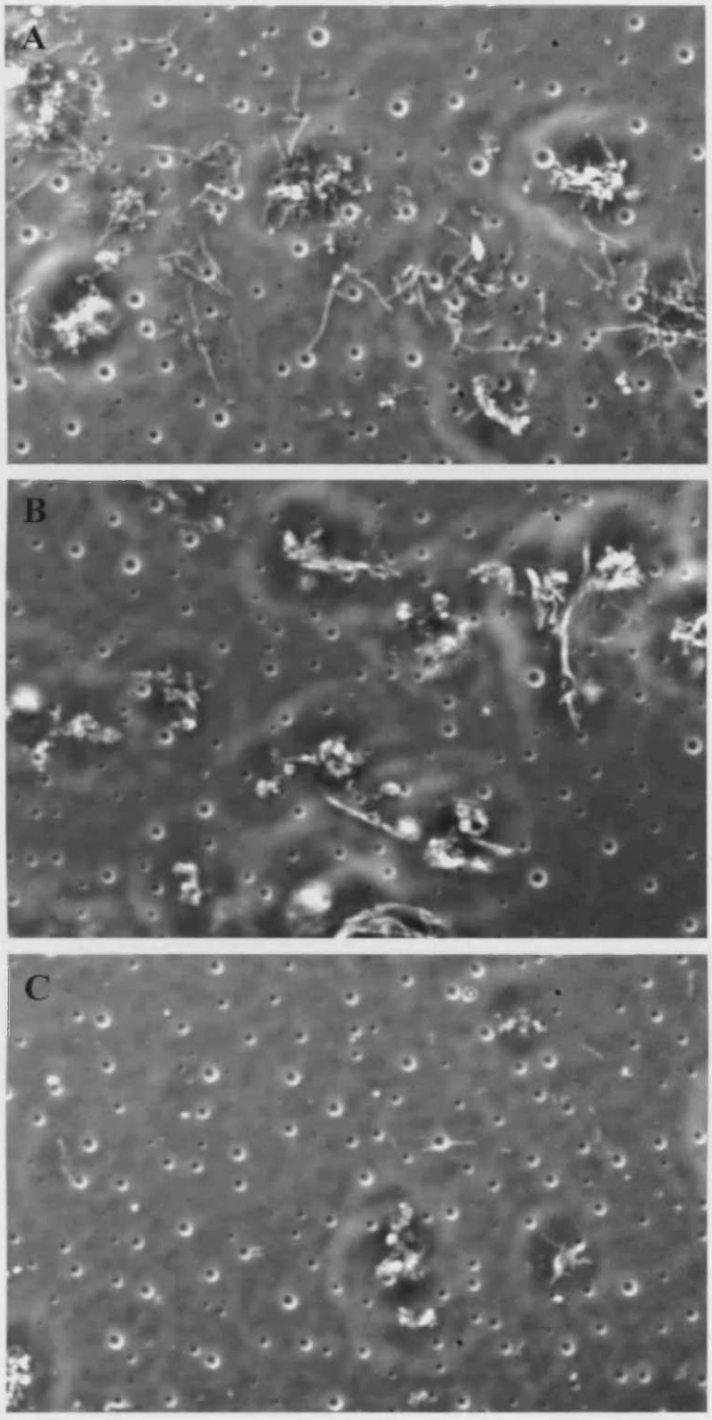

Figure 3.37: Structure of *P. mirabilis* strain BVJ14 biofilm on silicone after 5 hours.

Adherence of *P. mirabilis* control mutant BVJ14, to silicone–coated glass after 5 hours in parallel plate flow chamber. Cells were observed using phase contrast microscopy, and images **A-C** represent separate fields of view (0.014 mm) captured from three replicate experiments.

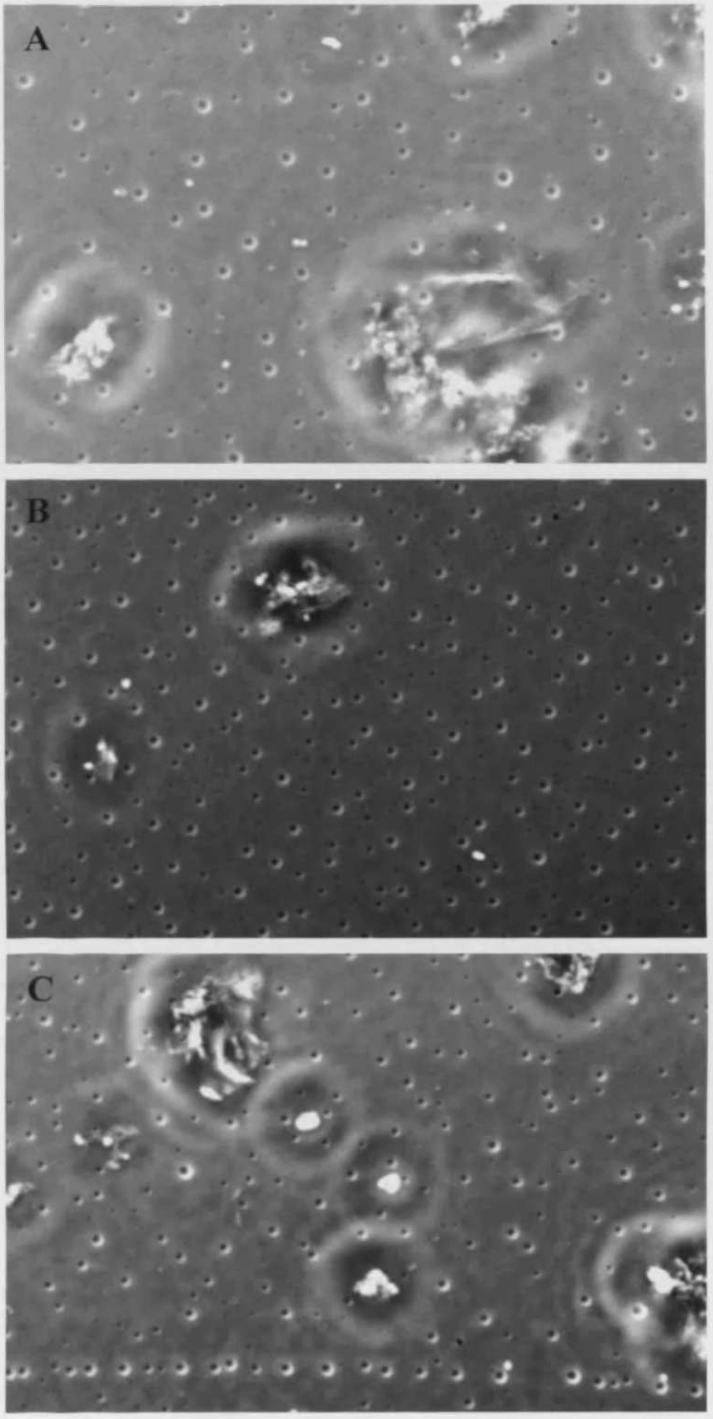

Figure 3.38: Structure of *P. mirabilis* strain BVJ15 biofilm on silicone after 5 hours.

Adherence of *P. mirabilis* control mutant BVJ15, to silicone–coated glass after 5 hours in parallel plate flow chamber. Cells were observed using phase contrast microscopy, and images **A-C** represent separate fields of view (0.014 mm) captured from three replicate experiments.

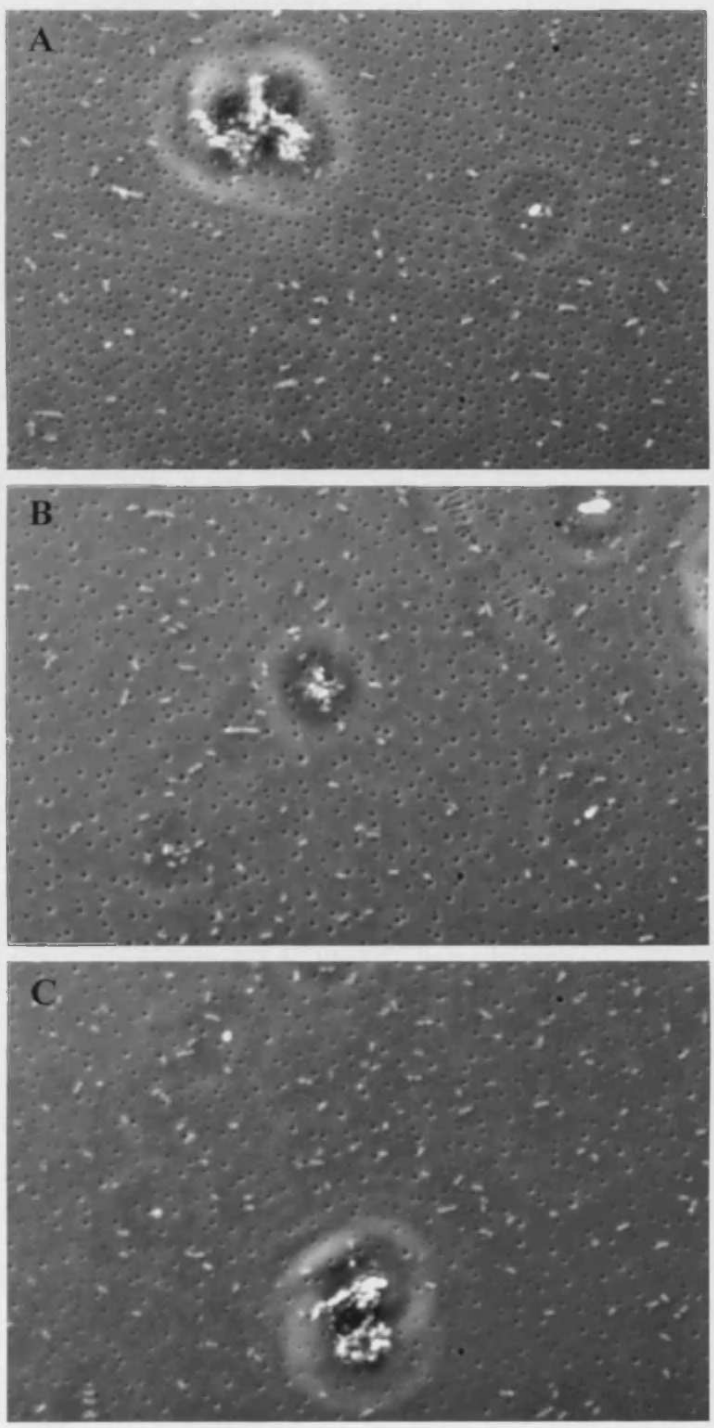

Figure 3.39: Structure of *P. mirabilis* strain G78 biofilm on silicone after 5 hours.

Adherence of *P. mirabilis* poor-swarming mutant G78, to silicone–coated glass after 5 hours in parallel plate flow chamber. Cells were observed using phase contrast microscopy, and images **A-C** represent separate fields of view (0.014 mm) captured from three replicate experiments.

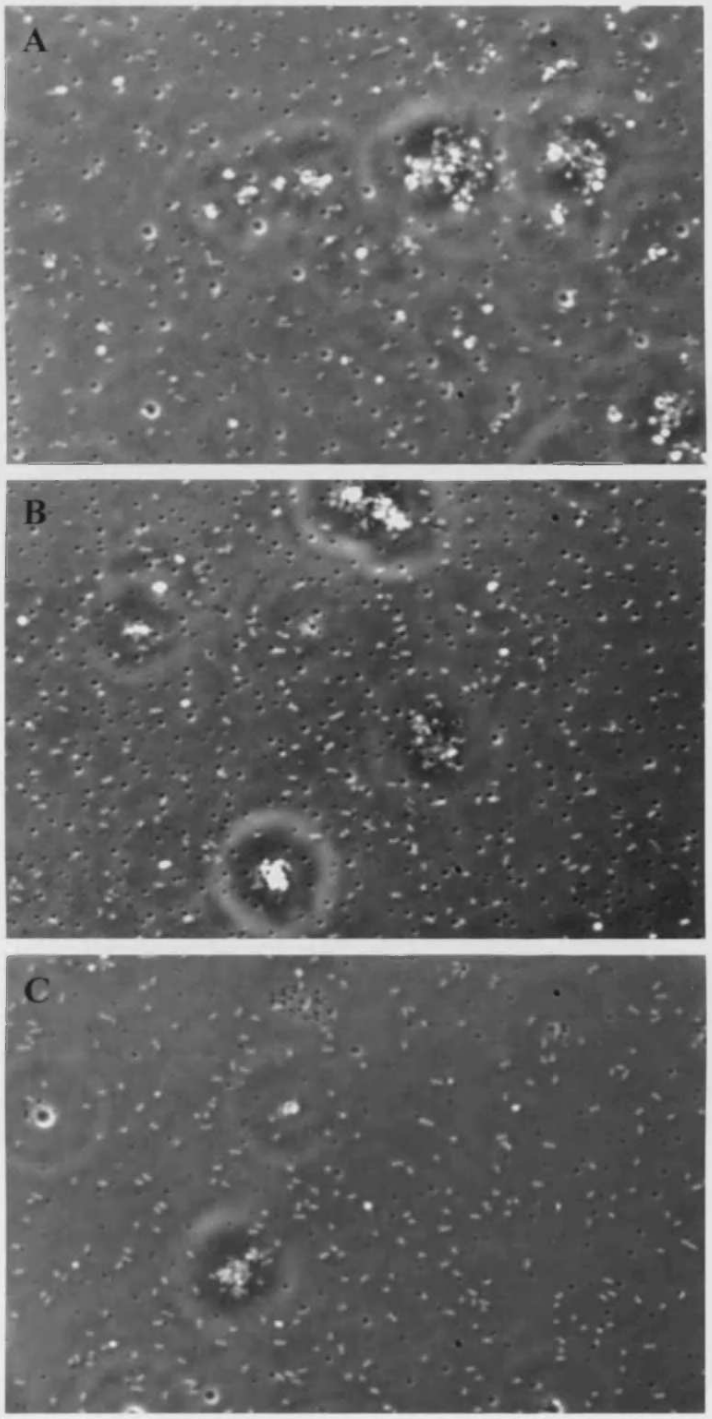

Figure 3.40: Structure of *P. mirabilis* strain G64 biofilm on silicone after 5 hours.

Adherence of *P. mirabilis* poor-swarming mutant G64, to silicone–coated glass after 5 hours in parallel plate flow chamber. Cells were observed using phase contrast microscopy, and images **A-C** represent separate fields of view (0.014 mm) captured from three replicate experiments.

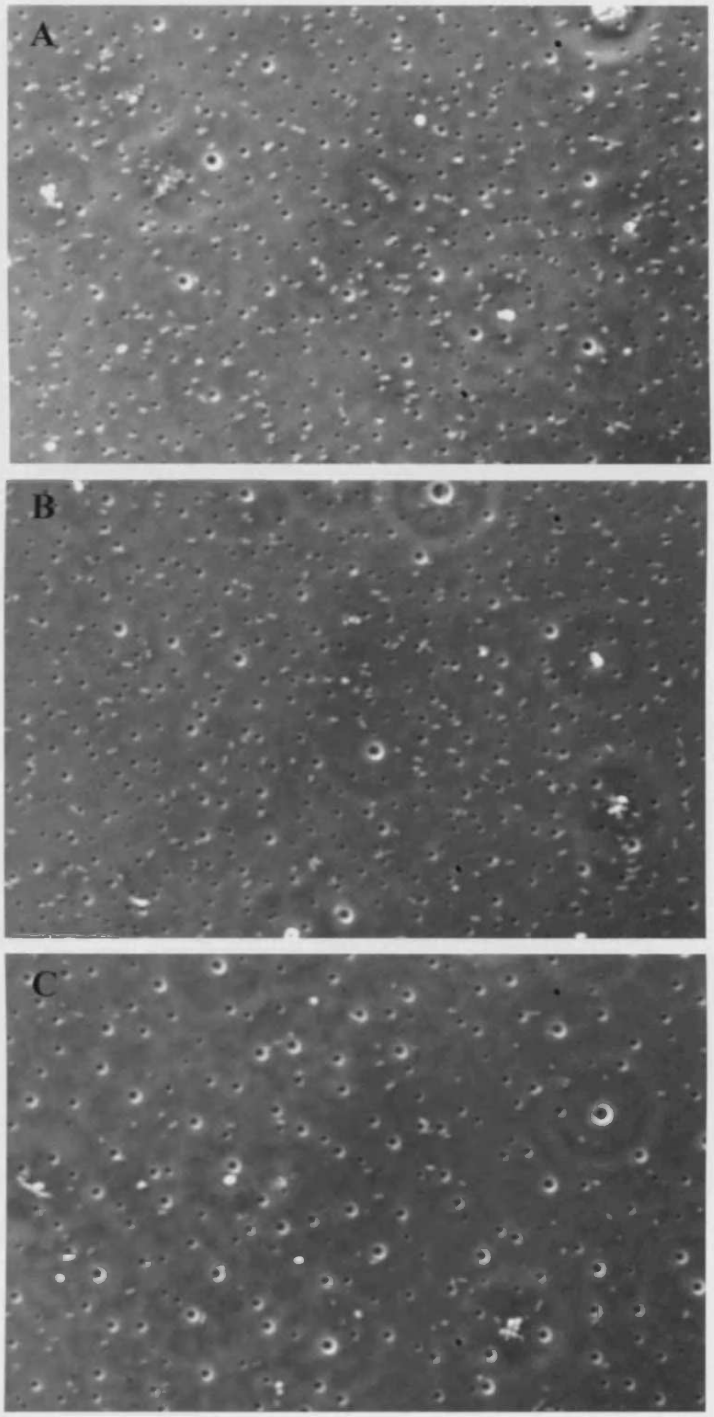

Figure 3.41: Structure of *P. mirabilis* strain G93 biofilm on silicone after 5 hours.

Adherence of *P. mirabilis* non-swarming mutant G93, to silicone–coated glass after 5 hours in parallel plate flow chamber. Cells were observed using phase contrast microscopy, and images **A-C** represent separate fields of view (0.014 mm) captured from three replicate experiments.

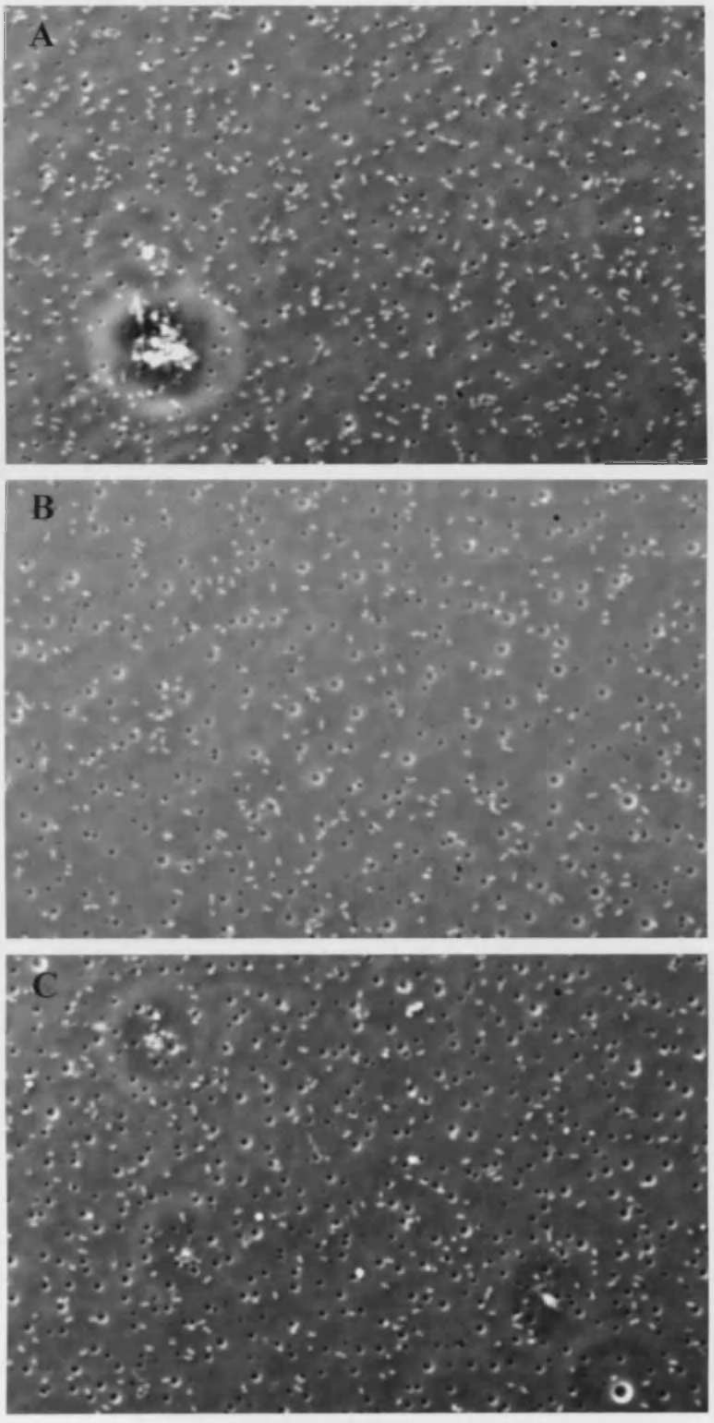

Figure 3.42: Structure of *P. mirabilis* strain G37 biofilm on silicone after 5 hours.

Adherence of *P. mirabilis* non-swarming mutant G37, to silicone–coated glass after 5 hours in parallel plate flow chamber. Cells were observed using phase contrast microscopy, and images **A-C** represent separate fields of view (0.014 mm) captured from three replicate experiments.

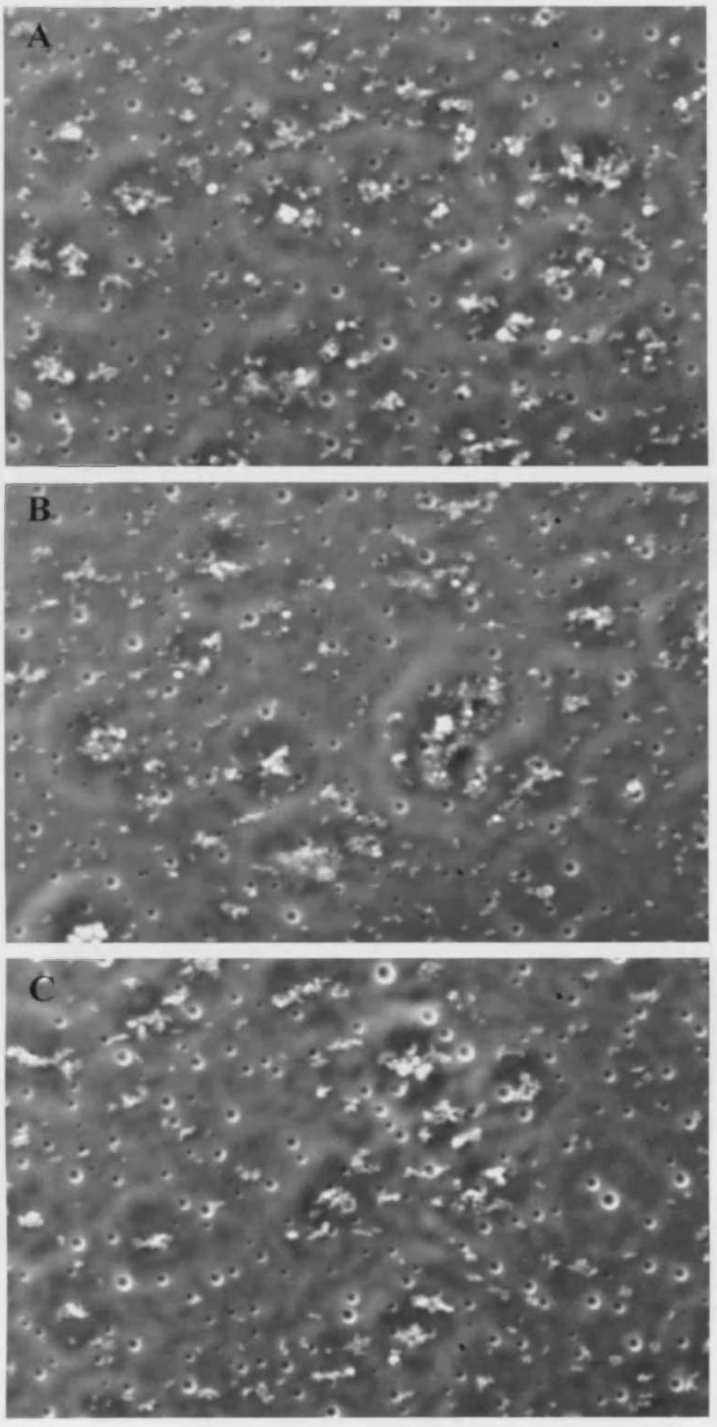

Figure 3.43: Structure of *P. mirabilis* strain NS63 biofilm on silicone after 5 hours.

Adherence of *P. mirabilis* non-swarming mutant NS63, to silicone–coated glass after 5 hours in parallel plate flow chamber. Cells were observed using phase contrast microscopy, and images **A-C** represent separate fields of view (0.014 mm) captured from three replicate experiments.

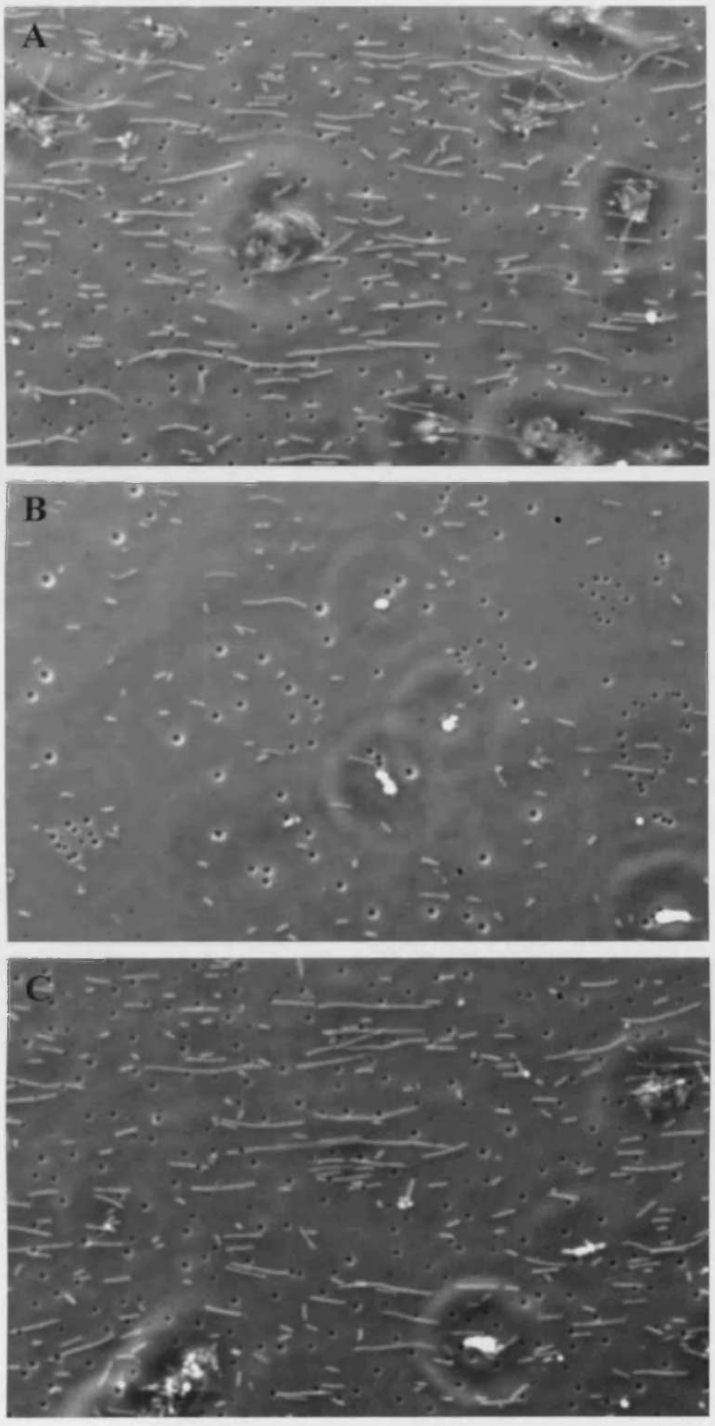

3.7 Models of Infection

The role of swarming in the pathogenesis of *P. mirabilis* catheter associated infections was investigated using *in vitro* infection models. The ability of the swarming-deficient mutants to migrate over catheter surfaces was investigated, to evaluate the contribution of swarming to colonisation of the catheterised urinary tract. The role of swarming in catheter encrustation and blockage was evaluated using a model of the catheterised urinary tract.

3.7.1 Migration of *P. mirabilis* over the surfaces of urinary catheters

The ability of the swarming-deficient mutants to migrate over the surfaces of all-silicone, and hydrogel-coated latex catheters was examined using the catheter bridge model described by Stickler & Hughes (1999). The migration indices of the swarming deficient mutants were all lower than that of the wild type, showing that swarming deficient mutants were less able to migrate over the surfaces of both types of catheter (Table 3.15). Non-swarming mutants were unable to migrate over all-silicone catheters, but those capable of swimming were able to migrate over hydrogel-coated latex catheters. The non-swarming, non-swimming mutant NS63 failed to migrate over any of the catheter sections. These experiments also indicated that migration occurred more readily over hydrogel-coated latex sections than the all-silicone sections (Table 3.15).

Table 3.15: The ability of *P. mirabilis* wild type strain B4, swarming-deficient mutants, and control mutants to migrate over the surfaces of all-silicone and hydrogel-coated latex catheters.

Group	Strain	Migration Index[a]	
		All-silicone	Hydrogel-coated latex
Wild type	B4	66.67	100
	U6450	50	75
Group 1: Control mutants	BVJ14	41.67	100
	BVJ12	41.67	100
	BVJ15	16.67	100
Group 2: Poor-swarming mutants	NS77	16.67	58.33
	G77	0	75
	PS92	0	75
	G78	8.33	58.33
	G64	0	58.33
Group 3: Non-swarming mutants	G93	0	66.67
	G37	0	50
	G33	0	33.3
Group 4: Non-swimming, non-swarming mutants	NS63	0	0
	U6450 *flhA*$^-$	0	0

[a] The migration index is calculated as the percentage of catheter sections crossed by each strain from twelve replicate tests.

3.7.2 Correlation of swarming and swimming ability with migration over catheter surfaces

The relationship between swarming and swimming ability, and migration over catheter surfaces was investigated. The swimming and swarming indices of the test strains were plotted against their migration indices for both catheter types on scatter graphs. This analysis indicated a possible correlation between both types of motility, and migration over both types of catheter (Figures 3.44, 3.45, 3.46, and 3.47).

The degree to which each type of motility was associated with migration over the catheter sections, was assessed by calculating the correlation coefficients for swarming and swimming indices vs the migration index over both catheter types. This indicated that swarming was the critical motility involved in migration over all-silicone catheters, and the contribution of swimming motility to migration over these surfaces was negligible (Table 3.16). In the case of hydrogel-coated latex catheters, correlation coefficients showed that both swimming and swarming ability was strongly linked to the ability to migrate over these surfaces (Table 3.16), although swimming ability was found to be the most significant factor in migration over these catheter sections (Table 3.16).

3.7.3 Migration of complemented mutants over sections of urethral catheter

The ability of the complemented mutants to migrate over sections of all-silicone, and hydrogel-coated latex catheters, was assessed using catheter bridge models. The migration indices of the complemented mutants was compared to those of their un-complemented equivalents. All of the complemented mutants showed an increase in their capacity for migration over both catheter types. G78comp was found to be fully restored in ability to migrate over hydrogel-coated latex sections (Table 3.17).

Figure 3.44: Correlation of swarming ability with migration over all-silicone catheter sections.
The swarming indices of test strains were plotted against their migration indices for all-silicone catheter sections, and analysed using linear regression (line).

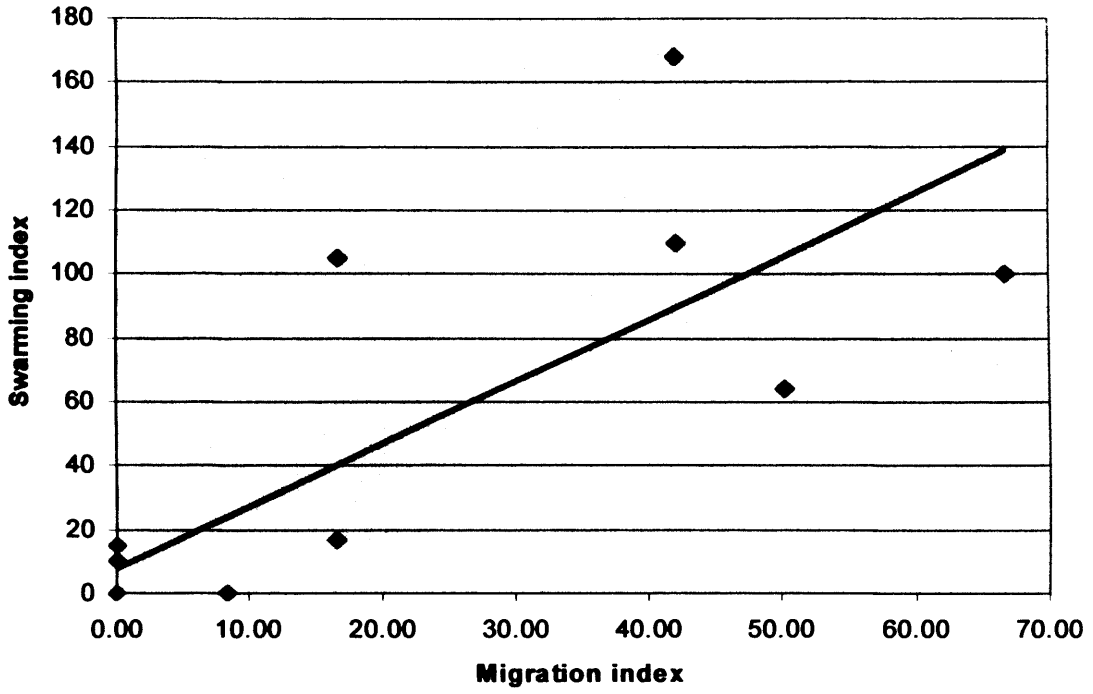

Figure 3.45: Correlation of swimming ability with migration over all-silicone catheter sections.
The swimming indices of test strains were plotted against their migration indices for all-silicone catheter sections, and analysed using linear regression (line).

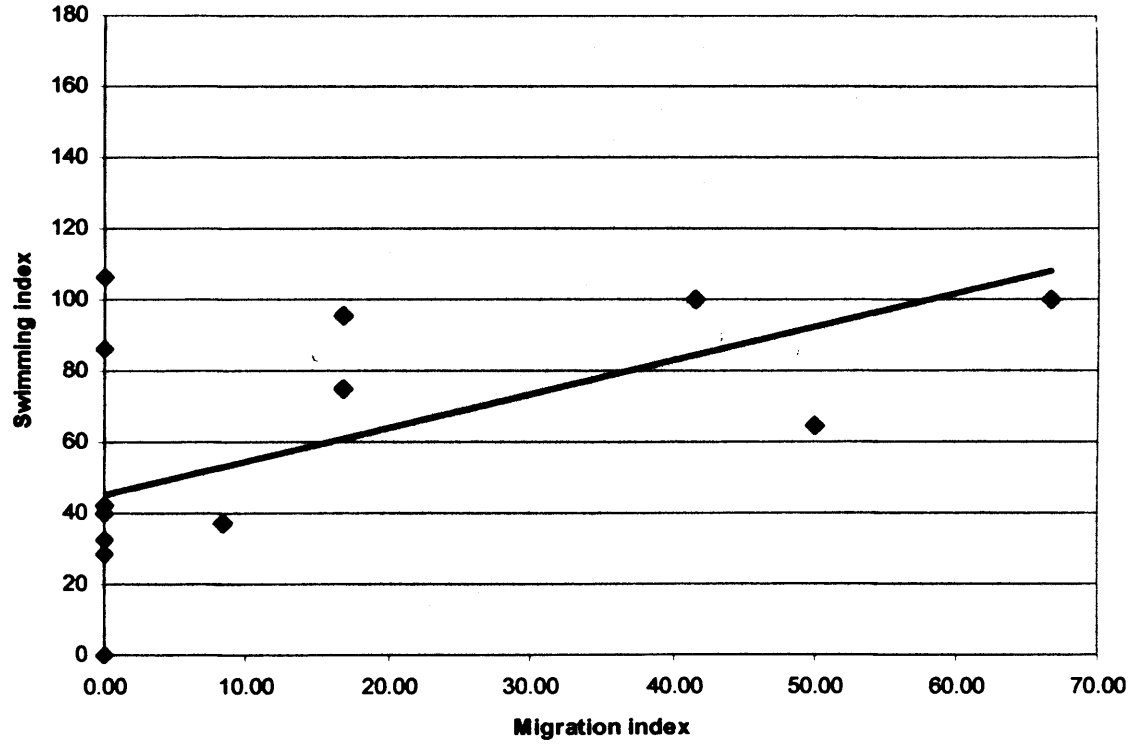

Figure 3.46: Correlation of swarming ability with migration over hydrogel-coated latex catheter sections.
The swarming indices of test strains were plotted against their migration indices for hydrogel-coated latex catheter sections, and analysed using linear regression (line).

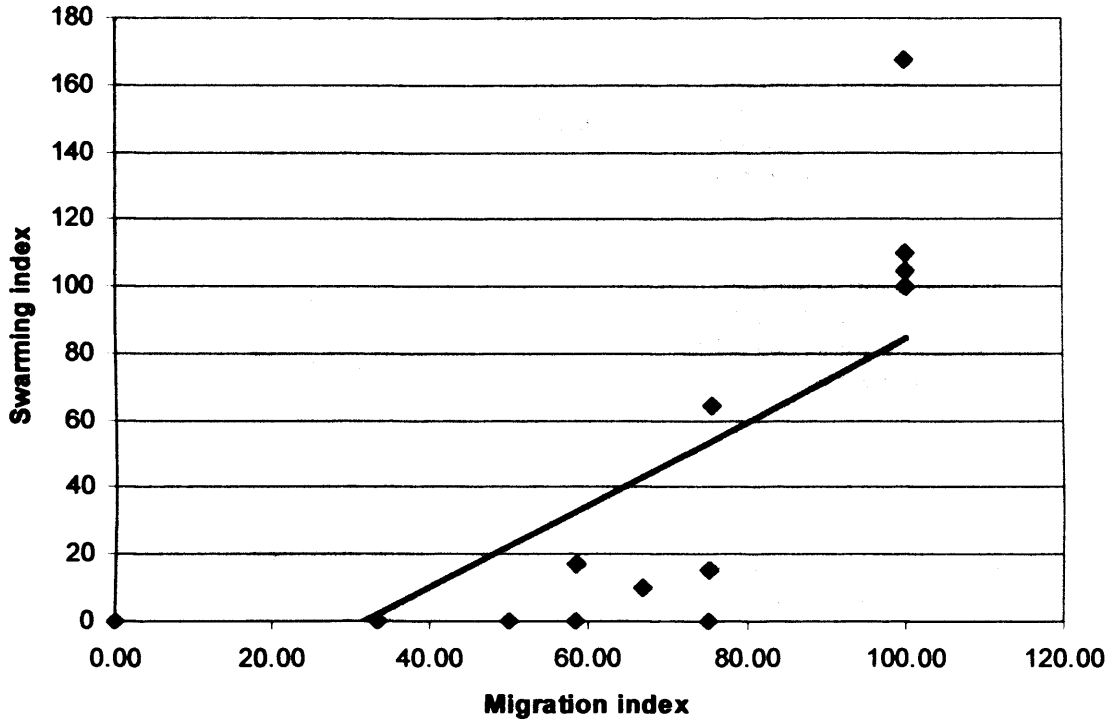

Figure 3.47: Correlation of swimming ability with migration over hydrogel-coated latex catheter sections.
The swimming indices of test strains were plotted against their migration indices for all-silicone catheter sections, and analysed using linear regression (line).

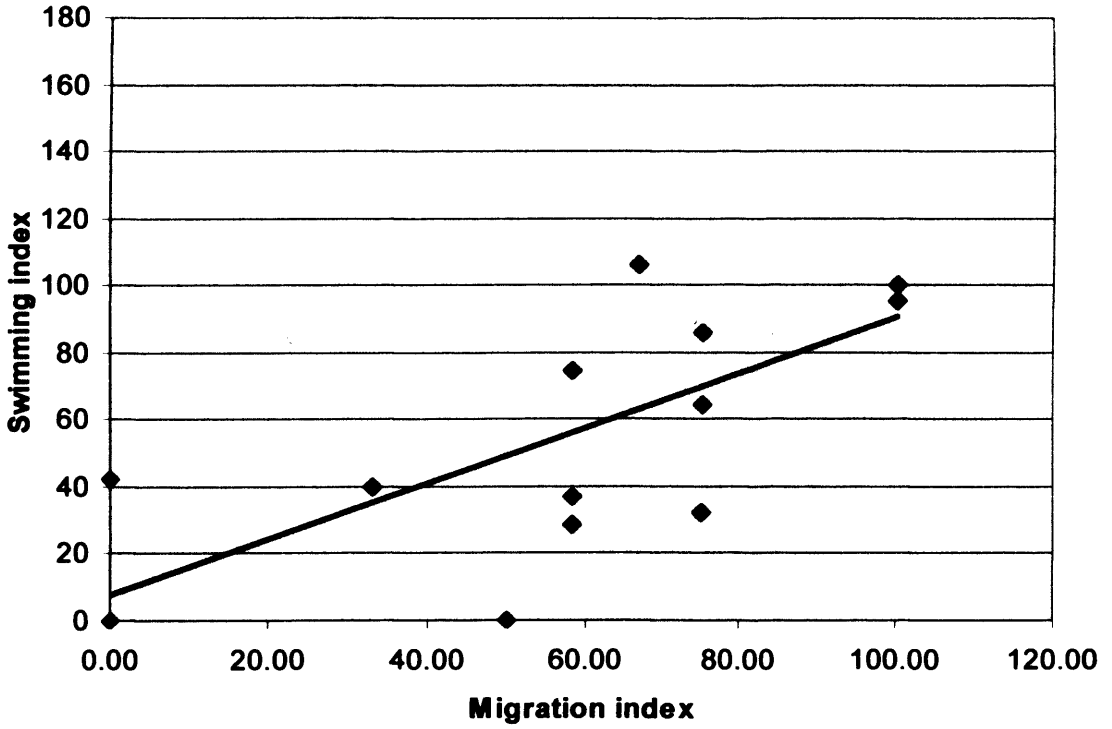

Table 3.16: Relationship between swarming and swimming ability and migration over all-silicone catheters.

Catheter type	Factors compared	Correlation coefficient [a]	Explanation
All-silicone	Swarming index vs. Migration index	0.799	Indicates a **strong positive correlation** between swarming ability and ability to migrate over all-silicone catheter sections
	Swimming index vs. Migration index	0.576	Indicates a **weak positive correlation** between swimming ability and ability to migrate over all-silicone catheter sections
Hydrogel-coated latex	Swarming index vs. Migration index	0.737	Indicates a **strong positive correlation** between Swarming ability and ability to migrate over hydrogel-coated latex sections
	Swimming index vs. Migration index	0.908	Indicates a **very strong positive correlation** between Swimming ability and ability to migrate over hydrogel-coated latex sections

[a] All correlation coefficients were significant at the 95% confidence level, as assessed using critical coefficient values presented by Fry (1993).

Table 3.17: Ability of complemented mutants to migrate over catheter surfaces.
The ability of the complemented mutants (NS63comp, G64comp, and G78comp) to move over the surfaces of all-silicone, and hydrogel-coated latex catheters was assessed. Ability to migrate over these surfaces was investigated using the catheter bridge models and compared to the migration ability of the un-complemented mutants NS63, G64, and G78.

Mutant type[a]	Strain	Migration index[b]	
		All-silicone	Hydrogel-coated latex
Un-complemented mutants	NS63	0	0
	G64	0	58.33
	G78	8.33	58.33
Complemented mutants	NS63comp	25	50
	G64comp	33.33	66.67
	G78comp	50	100

[a] Identifies complemented mutants and their un-complemented counterparts.

[b] Migration index represent the percentage of catheter sections that were successfully crossed from twelve replicate tests.

3.7.4 Blockage of all-silicone catheters by swarming-deficient mutants

The role of swarming in the blockage of indwelling urethral catheters was assessed using an *in vitro* model of the catheterised bladder (Section 2.11.2). The ability of control mutants, and swarming-deficient mutants to block all-silicone catheters was compared to that of the wild type strain B4. The pH of media in the model, and the numbers of viable cells was also assessed at the beginning of the experiments and upon blockage of catheters.

In general, strains exhibiting a reduction in swarming ability were found to block catheters more quickly than the wild type strain B4. In contrast, the control mutants which exhibit swarming abilities above that of the wild type, showed an apparent increase in the time taken to block the catheters (Table 3.18). However, statistical analysis of the data revealed that none of the test strains showed significant differences in time taken to block catheters ($P = 0.075$ or greater for all test strains when compared to the wild type by two-sample t-tests at the 95% confidence interval).

The numbers of viable cells, and the pH of media in models at the beginning and end of the experiments, were calculated for each test strain and compared to the wild type using a two-sample t-test (at the 95% confidence interval). The control mutant BVJ15 was found to have a significantly higher number of viable cells in models, at the beginning of experiments ($P = 0.01$), compared to the wild type. However, this did not result in a decreased time to blockage (Table 3.18). All other strains showed no significant differences in the number of viable cells at the start of the experiments ($P = 0.66$ or greater). No significant differences were observed in the number of viable cells after blockage of catheters ($P = 0.67$ or greater). Table 3.19 shows the number of viable cells in models at the beginning of experiments and after catheter blockage.

Table 3.18: Ability of *P. mirabilis* wild type strain B4, control mutants, and swarming-deficient mutants to block all-silicone catheters.

Group	Strain	Time to blockage (Hours) [a,b]
Wild type	B4	29.50 ± 2.97
Group1: Control mutants	BVJ14	41.14 ± 2.98
	BVJ15	30.04 ± 6.08
Group 2: Poor-swarming mutants	PS92	26.67 ± 5.34
	G78	25.72 ± 5.07
	G64	26.89 ± 1.34
Group 3: Non-swarming mutants	G93	29.93 ± 4.79
	G37	22.14 ± 0.25
Group 4: Non-swimming, non-swarming mutants	NS63	25.08 ± 0.84

[a] Values represent the means of three replicate experiments. Values following ± show the standard deviation of the mean.

[b] The time taken for each mutant to block the all-silicone catheters did not differ significantly form that of the wild type (P = 0.075 or greater). Mutants were compared using a two-sample t-test at the 95% confidence interval

Table 3.19: The number of viable cells in *in vitro* bladder models at the beginning of experiments and after catheter blockage.

Group	Strain	Viable cells in model at 0 hours [a,b]	Viable cells in model after blockage [a,b]
Wild type	B4	$3.27 \times 10^9 \pm 1.91 \times 10^{8}$	$2.05 \times 10^9 \pm 4.0 \times 10^{8}$
Group1: Control mutants	BVJ14	$1.10 \times 10^{10} \pm 4.80 \times 10^{8}$	$9.61 \times 10^9 \pm 3.66 \times 10^{8}$
	BVJ15	$1.95 \times 10^{10} \pm 1.44 \times 10^{9}$	$1.57 \times 10^{10} \pm 6.07 \times 10^{9}$
Group 2: Poor-swarming mutants	PS92	$1.59 \times 10^{10} \pm 4.16 \times 10^{8}$	$5.40 \times 10^9 \pm 1.35 \times 10^{8}$
	G78	$1.77 \times 10^{10} \pm 5.56 \times 10^{8}$	$3.30 \times 10^9 \pm 1.79 \times 10^{8}$
	G64	1.10×10^{10} *	$1.79 \times 10^9 \pm 4.94 \times 10^{8}$
Group 3: Non-swarming mutants	G93	$2.21 \times 10^{10} \pm 6.23 \times 10^{8}$	$5.56 \times 10^9 \pm 1.59 \times 10^{8}$
	G37	$1.43 \times 10^{10} \pm 4.32 \times 10^{8}$	$1.23 \times 10^{10} \pm 3.56 \times 10^{8}$
Group 4: Non-swimming, non-swarming mutants	NS63	$5.69 \times 10^9 \pm 4.64 \times 10^{8}$	$2.58 \times 10^9 \pm 4.78 \times 10^{8}$

[a] Values represent the means of three replicate experiments. Values following ± show the standard deviation of the mean.

[b] Viable cell counts of the mutants were not significantly different to those of the wild type, except for BVJ15 which showed a significantly greater number of viable cells in models at the beginning of experiments ($P = 0.01$). Mutants were compared to the wild type using a two-sample t-test at the 95% confidence interval.

* For G64, only one set of data was obtained for the number of viable cells in models at the beginning of experiments. For other replicates cells were too numerous to count and exceeded the presented value.

The control mutant BVJ14 exhibited a significantly lower pH of media at the start of experiments than the wild type, while the non-swarming mutant G37 possessed a significantly higher pH (Table 3.20). No significant differences were observed in the pH of media in models after blockage of catheters (P = 0.23 or greater).

3.7.5 Correlation of swimming, swarming, and adherence to silicone with catheter blockage

The association between the test strains ability to block catheters and their abilities to swim, swarm, and adhere to silicone (taken as the number of cells attached per cm^2 after 5 hours in the parallel plate flow chamber, Table 3.12), were explored. The various factors were compared as outlined in section 3.6.2. Scatter graphs and linear regression showed a positive correlation between swimming and swarming ability and the time taken to block catheters, but a negative correlation between the ability to adhere to silicone (Figures 3.48, 3.49, 3.50). Calculation of correlation coefficients confirmed these relationships, and indicated the extent to which the factors were associated (Table 3.21). This indicated that as swimming and swarming ability increased, the ability to block catheters was reduced, leading to an increased time to blockage. In contrast, as the ability to adhere to silicone increased, blockage of catheters was enhanced, leading to a decreased time to blockage.

Table 3.20: pH of the media in *in vitro* bladder models at the beginning of experiments and after blockage of catheters.

Group	Strain	pH at Start [a]	pH at End [a]	Significantly different to B4 [b]
Wild type	B4	9.01 ± 0.02	8.53 ± 0.10	-
Group1: Control mutants	BVJ14	8.85 ± 0.03	8.39 ± 0.13	Yes for pH at start (p 0.021) No for pH at end
	BVJ15	8.66 ± 0.12	8.52 ± 0.09	No
Group 2: Poor-swarming mutants	PS92	8.99 ± 0.06	8.48 ± 0.12	No
	G78	8.84 ± 0.13	8.38 ± 0.16	No
	G64	9.05 ± 0.03	8.80 ± 0.26	No
Group 3: Non-swarming mutants	G93	9.10 ± 0.04	8.77 ± 0.10	No
	G37	9.12 ± 0.01	8.66 ± 0.19	Yes for pH start (P 0.014) No for pH at end
Group 4: Non-swimming, non-swarming mutants	NS63	8.98 ± 0.05	8.85 ± 0.19	No

[a] Values represent the means of three replicate experiments. Values following ± show the standard deviation of the mean.

[b] Significant differences were assessed by comparing data for mutant to the wild type strain B4 using a two-sample t-test at the 95% confidence interval. Figures in parentheses represent P values.

Figure 3.48: Correlation of swarming ability and blockage of urethral catheters.
The swarming indices of test strains were plotted against the time taken to block all-silicone catheters in the *in vitro* bladder model, and analysed using linear regression (line).

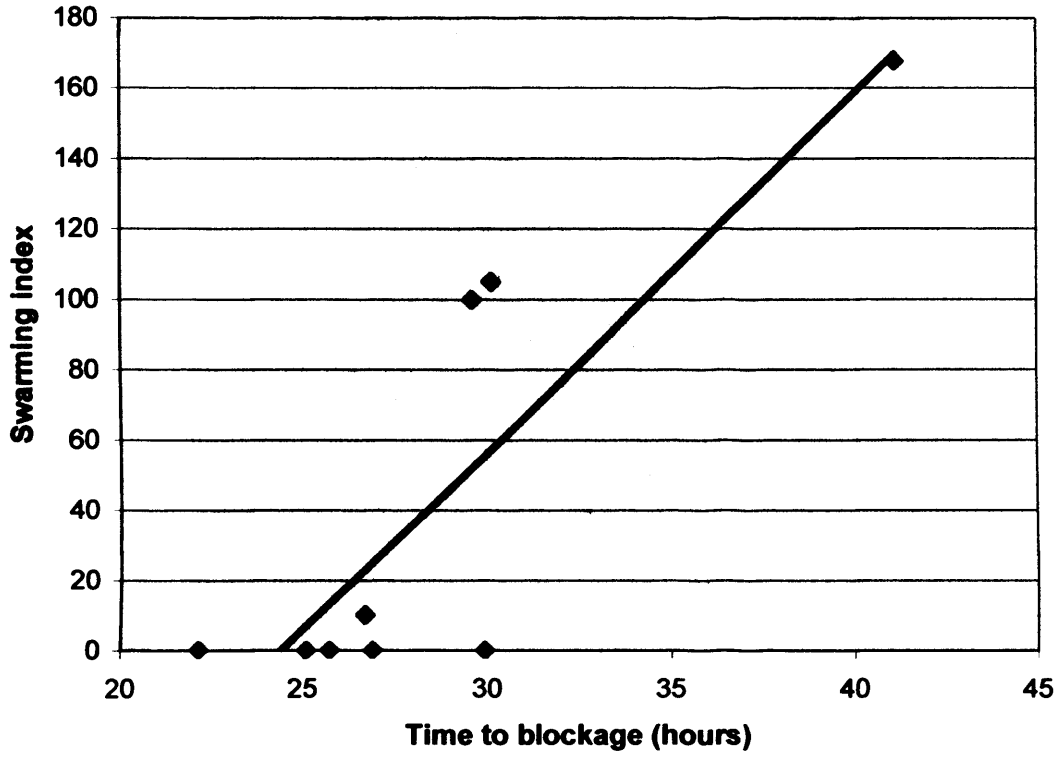

Figure 3.49: Correlation of swimming ability and blockage of urethral catheters.
The swimming indices of test strains were plotted against the time taken to block all-silicone catheters in the *in vitro* bladder model, and analysed using linear regression (line).

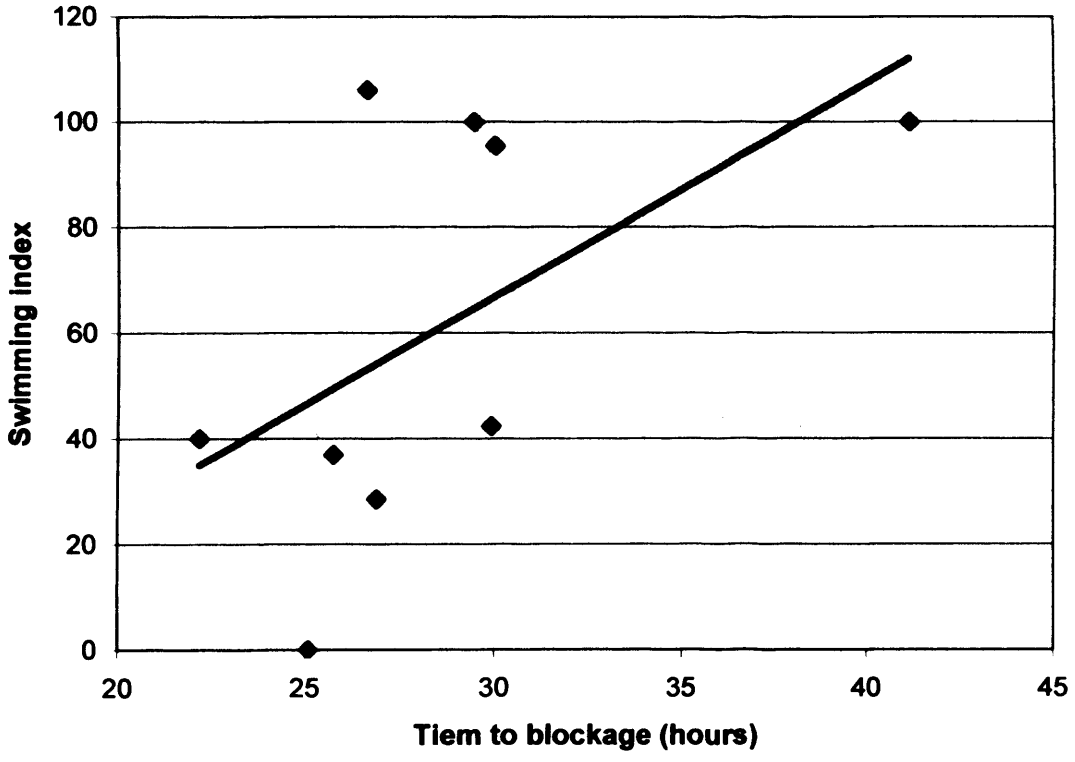

Figure 3.50: Correlation of swimming ability and blockage of urethral catheters.

The ability of test strains to adhere to silicone (taken as the number of cells attached per cm^2 after 5 hours in the parallel plate flow chamber, Table 3.9) were plotted against the time taken to block all-silicone catheters in the *in vitro* bladder model, and analysed using linear regression (line).

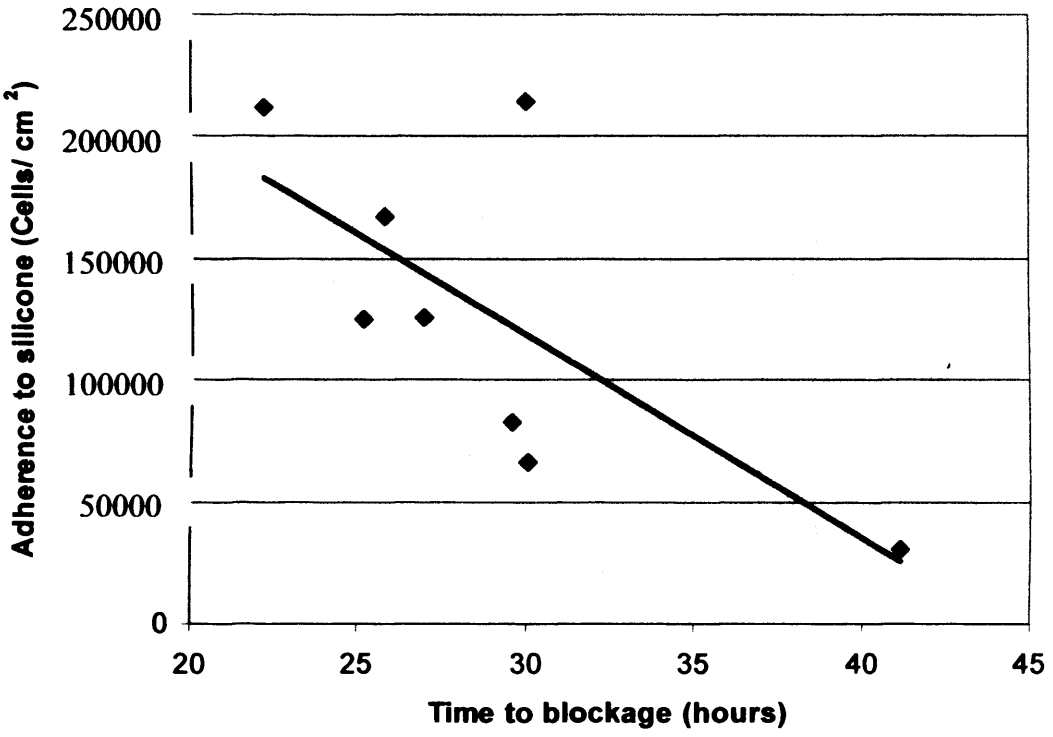

Table 3.21: Relationship between time taken to block all-silicone catheters in the *in vitro* bladder model, and ability to swim, swarm and adhere to silicone.

Factors compared	Correlation coefficient [b]	Explanation
Time to blockage vs. Swimming index	0.697	Indicates a **strong positive correlation** between swimming ability and time to blockage. As swimming ability increases, so does time to blockage.
Time to blockage vs. Swarming index	0.759	Indicates a **strong positive correlation** between swarming ability and time to blockage. As swarming ability increases, so does time to blockage.
Time to blockage vs. Ability to adhere to silicone [a]	-0.704	Indicates a **strong negative correlation** between ability to adhere to silicone and time to blockage. As adherence increases time to blockage decreases.

[a] Ability to adhere to silicone in the parallel plate flow chamber, taken as the number of cells attached per cm^2 after 5h (Table 3.12).

[b] All correlation coefficients were significant at the 95% confidence level, as assessed using critical coefficient values presented by Fry (1993).

Chapter 4: Discussion

4.1 Selection and mutagenesis of a *P. mirabilis* clinical isolate

4.1.1 Selection of a *P. mirabilis* clinical isolate for mutagenesis

In any investigation of pathogenesis and virulence mechanisms, the strain selected for study is a critical factor. The clinical relevance of a strain, its history, and the ability to use it in conjunction with the proposed methods are key issues (Miller & Mahenthiralingam 2003). The clinical relevance, and history of a strain are important in order to ensure the use of a pathogenic strain capable of initiating the infection to be studied. The genomes of different strains from the same species may vary considerably (Bergthorsson & Ochman 1998; Dobrint *et al.* 2002; Liang *et al.* 2001), and non-pathogenic strains are likely to completely lack many genes associated with virulence (Ørskov & Ørskov 1992; Nataro & Kaper 1998; Dobrint *et al.* 2002). Analysis of natural isolates of *E. coli* has shown that the genome size of this organism can vary by as much as 1 Mb (Bergthorssen & Ochman 1998).

Therefore, in order to identify genes associated with the pathogenicity of *P. mirabilis* in the catheterised urinary tract, it was important to use a target strain that was known to be capable of initiating catheter associated urinary tract infection, and blocking urethral catheters. The clinical isolates B1 - B6 were chosen for this study as they had recently been isolated from blocked and encrusted indwelling urethral catheters. However, it was important to identify which were suitable for investigation by the proposed random mutagenesis strategy, and therefore further characterisation of these isolates was required. The main considerations addressed by this analysis were: whether commonly used selectable markers were suitable for use with these isolates; whether any isolates harboured naturally occurring plasmids; and which isolates were amenable to genetic manipulation (such as isolates into which foreign plasmid DNA could be introduced).

Some pathogenic bacteria, such *Shigella flexneri* and *Agrobacterium tumefaciens*, possess plasmids that harbour a large number of virulence genes, and contribute greatly to the pathogenicity of these organisms (Venkatesan *et al.* 2001; Lan *et al.* 2001; Kado 2002). For the study of virulence mechanisms in such organisms, it is often essential to utilise strains possessing these virulence plasmids. For example, in *S. flexneri* the virulence plasmid plays such a major role in pathogenicity that strains lacking this replicon are no longer virulent (Lan *et al.* 2001). In the case of *P. mirabilis*, swarming has not been associated with the presence of any extra-chromosomal elements, and genes involved in this form of motility have been found to occupy closely linked loci on the *P. mirabilis* chromosome (Allison & Hughes 1991).

Some clinical isolates of *P. mirabilis* have been found to contain large plasmids associated with resistance to antibiotics (Mobley 1996). The presence of a native plasmid could reduce the efficacy of transposon mutagenesis in *P. mirabilis,* and may also interfere with other genetic manipulations. Plasmids resident in clinically isolated strains are likely to carry genes encoding resistance to antibiotics, and may therefore undermine the use of selective agents used to identify transposon mutants. In previous studies, the natural resistance of *P. mirabilis* isolates to certain selective agents has limited the transposable elements suitable for use (Belas *et al.* 1991a). Native plasmids could also hinder identification of disrupted genes, by reducing the efficiency with which DNA flanking transposon inserts could be sub-cloned. In addition, incompatibility issues between resident plasmids and plasmid vectors could impede complementation studies, by limiting the ability to introduce intact copies of disrupted genes into mutants (Brown 2001). Therefore, the presence of a naturally

occurring plasmid in the *P. mirabilis* strain subjected to transposon mutagenesis in this study would be undesirable.

Fortunately, only isolate B2 was found to carry a plasmid, which was designated pB2. Interestingly, B2 also showed resistance to several antibiotics at clinically relevant concentrations, including ampicillin. It is possible that these resistances may be encoded by the plasmid pB2 (Mobley 1996), however *P. mirabilis* clinical isolates which possessed chromosomally encoded resistance to ampicillin have been reported (Bret *et al.* 1998).

All isolates were found to be resistant to tetracycline (Table 3.2). This highlights the intrinsic resistance of *P. mirabilis* to this antibiotic (Mobley 1996). However, the designated resistance of *P. mirabilis* to tetracycline is based on concentrations achievable *in vivo* (Mobley 1996). *In vitro,* tetracycline can be used in sufficient concentration to inhibit the growth of *P. mirabilis,* and function as a selective agent for the identification of transposon mutants. For example high concentrations of tetracycline (300 μg/ml) have been successfully used for selection of *Burkholderia cenocepacia* Tn*5*-OT182 mutants (Sokol *et al.* 1999). Therefore, all of the commonly used selective agents assessed were suitable for use with *P. mirabilis*.

Screens for naturally occurring plasmids, and assessment of antibiotic sensitivities of the clinical isolates, indicated that only isolate B2 was unsuitable for transposon mutagenesis. However, experiments to identify isolates which were amenable to genetic manipulation, and into which plasmids could be introduced, showed that only isolates B3 and B4 were suitable for use in this study. The clinical isolate B4 was ultimately selected for mutagenesis, as this isolate was observed to swarm more

vigorously than B3, and produced more trans-conjugants after introduction of plasmid pOT182.

4.1.2 Mutagenesis of *P. mirabilis* strain B4

The widespread use of Tn*5* for mutagenesis has resulted in the generation of many distinct Tn*5* elements and delivery systems, designed to fulfil a variety of demands (Simon *et al.* 1989; de Lorenzo *et al.* 1990; Herrero *et al.* 1990; Merriman & Lamont 1993; Hansen *et al.* 1997). Two transposons and delivery systems were evaluated for use in strain B4, transposon Tn*5*-OT182 and the pOT182 delivery vector, and the pUTmini-Tn*5*Km2 system. Each transposon offered distinct advantages for the generation and analysis of *P. mirabilis* swarming deficient-mutants.

Merriman & Lamont (1993) constructed transposon Tn*5*-OT182, which contains the ColE1 origin of replication, to facilitate the cloning of DNA flanking the transposon insert. This transposon also possesses a promotorless *lacZ* gene which allows the expression of genes disrupted by this transposon to be monitored. However, this transposon suffers from disadvantages common to wild type Tn*5* elements. As described in Section 1.9.3, wild type transposons are large and difficult to handle often containing unwanted or inappropriate resistance genes (de Lorenzo *et al.* 1998); have a general lack of useful restriction sites, making cloning of disrupted genes potentially difficult; posses an active transposase gene making insertions unstable and inhibiting additional transposon mutagenesis; and the large repeated sequences at the ends also serve to promote genetic rearrangements in the host DNA. (Kleckner *et al.* 1991; Hensel & Holden 1996; de Lorenzo *et al.* 1998).

Herrero *et al.* (1990) and de Lorenzo *et al.* (1990) addressed these problems with the construction of a set of modified genetic elements based on Tn*5* and Tn*10*. The resulting constructs were named mini-transposons due to their reduced size, and include the mini-Tn*5*Km2 transposon used in this study (de Lorenzo *et al.* 1998). As such the mini-Tn*5*Km2 transposon is free of several disadvantages that impede the effectiveness of transposons more closely related to wild type Tn*5* elements (de Lorenzo *et al.* 1998), such as Tn*5*-OT182. The reduced size of mini-transposons facilitates handling and increases the frequency of insertion (Kleckner *et al.* 1991; de Lorenzo & Timmis 1994). The lack of an active transposase gene and the shortened inverted repeats of mini-transposons greatly increases the stability of inserts, and allows additional rounds of mutagenesis to be performed on strains already harbouring a transposon (de Lorenzo *et al.*1994). The advantages and disadvantages of Tn*5*-OT182, and mini-Tn*5*Km2 are summarised in Table 4.1.

However, it was the pOT182 delivery vector used with the Tn*5*-OT182 transposon that proved to be unsuitable for use with *P. mirabilis* B4, as pOT182 was maintained as a free replicon by B4. Despite the inability to use the Tn*5*-OT182 system, the maintenance of pOT182 in *P. mirabilis* B4 proved to be an extremely useful observation, and ultimately lead to the development of vector pB4 (Section 2.9.4 and 3.4.3).

In contrast to Tn*5*-OT182 and the pOT182 delivery vector, the pUTmini-Tn*5*Km2 system proved highly effective when applied to *P. mirabilis* B4. Mini-Tn*5* based elements have been used previously for mutagenesis based studies of *P. mirabilis,* mainly focused on swarming. Table 4.2 summarises several of these studies. The use of mini-Tn*5* elements for the mutagenesis of *P. mirabilis* was initially assessed by

Table 4.1: Summary of advantages and disadvantages offered by transposons Tn*5*-OT182, and mini-Tn*5*Km2.

Transposon	Advantages	Disadvantages
Tn*5*-OT182	Tn*5* based transposon, so suitable for use in a wide range of Gram negative bacteria. Multiple selectable markers "Self cloning" facilitates identification of disrupted genes Allows transcriptional analysis through promotorless *lacZ*.	Large size, unwanted restriction sites. Presence of active transposase gene and wild type inverted repeats decreased stability Transposase gene generates immunity to subsequent mutagenesis with Tn*5* elements.
Mini-Tn*5*Km2	Tn*5* based transposon, so suitable for use in a wide range of Gram negative bacteria. Small size, few unwanted restriction sites. Engineered to contain unique restriction sites useful for cloning of DNA flanking inserts. Generates stable inserts.(Does not contain active transposase gene, and inverted repeats greatly reduced in size.) Lack of transposase gene allows further mutagenesis of host containing a mini-Tn*5* element with other Tn*5* based elements.	Inserts are often highly polar due to stop codons at the end of mini-Tn*5* elements. pUT delivery vector may co-integrate with transposon.

Table 4.2: Summary of studies using mini-Tn*5* based transposons for mutagenesis based studies of *P. mirabilis*.

Study	Transposon used	Summary
Belas *et al.* 1991a/b	Mini-Tn*5*Cm and Mini-Tn*5*Sm/Sp	Evaluated the use of mini-Tn*5* elements in *P. mirabilis*, and analyses mutants defective in swarming.
Belas *et al.*1995	Mini-Tn5Cm	Characterised disrupted genes in *P. mirabilis* mutants unable to differentiate normally. Found that the majority possessed inserts in genes associated with flagella biosynthesis.
Hay *et al.*1997	Mini-Tn5Cm	The *lrp* (leucine-responsive protein) global regulator is involved in hyper flagellation and elongation of *P. mirabilis* swarmer cells. *lrp* acts with other regulators to control swarming.
Belas *et al.*1998	Mini-Tn5Cm	Identified precocious swarming mutants defective in *rsbA* (regulator of swarming behaviour). *RsbA* found to be homologous to histidine kinases of two-component regulatory protein family.
Hay *et al.*1999	Mini-Tn5Cm	Identified non-swarming mutant disrupted in *ccmA* gene (Curved cell morphology). Mutants exhibited abnormal cell morphology. Lack of swarming in these mutants thought to be due to inability to form multicellular rafts.
Murphy *et al.*1999	Mini-Tn5Cm and spontaneous mutagenesis	Genetic rearrangements occur between flagellin genes of *P. mirabilis* to produce antigenically and biochemicaly different flagellin proteins. Suggest possible role in evasion of host immune response.
Zhao *et al.*1999	STM with Mini-Tn*5*Km	Identified genes necessary for virulence in mouse model of urinary tract infection, including a collagenase precursor, and an open reading frame belonging to the *rpoN* operon.

Belas *et al.* (1991a), who reported that mini-Tn*5* transposon could be used to successfully generate stable mutants, with single transposon insertions, and that the *P. mirabilis* chromosome did not contain significant hotspots for mini-Tn*5* insertion (Belas *et al.* 1991a).

Southern hybridisation showed that mini-Tn*5*Km2 generally inserted at random, and in single copy, in *P. mirabilis* B4 (Figure 3.6). However, trans-conjugant BVJ16 appeared to possess multiple copies of the transposon. In addition, this analysis also suggested the existence of pUTmini-Tn*5*Km2 as a free replicon in BVJ16. Bands of similar size were observed for digested DNA from both BVJ16 (which generated multiple bands), and the *E. coli* donor strain S17.1λ*pir* (which generated a single band corresponding to the pUTmini-Tn*5*Km2 plasmid carried by this strain). Therefore, the multiple bands observed in BVJ16 could potentially indicate replication of pUTmini- Tn*5*Km2 in B4, and multiple transposition events. However, extraction of plasmid DNA and digest with *Bam*H1 confirmed loss of the pUT delivery vector from all trans-conjugants used to assess this system (BVJ10-17); (Figure 3.5).

This supports an alternative explanation for the Southern hybridisation results obtained with BVJ16; that the multiple bands observed are the result of contamination of isolate BVJ16 with other trans-conjugants. This could easily have occurred during isolation of BVJ16 from selective media, after matings to introduce pUTmini-Tn*5*Km2 into *P. mirabilis* B4. Although this is most likely the cause of the BVJ16 Southern hybridisation results, swarming-deficient mutants selected for further study were also confirmed as possessing single, random mini-Tn*5*Km2 inserts as a precaution (Figure 3.9).

As well as the advantages already discussed, the successful use of the mini-Tn*5*Km2 transposon, also provides an opportunity to utilise an alternative transposon based mutagenesis strategy. The mini-Tn*5*Km2 element used in this study was randomly selected from a pool of 96 transposons, each carrying a unique oligo-nucleotide tag. These transposons may be used to identify genes associated with virulence through signature tagged mutagenesis (STM); a powerful extension of the random transposon mutagenesis strategy (Hensel *et al.* 1995).

When using STM, mutants are generated from each of the 96 tagged transposons, and organised into pools of 96 individual mutants harbouring a transposon with a distinct tag. This allows large numbers of mutants to be screened directly in an infection model to identify genes necessary for survival *in vivo*, where mutants disrupted in genes necessary for survival in the model are lost (Hensel *et al.* 1995). Mutants that are unable to survive *in vivo* can be identified by screening those recovered from the model to discern tags that have been lost (Hensel *et al.* 1995). Mutants whose tags are absent can then be isolated from a master plate and subjected to further analysis.

In the case of catheter encrustation by *P. mirabilis*, the *in vitro* bladder model could be utilised to identify genes required for the encrustation and blockage of urinary catheters. Figure 4.1 illustrates how STM may be applied to study the pathogenesis of *P. mirabilis* in the catheterised urinary tract. STM has already been successfully applied to the study of *P. mirabilis* virulence attributes. Zhao *et al.* (1999), utilised STM to identify novel genes associated with the ability of *P. mirabilis* to infect the urinary tract. In this study pools were used to inoculate mice trans-urethrally, and harvested 2 days after infection from bladders and kidneys. Mutants disrupted in

genes homologous to a collagenase precursor, and an open reading frame belonging to the *rpoN* operon, which is responsible controlling expression of genes regulated by nitrogen.

Figure 4.1: Application of signature tagged mutagenesis to the study of *P. mirabilis* catheter associated urinary tract infection.
Modified from Hensel *et al.* (1995).

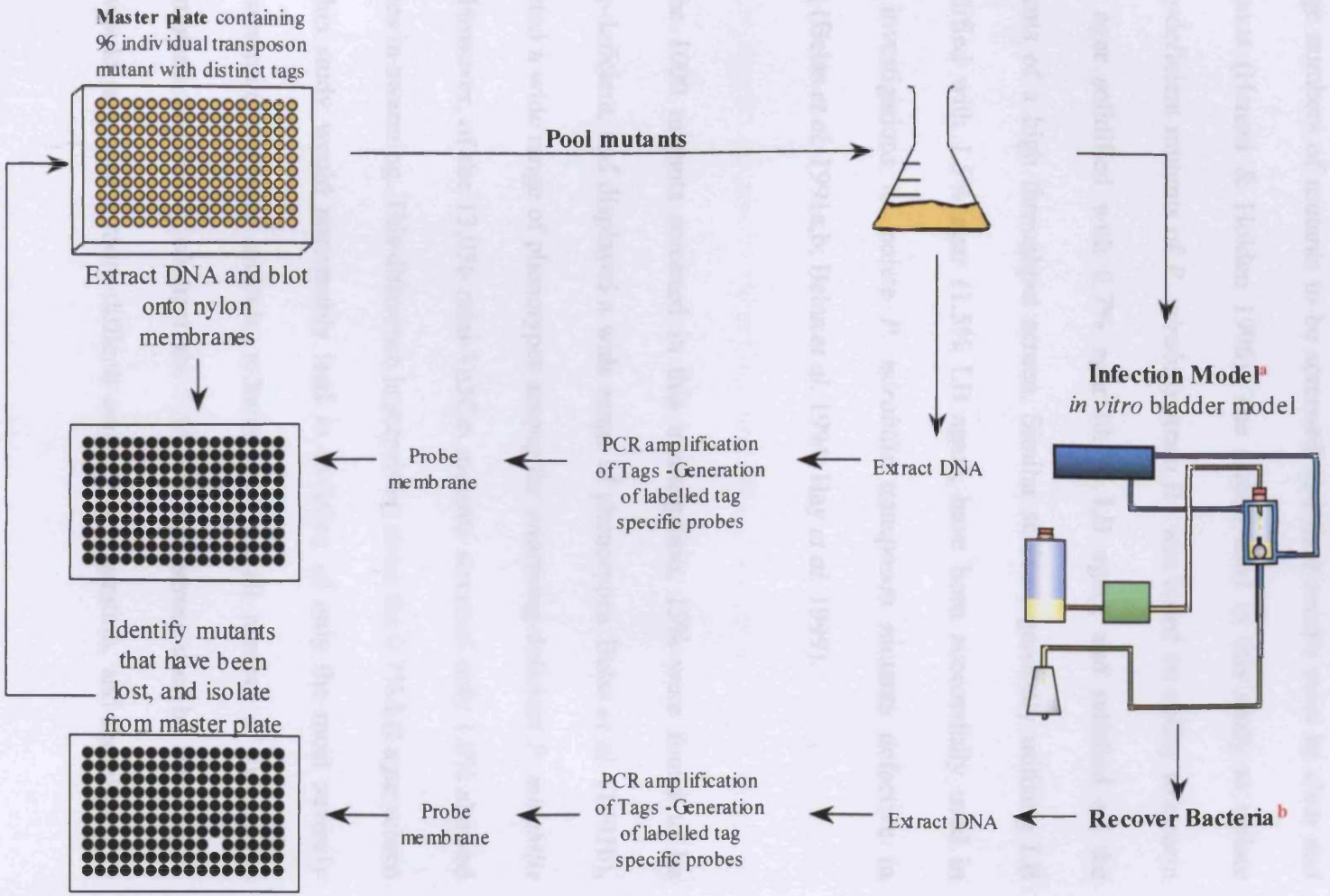

[a]**Models could be run in a variety of ways to investigate different aspects of *P. mirabilis* pathogenesis:**
1 - Models could be run as normal until blockage occurs. **2** - models could be run for set periods of time, for example 1-2 hours to investigate factors involved in the early stages of infection. **3** - models could be run using a variety of media, such as artificial urine, human urine, or minimal media.

[b]**Bacteria could be recovered from models in a variety of ways:**
1 - Could recover bacteria present in drainage bag only. Could use this method with model run for short time, and containing minimal media to enrich and positively select mutants unable to adhere to the catheter surface. **2** - Could harvest only bacteria adhering to catheter surface. **3** - Could recover all bacteria in model.

4.2 Isolation and characterisation of mutants

4.2.1 Isolation of swarming-deficient mutants

The design, and implementation of selective screens, to isolate mutants with a desired phenotype, is a vital factor in any study involving random transposon mutagenesis (Hensel & Holden 1996). Such screens must be high-throughput to allow large numbers of mutants to be screened, and their results must be clear and unambiguous (Hensel & Holden 1996). The screen used in this study to isolate swarming-deficient mutants of *P. mirabilis* strain B4 was based on ability to swarm over LB agar solidified with 0.7% agar (0.7% LB agar), and satisfied all the requirements of a high throughput screen. Similar screens, generally utilising LB agar solidified with 1.5% agar (1.5% LB agar), have been successfully used in previous investigations to isolate *P. mirabilis* transposon mutants defective in swarming (Belas *et al.* 1991a,b; Belas *et al.* 1994; Hay *et al.* 1999).

Out of the 1000 mutants screened in this investigation, 15% were found to be swarming-deficient, and displayed a wide range of phenotypes. Belas *et al.* (1991b), also reported a wide range of phenotypes among the swarming-deficient *P. mirabilis* mutants. However, of the 13,036 mini-Tn*5*Cm mutants screened only 1.6% showed deficiencies in swarming. This difference is surprising since the 0.7% LB agar screen used in this study would presumably lead to isolation of only the most severely crippled swarming-deficient mutants, reducing the overall number of swarming-deficient mutants isolated. In contrast, the 1.5% LB agar screen used by Belas *et al.* (1991b), would represent a more difficult surface for migration, and therefore this

screen should detect a greater number of swarming-deficient mutants. Rauprich *et al.* (1996) found that as agar concentration was increased swarming was inhibited to a corresponding degree.

The high number of swarming-deficient mutants isolated in this study may be partly due to the large numbers of genes thought to be involved in swarming. Based on the assumption that the chromosome size and coding capacity of *P. mirabilis* is equivalent to that of *E. coli*, Belas *et al.* (1991a) also estimated the number of genes involved in the *P. mirabilis* swarm cycle, and derived a figure of approximately 60 genes. Allison *et al.* (1991) also estimated the number of genes involved in the *P. mirabilis* swarm cycle, and suggested that around 40 genes are concerned with swarming. Although it is plausible that the number of genes associated with swarming could be in excess of 60, as around 40 - 50 genes are thought to be involved in flagella biogenesis alone (Macnab 1992; Fraser *et al.* 2000), this alone does not provide a satisfactory explanation for the high frequency of swarming-deficient mutants isolated in this study.

A more likely scenario is that the mini-Tn*5*Km2 transposon used in this investigation exhibits a degree of non-random insertion in *P. mirabilis* strain B4. Genes associated with swarming are generally thought to be closely clustered on the *P. mirabilis* chromosome (Allison *et al.* 1991), and the preferential insertion of mini-Tn*5*Km2 in a segment of DNA rich in swarming associated genes, could account for the high numbers of swarming-deficient mutants isolated. An alternative explanation may be

that in *P. mirabilis* strain B4 spontaneous swarming-deficient mutants occur at a high frequency. However data obtained from experiments designed to control for this scenario, indicated that this is not the case. In these experiments the frequency with which spontaneously swarming-deficient mutants occurred was investigated by screening 1000 wild type colonies using the 0.7% LB agar screen. Only 0.1% of the wild type colonies screened were found to be swarming-deficient.

An alternative explanation for the high numbers of swarming-deficient mutants that were obtained during this study may lie with factors associated with *P. mirabilis* strain B4 and the Tn*5* transposition mechanism. Several host factors, including DNA methylation, DNA gyrase, DNA polymerase I, and a host of other DNA modifications and DNA modifying proteins have been associated with the transposition of Tn*5* based elements (Reznikoff 2002). While these factors are not essential for transposition they may greatly influence the frequency at which transposition takes place (Reznikoff 2002). *P. mirabilis* B4 was selected for mutagenesis partly because of the large number of trans-conjugants obtained with this strain (Section 3.1.5). Therefore, B4 may provide a cellular environment more conducive to Tn*5* transposition than the *P. mirabilis* strains used in other studies, resulting in a higher frequency of transposition and greater numbers of mutants, including those with specific phenotypes such as swarming-deficiency. Tn*5* transposition has also been found to show some bias to negatively supercoiled DNA (Lodge & Berg 1990). In this study, the introduction of mini-Tn*5*Km2 and subsequent transposition was carried out on solid media, which would illicit

expression of genes involved in swarming. As these genes are thought to be closely linked on the *P. mirabilis* chromosome (Allison *et al.* 1991), the relaxation of DNA segments for expression of some of these genes, combined with the possible influence of host factors on transposition frequency, may have lead to an increase in the number of swarming-deficient mutants.

4.2.2 Co-integration of the pUT suicide delivery vector with mini-Tn*5*Km2

The co-integration of the pUT delivery vector observed in this study may also be related to aspects of Tn*5* transposition. Presence of the pUT delivery vector in recipient strains was also noted by de Lorenzo & Timmis (1994), based on an ampicillin resistant phenotype. These ampicillin resistant trans-conjugants usually occurred when the recipient strain was also *E. coli*, and was thought to be due to release of λ*pir* phage by the pUT donor strain which subsequent infected the recipient strain, and integrated into its chromosome. This then allowed replication of the pUT plasmid in the recipient strain (de Lorenzo & Timmis 1994). However, while λ*pir* phage may be capable of infecting *P. mirabilis* at low levels, due to the relatedness of the two species, no evidence of pUT replication was found in ampicillin resistant *P. mirabilis* trans-conjugants. Instead, segments of the pUT delivery vector were found to be integrated into the *P. mirabilis* chromosome, contiguous with the mini-Tn*5*Km2 transposon (Figures 3.7 and 3.8).

Swarming-deficient mutants isolated by the phenotypic 0.7% LB agar screen were subjected to tests for co-integration of the pUT suicide delivery vector into the *P.*

mirabilis chromosome. The co-integration of pUT into the *P. mirabilis* chromosome may be attributed to recombination between homologous sequences of pUT and *P. mirabilis* chromosomal DNA (de Lorenzo & Timmis 1994), but could be largely due to attributes of the Tn*5* transposition mechanism. This predicts that the formation of pUTmini-Tn*5*Km2 dimers would result in the co-transposition of segments of the donor DNA molecule, in this case pUT, with the mini-Tn*5*Km2 transposon (Berg & Berg 1983).

Co-integration of pUT was evident in ~30% of the swarming-deficient mutants isolated in this study. Similar results were obtained by Belas *et al.* (1991a), who reported a pUT co-integration frequency of 35% based on resistance to ampicillin. It has been suggested that mutants containing co-integrated pUT harbour all or most of the plasmid as a chromosomal insertion (Belas *et al.* 1991a; de Lorenzo & Timmis 1994). Characterisation of co-integrated pUT sequences during this investigation support this theory, as the majority of the plasmid could be amplified by PCR from ampicillin resistant, swarming-deficient mutants isolated during this study (Figure 3.8).

Belas *et al.* (1991a) found that the co-integration of pUT was stable within the *P. mirabilis* chromosome, and further analysis of such mutants was not hindered by its presence. However, the use of mutants harbouring chromosomally integrated pUT would seem to undermine several advantages of mini-transposons, and transposon mutagenesis in general. All of the swarming-deficient mutants containing co-

integrated pUT that were analysed by PCR, were found to contain segments of the plasmid encoding the Tn*5* transposase enzyme (Figure 3.8). Since the presence of the pUT ampicillin resistance gene was also confirmed by PCR and was shown to be functional, it is reasonable to assume that the transposase gene is also active when integrated into the *P. mirabilis* chromosome, and capable of mediating further transposition of the mini-Tn*5*Km2 transposon.

The presence of an active transposase gene eliminates one of the main advantages of mini-transposons, which is stability of the transposon insert (de Lorenzo 1998). While the pUT DNA would probably remain stably integrated at the original insertion site, maintaining the original mutant phenotype, the transposon could insert into and disrupt additional genes. Although as a necessity Tn*5* transposition has evolved to occur naturally at a low frequency, especially once integrated into the host chromosome (Reznikoff 2002), this does not preclude further transposition. Such events could be extremely difficult to detect and have no obvious phenotype, but may have serious implications for the results of experiments such as infection models. For example, in an infection model this could result in the false association of a gene with virulence, leading to flawed or incorrect conclusions, and misdirecting future research. In addition, the transposase would prevent further mutagenesis with other Tn*5* based elements (Reznikoff 2002), and the pUT DNA flanking transposon inserts may hamper identification of disrupted genes. Therefore, mutants exhibiting pUT co-integration were excluded from further study.

4.2.3 Selection and evaluation of mutants for further study

Mutants chosen for further study were selected at random, from those confirmed to be free of pUT co-insertion. In addition to pUT co-integration another potential problem related to the mutagenesis system was considered when selecting mutants for further study. This was the possibility that the mini-Tn*5*Km2 transposon itself could have an adverse effect on swarming ability, or other factors relevant to catheter blockage. For this reason several mutants that showed no reduction in swarming ability were included as controls. In addition, the growth rates and urease production of all mutants selected for further study was assessed, as these factors would be directly related to blockage and encrustation of urinary catheters in the *in vitro* bladder model.

If growth, swarming, or urease production were affected merely by the presence of the transposon, then the contribution to blockage of urethral catheters made by swarming in general, and the specific genes disrupted in each mutant, could not be accurately assessed. However, the control mutants (Table 3.5, group 1) showed that the presence of the mini-Tn*5*Km2 transposon in the host chromosome *per se* did not impair the swarming or swimming ability of strain B4. No significant differences were detected in growth or urease production in any of these control mutants. In addition, all of the mutants selected for further study including the control mutants, were confirmed to be stable and possess a single, random transposon inserts.

By investigating the swarming and swimming abilities of these stable transposon mutants, it was revealed that the majority of swarming-deficient mutants were also defective in swimming motility. Several other studies have reported that mutants isolated as deficient in swarming were also found to display deficiencies in swimming ability (Belas *et al.* 1991b; Gygi *et al.* 1995a; Hay *et al.* 1997; Gygi *et al.* 1997). With the exception of PS92, all swarming-deficient mutants showed decreased swimming ability when compared to the wild type (Table 3.5). Of the poor-swarming mutants, those with the lowest swarming indices (G64 and G78), also possessed the lowest swimming indices (Table 3.5, group 2). These results indicate that, excluding PS92, the mutants selected for this study generally appear to be disrupted in genes or processes common to both swimming and swarming motilities.

It is unusual that virtually all of the swarming-deficient mutants selected for further study also exhibit reductions in swimming motility. A reduction in swimming is not inevitable in swarming-deficient mutants, which would result from the disruption of genes and processes exclusive to swarming motility. This was illustrated by mutant PS92 which was deficient in swarming but not swimming. Swarming-deficient mutants with normal swimming ability have also been described in other studies (Gygi *et al.* 1995b; Lai *et al.* 1998; Hay *et al.* 1999). For example, Hay *et al.* (1999) described a swarming-deficient mutant which possessed normal swimming ability, but differentiation resulted in swarmer cells of abnormal shape which inhibited swarming. One possible explanation for the poor swimming ability observed in the majority of the mutants selected for further study may again relate to the 0.7% LB

agar screen used. Aspects of this screen for swarming-deficient mutants, discussed previously, may bias the type of mutants isolated towards those with the phenotypes observed here. This hypothesis is also reflected in the severe reductions in swarming observed in the poor-swarming mutants (Table 3.5, group 2).

The most obvious connection between swimming and swarming is the bacterial flagellum, as disruption of flagella biosynthesis or rotation would affect both activities (Belas *et al.* 1991b; Gygi *et al.* 1995a; Belas *et al.* 1995; Mobley 1996; Belas 1996; Gygi *et al.* 1997; Fraser *et al.* 2000). Belas *et al.* (1995) characterised the disrupted genes in non-swarming mini-Tn*5* mutants, and found that a large number were disrupted in genes associated with flagella biosynthesis. Genes associated with flagella biosynthesis were also found to be disrupted in the swarming-deficient mutants characterised by Gygi *et al.* (1995a), and Gygi *et al.* (1997), which also displayed reductions in swimming ability. However, further analysis of the mutants used in the current study (discussed in detail in subsequent sections) showed that the majority of transposon inserts were not in genes that could be directly associated with flagella production or swimming motility (see section 4.3).

Data obtained from quantification of swarming ability was also used to examine the periodicity of the swarm cycle in control and swarming-deficient mutants. Similar methods, which utilise migration velocity to measure progression of the swarming cycle, have also been used in other studies to investigate the temporal control of the swarm cycle (Gygi *et al.* 1995b; Rauprich *et al.* 1996; Belas *et al.* 1998; Lai *et al.*

1998). A major drawback with using this variable to deduce swarm cycle periodicity is that migration velocity only allows the timing of the swarm cycle to be investigated in mutants which exhibit active migration. However, mutants that do not exhibit migration may still exhibit normal temporal control over the swarm cycle, with cells differentiating, and dedifferentiating at the expected times. Hay *et al.* (1997), described a non-swarming *P. mirabilis* mutant which differentiated with kinetics similar to that of the wild, although elongation was less pronounced.

Analysis of the periodicity of the swam cycle in BVJ15 and BVJ12 revealed that both mutants possessed similar swarm cycle periodicity, but showed some differences in the timing of the swarm cycle compared to the wild type strain B4 (Figure 3.10). BVJ12 and BVJ15 accelerated faster than the wild type initially, but slowed before reaching peak migration velocity at around the same time as the wild type. This "stutter" in migration has been described in previous studies of *P. mirabilis* swarm cycle periodicity, and was attributed to the age of the culture used to inoculate the agar plate (Rauprich *et al.* 1996). However, the similarity in the measurements obtained for both mutants, and the fact that the data was derived for three replicate experiments using distinct cultures to inoculate agar plates, suggests that the "stutter" observed in migration of BVJ12 and BVJ15 was a controlled aspect of the swarm cycle in these mutants. BVJ12 and BVJ15 also showed a slower deceleration, resulting in an extended period of migration compared to the wild type. This slight increase in the duration of migration is probably why the swarming

indices of BVJ12 and BVJ15 were slightly above that of the wild type B4, at 110.1 and 105 respectively (Table 3.5).

The similarity between BVJ12 and BVJ15 suggests that a factor common to both mutants was responsible for the altered swarm cycle periodicity in these mutants. it is possible that these insertions were in the same gene. This is supported by the fact that in both mutants fragments of similar size were identified when genomic DNA was digested with *Pst*I, and analysed by Southern hybridisation using transposon specific probes (Figure 3.9).

A more pronounced difference in the swarm cycle was observed in BVJ14, which appeared to exhibit an accelerated swarming cycle compared to the wild type (Figure 3.10). This was also reflected in the high swarming index recorded by this mutant. Belas *et al.* (1999) also described a *P. mirabilis* transposon mutant with increased swarming ability, which initiated swarming sooner than the wild type and showed an accelerated swarming cycle (Belas *et al.* 1999).

The swarm cycle periodicity in the swarming-deficient mutants that could be assessed (G77, NS77, and PS92), indicated that all were also abnormal in the temporal control of the swarm cycle (Figure 3.11). These strains appeared to be delayed in the onset of migration, and show a greatly reduced migration velocity, which is consistent with the low swarming indices recorded for these mutants.

Therefore, the genes inactivated in these mutants contribute to the temporal control of the swarm cycle, although this may be an indirect effect.

While the periodicity data provides a useful indication of swarm cycle timing in the mutants tested, the differences observed were based on only one aspect of the swarming cycle, migration velocity. Therefore, these differences may be less significant when other variables such as haemolysin, urease, cell elongation, and flagellin production are also measured and incorporated into the analysis. In addition, measurement of other variables associated with swarming may provide a more detailed insight into the role of the genes disrupted in these mutants, and allow the swarm cycles of the non-swarming mutants to be investigated. As such, the genes disrupted in the mutants tested can only be tentatively associated with temporal control of the swarm cycle based on this data.

4.3 Identification of disrupted genes and complementation of swarming-deficient mutants

4.3.1 Identification of disrupted genes

One of the main advantages of transposon based mutagenesis strategies is that this strategy facilitates the identification of disrupted genes. Genes into which the transposon inserts are not only disrupted but also marked by the presence of the transposon. Because of the availability of the DNA sequence of most transposons used for mutagenesis based applications, including mini-Tn*5*Km2, a preliminary identification of the gene disrupted and assignment of a putative function can usually be easily accomplished. The sequence data of *P. mirabilis* chromosomal DNA flanking the transposon inserts in the mutants was used to identify genes homologous to those inactivated. This allowed a putative function to be assigned to disrupted genes, and hypotheses generated about their potential role in swarming and virulence of *P. mirabilis*.

Belas *et al.* (1995) characterised the inactivated genes in *P. mirabilis* transposon mutants defective in swarmer cell differentiation, and reported that the majority showed homology to flagella biosynthesis genes. In this study NS63 was the only swarming-deficient mutant found to be disrupted in a gene associated with flagella biosynthesis (Table 3.7). NS63 was disrupted in a *P. mirabilis flhA* gene, which has been shown to be important for the generation of flagella (Gygi *et al.* 1995a). *P. mirabilis flhA*$^{-}$ mutants were found to exhibit a non-swimming, non-swarming phenotype (Gygi *et al.* 1995a). This was also found to be the case in NS63 which was unable to either swim or swarm.

The FlhA protein is thought to be part of the flagella export apparatus, facilitating the secretion of flagellin subunits for filament assembly (Gygi *et al.* 1995a; Fraser *et al.* 2000), and homologues of *flhA* have been identified in numerous other flagellated bacteria (Gygi *et al.* 1995a). In addition, FlhA has homology to export proteins from other type III secretion systems, which are involved in bacterial interaction with host cells (Ginocchio *et al.* 1995; Collazo *et al.* 1997; Fleiszig *et al.* 2001). In *Pseudomonas aeruginosa, flhA* was found to be homologous to the *Salmonella* type III secretion protein *invA,* which is involved in the invasion of host cells (Collazo *et al.* 1997; Fleiszig *et al.* 2001). Studies of *Ps. aeruginosa flhA*$^{-}$ mutants revealed that this gene was also directly involved in the invasion of corneal epithelial cells by this organism, which was unrelated to the loss of motility (Fleiszig *et al.* 2001). Therefore, FlhA may also be involved in aspects of *P. mirabilis* pathogenicity within the urinary tract.

The control mutant BVJ15, which displayed normal swimming and swarming ability, was also disrupted in a gene associated with flagella formation. The gene disrupted showed good homology to *fliS* from *Salmonella enterica* serovar Typhimurium. In *S. typhimurium* the FliS protein is thought to act as an export chaperone of the flagellin protein (FliC), and prevent polymerisation of individual flagellin subunits in the cell (Auvray *et al.* 2001). Interestingly FliS appears to be dispensable for both swimming and swarming motility in *P. mirabilis*, although further studies are required to confirm *fliS* as the disrupted gene in BVJ15. For example, it is possible that the transposon has inserted at the terminal end of a neighbouring gene upstream and adjacent to *fliS*. Cloning and sequencing of DNA flanking this insert could then yield the sequence data of *fliS*, rather than the disrupted gene.

In *P. mirabilis* flagella genes have also been linked to the overall regulation of the swarm cycle and differentiation (Gygi 1995a; Belas 1996; Fraser *et al.* 2000). Mutants with disruptions in certain genes involved in flagella biosynthesis have been found to exhibit altered swarm cycle periodicity, although this is primarily through perturbations in swarm cell differentiation (Gygi 1995a; Belas 1996; Fraser *et al.* 2000). However, as discussed previously (Section 4.2.3), swarm cycle periodicity could not be investigated in NS63 using the methods employed in this study, but BVJ15 did exhibit some differences in swarm cycle timing that may be the result of *fliS* disruption (See Section 4.2).

Attempts were also made to identify the genes disrupted in other control mutants. DNA flanking the transposon insert in BVJ14 was successfully cloned and sequenced, but efforts to characterise BVJ12 in this way failed. The gene disrupted in BVJ14 was found to be homologous to *cjrC* from *E. coli*, which encodes the outer membrane receptor for colicin Js uptake. Colicins are small antibacterial proteins which have evolved to utilise outer membrane receptor proteins, usually responsible for nutrient uptake, to gain access to the target cell and inhibit growth (Šmajs & Weinstock 2001a,b). The outer membrane protein encoded by *E. coli cjrC* is homologous to a putative siderophore receptor from *Campylobacter jejuni* (Šmajs & Weinstock 2001b). The addition of Fe^{2+} to media has been found to allow *P. mirabilis* to over come the inhibitory effects of EDTA and initiate swarming (Jin & Murray 1988). The mutation in BVJ14 may therefore affect this aspect of *P. mirabilis* swarm cycle regulation and result in an accelerated swarm cycle.

Belas *et al.* (1998), also described a *P. mirabilis* mutant with increased swarming ability. This "precocious" swarming mutant was disrupted in RsbA an outer membrane protein homologous to membrane sensor histidine kinases. It was suggested that this protein is responsible for sensing external signals and triggering swarming behaviour. However, in this mutant the increased swarming ability was found to be solely due to an acceleration in swarm cycle timing, and the migration velocity was the same as the wild type. In contrast, BVJ14 does show a greater migration velocity as well as a more rapid progression through the swarming cycle, than the wild type strain B4 (Figure 3.10). The function of the inactivated protein in BVJ14 in the regulation of the *P. mirabilis* swarm cycle is unclear, but it seems likely to be an outer membrane receptor protein, and may therefore be involved in sensing external environmental signals. Interestingly, the precocious swarming phenotype of the mutant isolated by Belas *et al.* (1998), was thought to be due to a truncation of RsbA rather than a complete lack of functional protein. A similar scenario may also account for the increased swarming in BVJ14, but it appears that the disrupted gene in this mutant influences migration velocity as well as swarm cycle timing.

Analysis of the genes disrupted in swarming-deficient mutants, in which swarm cycle periodicity was investigated (NS77, G77, PS92), provided no obvious insights as to the mechanisms which had been disrupted (Table 3.7). Also no obvious function of these genes in swimming or swarming could be identified, based solely on the sequence data and the function of homologous genes. Attempts to identify the disrupted gene in PS92 were unsuccessful, while NS77 was found to be defective in a gene homologous to a hypothetical protein, or putative virulence factor of unknown function from *E. coli*. The disrupted gene in G77 showed no homology to any other

genes suggesting that this may be a novel gene involved in the regulation of swarming in *P. mirabilis*. Therefore, further characterisation of these mutants (G77 and NS77) may provide insight into virulence factors of both *E. coli* and *P. mirabilis*, and provide a greater understanding of the *P. mirabilis* swarming cycle.

Another potentially novel swarming associated gene was also identified in the poor-swarming mutant G78. The gene disrupted was homologous to *ansA* from *E. coli*, which encodes a cytoplasmic asparaginase enzyme. Although the association between this gene and swarming in *P. mirabilis* was initially unclear, further phenotypic analysis of this mutant, discussed in subsequent sections, highlighted a potential role for this gene in a novel aspect of the *P. mirabilis* swarming cycle (Section 4.4).

The disrupted genes in mutants G64, G37, and G93 were in keeping with the swarming-deficient phenotype of these mutants. In G64 the transposon had inserted into a region with homology to a *Salmonella enterica* serovar Typhimurium gene encoding a polysaccharide transport protein. The polysaccharide matrix through which *P. mirabilis* swarms acts as a surfactant, and lubricates the passage of migrating swarmer cells (Gygi *et al.* 1995b). Other swarming species have also been shown to produce a biosurfactant which facilitates swarming (Fraser *et al.* 2000). The best characterised of these are the serrawettin surfactants produced by *Serratia marcesens*, and *Serratia liquefaciens* during swarming (Matsuyama *et al.* 1992; Eberl *et al.* 1999). *P. mirabilis* mutants unable to synthesise a polysaccharide matrix have been found to exhibit a frequently consolidating phenotype, and subsequently reduced migration (Gygi *et al.* 1995b). Therefore, the transposon insertion in G64

may block, or hinder production of this polysaccharide matrix and result in the poor-swarming phenotype of this mutant.

This theory may also be extended to the non-swarming mutant G37. In this mutant the transposon was found to be inserted into a gene with homology to *wbdN* from *E. coli*, which encodes a putative glycosyl transferase enzyme. Glycosyl transferase enzymes have also been implicated in the formation of the bacterial polysaccharide capsule (Edwards *et al.* 1994; Annunziato *et al.* 1995), although the reduction in swimming ability exhibited by both G64 and G37 is not explained by a defect in capsule production. However, subsequent experiments suggested that in G37, a deficiency in capsule assembly is not the primary cause of the non-swarming phenotype, which will be discussed in subsequent sections (see Section 4.4).

An alternate possibility is that in G64 the mutation leads to abnormalities in lipopolysaccharide (LPS) production. LPS production appears to be important for swarming, and mutants of *Salmonella* and *P. mirabilis* deficient in swarming have been show to be defective in LPS production (Belas *et al.* 1995; Mireles II *et al.* 2001). Disruption of LPS structure may also have other effects, and in *E. coli* K12 has been shown to result in a non-motile phenotype (Parker *et al.* 1992). Therefore, such defects may account for both the swarming-deficient phenotype, and the reduced swimming ability of this mutant.

In G93 the disrupted gene was found to be homologous to a *Salmonella* gene *surA*, which encodes a periplasmic peptidyl-prolyl-*cis-trans*-isomerase enzyme (PPIase). The *surA* PPIase is responsible for facilitating folding of outer membrane proteins into functional conformations (Lazar & Kolter 1996). SurA homologues in *E. coli*

have been associated with long-term survival, and tolerance of high pH (Lazar *et al.* 1998). This may be particularly significant for *P. mirabilis,* which generates a highly alkaline environment during urinary tract infection and can persist for long periods of time in the bladders of infected patients (Kunin 1987; Stickler 1996a).

It has also been suggested that SurA is required for assembly of cell wall synthesizing apparatus in *E. coli* (Lazar *et al.* 1998). This raises the possibility that the non-swarming phenotype observed in G93 is due to a deficiency in cell wall synthesis, resulting in perturbations in cellular elongation and swarmer cell differentiation. However, in *E. coli* SurA has been shown to be a part of a set of parallel pathways of protein folding which show functional redundancy (Rizzitello *et al.* 2001). Due to this, it is possible that some consequences of SurA inactivation would be masked by other periplasmic PPIases which could perform the same functions.

Despite the functional redundancy displayed by these proteins in the *E. coli* periplasm, SurA has been shown to be important in virulence of *Salmonella* (Sydenham *et al.* 2000). While this mutant showed no reduction in stationary phase survival or tolerance to elevated pH, this mutant was attenuated in its ability to adhere to and invade eukaryotic cells, and infect mice (Sydenham *et al.* 2000). In *P. mirabilis* SurA appears to play an important role in swarming, and may possibly be required to fold outer membrane proteins required for swarmer cell development or multicellular raft formation, into functional conformations. Possible roles of SurA in swarming and virulence of *P. mirabilis* will be further explored in subsequent sections.

4.3.2 Complementation of swarming-deficient mutants

The sequence data of the DNA flanking the transposon inserts was also used to undertake complementation studies, in order to directly relate a disrupted gene to the phenotype of a specific mutant. Probably the major concern addressed by complementation studies is that the mutant phenotype is not generated by inactivation of the gene into which the transposon has inserted, but rather from suppression of distal genes though polar effects of the transposon (de Lorenzo *et al.*1990; Hensel & Holden 1996; de Lorenzo *et al.* 1998). This may also be the case for any of the mutants, but many show transposon inserts in genes that can be related to some aspect of the swarming cycle. However, further phenotypic and genetic analysis was required to directly relate the disruption of these genes with the phenotypes of the swarming-deficient mutants. Such experiments were necessary as simply identifying the gene into which the transposon had inserted is not sufficient to establish unambiguously a role for that gene in swarming.

In this study, three of the swarming-deficient-mutants were successfully complemented (NS63, G64, and G78), by providing intact copies of disrupted genes *in trans* on vector pB4. To accomplish this it was first necessary to generate a cosmid library of genomic DNA from *P. mirabilis* B4. Although the availability of the *P. mirabilis* genome sequence would eliminate the need for this in future studies. The cosmid library was then screened to identify clones which possessed intact copies of the disrupted genes which could then be sub-cloned and introduced to the appropriate mutant. The generation of this library was relatively straightforward, and was utilised for both complementation strategies employed in this study. In addition, the library may also be a useful resource in future studies of *P. mirabilis* pathogenicity.

G64 was complemented using a conventional strategy (Section 2.9.6), but this proved unsuitable for other mutants. Instead the random fractionation method using *Sau* 3A (Section 2.9.7) was devised and used to complement G78 and NS63. The results of these experiments indicated that the genes disrupted in NS63, G64, and G78 were responsible for the observed deficiencies in both swimming and swarming shown by these mutants (Table 3.10).

Of the complemented mutants (NS63comp, G64comp, and G78comp) only G64comp exhibited a complete restoration of swarming to wild type levels, and none showed wild type swimming ability. In addition, normal swarm cycle periodicity was not restored (Figure 3.19). In NS63comp, and G78comp, swarming was initiated later than in the wild type, but migration appeared to occur for a similar duration as in the wild type. The swarm cycle in G64comp appears to be accelerated and shows an increased migration velocity with each successive period of migration (Figure 3.19).

These results may reflect the complexity of the swarming processes, the regulation of which presumably requires tight control over its components. While the complementation of these mutants generates some restoration in function, the original regulatory balance is not restored and overall the process is still attenuated. For example, provision of the intact genes *in trans* on plasmid vectors results in the presence of multiple copies of these genes within the cell. This may result in the over expression of the inactivated protein, or sequestration of regulatory proteins required to control the transcription of other genes related to, and required for swarming. Thus the complementation strategy itself may disrupt the complex regulatory network of

the attribute under investigation, inhibiting full restoration of swarming in these mutants.

In G64comp, a possible explanation for the abnormal swarm cycle periodicity could be that the function of the deactivated gene has not been fully restored. The increases in migration velocity may be the result of an accumulation of the final product of the disrupted pathway. For example, if G64 is indeed defective in the assembly of the polysaccharide matrix, then a partial restoration of the disrupted pathway could account for the successive increases in migration velocity. As the lubricating polysaccharide matrix accumulates through successive cycle of swarming, so the ability of swarmer cells to overcome surface friction is also increased with each period of migration, resulting in corresponding increases in migration velocity. Although this hypothesis does not explain the acceleration in the timing of the swarm cycle.

In addition, the DNA fragments which complement these mutants have not yet been sequenced. As such it is possible that they restore swarming not through expression of the disrupted gene, but by expression of an uncharacterised locus close to the transposon insert (that may be suppressed by polar effects of the transposon insert). Alternatively the restoration in swarming may be from other swarming associated genes encoded by the complementing fragments, which are not disrupted by the original transposon insert, but compensate for the original mutation when over expressed. These considerations are particularly relevant to the mutants complemented using the *Sau* 3A approach, as identification of these fragments was based on their ability to restore swarming rather than the sequence of DNA flanking

the original insert. However, they were derived from cosmid clones positive for the presence of DNA sequences flanking the transposon inserts (Table 3.8, Figure 3.13).

There is strong evidence that the fragments do encode the genes inactivated in the mutants. For G64 the complementing fragment was identified using a probe homologous to the DNA sequence flanking the transposon insert, and this fragment was cloned directly into pB4. For G78, PCR with primers specific to the DNA sequence flanking the transposon insert generated a positive result when performed on pB4ANSA2 purified from G78comp (plasmid pB4 containing the DNA fragment which complements G78). This was also found to be the case when identical experiments were performed on pB4PST3 (plasmid pB4 containing the DNA fragment which complements G64). In the case of NS63, PCR assays could not confirm the presence of transposon flanking DNA in the complementing DNA fragment. However, the pB4FlhA3 plasmid (plasmid pB4 containing the DNA fragment which complements NS63) was successfully used to restore swarming in the U6450 *flhA*$^{-}$ mutant (Gygi *et al.* 1995a).

4.4 Characterisation of swarming-deficient mutants by electron microscopy

4.4.1 Demonstration of flagella production in swarming-deficient mutants

Many studies have utilised electron microscopy to study bacterial morphology, and surface associated structures, including the polysaccharide capsule, pilli, fimbriae, and flagella (Bahrani *et al.* 1991; Kanto *et al.*1991; Gygi *et al.* 1995a,b; Hay *et al.* 1999; Déziel *et al.* 2001). Both transmission and scanning electron microscopy have been used to study swimmer and swarmer cells of *P. mirabilis* (Bahrani *et al.* 1991; Allison *et al.* 1993; Gygi *et al.* 1995a,b; Hay *et al.* 1997; Hay *et al.* 1999). These techniques were also employed to investigate the swarming-deficient mutants generated during this study.

The application of transmission electron microscopy (TEM) allowed visualisation of the flagella filaments produced by swimmer cells of the wild type and mutants. It has been suggested that the flagella themselves may contribute significantly to the pathogenicity of *P. mirabilis* (Mobley 1996), and flagella synthesis and swimming motility have been identified as important processes in the formation of *Ps. aeruginosa*, and *Eschericia coli* biofilms (O'Toole & Kolter 1998a; Pratt & Kolter 1998).

The wild type *P. mirabilis* strain U6450, and a *flhA*$^{-}$ mutant of U6450, which had previously been described by as unable to generate flagella filaments (Gygi *et al.* 1995a), were included in this study as controls. Analysis of U6450, and U6450 *flhA*$^{-}$ confirmed that the negative staining procedure used in this study was capable of distinguishing flagella filaments during observation by TEM (Figure 3.20). This was

in agreement with other investigators who have used similar staining procedures to observe flagella filaments by TEM (Yokoseki *et al.* 1995; Deakin *et al.* 1999; Li *et al.* 2001; Kirov *et al.* 2002). Because flagella production by U6450 and the U6450 *flhA*⁻ mutant had already been characterised by TEM, observations of these strains also provided a reference for observations of the wild type and transposon mutants of strain B4.

Micrographs of the control mutants BVJ12, BVJ14, and BVJ15 (Figure 3.20) showed that flagella production was normal in these mutants, and that the presence of the mini-Tn*5*Km2 transposon in these strains did not affect flagella production. The normal flagella production of BVJ15 was of particular interest, although not unexpected as this mutant displayed normal swimming ability.

As discussed previously, BVJ15 contains a transposon insert in a gene homologous to *fliS* from *Salmonella* encoding an export chaperone for the flagellin subunit protein (Yokoseki *et al.* 1995; Auvery *et al.* 2001). Homologues of *fliS* have also been identified in *E. coli* and *Bacillus subtilis* (Kawagishi *et al.* 1992; Chen & Helman 1994). In *E. coli*, FliS has been found to be necessary for production of flagella, and *fliS*⁻ mutants are non-motile (Kawagishi *et al.* 1992) Conversely this gene has been found to be dispensable for flagella production in *Salmonella,* but *fliS* mutants generate short flagella filaments at a lower frequency than the wild type, and are deficient in swimming ability (Yokoseki *et al.* 1995).

TEM observations of the swarming-deficient mutants revealed that all were reduced in flagella production. Several mutants exhibited specific defects, but all swarming-deficient mutants generated fewer flagella than the wild type (Figure 3.21). Belas *et*

al. (1991b) also observed a general reduction in flagella production by swarming-deficient *P. mirabilis* transposon mutants. These observations may highlight the close association between genes involved in flagella production and the *P. mirabilis* swarm cycle, which has been indicated by other studies (Belas *et al.* 1991b; Belas *et al.* 1995; Gygi *et al.* 1995a; Fraser *et al.* 2000). Alternatively, these observations may reflect biases in the screens used to isolate swarming-deficient mutants.

The fact that the swarming-deficient mutants generated fewer flagella may also contribute to the general reduction in the swimming ability of these strains. Gygi *et al.* (1997), described a non-swarming mutant unable to produce FlgN, a putative facilitator of flagella filament assembly. This mutant produced fewer filaments than the wild type, and swimming was reduced to ~ 50% of wild type ability. It also seems probable that the altered flagella produced by G78 (altered flagella shape), G64 (decreased length of flagella), and G37 (flagella filaments dissociated from cell) account for the poor swimming ability of these mutants (Figure 3.21).

TEM observations also provide some insight into possible functions of the disrupted genes in the swarming-deficient mutants. The putative function of the disrupted gene in non-swimming, non-swarming mutant NS63 was confirmed by TEM observation of both complemented and uncomplemented NS63. The gene disrupted in this mutant was homologous to a *P. mirabilis* flagella biosynthesis gene *flhA*, and flagella were not produced by this mutant (Figure 3.21). This was not surprising considering the non-motile phenotype of NS63, which was similar to that of the U6450 *flhA*$^-$ mutant characterised by Gygi *et al.* (1995). Restoration of flagella production was seen in the complemented NS63 mutant (NS63comp) although remained below wild type levels (Figure 3.22). While it is unlikely that all the disrupted genes identified

have such a direct role in flagella production, TEM observations do indicate potential roles for some genes in aspects of flagella assembly, in particular those mutants exhibiting specific defects in flagella (G37, G64, G78).

The dissociation of the flagella filaments from the cell exhibited by G37 suggests that the gene disrupted in this mutant plays a role in producing functional flagella. As discussed in previous sections, the gene disrupted in G37 is homologous to *wbdN* form *E. coli* which encodes a putative glycosyl transferase enzyme. The flagella filaments of several bacteria have been found to be glycosylated, including *Helicobacter pylori*, *Ps. aeruginosa*, and *Campylobacter jejuni* (Doig *et al.*1996; Brimer & Montie 1998; Arora *et al.* 2001; Josenhans *et al.* 2002). If the gene disrupted in G37 does encode a glycosyl transferase enzyme, then the flagellin protein itself, or proteins which compose the flagella hook and basal body may be glycosylated by this enzyme.

The different regions of the bacterial flagellum are assembled in a sequential manner (Macnab 1992; Aldridge & Hughes 2002). Initially the basal body and hook complex is generated, then monomeric flagellin subunits pass through the central channel of the growing structure, and are incorporated at the distal end (Macnab 1992; Aldridge & Hughes 2002). In *H. pylori* inactivation of the *flmD* gene, which encodes a glycosyl transferase blocks filament assembly, and generates a non-motile phenotype, but basal-body and hook complexes are still formed (Josenhans *et al.* 2002). This led to the suggestion that glycosylation of the flagellin sub-units stabilises the protein, and influences interactions between individual flagellin sub-units, or with specific export and chaperone proteins, and is therefore required for filament assembly in *H. pylori* (Josenhans *et al.* 2002). However, as G37 generated

flagella filaments of apparently normal length, it seems likely that this mutant is not defective in the assembly of flagella filaments. Therefore, the protein encoded by the gene disrupted in G37 may be involved in interaction of the assembled flagella filament with the flagella basal body, possibly providing sufficient strength or flexibility to allow the structure to withstand the shear forces generated during flagella rotation and swimming.

Glycosylation of the flagellin filament may also be a protective mechanism, and may be a way of preventing damage caused by environmental factors such as high pH, possibly by serving to help maintain flagella shape. Alternatively glycosylation may render the flagella filament immune to degradation from proteolytic enzymes, possibly generated by other bacteria. In addition, flagella filaments are highly antigenic (Fraser *et al.* 2000), and glycosylation may also play a role in antigenic variation of this structure, potentially helping *P. mirabilis* evade the host immune response during urinary tract infection. A similar role has been suggested for flagella glycosylation in *C. jejuni* (Doig *et al.* 1996).

P. mirabilis has already been shown to vary the antigenic signature of its flagella filaments at the amino acid sequence level. Murphy *et al.* (1999) investigated a non-motile strain of *P. mirabilis* in which the flagellin gene *flaA* had been disrupted. As expected this mutant was unable to generate flagella, but at a low frequency, motile, flagella producing revertants were observed. These revertants were found to be the result of genomic rearrangements resulting in a fusion of the *flaA* gene with the normally silent, adjacent flagellin gene *flaB*. The flagellin produced by these revertants was antigenically and biochemically distinct from wild type flagellin.

In G78 and G64 evidence that the disrupted genes play a role in flagella assembly is strengthened by TEM observations of the complimented counterparts (G64comp, G78 comp) of these mutants (Figure 3.22). When DNA fragments (confirmed by PCR to encode sequences flanking the transposon inserts in these mutants) were introduced into the respective mutant, defects in flagella production were relieved, but the number of flagella produced remained below wild type levels.

For G78, the abnormal shape of the flagella filaments suggests that the protein encoded by the disrupted gene could be involved in generating flagella filaments of normal shape. In G78 the flagella filaments appear to be excessively curved. Those produced by G78comp have a morphology closer to that of the wild type filaments, but appear to be straighter with a longer wavelength. If the mutated gene in G78 performs a function involved with flagella shape, then the straighter shape of filaments in G78comp could be the result of over expression of the disrupted gene. Kanto *et al.* (1991) reported that *Salmonella typhimurium* mutants that produced flagella of abnormal shape were unable to swim normally. However, the altered flagella shapes of these mutants were due to mutations in the flagellin gene *fliC*, which altered the amino acid composition of the flagellin protein resulting in the abnormal shape (Kanto *et al.* 1991).

Amino acids responsible for flagella shape in *S. typhimurium* have been reported to be distributed at the terminal ends of the flagellin protein, and single amino acids substitutions are sufficient to drastically alter the shape of flagella filaments (Kanto *et al.* 1991). In *P. mirabilis* genomic rearrangements that fuse the *flaA* flagellin gene with the adjacent *flaB* flagellin gene results in a filament with altered wavelength (Morano, personal communication 2003). Production of these hybrid flagella has

been found to occur more frequently in response to certain environmental conditions, including high pH, and it has been postulated that the hybrid flagella is a more efficient propeller (Morano, personal communication 2003). If true, this has clear implications for pathogenesis of *P. mirabilis* urinary tract infection, and raises the question of bacteria possessing mechanisms to actively modify or maintain flagella shape, perhaps in response to environmental signals. In the case of bacterial pathogens such signals could reflect the environment encountered in the host.

In the case of G78, it is difficult to envisage how a protein homologous to an asparaginase enzyme could mediate a process influencing flagella shape. The altered flagella shape of G78 may be an indirect consequence of disruption of the AnsA homologue, but it is also possible that this gene plays a direct role in flagella morphology and it is conceivable that this gene is in some way involved in modification of the flagellin sub unit protein. However, the homology of the disrupted gene in G78 to *ansA* from *E. coli* is based on only a partial gene sequence. A more complete sequence analysis will hopefully provide more insight into the precise function of this protein and its role in flagella assembly.

The abnormal flagella generated by G64 swimmer cells is also difficult to relate to the genotype of this mutant, although is concordant with its greatly reduced swimming ability. A non-swarming mutant of *P. mirabilis,* with a transposon insert in a putative sugar transport protein was also described by Gygi *et al.* (1995b), but this mutant exhibited no reduction in swimming ability. In addition, G64comp generates flagella filaments of normal length and at a higher frequency than G64, clearly demonstrating a role for the disrupted gene in flagella assembly. Despite such evidence that this gene is necessary for efficient flagella production, SEM

observations of G64 swarmer cells show this mutant is able to generate apparently normal flagella on hyper-flagellated swarmer cells (Figure 3.25).

It is possible that the protein encoded by the gene mutated in G64 may perform a regulatory function that accounts for the abnormal flagella production in G64 swimmer cells. Up-regulation of flagella production during differentiation could compensate for the absence of this protein, resulting in normal flagella being produced by differentiated swarmer cells, but abnormal flagella production by swimmer cells.

Another possible explanation is that the protein encoded by the mutated gene in G64 is involved in lipopolysaccharide (LPS) synthesis, as some sugar transferases also play a role in LPS core modification (Gygi *et al.* 1995b). This explanation is also relevant to the defective disrupted gene in G37, as glycosyl transferase enzymes also play a role in LPS synthesis (Tomb *et al.* 1997; Benz & Schmidt 2002). Some defects in LPS synthesis in *E. coli* K-12 have been reported to generate a highly pleiotrophic phenotype, and impact on several aspects of bacterial physiology (Parker *et al.* 1992). Some mutations affecting LPS synthesis have also been linked with defects in motility of *P. mirabilis, S. typhimurium*, and *E. coli* (Parker *et al.* 1992; Belas 1996; Mireles *et al.* 2001). A subset of *P. mirabilis* mutants defective in swarming were found to be disrupted in genes associated with LPS production (Belas *et al.* 1995). In *E. coli* the deletion of genes involved in LPS core synthesis lead to an inability to generate flagella, and a non-motile phenotype (Parker *et al.* 1992). It has been suggested that in *P. mirabilis* swarmer cells, long-side-chain LPS is redistributed and concentrated at the bases of flagella (Armitage *et al.* 1979; Armitage 1982). This has been proposed to stabilise the outer membrane and prevent damage due to forces

created by flagella rotation (Armitage *et al.* 1979; Armitage 1982). Therefore, a defect in the production of long-side-chain LPS or its redistribution may account for the abnormal flagella production in G37 and G64. However, the fact that G64 is able to differentiate normally, and produce hyper-flagellated swarmer cells suggests this is not the case in this mutant.

4.4.2 *In situ* analysis of swarm fronts

Flagella are also key structures in *P. mirabilis* swarming (Gygi *et al.* 1995a, Belas 1996, Gygi *et al.* 1997, Dufour *et al.* 1998). *P. mirabilis* mutants unable to synthesise flagella were found not only to be non-motile, but were unable to differentiate into elongated swarmer cells (Belas *et al.* 1991b, Gygi *et al.* 1995a, Belas 1996). In addition, *P. mirabilis* mutants unable to produce flagella were attenuated in virulence in murine models of urinary tract infection (Allison *et al.* 1994, Mobley 1996).

The application of a novel vapour fixation protocol for specimen preparation, allowed the swarming-deficient mutants to be examined *in situ* on LB agar by SEM. These experiments allowed the cellular arrangements of these mutants to be studied, as well as their ability to generate elongated, hyper-flagellated swarm cells. The SEM observations of mutants *in situ* on LB agar also allowed the function of disrupted genes in swarming to be assessed. The control mutants BVJ12, BVJ14, and BVJ15 showed no defects in differentiation or cellular organisation compared to the wild type B4 (Figure 3.24 and 3.25). This indicates that the presence of the mini-Tn*5*Km2 transposon in these mutants also has no effect on this aspect of *P. mirabilis* swarming.

With the exception of NS63, non-swarming mutants were unable to differentiate (Figure 3.26, and 3.27). Fraser *et al.* (2000) suggested that a threshold number of flagella are required before differentiation and swarming of *P. mirabilis* can occur. SEM observations of the non-swarming mutants G33, G37, and G93 showed that these mutants are unable to differentiate normally (Figure 3.26), and a decrease in flagella production was revealed by TEM observations. The poor-swarming mutants however, also showed low levels of flagella production compared to the wild type, but were still able to differentiate and swarm (Figure 3.25). The lack of differentiation in non-swarming mutants is most likely due to disruption of specific processes which impact on their ability to transform into swarmer cells.

The inability of G37 to differentiate (Figure 3.26) may be related to the dissociation of flagella filaments from the cell observed to occur in this mutant (Figure 3.21). This defect in flagella production may impede the ability of G37 to sense contact with a solid surface, and initiate differentiation. The non-differentiating phenotype also fits with a possible defect in LPS synthesis in G37, discussed above. Defects in LPS could prevent cellular elongation (Belas *et al.* 1995), or contribute to dissociation of flagella if the proposed stabilising effect of long-side-chain LPS was inhibited (Armitage 1982; Armitage *et al.* 1979). The failure of G93 to differentiate supports the hypothesis that SurA is involved in the elongation of *P. mirabilis* during swarmer cell development, and the suggestion that this enzyme is required for assembly of cell wall synthesis apparatus (Lazar *et al.* 1998).

Interestingly, SEM observations of NS63, *in situ* on agar, revealed that this mutant had retained the ability to generate elongated cells, despite being unable to generate flagella (Figure 3.27). In contrast the *P. mirabilis flhA* mutant described by Gygi *et*

al. (1995a) was unable to generate elongated cells. This was also confirmed during this study by SEM observations of U6450 *flhA*$^-$, vapour fixed *in situ* on agar, after the same period of incubation as NS63 (Figure 3.27). While these differences in phenotype may be due to differences in the genetic backgrounds of each mutant (i.e. genetic variation between *P. mirabilis* strain B4 and U6450), a possible explanation for these contrasting phenotypes may lie in the site at which the transposon insertion occurred in each mutant.

Gygi *et al.* (1995a) reported that *P. mirabilis flhA* was a 2091bp gene, and that U6450 *flhA*$^-$ harboured a transposon insert between nucleotides 67 and 68. In NS63, comparison of the DNA sequence flanking the mini-Tn*5*Km2 insert, showed that in this mutant the transposon had inserted towards the distal end of the gene between nucleotides 1830 and 1831. Therefore, the majority of the gene is transcribed, and presumably results in the production of a truncated but largely intact FlhA protein in NS63. Apart from its role in flagellin export, this raises the possibility that FlhA is also required for cell elongation, either directly or indirectly, and that this function is preserved by the presence of a truncated FlhA in NS63. The transposon insert in NS63 could allow transcription of 610 of the 697 codons in the *flhA* gene. In comparison, the location of the transposon insert in U6450 *flhA*$^-$ would result in transcription of only the first 22 codons of *flhA*, which may be the cause of both the lack of flagella production, and cell elongation in this mutant. This model is illustrated in Figure 4.2.

Figure 4.2: Role of *flhA* in *P. mirabilis* flagella production and swarmer cell elongation.

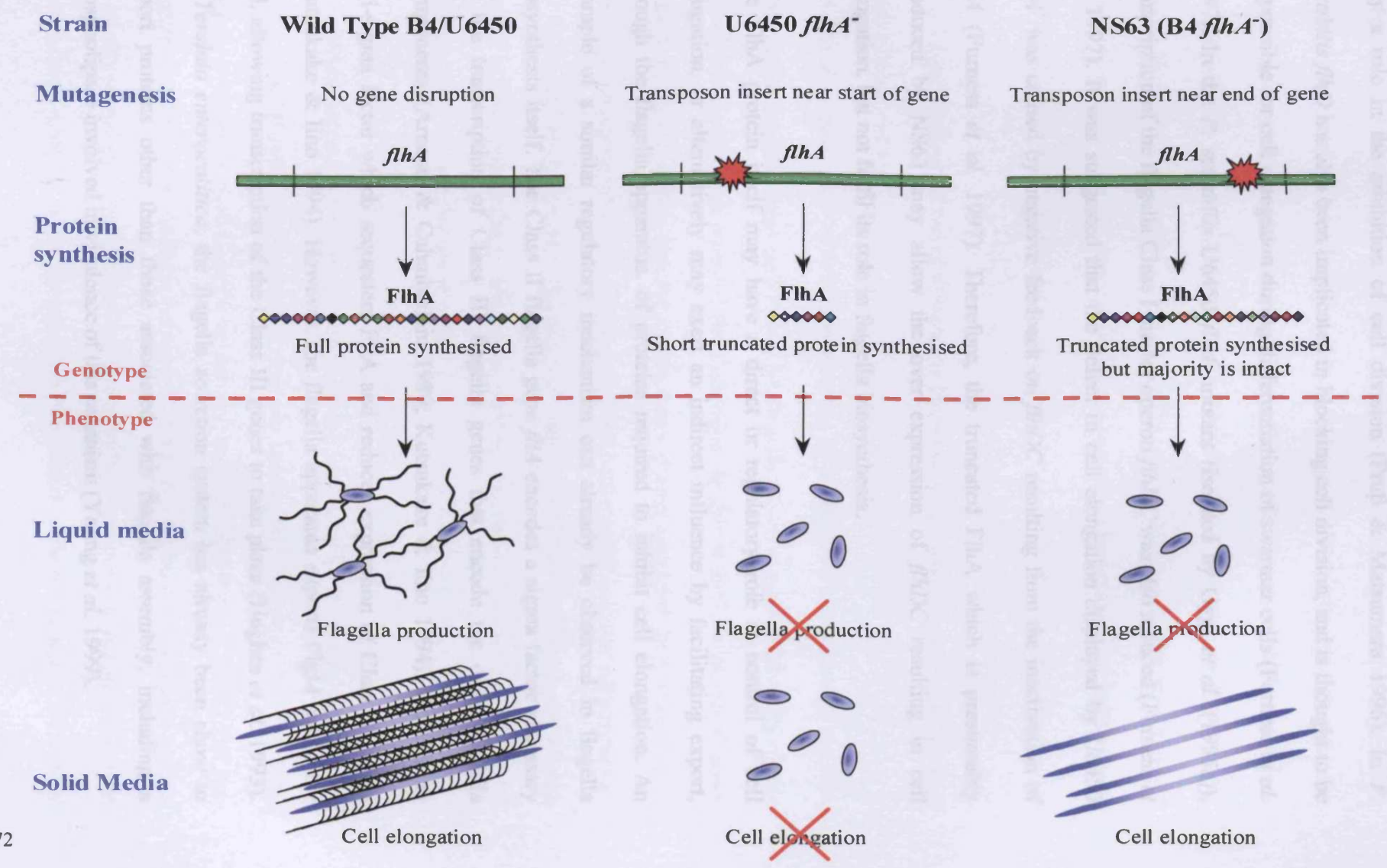

In *E. coli,* a component of the flagella Class I master operon, *flhD*, has been shown to play a role in the inhibition of cell division (Pruβ & Matsumara 1996). In *P. mirabilis flhD* has also been implicated in blocking cell division, and is thought to be responsible for cell elongation during differentiation of swarmer cells (Furness *et al.* 1997). In the *P. mirabilis* U6450 *flhA*$^-$ mutant (isolated by Gygi *et al.* (1995a)), transcription of the flagella Class I master operon *flhDC* was also reduced (Furness *et al.* 1997). It was suggested that the defect in cell elongation displayed by U6450 *flhA*$^-$ was caused by negative feedback on *flhDC* resulting from the inactivation of *flhA* (Furness *et al.* 1997). Therefore, the truncated FlhA which is presumably produced by NS63 may allow the over expression of *flhDC* resulting in cell elongation, but not fulfil its role in flagella biosynthesis.

The FlhA protein itself may have a direct or regulatory role in control of cell elongation, or alternatively may exert an indirect influence by facilitating export, through the flagella apparatus, of proteins required to inhibit cell elongation. An example of a similar regulatory mechanism can already be observed in flagella biosynthesis itself. The Class II flagella gene *fliA* encodes a sigma factor necessary for the transcription of Class III flagella genes that encode the distal flagella components (Arnosti & Cahmberlain 1989; Kutsukake & Iino 1994). FlgM is an anti-sigma factor which sequesters FliA and reduces expression of Class III genes (Kutsukake & Iino 1994). However, the flagella apparatus exports FlgM out of the cell, allowing transcription of the Class III genes to take place (Hughes *et al.* 1993). In *Yersinia enterocolitica*, the flagella secretion system has already been show to export proteins other than those associated with flagella assembly, including a phospholipase involved in virulence of this organism (Young *et al.* 1999).

Restoration of the *flhA* gene, *in trans*, restored normal elongation, flagella production, and swarming in U6450 (Gygi *et al.* 1995a). Complementation of NS63 also restored flagella production and swarming in this mutant, although the complementing fragment has not been confirmed as *flhA*. However, as discussed in a previous section (Section 2.3.2), the same fragment was also able to complement U6450 *flhA*$^{-}$. A more in depth characterisation of the disrupted locus in this novel class of mutant (NS63) may provide a greater understanding of swarm cell differentiation in *P. mirabilis*.

4.4.3 Identification of novel structures involved in formation and migration of mutlicellular rafts.

The role of flagella in *P. mirabilis* swarm cell differentiation has been well studied. In contrast the mechanisms underlying the flagella driven migration of multicellular rafts of swarm cells has received little attention. In this study, the vapour fixation method, and SEM used to observe swarm fronts during migration on 1.5% LB agar, permitted the resolution of novel structures involved in multicellular raft formation, and migration of *P. mirabilis* (Figure 3.23 and Table 3.11). These structures were termed helical connections, and were formed by the interweaving of flagella filaments from adjacent swarmer cells.

To our knowledge, this is the first report of this aspect of the *P. mirabilis* swarming cycle. Lateral flagella of swarming *Aeromonas* species have also been found to form linkages between individual cells on an agar surface (Kirov *et al.* 2002), but the formation of helical connections between *P. mirabilis* swarmer cells appears to be a far more ordered process. TEM observations of thin sections cut through wild type swarm fronts (Figure 3.29), along with the highly ordered structure of helical

connections observed by SEM (Figure 3.23), suggests a process of active organisation, where flagella filaments are arranged into these specific formations. In addition, observations of the wild type strain U6450 indicate that this is not a strain specific phenomenon, unique to B4 (Figure 3.23).

The function of helical connections in swarming may be diverse. The formation of helical connections may contribute to stability of multicellular rafts. The poor-swarming mutant PS92 possesses the ability to form helical connections, but does not generate them uniformly throughout the swarm front. PS92 rafts appear to lack cohesion, and cellular organisation is not maintained (Figure 3.25). Studies of the multicellular behaviour of *Salmonella typhimurium*, indicate that flagella play a similar role in pellicle formation by this organism, holding clumps of cells together (Römling & Rohde 1999).

Communication between swarmer cells may also be facilitated by formation of helical connections. These structures could hold swarmer cells at the optimum distance for, or play a more direct role in inter-cellular communication. Linking of flagella filaments through the formation of helical connections could form a network of tactile sensors, and may allow cells to co-ordinate certain aspects of the swarming cycle, such as migration velocity, and direction.

The organisation of flagella filaments into these structures appears to play an important role in the migration of multi-cellular rafts. Macnab (1992) estimated that in *E. coli* synthesis and operation of the 2-10 flagella used for swimming may require up to 2% of the cells energy resources. For the hyper-flagellated swarmer cell this is clearly a much larger commitment and therefore, it would be highly beneficial to

ensure that all filaments are oriented to provide optimal propulsion. Formation of helical connections could serve to co-ordinate flagella rotation in order to generate sufficient force for propulsion of multi-cellular rafts. SEM observations of the swarming deficient mutants showed that all poor-swarming mutants, with the exception of G64, exhibited defects in the production of helical connections (Figure 3.25), and these structures were not found in non-swarming mutants (Figure 3.26). The co-ordination of flagella would be particularly important for movement over surfaces exigent to migration, including some catheter biomaterials such as silicone.

Further evidence for a role of helical connections in multicellular raft migration come from the non-swarming, non-swimming mutant NS63, and the poor-swarming mutant G78, both of which recorded a swarming index of 0 (Table 3.5). No helical connections were generated by NS63, while G78 appeared to exhibit some flagella interweaving but produced helical connections with an abnormal morphology (Figure 3.25). The abnormal helical connections generated by G78 are presumably another aspect of the misshapen flagella filaments generated by this mutant, which inhibits the organisation of filaments. SEM observations of swarm fronts of complemented NS63 and G78, revealed formation of helical connections had been restored along with migration over LB agar (Figure 3.28). In NS63comp helical connections were evident, although were not as well developed as those formed by the wild type, nor were they as frequently observed. The helical connections generated by G78comp were indistinguishable from those of the wild type. However, swarming was not fully restored in these mutants. This could indicate that the formation of helical connections was not the only swarming related factor disrupted in these mutants, or that over expression of the restored genes (due to increased copy number) may have contributed to only partial restoration of swarming. It is most likely that the partial

restoration of swarming is due to aspects of the complementation approach, discussed in Section 4.2.

The normal helical connections generated by G64 would seem to question the role of helical connections in migration of multicellular rafts. However, the possibility that this mutant is defective in assembly of the exopolysaccharide matrix through which *P. mirabilis* swarms (Gygi *et al.* 1995b), would fit with the observed phenotype. In this scenario, G64 would be expected to exhibit normal differentiation and cellular organisation, including formation of helical connections, but the lack of migration in this mutant would be due to its inability to overcome surface friction. This hypothesis is strengthened by SEM observations of complemented G64 swarm fronts. G64comp was fully restored in its ability to migrate over LB agar, and showed no differences in production of helical connections when compared to either uncomplemented G64, or the wild type strain (Figure 3.28).

As with the TEM observations of flagella production, the fact that all but one of the swarming-deficient mutants display disruptions in formation of these structures, may initially be considered unusual. However, for many mutants the disruption of helical connections is likely to be an indirect consequence of the mutant phenotype, rather than a direct association between the inactivated gene and this process. This is almost certainly true for the non-swarming mutants which either do not generate flagella (NS63, Figure 3.27), or are defective in differentiation (Figure 3.26). For other mutants, such as G78 the disrupted gene appears to be closely associated with flagella production and formation of these structures.

In conclusion, the vapour fixation technique has revealed that rafts of *P. mirabilis* swarmer cells are held together by large numbers of flagella filaments, interwoven in phase, to form helical connections between adjacent swarmer cells. Initial studies also indicate that these structures may play a role in migration of these rafts over solid surfaces, and mutants lacking helical connections failed to swarm successfully. Possible functions of helical connections in swarming are summarised in Table 4.3.

Table 4.3: Potential functions of helical connections in formation and migration of mutlicellular rafts.

Aspect of Swarming	Possible function of helical connections
Raft propulsion	Co-ordination of flagella rotation to generate sufficient force for raft propulsion. Particularly important on surfaces exigent to migration
	Orient flagella filaments to ensure all contribute to migration
Raft Formation	Helical connections may contribute to raft stability and maintain cellular organisation during migration.
Communication	Helical connections could form a network of tactile sensors allowing the distribution of information throughout the raft to control migration velocity, timing of consolidation, or direction of migration.

4.5 Adhesion of *P. mirabilis* swarming-deficient mutants to silicone, and biofilm architecture in the parallel plate flow chamber

4.5.1 Adhesion of swarming-deficient mutants to silicone

The ability of bacteria to form biofilm communities on surfaces has become the focus of intensive study, and biofilm formation on implanted medical devices is common (Donlan & Costerton 2000; Donlan 2001; 2002). The initial stages of biofilm formation involve the attachment of cells to the substratum, and therefore bacterial adhesion to abiotic surfaces is a key process in biofilm formation (Watnick & Kolter 1999; Donlan 2001; Sauer *et al.* 2002; Klausen *et al.* 2003). Several factors are thought to influence the attachment of bacterial cells to a surface such as, the hydrodynamics of the medium, properties of the medium and substratum, and various characteristics of the bacterial cell including motility (Pratt & Kolter 1999; Donlan 2002).

The contribution of swarming to biofilm formation, and bacterial adhesion has been less thoroughly investigated. As biofilm formation is a key process in the encrustation and blockage of urethral catheters (Ohkawa *et al.* 1990; Clapham *et al.*1990; Dumanski *et al.* 1994; Winters *et al.* 1995; Stickler 1996b; Morris *et al.* 1997), the ability of the swarming-deficient mutants to adhere to and generate biofilms on silicone surfaces was investigated using a parallel plate flow chamber. This allowed the contribution to biofilm formation of swarming in general to be evaluated, as well as assessing the roles of the genes inactivated in individual mutants. The parallel plate flow chamber has been utilised in other investigations of bacterial adherence and biofilm formation (Tolker-Nielsen *et al.* 2000; Hughes 2001; Klausen *et al.* 2003).

For the purposes of this study the flow chamber offered the ability to study several aspects of *P. mirabilis* biofilm formation in the mutants, including adhesion and differences in biofilm architecture. However, phosphate buffer was used as a medium rather than human or artificial urine. This was necessary to standardise conditions, as increasing pH and crystal formation would hinder image analysis in both human and artificial urine. The flow rate was kept constant throughout the flow chamber experiments, but in a clinical setting would be expected to vary between patients, and may also vary in an individual over time.

Under these conditions only the poor-swarming mutant G78, and the non-swarming mutant G37 differed significantly from the wild type. Both these mutants demonstrated significantly greater adhesion to silicone when compared to the wild type individually using a two-sample t-test (Table 3.12). Biofilm formation is thought to require both the up-regulation and down-regulation of many genes (Pratt & Kolter 1999). This indicates that the down-regulation of the genes disrupted in G78 and G37 (Table 3.7) may be involved in *P. mirabilis* biofilm formation.

The role of these genes in adhesion is unclear, but may be related to aspects of their function during swarming. For G37 the possible inactivation of a glycosyl transferase enzyme has several potential outcomes which may affect adhesion to silicone. A lack of glycosylation of specific structures or proteins may also serve to enhance interactions between the cell and the silicone surface. The overall charge of the cell may have been altered if certain surface structures are not glycosylated, and may become more favourable to interactions between the cell and the surface. Alternatively, proteins which were previously unavailable due to glycosylation may now be available to strengthen or facilitate attachment, or the unmodified forms of

specific adhesion proteins may enhance their ability to interact with a surface. However, such changes may be detrimental to biofilm formation or general survival *in vivo,* or under other environmental conditions encountered by the cell.

Although it is unclear how the inactivated gene in G78 is involved in adhesion, the fact that it is implicated as influencing the overall shape of a protein, may provide some explanation. The disruption of this gene may affect the production of proteins that are antagonistic to attachment of *P. mirabilis*. For example, G78 generates fewer flagella than the wild type and it is possible that these structures interfere with the establishment of contact between the abiotic surface and components of the cell envelope. This hypothesis may also apply to G37, as this mutant also generates fewer flagella than the wild type. However, the majority of the swarming-deficient mutants also synthesise fewer flagella than the wild type, but show no significant differences in attachment (Table 3.12).

In general the results obtained suggest that neither swimming nor swarming motility are required for adhesion of *P. mirabilis* to silicone. The results obtained for many of the mutants suffering reductions in swimming motility, are in contrast to those obtained in studies of other biofilm forming bacteria. Swimming motility is thought to permit bacterial cells to overcome repulsive forces between the cell and the substratum, and restraints of medium flow, enabling contact between the cell and surface (Pratt & Kolter 1999). Studies of *Ps. aeruginosa* mutants deficient in flagella-mediated motility revealed these were also deficient in attachment, indicating that swimming motility was important for initial cell-to-surface interactions (O'Toole & Kolter 1998a). Swimming was also found to be important for initial interaction of *E. coli* with a surface (Pratt & Kolter 1998), while the

absence of a flagellum in *Vibro cholerae* lead to alterations in biofilm development (Watnick *et al.* 2001).

Conversely, the results of flow chamber experiments in this study would seem to suggest that swimming is inhibitory to adherence, and therefore biofilm formation, in *P. mirabilis*. A strong correlation was observed between swimming ability and adherence, although surprisingly this was a negative, indicating that as swimming ability increased adherence decreased (Table 3.13).

However, not all studies of biofilm formation have found that swimming motility is a requirement for attachment to a surface. Klausen *et al.* (2003) reported that flagella mediated motility was not necessary for initial attachment or biofilm formation in *Ps. aeruginosa* PA01. Biofilm formation by this organism has also been correlated with the emergence of phenotypic variants, defective in swimming, swarming and twitching motility (Déziel *et al.* 2001). The non-swarming phenotype associated with biofilm formation in *Ps. aeruginosa* is also relevant to *P. mirabilis* biofilm formation, and agrees with the results obtained in this study.

A strong negative correlation was also observed between swarming and adherence (Table 3.13). In general the swarming-deficient mutants exhibited higher rates of deposition than the wild type strain (Figures 3.31 and 3.32). Mutants such as BVJ14, possessing swarming indices greater than the wild type, exhibited deposition rates that were much slower than the wild type (Figure 3.33). This suggests that swarming is also inhibitory to biofilm formation. Similar results have been reported for biofilm formation in *Salmonella enterica* serovar Typhimurium (Mireles II *et al.* 2001).

In *S. typhimurium* mutants deficient in swarming, more cells were found to adhere to PVC in an assay of biofilm formation. The production of surfactin during differentiation, was found to inhibit biofilm formation in this organism (Mireles II *et al.* 2001). It is possible that the increased deposition rates observed in the swarming-deficient mutants could be attributed to a decrease in surfactin production. This would be particularly relevant to the non-swarming mutants G37 and G93, which do not generate differentiated swarmer cells (Figure 3.27) and displayed the greatest levels of attachment and deposition rates (Table 3.12, Figure 3.31). If surfactants do inhibit attachment of *P. mirabilis* to catheter biomaterials then this could potentially constitute an effective way to inhibit colonisation of indwelling urethral catheters, and manage *P. mirabilis* C-UTI infections. Additional experiments should be undertaken to evaluate this hypothesis.

It is perhaps unsurprising that the results of this study indicate that swarming is not required for initial cell-to-surface interactions in *P. mirabilis*. As differentiation and swarming are generally thought to be triggered by increased viscosity of the media, or contact with a solid surface (Belas 1996), a role for swarming in initial cell-to-surface interactions seems unlikely. Any contribution of swarming probably comes after initial attachment, and could be involved in the strengthening of interactions between pioneering cells and the surface.

Nevertheless, it is conceivable that this is only true under the conditions used in the flow chamber experiments, and that the lack of significant differences between the mutants may be due to aspects of the experimental design. As many patients undergoing long-term catheterisation are elderly, a flow rate of 1 ml/min was used to reflect the lower urinary output of these patients. Higher flow rates of 2-3 ml/min

have been shown to significantly reduce the numbers of *P. mirabilis* cells adhering in the flow chamber (Hughes 2001). It is possible that at higher flow rates the contribution of swarming, or swimming to adhesion would be more important, and a greater difference may be observed between the mutants and the wild type. Also the use of artificial or human urine may highlight differences between the mutants and wild type. Environmental factors such as elevated pH, crystal formation, and the establishment of a proteinaceous conditioning film on the abiotic surface may alter the adherence of the mutants compared to the wild type, and highlight a role for swarming or swimming motility in attachment.

In previous studies of *P. mirabilis* adhesion in the parallel plate flow chamber Hughes (2001), reported that non-swimming, non-swarming *P. mirabilis* mutants were inhibited in adhesion to a glass surface. The disparity between the results obtained by Hughes (2001), and those from this study may be caused by the different surfaces investigated, or may be attributed to the different genetic background of the mutants utilised. Hughes (2001), used *P. mirabilis* wild type strain U6450, and mutants strains U6450 *flhA*$^-$ (non-swimming, non-swarming) and U6450 *flgN*$^-$ (capable of swimming, but non-swarming). In this study *P. mirabilis* wild type strain B4 and mutants derived form B4 were used.

Bacteria may form biofilms though the expression of distinct, convergent, genetic pathways (Vidal *et al.* 1998; O'Toole & Kolter 1998b; Watnick *et al.* 1999; Prigent-Combaret *et al.* 2000). Studies of *Ps. fluorescens* WCS365 have indicated the existence of two or more overlapping genetic pathways, concerned with biofilm development in this organism (O'Toole & Kolter 1998b). Mutants defective in one such pathway did not require flagella-mediated motility to initiate biofilm formation

under the conditions tested (O'Toole & Kolter 1998b). Vidal *et al.* (1998) reported that increased expression of the *E. coli* surface adhesin protein, curli, could restore biofilm formation in non-motile *E. coli* mutants. It was suggested that under certain conditions swimming is not required for biofilm formation in this organism, and that an alternate pathway, dependant on curli overproduction is utilised (Vidal *et al.* 1998). In *E. coli* strains that generate functional flagella and over produce curli no deficiency in adhesion was observed when flagella production was blocked by inactivation of *fliC* (Prigent-Combaret *et al.* 2000).

Therefore, the contrasting contributions of flagella-mediated motility to *P. mirabilis* adhesion between this study, and that of Hughes (2001), may reflect the utilisation of different genetic pathways of biofilm development in *P. mirabilis* U6450 and B4. For example, mutants of *P. mirabilis* strain B4 may be capable of utilising an alternate pathway of biofilm formation which is not available to U6450, either through inactivation or incompatibility with adherence to a glass surface. This theory is strengthened when considered in relation to the U6450 *flhA*$^-$ mutant utilised by Hughes (2001), and the B4 *flhA*$^-$ mutant NS63 used in this study, which have transposon insertions in the same gene. Despite this U6450 *flhA*$^-$ was found to be deficient in attachment compared to wild type U6450, while NS63 exhibited increased attachment compared to the wild type B4. However, the differing phenotypes of these mutants may account for the observed variation in adherence, with the potentially greater surface area of NS63 cells compensating for the non-motile phenotype.

In *Aeromonas* spp. lateral flagella used for swarming have been shown to enhance adhesion to both abiotic and cell surfaces (Kirov 2003; Gavín *et al.* 2003). It is also possible in *P. mirabilis* that flagella may act as adhesins, directly anchoring cells to a surface. If this is the case, it seems probable that swarmer cell differentiation and hyper-flagellation would increase the strength of adherence once initial cell-to-surface contact has been established.

Assessment of the strength of adherence indicated that, differentiation did not increase the strength of adherence to silicone (Table 3.14). Wild type strain B4, control mutants, and poor-swarming mutants which are all capable of differentiation, showed no significant differences in strength of adherence compared to mutants G37 and G93 which are unable to differentiate. In addition, the non-flagellated mutant NS63 also showed no significant reduction in the strength of adherence, indicating flagella are not directly involved in adhesion in *P. mirabilis*. However, NS63 attached mainly as elongated cells, and has been observed to generate elongated cells in liquid media. Therefore, the increased surface area of these cells may compensate for the lack of flagella in this mutant.

Apart from flagella, other surface associated structures, such as pili have also been associated with adherence to abiotic surfaces. Although it appears unlikely that *P. mirabilis* would a possess pili or fimbriae specific to silicone, let alone other catheter biomaterials, it has been shown that in other bacteria pili are involved in non-specific interactions with abiotic surfaces (Pratt & Kolter 1999). In *E. coil* type I pili have been found to be important for attachment, and biofilm formation on several surfaces, including PVC, polystyrene and borosilicate glass (Pratt & Kolter 1999). In

V. cholerae the mannose-sensitive heamagglutinin pilus was found to be required for biofilm formation on borosilicate glass (Watnick *et al.* 1999).

P. mirabilis is known to express four distinct types of fimbriae, MR/P fimbriae (Mannose-resistant/*Proteus*-like), PMF fimbriae (*Proteus mirabilis* fimbriae), NAF (nonagglutinating fimbriae), and ATF fimbriae (ambient temperature fimbriae) (Mobley 1996). It is possible that such structures are expressed in greater numbers by the swarming-deficient mutants, as an indirect consequence of the general defects in swarming. Alternatively the presence of flagella may be antagonistic to interactions between any surface associated adhesins of *P. mirabilis* and the silicone surface. The reduced flagella production observed in the swarming-deficient mutants may initially decrease the number of cells that come into contact with the surface, but give a greater chance of interaction between adhesins and the silicone surface when cells do make contact.

4.5.2 Biofilm architecture

Another aspect of *P. mirabilis* biofilm formation investigated during the flow cell experiments was microcolony formation and biofilm architecture. Biofilm formation is thought to involve several distinct phases: (i) contact and initial adhesion of cells to a surface, (ii) microcolony formation, (iii) maturation of the biofilm and structural development (biofilm architecture; Tolker-Nielsen *et al.* 2000; Sauer *et al.* 2002; Klausen *et al.* 2003). After adhesion of cells to a surface, biofilm development is thought to begin with the formation of micro-colonies, which have been described as the "building blocks of biofilms" (Donlan & Costerton 2002). As such the ability to form micro-colonies may be a rate limiting step in *P. mirabilis* biofilm development which in terms of catheter encrustation correlates to the time taken for a catheter to

block. It has been suggested that the majority of biofilms then form complex three-dimensional structures composed of "mushrooms " and "stacks" of cells embedded in polysaccharide matrix (Donlan & Costerton 2002). This architecture also creates channels through which aqueous media can flow, distributing nutrients and minerals throughout the biofilm (Donlan & Costerton 2002).

The three-dimensional structure of *P. mirabilis* biofilms that develop on urinary catheters may contribute to the rate at which crystalline material is embedded in the biofilm matrix, and influence the speed at which biofilm mineralisation and encrustation occurs. For these reasons the flow cell experiments were also used as an indication of the test strains ability to from micro-colonies, and to assess the architecture of biofilms at the end of the experiments.

Differences in biofilm architecture were observed between the mutant strains assessed in flow chamber experiments, and the wild type (Figure 3.35 to 3.43). The wild type strains and control mutants appeared to generate biofilms with similar architecture, consisting of large aggregates with fewer individual cells attached. In contrast the biofilms of the non-swarming mutants appeared to be composed mainly of individual cells, or in the case of G37 many small aggregates, spread evenly over the surface. Poor-swarming mutants appeared to exhibit biofilms with an intermediate architecture. However, these observations are based on 5h biofilms, and may only reflect differences in early stages of biofilm formation, which are not evident in mature biofilms. Nevertheless, interesting differences are indicated between the different classes of mutants.

Several different processes are thought to contribute to the development of the mature biofilm structure including flagella mediated motility, twitching motility, exopolysaccharide (EPS) production, and cell to cell communication (Pratt & Kolter 1998; O'Toole & Kolter 1998a,b; Watnick *et al.* 1999; Tolker-Nielsen *et al.* 2000). Tolker-Nielsen *et al.* (2000), reported that interaction of cells between distinct microcolonies during later stages of biofilm development was mediated by flagella driven motility. Motility has also been reported to be important in the aggregation of cells to form microcolonies during *Ps. aeruginosa* biofilm formation (O'Toole & Kolter 1998a), and in *E. coli* it has been suggested that motility is necessary for migration of cells over the surface, and facilitates spreading of the biofilm as it develops (Pratt & Kolter 1998).

In *P. mirabilis* it has been suggested that swarming facilitates the spreading of the biofilm over the catheter surface (Stickler & Hughes 1999). But in general no association was observed between formation of microcolonies and either swimming or swarming ability. Similar results were also obtained during flow chamber studies of mixed species biofilms composed of *Ps. aeruginosa,* and *Ps. putida,* where initial microcolony formation was found to occur through clonal expansion of attached cells, rather than flagella mediated aggregation of cells (Tolker-Nielsen *et al.* 2000). The results of this study suggest that flagella-mediated motility is not required for microcolony formation in *P. mirabilis,* but does not preclude its involvement in later stages of biofilm development.

However, apart from migration over solid surfaces, other aspects of differentiated swarmer cells may be pertinent to biofilm architecture. Differentiated swarmer cells produce an extensive exopolysaccharide matrix, abundant flagella filaments, and

exhibit changes to the cell membrane (Belas 1996), all of which may potentially influence biofilm architecture in *P. mirabilis*. It is interesting that those strains capable of differentiation, with the exception of G64, produced larger cellular aggregates than those found to be unable to differentiate (G37 and G93). G37 and G93 appeared to produce smaller microcolonies, although G37 appeared to generate large numbers of these structures.

Elongated cells were observed in biofilms of the wild type strain B4, non-swarming mutant NS63, and the control mutant BVJ12 (Figures 3.36, and 3.43). In the control mutants and the wild type, elongated cells were associated with large cellular aggregates, which were not observed in the swarming-deficient mutants tested. This may indicate that differentiated swarmer cells act as a nuclei for formation of the larger cellular aggregates observed in the wild type and control mutants. The large numbers of flagella present on swarmer cells may form intercellular linkages that hold cells together. Flagella have been found to perform a similar function during formation of pellicles in *S. typhimurium* (Römling & Rhode 1999). The increased EPS production of swarmer cells may also contribute to formation of these structures.

The apparent attenuation in microcolony formation exhibited by G64, G93, and the excessive microcolony production observed in G37 may be directly related to the genes inactivated in these mutants. If G64 is indeed deficient in EPS production, then the aggregation of cells may be inhibited in this mutant. For G37, the potential loss a glycosyl transferase may again cause defects in EPS assembly. Alternatively certain surface structures responsible for generating cell-cell contacts and cellular aggregation, may not function effectively unless glycosylated. A similar scenario can

be envisaged for G93. The potential loss of the PPIase SurA in this mutant may result in reduced cellular aggregation if for example, SurA is required to produce functional conformations of outer membrane proteins involved in microcolony development.

Differing flow rates found in catheterised patients may also contribute to the phenotype of the biofilm formed. An increase in flow rate and subsequently greater shear forces would presumably result in a biofilm with higher tensile strength, as has been described for other species (Donlan & Costerton 2002). In addition, biofilms formed *in vivo* are likely to be polymicrobial, and the complex interaction between different species of bacteria will almost certainly have a profound effect on the properties of the biofilm.

4.6 Models of Infection

4.6.1 Catheter bridge models

P. mirabilis has the ability to swarm over urethral catheters (Stickler & Hughes 1999). Therefore, the capability of the swarming-deficient mutants to migrate over catheter biomaterials and the potential role of swarming in the initiation of *P. mirabilis* C-UTI was investigated. Few studies have investigated the migration of bacteria over catheter surfaces. Darouchie *et al.* (1997) reported that of the four bacterial species tested, *Ps. aeruginosa* was the most mobile in a model of bladder colonisation, where it took 12 days to migrate along a 10 cm length of all-silicone catheter. In view of its importance as a pathogen of the catheterised urinary tract, it was surprising that *P. mirabilis* was omitted from the latter study. Sabbuba *et al.* (2002) demonstrated that *P. mirabilis* and *P. vulgaris* swarmer cells migrated more successfully over all-silicone catheter sections than nine other urinary tract pathogens, including *Ps. aeruginosa.*

The results of the catheter bridge experiments (Table 3.15) showed that swarming is important for migration of *P. mirabilis* over catheter surfaces. In general, mutants deficient in swarming were less able to move over both types of catheter, but for hydrogel-coated latex catheters it was clear that swimming motility was also involved. Therefore, the degree to which each type of motility (swimming or swarming) was involved in migration over the two types of catheter was assessed by calculating correlation coefficients (Table 3.16). As with other aspects of *P. mirabilis* pathogenicity, the individual contributions of swimming and swarming motility are difficult to evaluate. Correlation coefficients provide an indication of the relationship between two variables but must be interpreted with care, and cannot be used to draw conclusions without additional evidence. Due to the difficulty in separating

swimming and swarming motility, it is possible that these calculations may not reflect a true relationship between the variables investigated, as the best swarmers also tend to be the best swimmers. However, in this study direct observations of catheter bridge experiments supported the relationships highlighted by these calculations.

Correlation coefficients for swimming or swarming ability and migration over each catheter surface indicated that swarming was clearly the most important factor in migration over all-silicone. Non-swarming mutants failed completely to cross all-silicone sections, and many poor-swarming mutants were also unable to migrate over any sections. In the case of hydrogel-coated latex sections both swimming and swarming appeared to be linked to migration over these surfaces. The correlation coefficients showed that both swimming and swarming ability had a similar influence on migration over hydrogel-coated latex sections, and non-swarming mutants which had retained the ability to swim were still able to migrate over these sections. These observations raise the possibility that the contribution of each form of motility, to colonisation of the catheterised urinary tract by *P. mirabilis*, is modulated by the type of catheter used. Similar results were also reported by Sabbuba *et al.* (2000) who investigated the migration of *P. mirabilis* over all-silicone, and hydrogel-coated latex catheters, under conditions which inhibited swarming.

In this study the role of swarming in migration of *P. mirabilis* over these surfaces was reinforced by experiments with the complemented mutants, NS63comp, G64comp, and G78comp (Table 3.17). These showed that as swarming was restored to these mutants, their ability to move over both types of catheter increased. This observation was most notable for all-silicone catheter sections, over which NS63 and

G64 were completely unable to migrate, while G78 only managed to migrate over a very low percentage of sections. The catheter bridge experiments with G78comp may also indicate that while both swimming and swarming motility are undoubtedly involved in migration of *P. mirabilis* over hydrogel-coated latex catheters, swarming may play a more important role.

The ability of G78comp to migrate over hydrogel-coated latex was completely restored. However, comparison of the swimming, swarming, and migration indices of G78comp with those of the poor-swarming mutants NS77, G77, and PS92, indicated that the increase in swarming ability (rather than in swimming ability) was responsible for the enhanced migration of G78comp over hydrogel-coated latex catheters. PS92 possessed wild type swimming ability, while G77 and NS77 had similar or greater swimming indices than G78comp. Swarming indices of all strains were also well below that of G78comp. However, PS92 and G77 were unable to migrate over more that 75% of hydrogel-coated latex sections, and NS77 was only able to move over 58.33% of sections. In contrast, G78comp could migrate over 100% of hydrogel-coated latex sections. This suggests that swimming may be less efficient for the colonisation of catheter surfaces than swarming. While the differences in swimming and swarming ability produce only relatively small differences *in vitro*, these may be of greater importance *in vivo*.

Studies of the complemented mutants also indicate a potential role for the formation of helical connections in the migration of *P. mirabilis* over catheter surfaces. The poor-swarming mutant G78 was severely reduced in migration over all-silicone catheters, while NS63 was unable to move over any catheter sections. Complementation restored swarming ability and greatly increased migration over all-

silicone catheters in these strains. Interestingly the swarming index of G78comp was similar to that of NS63comp; however, G78comp was able to move over twice as many all-silicone sections as NS63comp. This may be due to the fact that while both strains can generate helical connections, those produced by G78comp are more organised and similar in appearance to those seen in wild type swarm fronts (Figure 3.28). This may indicate that the ability to generate helical connections, rather than swarming ability in general is the important factor in migration over surfaces such as silicone.

Stickler & Hughes (1999) showed that *P. mirabilis* moves over catheter surfaces as discreet rafts of swarmer cells. The organisation of flagella into helical connections may be required to generate sufficient force for propulsion of rafts over these materials. Alternatively, the apparent contribution of helical connections to raft formation and stability, may hold rafts together as they move over catheter surfaces. Therefore, genes related to swarming in general, and formation of helical connections are important for the colonisation of urethral catheters by *P. mirabilis*.

4.6.2 *In vitro* bladder models.

Other investigations of the role of swarming and swimming, in *P. mirabilis* urinary tract infection, have generally considered the uncomplicated urinary tract (Zunnino *et al.* 1994; Mobley 1996; Belas 1996; Legnani-Fajardo *et al.* 1996; Zhao *et al.* 1999; Schneider *et al.* 2002; Jansen *et al.* 2003). The results obtained from these studies present conflicting views on the role of swarming in *P. mirabilis* UTI. Potential functions of swarming in the pathogenesis of *P. mirabilis* urinary tract infections are illustrated in Figure 4.3. Mutants deficient in flagella production and swarming have been found to be less virulent in a murine model of infection (Mobley 1996), and

Figure 4.3: Potential functions of swarming in *P. mirabilis* pathogenesis in the catheterised urinary tract.

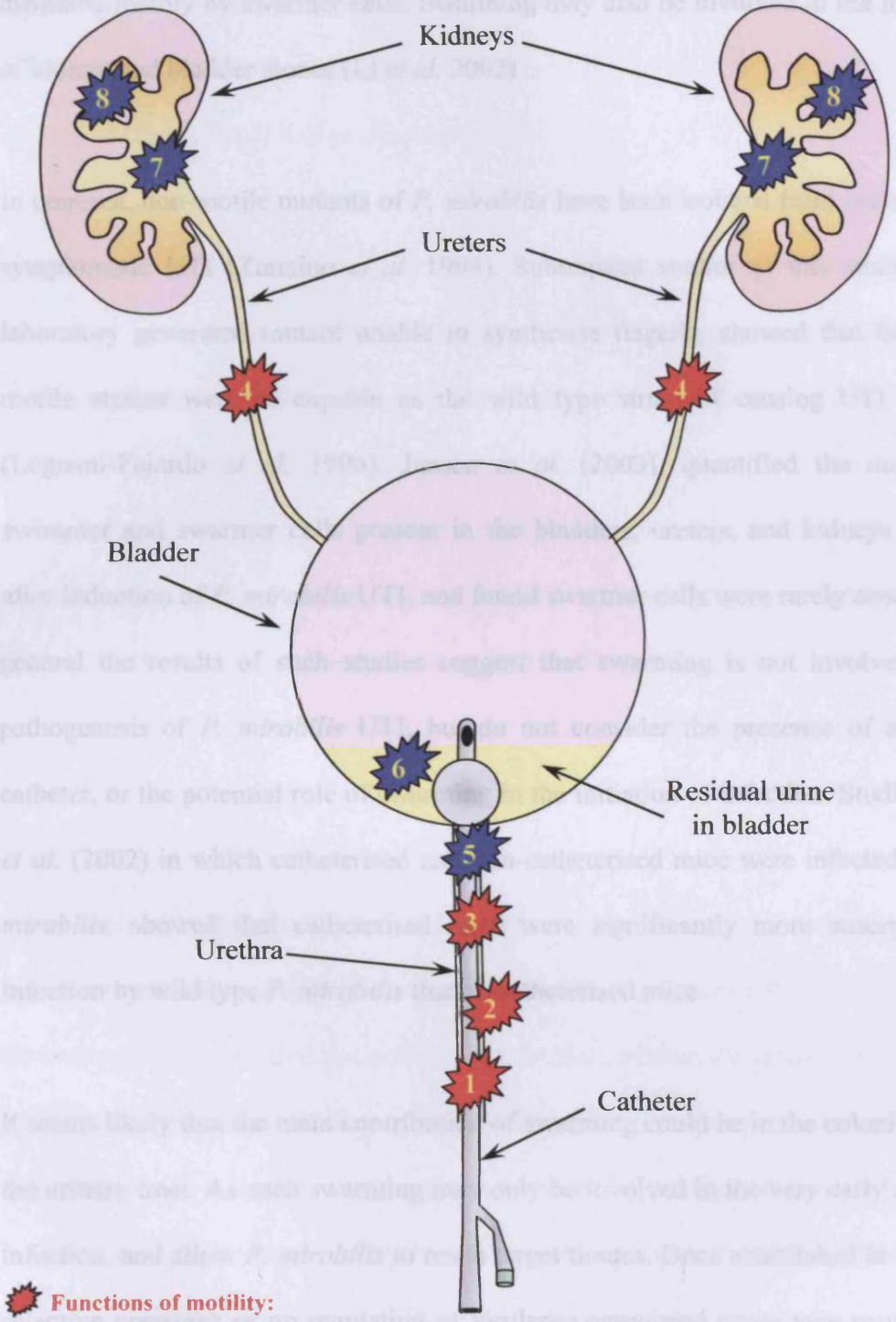

Functions of motility:

1. Migration over catheter lumen to colonise bladder
2. Migration over external surfaces of catheter to colonise bladder
3. Spreading of biofilm over catheter
4. Migration along ureters to colonise kidneys

Functions of increased virulence factor expression by swarmer cells (particularly urease):

5. Increased mineralisation of biofilm
6. Increased formation of bladder stones in residual urine.
7. Increased formation of kidney stones
8. Invasion of kidney epithelial cells

Allison *et al.* (1992) concluded that invasion of kidney cells by *P. mirabilis* was mediated mainly by swarmer cells. Swarming may also be involved in the formation of kidney and bladder stones (Li *et al.* 2002)

In contrast, non-motile mutants of *P. mirabilis* have been isolated from patients with symptomatic UTI (Zunnino *et al.* 1994). Subsequent studies of this strain, and a laboratory generated mutant unable to synthesise flagella, showed that both non-motile strains were as capable as the wild type strain of causing UTI in mice (Legnani-Fajardo *et al.* 1996). Jansen *et al.* (2003), quantified the number of swimmer and swarmer cells present in the bladders, ureters, and kidneys of mice after induction of *P. mirabilis* UTI, and found swarmer cells were rarely observed. In general the results of such studies suggest that swarming is not involved in the pathogenesis of *P. mirabilis* UTI, but do not consider the presence of a urinary catheter, or the potential role of swarming in the initiation of infection. Studies by Li *et al.* (2002) in which catheterised and non-catheterised mice were infected with *P. mirabilis,* showed that catheterised mice were significantly more susceptible to infection by wild type *P. mirabilis* than uncatheterised mice.

It seems likely that the main contribution of swarming could be in the colonisation of the urinary tract. As such swarming may only be involved in the very early stages of infection, and allow *P. mirabilis* to reach target tissues. Once established in the host, selective pressures or up regulation of virulence associated genes may result in the vegetative swimmer cells emerging as the dominant morphotype. For example, the highly immunogenic swarmer cell, with its thousands of flagella may be cleared more rapidly by the host immune system than swimmer cells. Fimbriae implicated as important for colonisation of the host, such as the MR/P fimbriae, have been shown

to be expressed by swimmer cells only (Li *et al.* 2001; Jansen *et al.* 2003). Thus once target tissues have been reached, swarming may no longer be required or appropriate. This may account for the lack of swarmer cells observed by Jansen *et al.* (2003), who studied tissues at 2 and 4 days after inoculation.

The catheter bridge results suggest that at least in the case of all-silicone catheters, swarming is involved in the migration of *P. mirabilis* from the periurethral skin, along the catheter surface and into the bladder, thus initiating C-UTI. Hydrogel coatings appear to facilitate the migration of *P. mirabilis* over latex catheters. Both Sabbuba *et al.* (2000), and Stickler & Hughes (1999), reported that *P. mirabilis* migrates more easily over the surfaces of hydrogel-coated latex catheters than all-silicone catheters. This suggests that hydrogel-coatings may in fact assist the colonisation of the catheterised urinary tract by *P. mirabilis* and other uropathogenic bacteria.

It has been suggested that inhibition of swarming may constitute a novel strategy for the prevention of C-UTI by *P. mirabilis* (Stickler & Hughes 1999). By preventing swarming it is hoped that the colonisation of the catheterised urinary tract may be inhibited. However, while this study indicates that swarming is important in the migration of *P. mirabilis* over catheter surfaces, it is also clear that swimming motility also contributes to migration over certain surfaces. As such, the role played by swimming and swarming motility *in vivo* may depend on the catheter type used, and could be influenced by other factors such as the use of hydrogel based lubricating gels to assist the insertion of catheters.

Any strategies seeking to inhibit *P. mirabilis* C-UTI by specifically blocking swarming motility, may be undermined by colonisation of the catheterised urinary tract through swimming motility. Therefore, such strategies may require the inhibition of motility in general in order to be broadly applicable. However, it seems likely that physical barriers to migration present *in vivo*, such as urine flow, or the mucous layer overlying urethral epithelial cells, would require the concerted effort of swarming to overcome (Belas 1996). Agents which disrupt normal flagella synthesis or function may form the basis of such strategies, and a greater understanding of swarming and flagella biosynthesis in *P. mirabilis* will hopefully identify prospective bacterial therapeutic targets.

The results of catheter bridge experiments with the poor-swarming mutant G64 also suggest possible strategies for prevention of *P. mirabilis* C-UTI. The putative defect in production of exopolysaccharide which may inhibit swarming in this mutant, also appears to greatly reduce its ability to migrate over catheter surfaces. As such, a potential method for inhibiting *P. mirabilis* swarming could focus on disruption of the EPS matrix through which *P. mirabilis* swarms. This may also have the added bonus of inhibiting biofilm development and could possibly disrupt mature biofilms.

Swarming has also been suggested to play a role in development of the crystalline biofilm on the catheter surface (Stickler & Hughes 1999; Sabbuba *et al.* 2002), and may be involved in the formation of kidney and bladder infection stones (Li *et al.* 2002). Swarming by *P. mirabilis* may facilitate the spread of the biofilm over the catheter surface, while the increased production of urease by swarmer cells (Allison *et al.* 1992) could accelerate mineralisation. This increased urease production by swarmer cells may also be relevant to the formation of infection stones. *P. mirabilis*

swarmer cells have been observed on the surface of, and within the matrix of infection stones, and it has been suggested that the increased expression of urease by differentiated swarmer cells may be a factor in the development of these structures (Li *et al.* 2002).

The ability of the swarming-deficient mutants to block all-silicone catheters was assessed using *in vitro* bladder models. However, no statistically significant differences were found between the time taken for mutants to block catheters, when compared to the wild type (Table 3.18). Although the *in vitro* bladder model represents a very stringent test, and may be thought of in terms of catheterising a patient with an already heavily infected urinary tract. As such the differences observed during these experiments may be of greater significance in a clinical setting.

Interestingly, these results indicated that non-swarming mutants were generally more capable of blocking catheters than the wild type. Calculation of correlation coefficients indicated that as swarming decreased, ability to block catheters increased. This was also found to be the case for swimming motility. In contrast, an investigation of the relationship between the mutants ability to adhere to silicone in the parallel plate flow chamber, and the time taken to block all-silicone catheters, indicated a strong negative correlation (Table 3.21). This suggests that strains which exhibit the greatest adherence to silicone block catheters in the shortest time. Therefore, the increase in time to blockage observed in the mutants with higher swarming ability, is likely a reflection of the relationship between swarming and adherence to silicone identified during parallel plate flow chamber experiments (Section 3.6, Table 3.13).

These results indicate that neither swimming nor swarming motility were required for the formation of crystalline biofilms on all-silicone catheters. However, they do not preclude a role for either motility in the colonisation of the catheterised urinary tract, or initiation of infection. Such aspects of infection are not tested by the *in vitro* bladder model, in which the "bladder" has already been colonised and become bacteriuric.

No significant differences were found in the number of cells with which models were inoculated, nor in the number of cells persisting in bladders after blockage of catheters. The pH of media in the bladders was also measured at the start and end of experiments. This showed that differences in time to blockage between the mutants and wild type were not due to defects in growth, the ability to elevate pH to levels sufficient for crystal formation, or tolerance of high pH.

This is particularly relevant to the non-swarming mutant G93, which contains a transposon insertion in a gene homologous to *surA*. As discussed previously (Section 3.4, Table 3.7), in *E. coli* defects in SurA production have been linked with an inability to persist in stationary phase and tolerate high pH (Lazar *et al.* 1998). This is obviously not the case in *P. mirabilis*, as has been found with *Salmonella surA* mutant. However, in *E. coli* the attenuation was linked with additional mutations, which may also reduce the long term survival of *P. mirabilis surA* mutants, and its ability to tolerate high pH. Further investigation of this aspect of *P. mirabilis* physiology may lead to novel strategies for the control of *P. mirabilis* C-UTI.

Taken together, the results of the catheter bridge experiments and *in vitro* bladder models suggest that swarming is important in the initial colonisation of the

catheterised urinary tract, but not directly involved in the formation of crystalline biofilms and catheter blockage. Overall these results support the hypothesis that swarming is important for the early stages of infection, but is less important once *P. mirabilis* is established in the host.

4.7 General discussion and future work

4.7.1 Mutagenesis of *P. mirabilis* strain B4, isolation and complementation of swarming-deficient mutants

The molecular genetic approach to the study of bacterial virulence is a powerful way in which individual genes, and the processes that they control, can be investigated with regard to their role during infection. In the case of *P. mirabilis* crystalline biofilm formation, random transposon mutagenesis offers many advantages over other molecular approaches. Problems associated with the application of strategies involving gene transfer, and the lack of knowledge about genes involved in crystalline biofilm formation and colonisation of the catheterised urinary tract by *P. mirabilis* favour this mutagenesis strategy.

It is clear from the results of this study that the application of random transposon mutagenesis to investigate the contribution of swarming to catheter blockage, allowed the identification of novel genes and processes important to both swarming, and encrustation of urinary catheters by *P. mirabilis*. Modifications to the methods described here may allow many different aspects of *P. mirabilis* pathogenesis to be studied.

A key part of the mutagenesis strategy employed was the use of a simple high throughput screen to identify swarming-deficient mutants. The development of additional screens would also allow other processes to be investigated in relation to catheter blockage. For example, the factors associated with adherence of *P. mirabilis* to abiotic surfaces could be investigated by isolating mutants defective in attachment to a surface. O'Toole & Kolter (1998a) developed a simple high-throughput assay to

identify mutants unable to form biofilms on PVC. This screen could be adapted to investigate *P. mirabilis* biofilm formation on catheter biomaterials.

Alternatively, the bladder model itself may be used as a screen to identify genes necessary for survival in the catheterised urinary tract. This may be accomplished using modifications of the random transposon mutagenesis method such as signature tagged mutagenesis (STM). A description of how STM may be applied to the investigation of catheter encrustation by *P. mirabilis* is provided in Section 4.1.2. The bladder model may also be used to investigate the genetic basis of *P. mirabilis* catheter encrustation through the use of DNA microarrays. With the sequencing of the *P. mirabilis* genome currently underway, this option should soon be feasible. The use of DNA microarrays would potentially allow the identification of the majority of genes expressed during encrustation of the catheterised urinary tract. Therefore, this approach would potentially generate much valuable data regarding the genes involved in the pathogenesis of *P. mirabilis*.

The completion of the *P. mirabilis* genome sequence would also facilitate further genetic analysis of the mutants generated during this study. For those mutants that were not complemented, a genome sequence would greatly improve the efficiency with which this could be accomplished. Although three mutants were successfully complemented during this study, many interesting results were obtained form mutants that were not successfully complemented. It would be advantageous to perform complementation studies (possibly utilising the *Sau* 3a based random digestion approach which was not attempted for all mutants) on all the mutants and perform further phenotypic and genotypic analysis.

The complemented mutants provide very strong evidence that the genes disrupted in NS63, G64, and G78 are important in swarming by *P. mirabilis*. However, without sequence data on the complementing fragments, it is not possible to say with absolute certainty that the genes disrupted are responsible for the mutant phenotypes. In addition, analysis of the sequence data could provide a more in-depth understanding of the processes disrupted in these mutants, and provided a greater understanding of the function performed by the disrupted genes. Following verification of the role of each disrupted gene by complementation studies and sequence analysis, more specific phenotypic studies of individual mutants should be undertaken to evaluate hypotheses regarding the role of the disrupted genes in swarming. Experiments which should be carried out for each mutants are listed in section 4.7.5.

4.7.2 Characterisation of swarming-deficient mutants by electron microscopy

The studies on the swarming-deficient mutants and the complemented mutants allowed the role of swarming in the pathogenesis of C-UTI to be assessed, and the elucidation of novel structures involved in swarming. In general, investigation of flagella production by the mutants indicated a close association between flagella biogenesis and swarm cell differentiation, as has been previously suggested (Belas *et al.* 1991b; Belas *et al.* 1995; Gygi *et al.* 1995a; Fraser *et al.* 2000).

The application of the novel vapour fixation technique and electron microscopy allowed the resolution of structures involved in swarming by *P. mirabilis*. The formation of these structures was found to be due to the organisation of individual flagella filaments into helical connections between adjacent swarmer cells. This is a novel aspect of the *P. mirabilis* swarm cycle, and subsequent studies indicated that

these structures may play diverse roles in formation and migration of multicellular rafts.

A role for these structures in swarming was confirmed by analysis of the complemented mutants, which revealed that as swarming was restored, so too was the production of helical connections. These structures may perform a number of functions during swarming, but initial experiments indicate that they play a role in holding cells in formation and generating sufficient force for raft propulsion. This is reinforced by the potential role of these helical connections in migration over all-silicone catheters indicated by catheter bridge experiments.

Further investigation of the structure and function of helical connections during swarming could potentially lead to a greater understanding of this behaviour. The observation that these structures may be important to migration over catheter biomaterials should also be explored further. If formation of helical connections is indeed an important process in migration of *P. mirabilis*, and these structures are particularly important for migration over unfavourable surfaces as is suggested by catheter bridge experiments, then their disruption could constitute part of novel strategy for prophylaxis of *P. mirabilis* C-UTI.

The examination of the mutants *in situ* on agar also provided additional insights into the functions of previously described genes, and the mechanisms that are thought to control *P. mirabilis* swarm cell differentiation. Observations of the non-swarming mutant NS63 revealed that although this mutant is lacking in flagella, it has retained the ability to generate elongated cells. This is particularly interesting as the gene potentially disrupted, *flhA,* has been previously reported to be inactivated in a non-

swimming, non-swarming mutant of *P. mirabilis,* where it was found to be involved in flagella biosynthesis (Gygi *et al.* 1995a). Therefore the observations of NS63 may highlight an additional role of *flhA* in swarmer cell differentiation (discussed in detail in Section 4.4.2), and in general may indicate that inhibition of flagella rotation is not the only mechanism by which *P. mirabilis* senses contact with a solid surfaces and initiates differentiation.

4.7.3 Biofilm formation and adhesion of swarming-deficient mutants to silicone.

The ability of *P. mirabilis* to adhere to catheter surfaces and generate biofilms is a key event in catheter blockage. However, the contribution of swarming to this process is not well understood. In general the results of parallel plate flow chamber experiments with the swarming-deficient mutants indicated that neither swarming, swimming, or flagella production are necessary for this aspect of *P. mirabilis* C-UTI. However, adhesion and biofilm formation in *P. mirabilis* is undoubtedly a complex multi-factorial process, and as such these results must be interpreted with care. The conditions used in the parallel plate flow chamber experiments do not accurately reflect those likely to be encountered *in vivo*. It is likely that under the conditions found *in vivo*, swimming or swarming may have a greater or lesser contribution to adherence and other aspects of biofilm development.

Very little is known about the genetics of biofilm formation in *P. mirabilis*, or indeed if multiple convergent genetic pathways of biofilm formation, such as those identified in *Ps. fluorescens* WCS365 (O'Toole & Kolter 1998), exist in this organism. The contrasting results obtained in this study and that of Hughes (2001), may constitute tentative evidence that such pathways are present in *P. mirabilis*. If true, this raises the possibility that conditions *in vivo* may stimulate the use of

alternative pathways of biofilm formation not seen under the conditions used in the flow chamber experiments. *In vivo*, formation of a conditioning film of host proteins on the catheter surface (Ohkawa *et al.* 1990), and the presence of crystalline material may influence adhesion, could modulate the mechanisms used to attach to catheter surfaces. In addition, swimming and swarming may be more significant to adherence and biofilm formation on catheter biomaterials other than silicone.

Investigation of this aspect of *P. mirabilis* biofilm formation may be of use in developing strategies for the inhibition of catheter blockage. This would be of particular importance for the development of a widely applicable strategy to inhibit *P. mirabilis* biofilm formation. If environmental factors and the composition of the substratum to be colonised modulate the mechanisms which *P. mirabilis* uses to adhere to a surface, then strategies seeking to inhibit biofilm formation would need to work against targets common to all pathways of biofilm formation.

In *Ps. aeruginosa,* different pathways of biofilm formation were identified by supplementing media with nutrients such as citrate, glutamate, or iron (O'Toole & Kolter 1998). Different supplements restored biofilm formation in particular subsets of mutants, which presumably had defects in genes associated with distinct pathways of biofilm development (O'Toole & Kolter 1998). Similar studies could be undertaken in an effort to examine the possibility that *P. mirabilis* does indeed possess multiple pathways for biofilm development. Of particular interest would be the effects of supplementing the flow cell media used in this study with glutamine, as this amino acid has been implicated as a signal for swarm cell differentiation (Allison *et al.* 1993).

The lack of significant differences between the mutants and wild type in the flow chamber may also be due to other aspects of the experimental design. As many patients undergoing long-term catheterisation are elderly, a flow rate of 1 ml/min was used to reflect the lower urinary output of these patients. Higher flow rates of 2-3 ml/min have been shown to significantly reduce the numbers of *P. mirabilis* cells adhering to a glass surface in the flow chamber (Hughes 2001). It is possible that at higher flow rates the contribution of swarming, or swimming to adhesion would be more important, and a greater difference may be observed between the mutants and the wild type.

Interestingly, the flow chamber experiments indicated that increased swimming or swarming ability was antagonistic to adherence. In the case of swarming, similar results were obtained with non-swarming mutants of *S. typhimurium* and indicated that surfactin generated by swarmer cells was antagonisitic to biofilm formation (Mireles II *et al.* 2001). This may constitute another potential method by which catheter encrustation could be controlled, and therefore additional flow chamber experiments should be undertaken to determine the effect of similar compounds on *P. mirabilis* biofilm formation.

Studies of the early biofilm architecture of swarming-deficient mutants also indicated that aspects of swarming or swarm cell differentiation may influence the three dimensional structure of mature biofilms. A greater understanding of how this three dimensional structure develops, and how it affects catheter blockage may also aid in developing strategies for managing the catheterised urinary tract. Confocal laser microscopy could be employed to study the development of *P. mirabilis* in three

dimensions. It would be particularly interesting to use this technique in conjunction with the parallel plate flow chamber, and urine cultures of *P. mirabilis*.

4.7.4 Models of infection

The results of the flow chamber experiments were reflected in the results of the bladder model experiments. Mutants with the greatest swarming ability were also the least proficient at blocking all-silicone catheters. Closer analysis revealed that this was most likely due to their ability to adhere to silicone than a direct link between swarming or swimming (Section 4.6.2). As mentioned above, non-swarming mutants of *S. typhimurium* were also found to be more proficient at biofilm formation than the wild type strain (Mireles II *et al.* 2001), and may highlight a potential strategy for the prevention of catheter blockage by *P. mirabilis*. Together, the bladder model and flow chamber experiments suggest that increased swarming may inhibit the formation of *P. mirabilis* biofilms at least on the surface of all-silicone catheters, and may also be true for other catheter biomaterials. As with flow chamber experiments, swarming may also have a greater or lesser contribution under conditions encountered *in vivo*.

The bladder model experiments also suggest that disrupting genes required for swarming could increase the rate at which biofilm formation, and therefore catheter encrustation occurs. Although not statistically significant, an increased ability to block catheters was evident in all but one swarming-deficient mutant (G93), while the results from control mutants, which have an increased swarming ability, showed an extended in time to blockage. This suggests that the reduced blockage time in swarming-deficient mutants was a result of a general reduction in swarming, rather than specific defects in individual mutants. This is particularly significant for the

development of strategies that seek to prevent *P. mirabilis* colonisation of the urinary tract through the inhibition of swarming.

In contrast to adherence and biofilm formation, swarming was found to be highly important for the migration of *P. mirabilis* over the surfaces of catheters. Swarming-deficient mutants were less able to migrate over both hydrogel-coated latex, and all-silicone catheters. However, while swarming was clearly a prerequisite for migration over all-silicone catheters, this was not the case with hydrogel-coated latex catheters. Hydrogel-coated latex appeared to be a more favourable surface for migration, and all motile strains were able to move over a greater number these sections than all-silicone. This included the non-swarming mutants, which managed to migrate over these catheters by swimming motility. Therefore catheter materials that are resistant to the migration of *P. mirabilis* may prevent or delay the initiation of C-UTI by this organism.

In general, analysis of the swarming-deficient mutants indicated that swarming is important for the initial colonisation of the catheterised urinary tract. Flow chamber experiments, and *in vitro* bladder models, showed that swarming is not directly involved in the formation of crystalline biofilms and blockage of catheters. The formation of helical connections appeared to contribute greatly to the ability of *P. mirabilis* to migrate over all surfaces tested, and methods which disrupt or inhibit formation of these structures may also inhibit the ability of *P. mirabilis* to colonise the catheterised urinary tract. In addition, the observation that swimming may also contribute to migration of *P. mirabilis* over certain catheter types suggests that any inhibition of swarming alone would not be sufficient to prevent initiation of C-UTI.

4.7.5 Future work

The following aims should be sought in future studies:

- Develop additional high-throughput screens to allow investigation of other aspects of catheter encrustation by *P. mirabilis*. For example, high-throughput screens for mutants defective in biofilm formation and adherence to catheter biomaterials to identify genes specifically involved in attachment and development of crystalline biofilms.

- Investigate the use of additional molecular genetic approaches such as STM and microarrays, in conjunction with the *in vitro* bladder model to identify genes involved in catheter blockage.

- Complementation of all swarming-deficient mutants, and sequencing of complementing fragments to fully characterise disrupted genes.

- Further phenotypic characterisation of swarming-deficient mutants to establish the precise role of disrupted genes in swarming, biofilm formation and catheter encrustation.

- The formation of helical connections and their function during swarming should be investigated further, to ascertain their role in *P. mirabilis* swarming and pathogenesis. The generation of helical connections in other strains of *P. mirabilis*, both clinical and environmental should be investigated.

- The formation of helical connections during the swarm cycle could be further examined by using SEM to observe cells fixed *in situ* by vapour fixation at different stages during the swarm cycle.

- Attempts should be made to investigate the possibility that *P. mirabilis* possesses multiple convergent pathways of biofilm development. Possibly such experiments could be based on those described by O'Toole & Kolter (1998a,b).

- The ability of swarming-deficient mutants to block catheters other than all-silicone could be investigated using the *in vitro* bladder model. This may reveal if the contribution of swarming to blockage of urethral catheters is influenced by the properties of different catheter biomaterials.

Chapter 5: Conclusions

5.0 Conclusions

- The pUT suicide delivery vector and the mini-Tn*5*Km2 transposon can be used to generate random, single-insert transposon mutants in *P. mirabilis* B4.

- The pUT suicide delivery vector exhibits a high frequency (~30%) of co-integration with the mini-Tn*5*Km2 transposon among swarming-deficient mutants, and co-integrates with the mini-Tn*5*Km2 transposon in a contiguous fashion.

- Swarming-deficient mutants harbouring co-integrated segments of the pUT vector can be identified by resistance to ampicillin (100 μg/ml).

- In general, mutants deficient in swarming also display deficiencies in swimming ability when assessed by spreading through LB media solidified with 0.3% agar.

- The presence of the mini-Tn*5*Km2 transposon *per se* in the *P. mirabilis* genome did not affect swarming, swimming, urease production, or the growth of *P. mirabilis*.

- The genes disrupted in mutants NS63, G64, and G78 are involved in swarming of *P. mirabilis*.

- The reduced flagella production exhibited by all swarming-deficient mutants indicates a close association between the regulation of flagella production and swarming.

- The flagella filaments of *P. mirabilis* are highly organised during migration of multicellular rafts. Individual filaments are interwoven in phase to form helical connections between adjacent swarmer cells.

- Helical connections result from the interweaving of flagella in a criss-cross pattern. Flagella filaments are interwoven both with and against the direction of migration indicating that these structures are formed by an active process.

- Flagella organisation and formation of helical connections is important for the migration of *P. mirabilis* over agar surfaces. Mutants that are unable to form these structures are deficient in swarming.

- The genes disrupted in mutants NS63, G78, and G64 are invloved in flagella production.

- The gene disrupted in G78 affects the shape of flagella filaments, and is involved in the formation of helical connections.

- The presence of the mini-Tn*5*Km2 transposon *per se* in the *P. mirabilis* genome does not affect flagella production, flagella shape, formation of multicellular rafts, or formation of helical connections.

- Swarming or swimming motility are not required for adhesion of *P. mirabilis* to a silicone surface. Flow chamber experiments showed no significant differences in adherence to silicone between the wild type and swarming-deficent mutants.

- Swarming ability does not significantly influence the strength with which *P. mirabilis* adheres to silicone in the flow chamber experiments.

- Flagella production is not required for adherence of *P. mirabilis* to silicone in the parallel plate flow chamber.

- Swarm cell differentiation and/or swarming motility may influence biofilm architecture, although swarming or swimming motility are not required for microcolony formation by *P. mirabilis*.

- Swarming facilitates the migration of *P. mirabilis* over the surfaces of urethral catheters, and is essential for migration over all-silicone catheters.

- *P. mirabilis* can migrate over hydrogel-coated latex catheters using swimming motility, and migration occurs more readily over these surfaces compared with all-silicone catheters.

- Swarming ability was not significantly associated with the ability to encrust and block all silicone catheters in *in vitro* bladder models.

- Ability to adhere to silicone in the parallel plate flow chamber was strongly associated with ability to block all-silicone catheters in *in vitro* bladder models.

- Swarming is not required for encrustation of urethral catheters, but catheter-bridge experiments indicate a role in colonisation of the catheterised urinary tract.

Chapter 6: References

6.0 References

Aldridge, P., and K. T. Hughes. 2002. Regulation of flagella assembly. *Curr. Opin. Microbiol.* **5**:160 - 165.

Allison, C., and C. Hughes. 1991. Closely linked genetic loci required for swarm cell- differentiation and multicellular migration by *Proteus mirabilis*. *Mol. Microbiol.* **5**:1975 - 1982.

Allison, C., H. C. Lai, and C. Hughes. 1992. Coordinate expression of virulence genes during swarm-cell differentiation and population migration of *Proteus mirabilis*. *Mol. Microbiol.* **6**:1583 - 1591.

Allison, C., H. C. Lai, D. Gygi, and C. Hughes. 1993. Cell differentiation of *Proteus mirabilis* is initiated by glutamine, a specific chemoattractant for swarming cells. *Mol. Microbiol.* **8**:53 - 60.

Allison, C., L. Emody, N. Coleman, and C. Hughes. 1994. The role of swarm cell-differentiation and multicellular migration in the uropathogenicity of *Proteus mirabilis*. *J. Infect. Dis.* **169**:1155-1158.

Alm, R. A., L-S. L. Ling, D. T. Moir, B. L. King, E. D. Brown, P. C. Doig, D. R. Smith, B. Noonan, B. C. Guild, B. L. deJonge, G. Carmel, P. J. Tummino, A. Caruso, M. Uria-Nickelsen, D. M. Mills, C. Ives, R. Gibson, D. Merberg, S. D. Mills, Q. Jiang, D. E. Taylor, G. F. Vovis, and T. J. Trust. 1999. Genomic-sequence comparison of two unrelated isolates of the human gastric pathogen *Helicobacter pylori*. *Nature.* **397**:176 -180.

Annunziato, P. W., L. F. Wright, W. F. Vann, and R. P. Silver. 1995. Neucleotide sequence and genetic analysis of the *neuD* and *neuB* genes in region 2 of the polysialic acid gene cluster of *Eschericia coli* K1. *J. Bacteriol.* **177**:312 - 319.

Anwar, H., J. L. Strap, K. Chen, and J. W. Costerton. 1992. Dynamic interactions of biofilms of mucoid *Pseudomonas aeruginosa* with tobramycin and piperacillin. *Antimicrob. Agents Chemother.* **36**:1208 - 1214.

Armitage, J. P. 1982. Changes in the organization of the outer membrane of *Proteus mirabilis* during swarming: Freeze fracture structure and membrane fluidity analysis. *J. Bacteriol.* **150**:900 - 904.

Armitage, J. P., D. G. Smith, and R. J. Rowbury. 1979. Alterations in the cell envelope composition of *Proteus mirabilis* during the development of swarmer-cells. *Biochim. Biophys. Acta.* **584**:389 - 397.

Arnosti, D. N., and M. J. Chamberlin. 1989. Secondary σ factor controls transcription of flagellar and chemotaxis genes in *Eschericia coli*. *Proc. Natl. Acad. Sci. USA.* **86**:830 - 834.

Arora, S. K., M. Bangera, S. Lory, and R. Ramphal. 2001. A genomic island in *Pseudomonas aeruginosa* carries the determinants of flagellin glycosylation. *Proc. Natl. Acad. Sci. USA.* **98**:9342 - 9347.

Auvrey, F., J. Thomas, G. M. Fraser, and C. Hughes. 2001. Flagellin polymerisation control by a cytosolic export chaperone. *J. Mol. Biol.* **308**:221 - 229.

Bahrani, F. K., D. E. Johnson, D. Robbins, and H. L. T. Mobley. 1991. *Proteus mirabilis* flagella and MR/P fimbriae: Isolation, purification, N-terminal analysis, and serum antibody response following experimental urinary tract infection. *Infect. Immun.* **59**:3574 - 3580.

Bahrani, F. K., G. Massad, C. V. Lockatell, D. E. Johnson, R. G. Russell, J. W. Warren, and H. L. T. Mobley. 1994. Construction of an MR/P fimbrial mutant of *Proteus mirabilis*: Role in virulence in a mouse model of ascending urinary tract infection. *Infect. Immun.* **62**:3363 - 3371.

Bassler, B. L. 1999. How bacteria talk to each other: Regulation of gene expression by quorum sensing. *Curr. Opin. Microbiol.* **2**:582 - 587.

Belas, R., D. Erskine, and D. Flaherty. 1991a. Transposon mutagenesis in *Proteus mirabilis*. *J. Bacteriol.* **173:**6289 - 6293.

Belas, R., D. Erskine, and D. Flaherty. 1991b. *Proteus mirabilis* mutants defective in swarmer cell differentiation and multicellular behaviour. *J. Bacteriol.* **173:**6279 - 6288.

Belas, R. 1994. Expression of multiple flagellin-encoding genes of *Proteus mirabilis*. *J. Bacteriol.* **176:**7169 - 7181.

Belas, R., and D. Flaherty. 1994. Sequence and genetic analysis of multiple flagellin encoding genes from *Proteus mirabilis*. *Gene* **148:**33 - 41.

Belas, R., M. Goldman, and K. Ashliman. 1995. Genetic analysis of *Proteus mirabilis* mutants defective in swarmer cell elongation. *J. Bacteriol.* **177:**823 - 828.

Belas, R. 1996. *Proteus mirabilis* swarmer cell differentiation and urinary tract infection. In: *Urinary Tract Infections, Molecular Pathogenesis and Clinial Management.* **ASM Press, Washington D.C. Eds: H. L. T. Mobley & J. W. Warren:p**271 - 293.

Belas, R., R. Schneider, and M. Melch. 1998. Characterization of *Proteus mirabilis* precocious swarming mutants: identification of *rsbA*, encoding a regulator of swarming behaviour. *J. Bacteriol.* **180:**6126 - 6139.

Benz, I., and A. M. Schmidt. 2002. Never say never again: Protein glycosylation in pathogenic bacteria. *Mol. Microbiol.* **45:**267 - 276.

Berg, D. E. 1989. Transposon Tn*5*. In: *Mobile DNA* **American Society for Microbiology, Wahsington DC, Eds. Douglas E. Berg, Martha M. Howe: p**185 - 210.

Berg, D. E., and C. M. Berg. 1983. The prokaryotic transposable element Tn*5*. *Biotechnology* **1:**417 - 435.

Bergthorsson, U., and H. Ochman. 1998. Distribution of chromosome length variation in natural isolates of *Escherichia coli*. *Mol. Biol. Evol.* **15:**6 - 16.

Bibby, J. M., A. J. Cox, and D. W. L. Hukins. 1995. Feasibility of preventing encrustation of urinary catheters. *Cells Materials* **2:**183 - 195.

Bradley, C., J. Babb, J. Davies, and G. A. J. Ayliffe. 1986. Urinary tract infections in catheterised patients can be prevented. *Nursing Times.* **March 5th:** 70 - 73.

Bret, L., C. Chanal-Claris, D. Sirot, E. B. Chaibi, R. Labia, and J. Sirot. 1998. Chromosomally encoded AmpC-Type β-Lactamase in a clinical isolate of *Proteus mirabilis*. *Antimicrob. Agents Cemother.* **42:**1110 - 1114.

Brimer, C. D., and T. C. Montie. 1998. Cloning and comparison of *fliC* genes and identification of glycosylation in the flagellin of *Pseudomonas aeruginosa* a-Type strains. *J. Bacteriol.* **180:**3209 - 3217.

Brown, T. A. 2001. *Gene Cloning*, 4th Ed. Stanley Thomas Ltd.

Burke, J. P., R. A. Garibaldi, M. R. Britt, J. A. Jacboson, M. Conti, and D. W. Alling. 1981. Prevention of catheter-associated urinary tract infections: Efficacy of daily meatal care regimens. *Am. J. Med.* **70:**665 - 668.

Burke, J. P., J. A. Jacobson, R. A. Garibaldi, M. T. Conti, and D. W. Alling. 1983. Evaluation of daily meatal care with poly-antibiotic ointment in prevention of urinary catheter-associated bacteriuria. *J. Urol.* **129:**331 - 334.

Bultitude, M. I., and S. Eykyn. 1973. The relationship between the urethral flora and urinary tract infection in the catheterised male. *Br. J. Urol.* **45:**678 - 683.

Calvo, J. M., and R. G. Matthews. 1994. Leucine responsive regulatory protein - a global regulator of metabolism in *Eschericia coli*. *Microbiol. Rev.* **58:**466 - 490.

Chen, L., and J. D. Helman. 1994. The *Bacillus subtilis* sigmaD-dependant operon encoding the flagellar proteins FliD, FliS, and FliT. *J. Bacteriol.* **176:**3093 - 3101.

Chiang, S. L., J. J. Mekalanos, and D. W. Holden. 1999. *In vivo* genetic analysis of bacterial virulence. *Annu. Rev. Microbiol.* **53:**129 - 154.

Chiang, S. L., and J. J. Mekalanos. 1998. Use of signature-tagged transposon mutagenesis to identify *Vibrio cholerae* genes critical for colonization. *Mol. Microbiol.* **27:**797 - 805.

Clapham, L., R. J. C. McLean, J. C. Nickel, J. Downey, and J. W. Costerton. 1990. The influence of bacteria on struvite crystal habit and its importance in urinary stone formation. *J. Crystal Growth* **104:**475 - 484.

Clayton, C. L., J. C. Chawala, and D. J. Stickler. 1982. Some observations on urinary tract infections in patients undergoing long-term bladder catheterisation. *J. Hosp. Infect.* **3:**39 - 47.

Codling, C. E. 2004. Aspects of the antimicrobial mechanisms of action of a polyquaternium and an amidoamine. PhD Thesis. Welsh School of Pharmacy, Cardiff University, Cardiff.

Coker, C., A. C. Poore, X. Li, and H. L. T. Mobley. 2000. Pathogenesis of *Proteus mirabilis* urinary tract infection. *Microbes Infect.* **2:**1497 - 1505.

Collazo, C. M., and J. E. Galán. 1997. The invasion-associated type III system of *Salmonella typhimurium* directs the translocation of Sip proteins into the host cell. *Mol. Microbiol.* **24:**747 - 756.

Costerton, J. W., K. J. Cheng, G. G. Geesey, T. I. Ladd, J. C. Nickel, M. Dasgupta, and T. J. Marrie. 1987. Bacterial biofilms in nature and disease. *Annu. Rev. Microbiol.* **41:**435 - 464.

Costerton, W. J., Z. Lewandowski, D. E. Caldwell, D. R. Korber, and H. M. Lappin-Scott. 1995. Microbial biofilms. *Annu. Rev. Microbiol.* **49:**711 - 745.

Cowan, M. M., T. M. Warren, and M. Fletcher. 1991. Mixed species colonisation of solid surfaces in laboratoty biofilms. *Biofouling* **9:**23 - 34.

Cowan, S. T., and K. J. Steele. 1993. *Manual for the identification of medical bacteria.* 3rd ed. Cambridge: Cambridge University Press.

Cox, A. J., and D. W. L. Hukins. 1989. Morphology of mineral-deposits on encrusted urinary catheters investigated by scanning electron-microscopy. *J. Urol.* **142:**1347 - 1350.

Creno, R. J., R. E. Wenk, and P. Bohlig. 1970. Automated micromeasurement of urea using urease and the Berthelot reaction. *A. J. C. P.* **54:** 828 - 832.

Daifuku, R., and W. E. Stamm. 1984. Association of rectal and urethral colonization with urinary-tract infection in patients with indwelling catheters. *JAMA.* **252:**2028 - 2030.

Darouchie, R. O. 1999. Anti-infective efficacy of silver-coated medical prostheses. *Clin. Infect. Dis.* **29:**1371 - 1377.

Darouiche, R. O., H. Safar, and I. I. Raad. 1997. *In vitro* efficacy of antimicrobial-coated bladder catheters in inhibiting bacterial migration along catheter surfaces. *J. Infect. Dis.* **176:**1109 - 1112.

Davies, D. G., M. R. Parsek, J. P. Pearson, B. H. Iglewski, J. W. Costerton, and E. P. Greenberg. 1998. The involvement of cell-to-cell signals in the development of a bacterial biofilm. *Science.* **280:**295 - 298.

de Lorenzo, V., M. Herrero, U. Jakubzik, and K. N. Timmis. 1990. Mini-Tn*5* transposon derivatives for insertion mutagenesis, promotor probing, and chromosomal insertion of cloned DNA in Gram-negative eubacteria. *J. Bacteriol.* **172:**6568 - 6572.

de Lorenzo, V., and K. N. Timmis. 1994. Analysis and construction of stable phenotypes in Gram-negative bacteria with Tn*5*- and Tn*10*-derived mini-transposons. *Methods Enzymol.* **235**:386 - 405.

de Lorenzo, V., M. Herrero, J. M. Sanchez, and K. N. Timmis. 1998. Mini-transposons in microbial ecology and environmental biotechnology. *FEMS Microbiol. Ecol.* **27**:211 - 224.

Deakin, W. J., V. E. Parker, E. L. Wright, K. J. Ashcroft, G. J. Loake, and C. H. Shaw. 1999. *Agrobacterium tumefaciens* possesses a fourth flagellin gene located in a large gene cluster concerned with flagellar structure, assembly and motility. *Microbiology.* **145**:1397 - 1407.

Déziel, E., Y. Comeau, and R. Villemur. 2001. Initiation of biofilm formation by *Pseudomonas aeruginosa* 57RP correlates with emergence of hyperpiliated and highly adherent phenotypic varients deficient in swimming, swarming, and twitching motilities. *J. Bacteriol.* **183**:1195 - 1204.

Dobrint, U., F. Agerer, K. Michaelis, A. Janka, C. Buchrieser, M. Samuelson, C. Svanborg, G. Gottschalk, H. Karch, and J. Hacker. 2003. Analysis of genome plasticity in pathogenic and commensal *Eschericia coli* isolates by use of DNA arrays. *J. Bacteriol.* **185**:1831 - 1840.

Doig, P., N. Kinsella, P. Guerry, and T. J. Trust. 1996. Characterization of a post-translational modification of *Campylobacter* flagellin: identification of a sero-specific glycosyl moiety. *Mol. Microbiol.* **19**:379 - 389.

Donlan, R. M. 2001. Biofilms and device-associated infections. *Emerg. Infect. Dis.* **7**:277 - 281.

Donlan, R. M. 2002. Biofilms: Microbial life on surfaces. *Emerg. Infect. Dis.* **8**:881 - 890.

Donlan, R. M., and J. W. Costerton. 2002. Biofilms: Survival mechanisms of clinically relevant microorganisms. *Clin. Microbiol. Rev.* **15**:167 - 193.

Dufour, A., R. B. Furness, and C. Hughes. 1998. Novel genes that upregulate the *Proteus mirabilis flhDC* master operon controlling flagellar biogenesis and swarming. *Mol. Microbiol.* **29**:741 - 751.

Dumanski, A. J., H. Hedelin, A. Edinliljegren, D. Beauchemin, and R. J. C. McLean. 1994. Unique ability of the *Proteus mirabilis* capsule to enhance mineral growth in infectious urinary calculi. *Infect. Immun.* **62**:2998 - 3003.

Eberel, L., S. Molin, and M. Givskov. 1999. Surface motility of *Serratia liquefaciens* MG1. *J. Bacteriol.* **181**:1703 - 1712.

Edwards, U., A. Muller, S. Hammerschmidt, R. Gerardy-Schahn, and M. Frosch. 1994. Molecular analysis of the biosynthesis pathway of the alpha-2,8 polysialic acid capsule by *Neisseria meningitidis* serogroup B. *Mol. Microbiol.* **14**:141 - 149.

Esipov, S. E., and J. A. Shapiro. 1998. Kinetic model of *Proteus mirabilis* swarm colony development. *J. Math. Biol.* **36**:249 - 268.

Fawcett, C., J. C. Chawla, A. Quoraishi, and D. J. Stickler. 1986. A study of the skin flora of spinal-cord injured patients. *J. Hosp. Infect.* **8**:149 - 158.

Fleiszig, S. J. M., S. K. Arora, R. Van, and R. Ramphal. 2001. FlhA, a Component of the flagellum assembly apparatus of *Pseudomonas aeruginosa*, plays a role in internalization by corneal epithelial cells. *Infect. Immun.* **69**:4931 - 4937.

Fraser, G. M., R. B. Furness, and C. Hughs. 2000. Swarming migration by *Proteus* and related bacteria In: *Prokaryotic Development.* **American Society for Microbiology, Washington, DC. Eds: Brun, Y. V., and Shimkets, L. J:** p381 - 401.

Fraser, G. M., and C. Hughes. 1999. Swarming motility. *Curr. Opin. Microbiol.* **2**:630 - 635.

Fry, J. C. 1993. *Biological data analysis: A practical approach.* Oxford Universtiy Press, Oxford, United Kingdom.

Furness, R. B., G. M. Fraser, N. A. Hay, and C. Hughes. 1997. Negative feedback from a *Proteus* class II flagellum export defect to the *flhDC* master operon controlling cell division and flagellum assembly. *J. Bacteriol.* **179**:5585-5588.

Ganderton, L., J. Chawla, C. Winters, J. Wimpenny, and D. Stickler. 1992. Scanning electron-microscopy of bacterial biofilms on indwelling bladder catheters. *Eur. J. Clin. Microbiol. Infect. Dis.* **11**:789 - 796.

Gavín, R., S. Merino, M. Altarriba, R. Canals, J. G. Shaw, and J. M. Tomás. 2003. Lateral flagella are required for increased cell adherence, invasion and biofilm formation by *Aeromonas* spp. *FEMS Microbiol. Let.* **224**:77 - 83.

Getliffe, K. A., and A. B. Mulhall. 1991. The encrustation of indwelling catheters. *Br. J. Urol.* **67**:337 - 341.

Gillespie, W. A., J. E. Jones, C. Teasdale, R. A. Simpson, L. Nashef, and D. C. E. Speller. 1983. Does the addition of disinfectant to urine drainage bags prevent infection in catheterized patients. *Lancet.* **i**:1037 - 1039.

Ginnocchio, C. C., and J. E. Galán. 1995. Functional conservation among members of the *Salmonella typhimurium* InvA family of proteins. *Infect. Immun.* **63**:729 - 732.

Griffith, D. P., J. R. Gibson, C. W. Clinton, and D. M. Musher. 1978. Acetohydroxamic acid: Clinical studies of a urease inhibitor in patients with staghorn calculi. *J. Urol.* **119**:9 - 15.

Griffith, D. P., Musher D. M., and Itin C. 1976. Urease: The preliminary cause of infection induced urinary stones. *Invest. Urol.* **13**:346 - 350.

Groisman, E. A., M. A. Sturmoski, F. R. Solomon, R. Lin, and H. Ochman. 1993. Molecular, functional, and evolutionary analysis of sequences specific to *Salmonella*. *Proc. Natl. Acad. Sci. USA.* **90**:1033 - 1037.

Gygi, D., M. J. Bailey, C. Allison, and C. Hughes. 1995a. Requirement for FlhA in flagella assembly and swarm-cell differntiation by *Proteus mirabilis*. *Mol. Microbiol.* **15**:761 - 769.

Gygi, D., G. Fraser, A. Dufour, and C. Hughes. 1997. A motile but non-swarming mutant of *Proteus mirabilis* lacks FlgN, a facillitator of flagella filament assembly. *Mol. Microbiol.* **25**:597 - 604.

Gygi, D., M. M. Rahman, H. C. Lai, R. Carlson, J. Guardpetter, and C. Hughes. 1995b. A cell-surface polysaccharide that facilitates rapid population migration by differentiated swarm cells of *Proteus mirabilis*. *Mol. Microbiol.* **17**:1167 - 1175.

Hansen, L. H., S. J. Sorensen, and L. B. Jensen. 1997. Chromosomal insertion of the entire *Escherichia coli* lactose operon, into two strains of *Pseudomonas*, using a modified mini-Tn*5* delivery system. *Gene* **186**:167 - 173.

Hay, N. A., D. J. Tipper, D. Gygi, and H. C. 1999. A novel membrane protien influencing cell shape and multicellular swarming of *Proteus mirabilis*. *J. Bacteriol.* **181**:2008 - 2016.

Hay, N. A., D. J. Tipper, D. Gygi, and C. Hughes. 1997. A nonswarming mutant of *Proteus mirabilis* lacks the Lrp global transcriptional regulator. *J. Bacteriol.* **179**:4741 - 4746.

Hedelin, H., A. Eddeland, L. Larsson, S. Pettersson, and S. Ohman. 1984. The composition of catheter encrustations, including the effects of allopurinol treatment. *Br. J. Urol.* **56**:250 - 254.

Henrichsen, J. 1972. Bacterial surface translocation: a survey and a classification. *Bacteriol. Rev.* **36**:478 - 503.

Hensel, M., and D. W. Holden. 1996. Molecular genetic approaches for the study of virulence in both pathogenic bacteria and fungi. *Microbiology.* **142**:1049 - 1058.

Hensel, M., J. E. Shea, C. Gleeson, M. D. Jones, E. Dalton, and D. W. Holden. 1995. Simultaneous identification of bacterial virulence genes by negative selection. *Science.* **269:**400 - 403.

Herrero, M., V. de Lorenzo, and K. N. Timmis. 1990. Transposon vectors containing non-antibiotic resistance selection markers for cloning and stable chromosomal insertion of foreign genes in Gram-negative bacteria. *J. Bacteriol.* **172:**6557 - 6567.

Hughes, G. G. 2001. A study of *Proteus mirabilis* biofilm formation on indwelling urethral catheters. PhD Thesis: Cardiff School of Biosciences, Cardiff University. Cardiff.

Hughes, K. T., K. L. Gillen, M. J. Semon, and J. E. Karlinsey. 1993. Sensing structural intermediates in bacterial flagellar assembly by export of a negative regulator. *Science.* **262:**1277 - 1280.

Isberg, R. R., and S. Falkow. 1985. A single genetic locus encoded by *Yersinia pseudotuberculosis* permits invasion of cultured animal cells by *Escherichia coli* K12. *Nature* **317:**263 - 264.

Jansen, A. M., V. C. Lockatell, D. E. Johnson, and H. L. T. Mobley. 2003. Visualization of *Proteus mirabilis* morphotypes in the urinary tract: The elongated swarmer cell is rarely observed in ascending urinary tract infection. *Infect. Immun.* **71:**3607 - 3613.

Jepsen, O. B., Olesen Larsen S., D. F. Dankert J., Gronroos P., Meers P.D., Nystrom B., Rotter M., and Sander J. 1982. Urinary-tract infection and bacteraemia in hospitalized medical patients - a European multicentre prevalence survey on nosocomial infection. *J. Hosp. Infect.* **3:**241 - 252.

Jewes, L. A., W. A. Gillespie, A. Leadbetter, B. Myers, R. A. Simpson, M. J. Stower, and A. C. Viant. 1988. Bacteriuria and bacteraemia in patients with long-term indwelling catheters - a domiciliary study. *J. Med. Microbiol.* **26:**61 - 65.

Jin, T., and R. G. Murray. 1988. Further studies of swarmer cell differentiation of *Proteus mirabilis* PM32: A requirement for iron and zinc. *Can. J. Microbiol.* **34:**588 - 593.

Johnson, D. E., R. G. Russell, C. V. Lockatell, J. C. Zulty, J. W. Warren, and H. L. T. Mobley. 1993. Contribution of *Proteus mirabilis* urease to persistence, urolithiasis, and acute pyelonephritis in a mouse model of ascending urinary tract infection. *Infect. Immun.* **61:**2748 - 2745.

Johnson, J. R., P. L. Roberts, R. J. Olsen, K. A. Moyer, and W. E. Stamm. 1990. Prevention of catheter-associated urinary tract infection with a silver oxide-coated urinary catheter: Clinical and microbiological correlates. *J. Infect. Dis.* **162:**1145 - 1150.

Josenhans, C., L. Vossebein, S. Friedrich, and S. Suerbaum. 2002. The *neuA/flmD* gene cluster of *Helicobacter pylori* is involved in flagellar biosynthesis and flagellin glycosylation. *FEMS Microbiol. Lett.* **210:**165 - 172.

Kado, C. I. 2002. Native transcriptional regulation of virulence and oncogenes of the Ti-plasmid by Ros bearing a conserved C2H2-zinc finger motif. *Plasmid.* **48:**179 - 185.

Kanto, S., H. Okino, and S-I. Aizawa. 1991. Amino acids responsibe for flagellar shape are distributed in terminal regions of flagellin. *J. Mol. Biol.* **219:**471 - 480.

Kass, E. H., and L. J. Schneiderman. 1957. Entry of bacteria into the urinary tracts of patients with inlying catheters. *N. Engl. J. Med.* **256:**556 - 557.

Kawagishi, I., V. Müller, A. W. Williams, V. M. Irikura, and R. M. Macnab. 1992. Subdivision of flagellar region III of the *Eschericia coli* and *Salmonella typhimurium* chromosomes and identification of two additional flagellar genes. *J. Gen. Microbiol.* **138:**1051 - 1065.

Kirov, S. M. 2003. Bacteria that express lateral flagella enable dissection of the multifunctional roles of flagella in pathogenesis. *FEMS Microbiol. Lett.* **224:**151 - 159.

Kirov, S. M., B. C. Tassell, A. B. T. Semmler, O'Donavan. L. A., A. A. Rabaan, and J. G. Shaw. 2002. Lateral flagella and swarming motility in *Aeromonas* Species. *J. Bacteriol.* **184:**547 - 555.

Klausen, M., A. Heydorn, P. Ragas, L. Lambersten, A. Aaes-Jorgensen, S. Molin, and T. Tolker-Nielsen. 2003. Biofilm formation by *Pseudomonas aeruginosa* wild type, flagella and type IV pili mutants. *Mol. Microbiol.* **48:**1511 - 1524.

Kleckner, N. 1989. Transposon Tn*10* In: *Mobile DNA.* **American Society for Microbiology, Wahsington DC, Eds. Douglas E. Berg, Martha M. Howe:** p227 - 268.

Kleckner, N., J. Bender, and S. Gottesman. 1991. Uses of transposons with emphasis on Tn*10*. *Methods Enzymol.* **204:**139 - 180.

Kunin C.M. 1987. *Detection, Prevention and Management of Unrinary Tract Infections* 4th Ed, Lea and Febiger, Philadelphia.

Kunin, C. M., Q. F. Chin, and S. Chambers. 1987. Formation of encrustations on indwelling urinary catheters in the elderly: A comparison of different types of catheter materials in "blockers" and "nonblockers". *J. Urol.* **138:**899 - 902.

Kunin, C. M. 1989. Blockage of urinary catheters: Role of microorganisms and constituents of the urine on formation of encrustations. *J. Clin. Epidemiol.* **42:**835 - 842.

Kunin C. M., S. Douthitt, Dancing J., Anderson J., and Moeschberger M. 1992. The association between the use of urinary catheters and morbidity and mortality among elderly patiens in nursing homes. *Am. J. Epidemiol.* **135:**291 - 301.

Kutsukake, K., and T. Iino. 1994. Role of the FliA-FlgM regulatory system on the transcriptional control of the flagellar regulon and flagellar formation in *Salmonella typhimurium. J. Bacteriol.* **176:**3598 - 3605.

Lai, H. C., D. Gygi, G. M. Fraser, and C. Hughes. 1998. A swarming-defective mutant of *Proteus mirabilis* lacking a putative cation-transporting membrane P-type ATPase. *Microbiology.* **144:**1957 - 1961.

Lan, R., B. Lumb, D. Ryan, and P. R. Reeves. 2001. Molecular evolution of large virulence plasmid in *Shigella* clones and enteroinvasive *Escherichia coli. Infect. Immun.* **69:**6303 - 6309.

Lazar, S. W., and R. Kolter. 1996. SurA assists the folding of *Eschericia coli* outer membrane proteins. *J. Bacteriol.* **178:**1770 - 1773.

Lazar, S. W., M. Almirón, A. Tormo, and R. Kolter. 1998. Role of the *Escherichia coli* SurA protein in stationary-phase survival. *J. Bacteriol.* **180:**5704 - 5711.

Legnani-Fajardo, C., P. Zunino, C. Piccini, A. Allen, and D. Maskell. 1996. Defined mutants of *Proteus mirabilis* lacking flagella cause ascending urinary tract infection in mice. *Microb. Pathog.* **21:**395 - 405.

Leigh, J. A., and G. C. Walker. 1994. Exopolysaccharides of *Rhizobium*: synthesis, regulation and symbiotic function. *Trends Gent.* **10:**63 - 67.

Leigh, J. A., E. R. Singer, and G. C. Walker. 1985. Exopolysaccharide-deficient mutants of *Rhizobium meliloti* that form ineffective nodules. *Proc. Natl. Acad. Sci. USA* **82:**6231 - 6235.

Lewenza, S., B. Conway, E. P. Greenberg, and P. A. Sokol. 1999. Quorum sensing in *Burkholderia cepacia*: Identification of the LuxRI homologs CepRI. *J. Bacteriol.* **181:**748-756.

Li, X., D. A. Rasko, V. C. Lockatell, D. E. Johnson, and H. L. T. Mobley. 2001. Repression of bacterial motility by a novel fimbrial gene product. *EMBO J.* **20:**4854 - 4862.

Li, X., H. Zhao, C. V. Lockatell, C. B. Drachenberg, D. E. Johnson, and H. L. T. Mobley. 2002. Visualisation of *Proteus mirabilis* within the matrix of urease-induced bladder stones during experimental urinary tract infection. *Infect. Immun.* **70:**389 - 394.

Liang, X., X-Q. T. Pham, M. V. Olson, and S. Lory. 2001. Identification of a genomic island present in the majority of pathogenic isolates of *Pseudomonas aeruginosa*. *J. Bacteriol.* **183:**843 - 853.

Liedberg, H., and T. Lundberg. 1990. Silver alloy coated catheters reduce catheter-associated bacteriuria. *Br. J. Urol.* **65:**379 - 381.

Lindum, P. W., U. Anthoni, C. Christophersomn, L. Eberl, S. Molin, and M. Givskov. 1998. *N*-acyl-L-homoserine lactone autoinducers control production of an extracellular lipopeptide biosurfactant required for swarming motility of *Serratia liquefaciens* MG1. *J. Bacteriol.* **180:**6384 - 6388.

Locke, J. R., D. E. Hill, and Y. Walzer. 1985. Incidence of squamous-cell carcinoma in patients with long-term catheter drainage. *J. Urol.* **133:**1034 - 1035.

Lodge, J. K., and D. E. Berg. 1990. Mutations that affect Tn*5* insertion into pBR322: Importance of local DNA supercoiling. *J. Bacteriol.* **172:**5956 - 5960.

Lominski, I., and A. C. Lendrum. 1947. The mechanism of swarming of *Proteus*. *J. Pathol. Bacteriol.* **59:**688 - 691.

Lundberg, T. 1986. Prevention of catheter-associated urinary tract infections by use of silver-impregnated catheters. *Lancet.* **I:**1031.

Macnab, R. M. 1992. Genetics and biogenesis of bacterial flagella. *Annu. Rev. Genet.* **26:**131 - 158.

Mahan, M. J., J. M. Slauch, and J. J. Mekalanos. 1993. Selection of bacterial virulence genes that are specifically induced in host tissues. *Science.* **259:**686 - 688.

Mahenthiralingam, E., B-I. Marklund, L. A. Brooks, D. A. Smith, G. J. Bancroft, and R. W. Stokes. 1998. Site-directed mutagenesis of the 19-Kilodalton lipoprotein antigen reveals no essential role for the protein in the growth and virulence of *Mycobacterium intracellulare*. *Infect. Immun.* **66:**3626 - 3634.

Matsuyama, T., K. Kaneda, Y. Nakagawa, K. Isa, H. Hara-Hotta, and I. Yano. 1992. A novel extracellular cyclic lipopeptide which promotes flagellum-dependant and independant spreading growth of *Serratia marcesens*. *J. Bacteriol.* **174:**1769 - 1776.

McLean, R. J. C., J. R. Lawrence, D. R. Korber, and D. E. Caldwell. 1991. *Proteus mirabilis* biofilm protection against struvite crystal dissolution and its implications in struvite urolithiasis. *J. Urol.* **146:**1138 - 1142.

McLean, R. J. C., M. Whiteley, D. J. Stickler, and W. C. Fuqua. 1997. Evidence of autoinducer activity in naturally occurring biofilms. *FEMS Microbiol. Lett.* **154:**259 - 263.

Meers, P. D., Ayliff G. A. J., and Emmerson A. M. 1980. National survey of infection in hospitals. part 2: Urinary tract infection. *J. Hosp. Infect.* **Supplement 2:**23 - 28.

Merriman, T. R., and I. L. Lamont. 1993. Construction and use of a self-cloning promoter probe vector for Gram-negative bacteria. *Gene.* **126:**17 - 23.

Miller, D. A., and E. Mahenthiralingam. 2003. Sequencing of the *Pseudomonas aeruginosa* and *Burkholderia cepacia* genomes and their applications in relation to cystic fibrosis. *J. Royal Soc. Med.* **96(Suppl 43):** 1 - 9.

Miller, J. M. 1975. The effect of hydron on latex urinary catheters. *J. Urol.* **113:**530.

Miller, V., and J. Mekalanos. 1988. A novel suicide vector and its use in construction of insertion mutants: Osmoregulation of outer membrane proteins and virulence determinants in *Vibrio cholerae* requires *toxR*. *J. Bacteriol.* **170:**2575 - 2583.

Mireles II, J. R., A. Toguchi, and R. M. Harshey. 2001. *Salmonella enterica* serovar *Typhimurium* swarming mutants with altered biofilm-forming abilities: Surfactin inhibits biofilm formation. *J. Bacteriol.* **183**:5848 - 5854.

Mobley, H. L. T. 1996. Virulence of *Proteus mirabilis*. In: *Urinary tract infections, molecular pathogenesis and clinial management.* **ASM Press, Washington D.C. Eds: H. L. T. Mobley & J. W. Warren:** p245 - 265.

Mobley, H. L. T., M. D. Island, and R. P. Hausinger. 1995. Molecular biology of microbial ureases. *Microbiol. Rev.* **59**:451 - 480.

Mobley, H. L. T., and J. W. Warren. 1987. Urease-positive bacteriuria and obstruction of long-term urinary catheters. *J. Clin. Microbiol.* **25**:2216 - 2217.

Morano, J. 2003. Personal communication.

Morris, N. S., D. J. Stickler, and C. Winters. 1997. Which indwelling urethral catheters resist encrustation by *Proteus mirabilis* biofilms? *Br. J. Urol.* **80**:58 - 63.

Muder, R. R., C. Brennen, M. M. Wagener, and A. M. Goetz. 1992. Bactereamia in a long-term-care facility: a five year prospective study of 163 consecutive episods. *Clin. Infect. Dis.* **14**:647 - 654.

Murphy, C. A., and R. Belas. 1999. Genomic rearrangements in the flagellin genes of *Proteus mirabilis*. *Mol. Microbiol.* **31**:679 - 690.

Nataro, J. P., and J. B. Kaper. 1998. Diarrheagenic *Eschericia coli*. *Clin. Microbiol. Rev.* **11**:142 - 201.

Nickel J. C. 1991. Catheter-associated urinary tract infection: New perspectives on old problems. *Can. J. Infect. Cont.* **6**:38 - 42.

Ørskov, F., and I. Ørskov. 1992. *Eschericia coli* serotyping and disease in man and animals. *Can. J. Microbiol.* **38**:699 - 704.

Ohkawa, M., T. Sugata, M. Sawaki, T. Nakashima, H. Fuse, and H. Hisazumi. 1990. Bacterial and crystal adherence to the surfaces of indwelling urethral catheters. *J. Urol.* **143**:717 - 721.

O'Toole, G. A., and R. Kolter. 1998a. Flagellar and twitching motility are necessary for *Pseudomonas aeruginosa* biofilm development. *Mol. Microbiol.* **30**:295-304.

O'Toole, G. A., and R. Kolter. 1998b. Initiation of biofilm formation in *Pseudomonas fluorescens* WCS365 proceeds via multiple, convergent signalling pathways: a genetic analysis. *Mol. Microbiol.* **28**:449-461.

Parker, C. T., A. W. Kloser, C. A. Schnaitman, M. A. Stein, S. Gottesman, and B. W. Gibson. 1992. Role of the *rfaG* and *rfaP* genes in determining the lipopolysaccharide core structure and cell surface properties of *Escherichia coli* K-12. *J. Bacteriol.* **174**:2525 - 2538.

Platt, R., B. Murdock, B. F. Polk, and B. Rosner. 1983. Reduction of mortality associated with nosocomial urinary-tract infection. *Lancet* **i**:893 - 897.

Platt, R., B. F. Polk, B. Murdock, and B. Rosner. 1982. Mortality associated with nosocomial urinary-tract infection. *N. Engl. J. Med.* **307**:637-642.

Pratt, L. A., and R. Kolter. 1999. Genetic analysis of biofilm formation. *Curr. Opin. Microbiol.* **2**:598 - 603.

Pratt, L. A., and R. Kolter. 1998. Genetic analysis of *Escherichia coli* biofilm formation: roles of flagella, motility, chemotaxis and type I pili. *Mol. Microbiol.* **30**:285 - 293.

Prigent-Combaret, C., G. Prensier, T. T. L. Thi, O. Vidal, P. Lejeune, and C. Dorel. 2000. Developmental pathway for biofilm formation in curli-producing *Escherichia coli* strains: Role of flagella, curli and colanic acid. *Environ. Microbiol.* **2**:450 - 464.

Prüß, B. M., and P. Matsumura. 1996. A regulator of the flagellar regulaon of *Escherichia coli flhD*, also affects cell division. *J. Bacteriol.* **178**:668 - 674.

Ramsey, J. W. A., A. J. Garnham, A. B. Mulhall, R. A. Crow, J. M. Bryan, I. Eardley, J. A. Vale, and H. N. Whitfield. 1989. Biofilms, bacteria, and bladder catheters. *Br. J. Urol.* **64**:395 - 398.

Rauprich, O., M. Matsushita, C. J. Weijier, F. Siegert, S. E. Esipov, and J. A. Shapiro. 1996. Periodic phenomena in *Proteus mirabilis* swarm colony development. *J. Bacteriol.* **178**:6525 - 6538.

Reznikoff, W. S. 2002. Tn*5* transposition. *Mobile DNA 2.* **ASM press Washington D. C. Eds: Craig, N. L., Craigie R., Gellent M., Lambowitz A. M:** p403 - 422.

Rizzitello, A. E., J. R. Harper, and T. J. Silhavy. 2001. Genetic evidence for parallel pathways of caperone activity in the periplasm of *Escherichia coli. J. Bacteriol.* **183**:6794 - 6800.

Römling, U., and M. Rhode. 1999. Flagella modulate the multicellular behavior of *Salmonella typhimurium* on the community level. *FEMS Microbiol. Lett.* **180**:91 - 102.

Rudman, D., A. Hontanosas, Z. Cohen, and D. E. Matteson. 1988. Clinical correlates of bactereamia in a veterans administration extended care facility. *J. Am. Geriatr. Soc.* **36**:726 - 732.

Sabbuba, N., G. Hughes, and D. J. Stickler. 2002. The migration of *Proteus mirabilis* and other urinary tract pathogens over Foley catheters. *Br. J. Urol.* **89**:55 - 60.

Sabbuba, N. A., E. Mahenthiralingam, and D. J. Stickler. 2003. Molecular epidemiology of *Proteus mirabilis* infections of the catheterized urinary tract. *J. Clin. Microbiol.* **41**:4961 - 4965.

Saint, S., and B. A. Lipsky. 1999. Preventing catheter-related bacteriuria - Should we? Can we? How? *Arch. Intern. Med.* **159**:800 - 808.

Sambrook, J., E. F. Fritsch, and T. Maniatis. 1989. *Molecular cloning: a laboratory manual.* 2nd cd. Cold Spring Harbour Laboratory Press Cold Spring Harbour NY.

Sauer, K., A. K. Camper, G. D. Ehrlich, W. J. Costerton, and D. G. Davies. 2002. *Pseudomonas aeruginosa* displays multiple phenotypes during development as a biofilm. *J. Bacteriol.* **184**:1140 - 1154.

Scott, A. C. 1989. Laboratory control of antimicrobial therapy. In*: Mackie & McCarteny practical medical microbiology*, 13th ed. **Churchill Livingston. Eds: J. G. Collee, J. P. Dogvid, A. G. Fraser, B. D. Marmion**: p161 - 181.

Schaeffer, A. J., and J. Chmiel. 1983. Urethral meatal colonization in the pathogenesis of catheter-associated bacteriuria. *J. Urol.* **130**:1096 - 1099.

Schneider, R., V. C. Lockatell, D. Johnson, and R. Belas. 2002. Detection and mutation of a *luxS*-encoded autoinducer in *Proteus mirabilis. Microbiology.* **148**:773 - 782.

Sherratt, D. 1989. Tn*3* and related transposible elements: Site-specific recombination and transposition. In: *Mobile DNA.* **American Society for Microbiology, Wahsington DC, Eds. Douglas E. Berg, Martha M. Howe:** p163 - 184.

Simon, R., J. Quandt, and W. Klipp. 1989. New derivatives of transposon Tn*5* suitable for mobilization of replicons, generation of operon fusions and induction of genes in Gram-negative bacteria. *Gene.* **80**:161 - 169.

Šmajs, D., and G. M. Weinstock. 2001a. Genetic organisation of plasmid ColJs, encoding Colicin Js activity, immunity, and release genes. *J. Bacteriol.* **183**:3949 - 3957.

Šmajs, D., and G. M. Weinstock. 2001b. The iron- and tempterature-regulated *cjrBC* genes of *Shigella* and enteroinvasive *Escherichia coli* strains code for colicin Js uptake. *J. Bacteriol.* **183:**3586 - 3966.

Sokol, P. A., P. Darling, D. E. Woods, E. Mahenthiralingam, and C. Kooi. 1999. Role of ornibactin biosynthesis in the virulence of *Burkholderia cepacia*: Characterization of *pvdA*, the gene encoding *L*-ornithine N^5-oxygenase. *Infect. Immun.* **67:**4443 - 4455.

Southampton Infection Control Team. 1982. Evaluation of aseptic techniques and chlorhexidine on the rate of catheter-associated urinary-tract infection. *Lancet* **319:**89 - 91.

Stamm, W. E. 1991. Catheter-associated urinary tract infections: Epidemiology, pathogenesis, and prevention. Am. J. Med. **91(suppl 3b):**65 - 71.

Stickler, D., and G. Hughes. 1999. Ability of *Proteus mirabilis* to swarm over urethral catheters. *Eur. J. Clin. Microbiol. Infect. Dis.* **18:**206 - 208.

Stickler, D., N. Morris, M. C. Moreno, and N. Sabbuba. 1998b. Studies on the formation of crystalline bacterial biofilms on urethral catheters. *Eur. J. Clin. Microbiol. Infect. Dis.* **17:**649 - 652.

Stickler, D. J. 1996a. Biofilms, catheters and urinary tract infections. *Eur. Urol. Update Series.* **5:**1 - 8.

Stickler, D. J. 1996b. Bacterial biofilms and the encrustation of urethral catheters. *Biofouling.* **9:**293 - 305.

Stickler, D. J. 2002. Susceptibility of antibiotic-resistant Gram-negative bacteria to biocides: A perspective from the study of catheter biofilms. *J. Appl. Microbiol. Symposium Supplement* **92:**163S - 170S.

Stickler, D. J., L. Ganderton, J. King, J. Nettleton, and C. Winters. 1993. *Proteus mirabilis* biofilms and the encrustation of urethral catheters. *Urol. Res.* **21:**407 - 411.

Stickler, D. J., R. Young, G. Jones, N. Sabbuba, and N. Morris. 2003. Why are Foley catheters so vulnerable to encrustation and blockage by crystalline bacterial biofilm? *Urol. Res.* **31:**306 - 311.

Stickler, D. J., and J. C. Chawla. 1987. The role of antiseptics in the management of patients with long-term indwelling bladder catheters. *J. Hosp. Infect.* **10:**219 - 228.

Stickler, D. J., and R. J. C. McLean. 1995. Biomaterials associated infections - the scale of the problem. *Cells Materials.* **5:**167 - 182.

Stickler, D. J., N. S. Morris, R. J. C. McLean, and C. Fuqua. 1998a. Biofilms on indwelling urethral catheters produce quorum-sensing signal molecules *in situ* and *in vitro*. *Appl. Environ. Microbiol.* **64:**3486 - 3490.

Stickler, D. J., and J. Zimakoff. 1994. Complications of urinary-tract infections associated with devices used for long-term bladder management. *J. Hosp. Infect.* **28:**177 - 194.

Stover, S. L., L. K. Lloyd, K. B. Waites, and A. B. Jackson. 1991. Neurogenic urinary tract infection. *Neurol. Clin.* **9:**741 - 755.

Sutherland, I. W., L. C. Skillman, and K. A. Hughes. 1999. Polysaccharides in biofilms and their interactions with phage and antimicrobials. In: *Biofilms: the good, the bad, and the ugly.* 4th Annual meeting of the biofilm club. **Cardiff Bioline, Eds: J. Wimpenny, P. Gilbert, J. Walker, M. Broding, R. Baystone:** p179 - 187.

Sydenham, M., G. Douce, F. Bowe, S. Ahmed, S. Chatfield, and G. Dougan. 2000. *Salmonella enterica* serovar *Typhimurium surA* mutants are attenuated and effective live oral vaccines. *Infect. Immun.* **68:**1109 - 1115.

Tolker-Nielsen, T., U. C. Brinch, P. C. Ragas, J. B. Andersen, C. S. Jacobsen, and S. Molin. 2000. Development and dynamics of *Pseudomonas* sp. biofilms. *J. Bacteriol.* **182:**6482 - 6489.

Tomb, J-F., O. White, A-R. Kerlavage, R. A. Clayton, G. G. Sutton, R. D. Fleischmann, K. A. Ketchum, H. P. Klenk, S. Gill, B. A. Dougherty, K. Nelson, J. Quackenbush, L. Zhou, E. F. Kirkness, S. Peterson, B. Loftus, D. Richardson, R. Dodson, H. G. Khalak, A. Glodek, K. McKenney, L. M. Fitzegerald, N. Lee, M. D. Adams, E. K. Hickey, D. E. Berg, J. D. Gocayne, T. R. Utterback, J. D. Peterson, J. M. Kelley, M. D. Cotton, J. M. Weidman, C. Fujii, C. Bowman, L. Watthey, E. Wallin, W. S. Hayes, M. Borodovsky, P. D. Karp, H. O'Smith, C. M. Fraser, and J. C. Venter. 1997. The complete genome sequence of the gastric pathogen *Helicobacter pylori*. *Nature* **388:**539 - 547.

Totten, P. A., C. J. Lara, and S. Lory. 1990. The *rpoN* gene product of *Pseudomonas aeruginosa* is required for expression of diverse genes, including the flagellin gene. *J. Bacteriol.* **172:**389 - 396.

Tribe, C. R., and J. R. Silver. 1969. Renal failure in paraplegia. *Pitman medical publishing Co.*

Venkatesan, M. M., M. B. Goldberg, D. J. Rose, E. J. Grotbeck, V. Burland, and F. R. Blattner. 2001. Complete DNA sequence and analysis of the large virulence plasmid of *Shigella flexneri*. *Infect. Immun.* **69:**3271 - 3285.

Vidal, O. L., R. C. Prigent-Combaret, C. Dorel, M. Hoorman, and P. Lejune. 1998. Isolation of an *Eschericia coli* K-12 mutant strain able to form biofilms on inert surfaces: involvement of a new *ompR* allele that increases curli expression. *J. Bacteriol.* **180:**2442 - 2449.

Walker, K. E., S. Moghaddame-Jafari, V. C. Lockatell, D. Johnson, and R. Belas. 1999. ZapA, the IgA-degrading metallopprotease of *Proteus mirabils*, is a virulence factor expressed specifically in swarmer cells. *Mol. Microbiol.* **32:**825 - 836.

Warren J. W. 1991. The catheter and urinary tract infection. *Med. Clin. North Am.* **75:**481 - 493.

Warren, J. W., H. L. Muncie Jr., and M. Hall-Craggs. 1988. Acute pyelonephritis associated with bacteriuria during long-term catheterization: a prospective clinopathological study. *J. Urol.* **158:**1341 - 1346.

Warren, J. W. 1996. Clinical presentations and epidemiology of urinary tract infections. In: *Urinary tract infections, molecular pathogenesis and clinical management.* **ASM Press, Washington D.C. Eds: H. L. T. Mobley & J. W. Warren:** p3 - 27.

Warren, J. W., R. Platt, T. R. J., B. Rosner, and E. H. Kass. 1978. Antibiotic irrigation and catheter associated urinary tract infections. *N. Engl. J. Med.* **299:**570 - 573.

Warren, J. W., H. L. Muncie, E. J. Bergquist, and J. M. Hoopes. 1981. Sequelae and management of urinary-infection in the patient requiring chronic catheterization. *J. Urol.* **125:**1 - 8.

Watnick, P. I., K. J. Fullner, and R. Kolter. 1999. A role for the mannose-sensitive hemagglutinin in biofilm formation by *Vibrio cholerae* El Tor. *J. Bacteriol.* **181:**3606 - 3609.

Watnick, P. I., and R. Kolter. 1999. Steps in the development of a *Vibrio cholerae* El Tor biofilm. *Mol. Microbiol.* **34:**586 - 595.

Watnick, P. I., C. M. Lauriano, K. E. Klose, L. Croal, and R. Kolter. 2001. The absence of a flagellum leads to altered colony morphology, biofilm development and viurulence in *Vibrio cholerae* O139. *Mol. Microbiol.* **39:**223 - 235.

Wigfield, S. M., G. P. Rigg, M. Kavari, A. K. Webb, R. C. Mattews, and J. P. Burnie. 2002. Identification of an immunodominat drug efflux pump in *Burkholderia cepacia*. *J. Antimicrob. Chemother.* **49:**619 - 624.

Williams, F. D., D. M. Anderson, P. S. Hoffman, R. H. Schwarzhoff, and S. Leonard. 1976. Evidence against the involvement of chemotaxis in swarming of *Proteus mirabilis*. *J. Bacteriol.* **127:**237 - 248.

Williams, F. D., and R. H. Schwarzhoff. 1978. Nature of the swarming phenomenon in *Proteus*. *Annu. Rev. Microbiol.* **32:**101 - 122.

Williams, J. J., J. S. Rodman, and C. M. Peterson. 1984. A randomized double-blind study of acetohydroxamic acid in struvite nephrolithiasis. *N. Engl. J. Med.* **311:**760 - 764.

Williams, L, W. A. Venables, D. Lloyd, F. Paul, and I. Critchley. 1997. The effects of adherence to silicone surfaces on antibiotic susceptibility in *Staphylococcus aureus*. *Microbiol.* **143:**2407-2413.

Winters, C., D. J. Stickler, T. J. Howe, N. Wilkinson, and C. J. Buckley. 1995. Some observations on the structure of encrusting biofilms of *Proteus mirabilis* on urethral catheters. *Cells Materials* **5:**245 - 253.

Yokoseki, T., T. Iino, and K. Kutsukake. 1996. Negative regulation by FliD, FliS, and FliT of the export of the flagellum-specific anti-sigma factor, FlgM, in *Salmonella typhimurium*. *J. Bacteriol.* **178:**899 - 901.

Yokoseki, T., K. Kutsukake, K. Ohnishi, and T. Iino. 1995. Functional analysis of the flagellar genes in the *fliD* operon of *Salmonella typhimurium*. *Microbiology.* **141:**1715 - 1722.

Young, G. M., D. H. Schmiel, and V. L. Miller. 1999. A new pathway for the secretion of virulence factors by bacteria: The flagellar export system apparatus functions as a protein-secretion system. *Proc. Natl. Acad. Sci. USA.* **96:**6456 - 6461.

Zhao, H., X. Li, D. E. Johnson, and H. T. L. Mobley. 1999. Identification of protease and *rpoN*-associated genes of uropathogenic *Proteus mirabilis* by negative selection in a mouse model of ascending urinary tract infection. *Microbiology.* **145:**185 - 195.

Zimakoff, J., B. Pontoppidan, S. O. Larsen, and D. J. Stickler. 1993. Management of urinary-bladder function in Danish hospitals, nursing-homes and home care. *J. Hosp. Infect.* **24:**183-199.

Zunino, P., L. Geymonat, A. G. Allen, A. Preston, V. Sosa, and D. J. Maskell. 2001. New aspects of the role of MR/P fimbriae in *Proteus mirabilis* urinary tract infection. *FEMS Immunol. Med. Microbiol.* **31:**113 - 120.

Zunino, P., C. Piccini, and Legnani-Fajardo. 1994. Flagellate and non-flagellate *Proteus mirabilis* in the development of experimental urinary tract infection. *Microb. Pathog.* **16:**379 - 385.